



# PROGRAM

icavs.org



Vienna, AUSTRIA

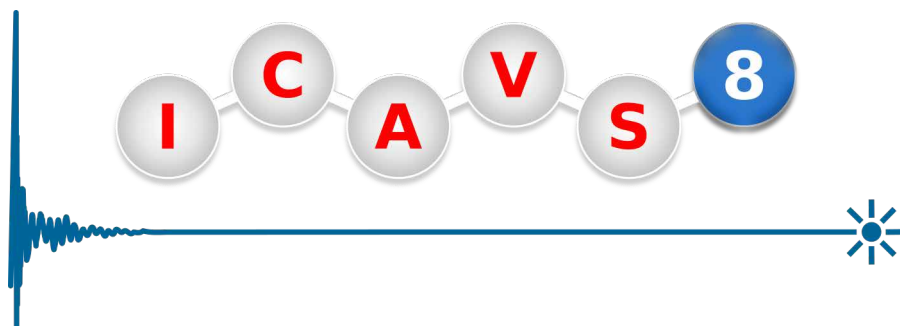
July 12-17, 2015

Platinum Sponsors



Gold Sponsors





# 8<sup>th</sup> International Conference on Advanced Vibrational Spectroscopy

TU Wien, July 12-17, 2015



## **Impressum**

Vienna, July 2015

Editors: Bernhard Lendl, Cosima Koch, Martin Kraft, Johannes Ofner, Georg Ramer

Layout: Manuel Dauböck

Typeface: Dejavu Sans, Humanist 777, Times New Roman, Calibri

Printer: druck.at

# Welcome

The Technische Universität Wien (TU Wien) is proud to have been entrusted with hosting the eighth International Conference on Advanced Vibrational Spectroscopy.

It is now the third time that Infrared and Raman spectroscopy brings researchers from all over the world together in Vienna. Following a highly successful ICOFTS - International Conference on Fourier Transform Spectroscopy event in 1987, which focussed on infrared spectroscopy, the third event of the Advanced Infrared and Raman Spectroscopy (AIRS) series took place at the TU Wien in 1998. Inspired by the momentum and the enthusiasm generated by AIRS and its widened topical coverage of emerging topics in vibrational spectroscopy, it was then decided to merge ICOFTS and AIRS into a new series – ICAVS – whose eighth meeting will now take place from July 12-17, 2015, once more at the TU Wien in the very heart of Vienna.

The aim of the ICAVS Conference Series is to bring together researchers, application scientists and instrumentation developers from universities, research institutes and industry and provide a forum for presenting and discussing recent developments in all fields related to infrared and Raman spectroscopies. In this, ICAVS is particularly focused on showcasing leading-edge developments in vibrational spectroscopy and covering related applications over a wide range of disciplines.

We thank the 600+ scientists from over 40 countries who have accepted our invitation to attend ICAVS 8 for their interest and participation, as well as the sponsoring Austrian and International institutions and the exhibiting and sponsoring companies for their support. With their help, over 50 student bursaries could be provided for this year's conference to encourage the activities of students and young people at the early stage of their careers in vibrational spectroscopy.

On behalf of all organizers, we wish you all a fruitful and enjoyable meeting and a rewarding scientific and human experience at ICAVS 8 in Vienna.



Bernhard Lendl



Mike George

# Content

## General Information

Committees .....	3
Venue.....	4
TU Wien: 200 Years.....	6
Systematic of Presentation Numbers .....	8
Oral Presentations .....	8
Poster Presentations .....	8
What's Hot Session.....	8
Registration & Information.....	9
WiFi .....	9
Emergency Information .....	9
Plotting Services .....	9
Awards and Poster Prizes.....	9
Conference Regulations.....	10
Public Transport.....	10
Conference App .....	11
Exhibition.....	12
Sponsors.....	12
Social Program.....	14
Pre-Conference Workshops.....	16

## Program

Overview.....	18
Monday Plenaries.....	20
Monday Contributed Sessions .....	25
Monday Poster Session.....	37
Tuesday Plenaries .....	60
Tuesday Contributed Sessions .....	65
Tuesday Poster Session.....	77
Wednesday Plenaries.....	100
Wednesday Contributed Sessions .....	105
Thursday Plenaries.....	110
Thursday Contributed Sessions.....	115
Thursday Poster Session .....	127
Friday Plenaries .....	148
Friday Invited Session.....	153

## Exhibition

Company Descriptions.....	156
---------------------------	-----

<b>Author Index</b> .....	164
---------------------------	-----

<b>Maps</b> .....	188
-------------------	-----

## Program Committee

Mike George (program chair UK)  
Katherine Bakeev (USA)  
Vasile Chis (Romania)  
Keith Gordon (New Zealand)  
Peter Griffiths (USA)  
Hiro-o Hamaguchi (Taiwan)  
Takeshi Hasegawa (Japan)  
Koichi Iwata (Japan)  
Young Mee Jung (South Korea)  
Johannes Kunsch (Germany)

Bernhard Lendl (Austria)  
Ian Lewis (USA)  
Curt Marcott (USA)  
Pavel Matousek (UK)  
Boris Mizaikoff (Germany)  
Laurence A. Nafie (USA)  
Christian Pellerin (Canada)  
Zhong-Qun Tian (China)  
Sylvia Turrell (France)

## International Steering Committee

Alexandre G. Brolo (Canada)  
Peter Fredericks (Australia)  
Mike George (UK)  
Takeshi Hasegawa (Japan)  
James de Haseth (USA) - incoming chair

Dennis Hore (Canada)  
Bernhard Lendl (Austria)  
Curt Marcott (USA)  
Don Mc Naughton (Australia) - outgoing chair  
Yukihiko Ozaki (Japan)

## Local Scientific Committee

Hinrich Grothe (TU Wien)  
Christoph Herwig (TU Wien)  
Helmuth Hoffman (TU Wien)  
Cosima Koch (TU Wien)  
Martin Kraft (Carinthian Tech Research)

Bernhard Lendl (TU Wien)  
Johannes Ofner (TU Wien)  
Manfred Schreiner (academy of fine arts vienna)  
Gottfried Strasser (TU Wien)  
Peter Weinberger (TU Wien)

## Local Organising Committee

Mirta Raquel Alcaraz  
Anna Balbekova  
Christoph Gasser  
Andreas Genner  
Cosima Koch  
Martin Kraft  
Christian Kristament  
Bernhard Lendl

María del Pilar Maldonado de Lendl  
Harald Moser  
Johannes Ofner  
Georg Ramer  
Judith Schmitzer  
Andreas Schwaighofer  
Johannes Waclawek  
Karin Wieland

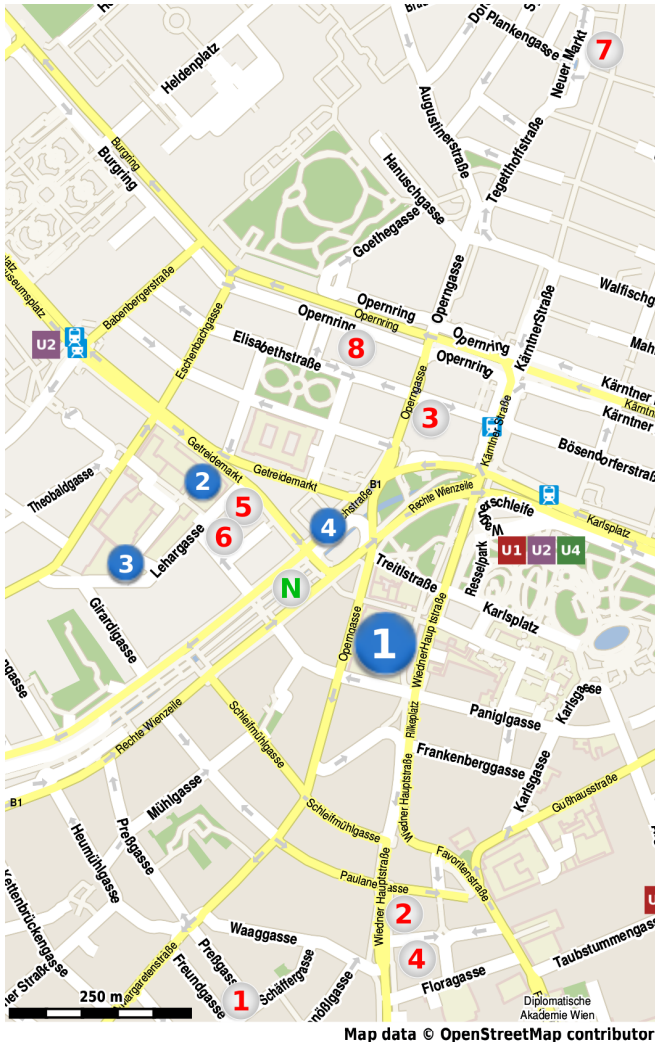
# Venue

The conference will be held at the Freihaus building of TU Wien, Wiedner Hauptstrasse 8-10, 1040 Wien. The plenary lectures, as well as the opening and closing ceremony will take place in the lecture hall HS1, which is located in the red part of the Freihaus building. Entrance to this lecture hall is from the first and the second floor.

Due to the high number of participants there will be a live video broadcast of the plenary lectures to HS5 located in the green part of the Freihaus building.

Invited and contributed talks will take place in parallel sessions in the lecture halls HS1, HS5, HS6 and HS8. Access to lecture halls HS5, HS6 and HS8 is from the second floor only.

Poster sessions and coffee breaks will be held in the exhibition area on the first and second floor of the Freihaus building.



## ICAVS-8 Venues

- 1 TU Freihaus: Main Venue, Workshops
- 2 TU Building BA: Workshops
- 3 Shimadzu Young Scientists Event
- 4 Seccession bus station

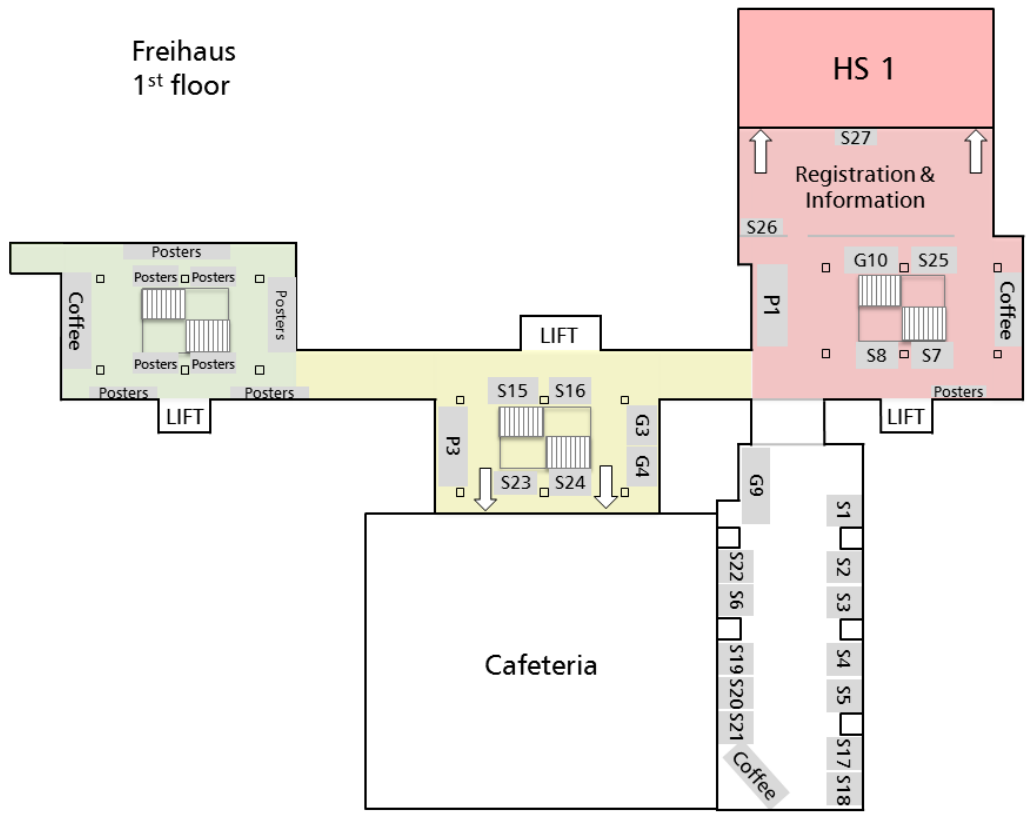
## Hotels

- 1 AllYouNeed Hotel
- 2 Hotel Papageno
- 3 Motel One Wien-Staatsoper
- 4 Hotel Erzherzog Rainer
- 5 Hotel Mercure Seccession
- 6 Hotel Beethoven
- 7 Austria Trend Hotel Europa
- 8 Hotel Le Meridien

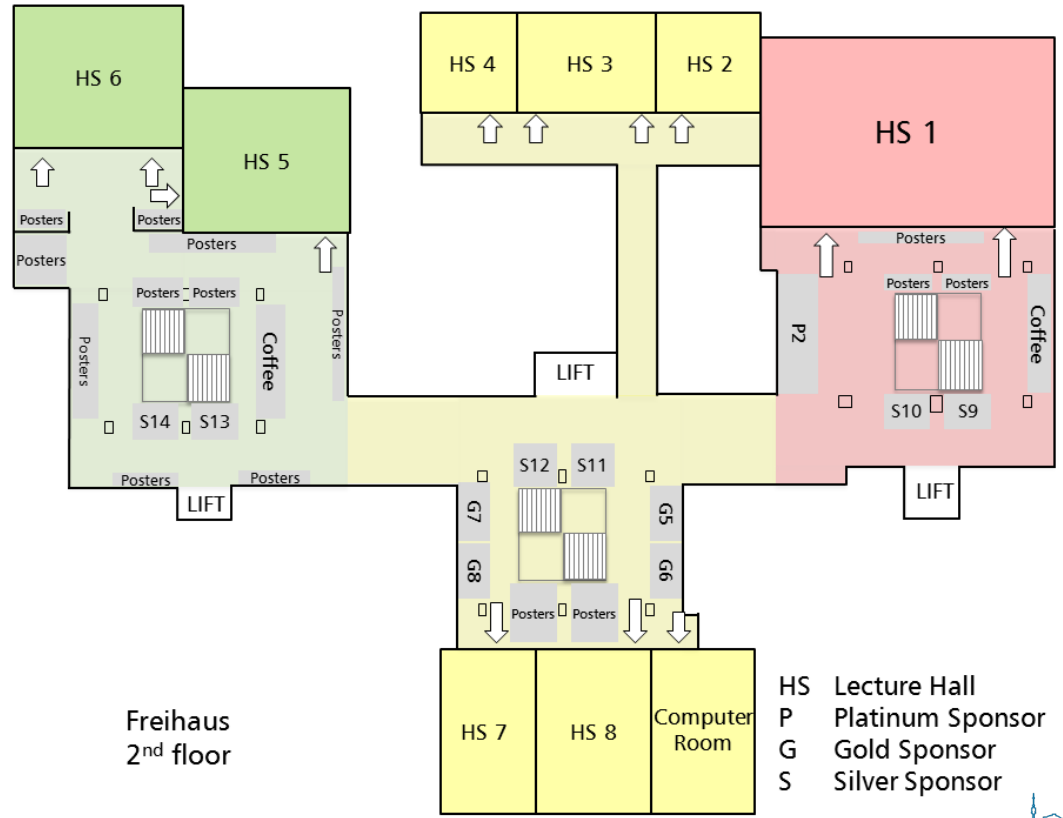
N Naschmarkt

Map data © OpenStreetMap contributors

### Freihaus 1<sup>st</sup> floor



### Freihaus 2<sup>nd</sup> floor



- HS Lecture Hall
- P Platinum Sponsor
- G Gold Sponsor
- S Silver Sponsor



# TU Wien: 200 Years Research - Teaching - Innovation

Through our research, we develop scientific excellence, and through our teaching, we enhance comprehensive competence.

On November 6th 2015 TU Wien is celebrating its 200th anniversary. Following the mission “technology for people”, TU Wien has been a place of research, teaching and learning in the service of progress.

Today, TU Wien is among the most successful technical universities in Europe and is developing scientific excellence of high international level. The university’s strength is the inherent combination of basic and applied research, as innovation occurs when least expected. Innovation means development, but also the explicit encouragement of development processes and the establishment of respective frameworks. Graduates and researchers of TU Wien substantially contribute to the knowledge and technology transfer into society and economy and provide – today as 200 years ago – an essential input to international competitiveness. To mark the 200-year-jubilee, TU Wien has opened the doors to the wider public to present our achievements and core competences in various ways.

Research at the University is of national and international significance. As one of Europe’s leading research universities, our focus is not only on the harmony of solid basic research with applied practical research, but also the high quality results that stem from research and close cooperation with the economy.

In teaching, great value is placed on the combination of theory and practice. Through this, and by passing on solid core principles, TU Wien allows interest-specific specializations to develop. The University’s maxim of research-driven teaching is supported by the active involvement of students in ongoing research projects. The selection of courses is diverse and ranges from architecture and engineering technology through to the natural sciences. TU Wien also sets itself the challenge of encouraging “lifelong learning”. A high priority is therefore placed on continuing education and training.

Through the fusion of companies and cooperation with the economy, a growing international and regional environment is promoted, in which our alumni are highly sought after employees in industry, the economy and the public sector, immediately after graduation. In this way, our alumni make a significant contribution to the stimulation of the domestic economy.

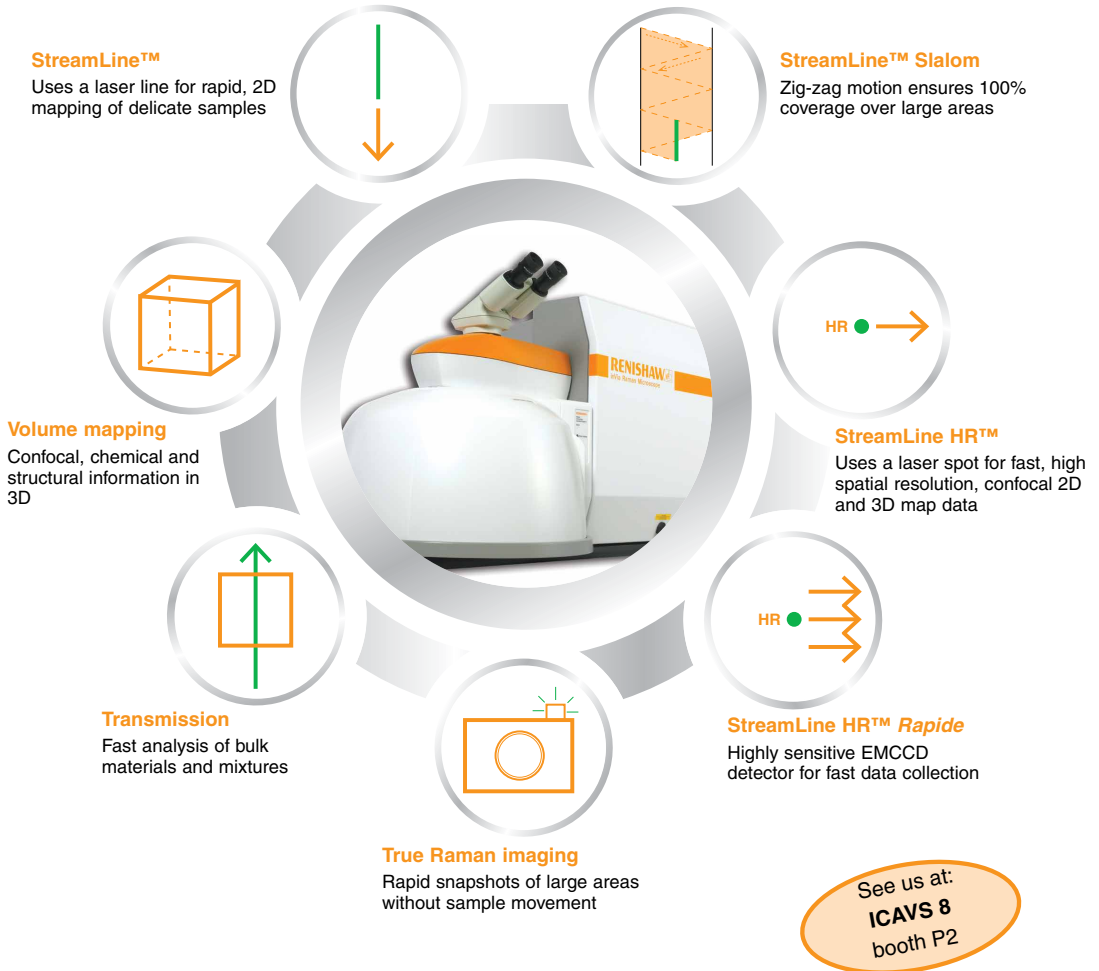
[www.tu200.at](http://www.tu200.at)



**1815 – 2015**

200 Jahre Zukunft

# inVia: innovative Raman imaging



## The Renishaw inVia confocal Raman microscope.

Don't limit your imaging capabilities.

The inVia's comprehensive range of imaging techniques allows you to generate high quality Raman images whatever your sample.

Discover more at [www.renishaw.com/ramanimages](http://www.renishaw.com/ramanimages)

# Systematics of Presentation Numbers

The day and location of oral presentations is encoded in the paper numbers as follows: The letters indicate the day of the presentation (MO, TU, WE ...), the first number indicates the lecture hall where the presentation will take place (lecture halls 1, 5, 6 or 8), and the last two numbers define the sequence of the presentations.

At ICAVS 8 poster Session A will take place on Monday, July 13, Poster Session B on Tuesday, July 14, and Poster Session C on Thursday, July 16. Each poster number includes the letter of the respective poster session. The poster boards are ordered by increasing poster number. The suffix –pdp indicates a post-deadline-poster.

## Oral Presentations

Speakers will be required to report to the technical support staff in the lecture hall of their respective session at least 15 minutes prior to the start of the session.

Computers running Windows 7 and equipped with both Microsoft Office Powerpoint 2013 and the Adobe PDF Reader will be provided for presentations in each lecture hall. Please give your presentation on a USB flash drive to the person in charge, who will upload it to the presentation PC and have it ready at the start of your presentation. The presentations will be deleted from the computers after each session. Alternatively, it is possible to connect your own laptop via a standard VGA interface.

All lecture halls are equipped with:

- Windows laptops
- LCD projector with single-screen projection configured for 4:3 display aspect ratio
- Wireless remote presenter and laser pointer
- Wireless lavalier microphone
- Speaker timer

Regarding the length of your presentation (12+3 min for contributed talks, 17+3 min for invited presentations and 30+5 min for plenaries) please refer to the scientific program starting at page 18. As there will be four sessions in parallel, we kindly ask you to strictly keep the time.

## Poster Presentations

Poster sessions are scheduled from 16:20 – 18:00 on Monday, Tuesday and Thursday.

Posters should be put up in the morning of the respective poster session and have to be removed immediately after the poster session finishes.

Please mount your poster on the board with your assigned poster number, e.g. A050. Posters have to be mounted to poster boards using adhesive tape, which will be provided.

## What's Hot Session

Platinum and Gold sponsors of ICAVS 8 have been invited to report on their most recent developments in a “What's Hot” session scheduled for Wednesday, July 15. The What's Hot Session will be held in HS1 and start at 12:20.

## Registration & Information

The registration and information desk is located at the first floor of the Freihaus building in front of lecture hall HS1. Registration will start on Sunday, July 12 at 12:00. The conference desk will be staffed until 20:00 on Sunday, and from 8:00 through 18:00 on Monday, Tuesday and Thursday. On Wednesday and Friday opening hours of the conference desk will be 8:00 - 14:00.

## Complimentary WIFI

Wifi connection is available throughout the conference venue. You will receive your personal access code during registration. Furthermore, EDUROAM is available throughout the TU Wien.

## Emergency Information

European Emergency Number: 112

Medical Emergencies: 144

Emergencies at the conference venue: alert conference staff

## Plotting Services

There are several plotting/printing services in close proximity to the conference venue (Freihaus):

- Grafisches Zentrum HTU GmbH: Freihaus, ground floor
- die Kopie 04: Wiedner Hauptstraße 5, 1040 Vienna
- Albert Schiessling Plotservice: Operngasse 20 b, 1040 Vienna

## Awards and Poster Prizes

For the first time at an ICAVS conference, the "Raman Young Investigator Award" sponsored by Horiba Scientific will be awarded to a participant of ICAVS 8 in recognition of an outstanding oral or poster presentation. The awardee, who will be selected by members of the ICAVS Program Committee, will receive the 1,000 US \$ award from the hands of a representative of Horiba Scientific during the conference dinner at the Palais Ferstel.

The Federation of Analytical Chemistry and Spectroscopy Societies (FACSS) kindly sponsors three non-local speakers in form of travel grants to support their participation in ICAVS 8. FACSS and these three awardees will be briefly introduced after the plenaries on Wednesday, July 15<sup>th</sup>.

Finally, several Poster Prizes sponsored by Springer (ABC), The Royal Society of Chemistry (The Analyst), John Wiley & Sons and Spectroscopy will be awarded to Young Scientists during ICAVS 8. These prizes will be presented July 17<sup>th</sup> as part of the closing ceremony of ICAVS 8.



# Conference Regulations

For security reasons, please always wear your ICAVS 8 badge while on the conference premises. Smoking is permitted only outside the conference venues. Photography and recording is not permitted in any oral or poster session.

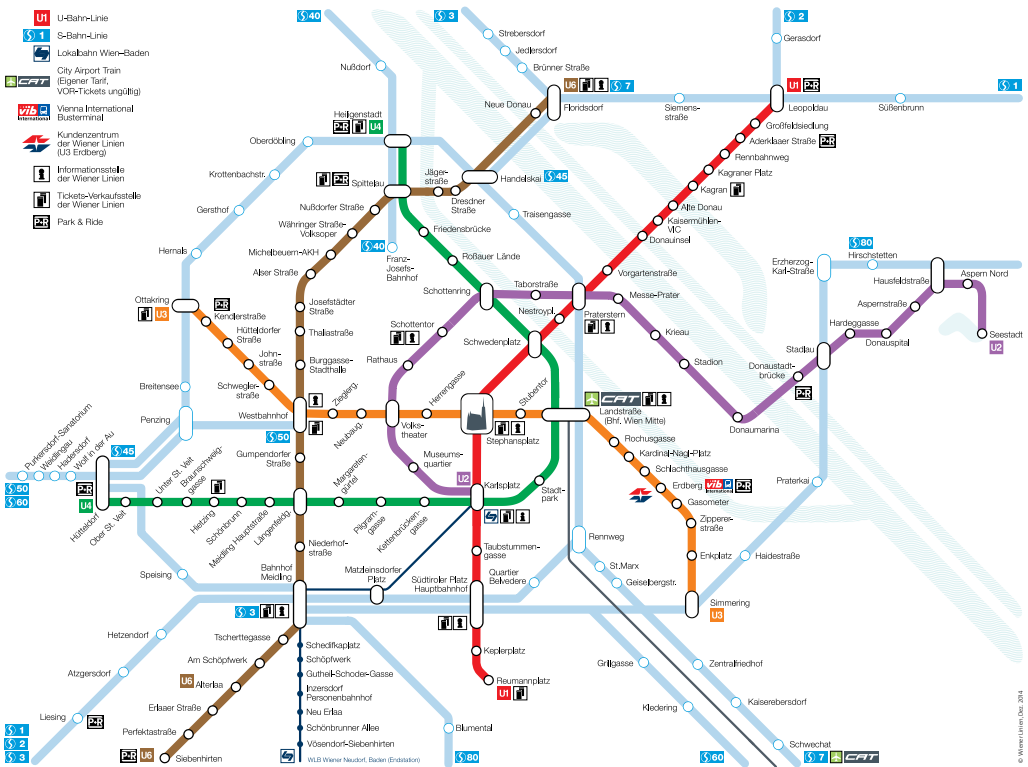
We will have a small film team on location to cover ICAVS 8. If you do not wish to be filmed, please approach them and indicate so.

## Public Transport

Vienna has an excellent public transport network comprising underground (U-Bahn) lines, trams (Straßenbahn), buses and commuter trains (S-Bahn). Before travel, a ticket must be validated once by punching it in a ticket validating machine, which are conveniently located at the entrances to underground station platforms and inside buses and trams.

A weekly ticket valid for all means of public transport within the city of Vienna is included in your conference package. This ticket is valid for one Monday-to-Sunday period once validated.

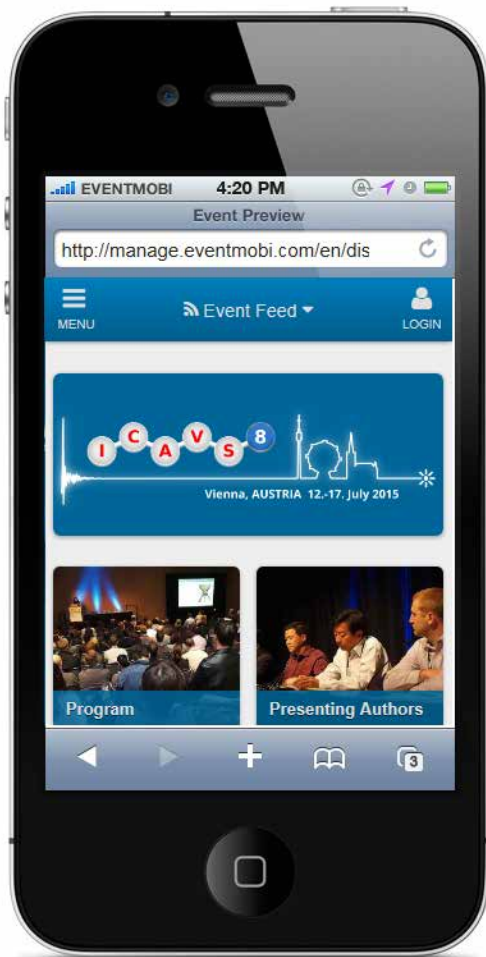
## Der Plan der schnellsten Wege.



# Conference App

At ICAVS 8 we will provide the attendees with a “conference app” for Android, Apple, Blackberry and Microsoft mobile devices. Please download and install the app and then validate your ICAVS 8 participation.

Announcements concerning changes to the program, updated information on the social program etc. will be made primarily through the app. In addition, announcements will be posted to a message board located on the first floor in front of lecture hall HS 1 close to the registration and information desk.



# Exhibition

The exhibition will take place at the first and second floor of the Freihaus building during the conference hours from Monday morning through Thursday evening. A detailed list of exhibitors can be found on page 156.

## Sponsors

### Platinum Sponsors



### Gold Sponsors



### Silver Sponsors



Zurich Instruments





### Logo Sponsors



# Social Program

*Sunday July 12, 18:00 – 20:00*

## **Bruker Welcome Mixer**

TU Wien - Freihaus, Cafeteria

The Bruker Welcome Mixer will be held in the Cafeteria of the TU Wien Freihaus (1<sup>st</sup> floor) directly opposite our conference venue on Sunday evening from 18.00 – 20.00.

*Tuesday July 14, 19:30 – 24:00*

## **Shimadzu Young Scientists Event**

Atelierhaus der Akademie der bildenden Künste Wien (“Semperdepot“), Lehargasse 6-8, 1060 Wien

Hosting this casual evening event, ICAVS 8 aims at fostering free and easy networking, especially of young/early career scientists. Finger food, drinks, music and games in a historical and but not traditional setting will provide a relaxed and enjoyable atmosphere.

All conference attendees are invited to join the event. Persons who have registered as a Young Scientist during registration will receive special benefits.

*Wednesday July 15, 14:00 – 22:00*

## **Excursions & Heuriger**

To help you get the “feel” of Vienna, visit places you always wanted to see or re-visit memories from past visits, you have a choice between four different excursions. The common final station of all is a typical Viennese wine tavern, a “Heuriger”, where we will all meet for a casual dinner.

### **Excursion 1: Walk through the “Old Vienna“**

Meeting point and time: TU Wien Freihaus, red area - ground floor at 15:00

Duration: approx. 2 hours

The purpose of this walk is to present parts of old Vienna that are typically not shown to the visitor. Our walk takes us past the Imperial Palace, the winter residence of the Imperial family. After a walk through the Volksgarten we reach the Augustinian church, the wedding church of the Habsburgs which is also famous for its unparalleled acoustics. Many music concerts take place here, all year round. Subsequently, our walk leads us to St. Stephen's Cathedral. At the end of the tour, a direct bus transfer to the Heurigen will be available.

### **Excursion 2: Walking tour: Vienna - City of Music**

Meeting point and time: TU Wien Freihaus, red area - ground floor at 15:00

Duration: approx. 2 hours

Vienna hosted numerous musicians who lived and worked in this city. On our tour we will pass the residences of Josef Haydn, Wolfgang Amadeus Mozart and Ludwig van Beethoven, to mention just a few. From the Vienna State Opera, one of the most famous Opera Houses in the World, we walk across the Augustinerstrasse to the Michaelerplatz. Finally you visit the House of Music where you can enjoy all conveniences an interactive museum has to offer. At the end of the tour a direct bus transfer to the Heurigen will be available.

### Excursion 3: Bus tour: Historical Vienna with tour through Schönbrunn Palace

Meeting point and time: Secession bus station (see map on page 4) at 14:30

Duration: approx. 3 hours

To provide you first with an impression of the city center, we start our tour at Ringstrasse. This boulevard with an approximate length of 4 km was created in the course of the city's expansion in the middle of the 19th century on the area of the former Glacis. We will see buildings like the Museum of Fine Arts, the Museum of Natural History, the City Hall, the Burgtheater, the Parliament, the University, and many more. The highlight of our excursion is a tour through Schönbrunn Palace, the summer residence of the former Imperial House of Austria. The bus will then take you to the Heurigen for dinner.

### Excursion 4: Bus & boat tour: Panoramic Danube

Meeting point and time: Secession bus station (see map on page 4) at 14:00

Duration: approx. 3.5 hours

We start our tour at Ringstrasse passing the Vienna State Opera, Burgtheater, Parliament and many more. The highlight of the tour is a boat ride on the Danube and the Danube Canal from the city center to the Reichsbrücke. Afterwards we take you to Cobenzl, a vantage point from which you have a panoramic view on the Wienerwald and the vineyards that encircle the city, the city itself and the Danube. The bus will then take you to the Heurigen for dinner.

## Heuriger

Heuriger Fuhrgassl-Huber, Neustift am Walde 68, 1190 Vienna

After the excursions, we will meet up at a typical Viennese wine tavern, a "Heuriger", for a casual dinner. For those who do not participate in any excursion, a direct bus transfer will be available from Secession bus station (see map page 4), leaving at 17:30.

Busses for the return journey to Secession bus station will start leaving the Heurigen at 21:00. Alternatively, you also can return to the City Center by public transport using the ticket included in your conference package.

*Thursday July 16, 19:30 – 22:30*

## Conference Dinner

Palais Ferstel, Strauchgasse 4, 1010 Vienna

The splendid Ferstel Palace on the Freyung was originally built in 1860 by the Viennese architect Heinrich von Ferstel as a bank and stock exchange building. Built in the romantic historicism style, the Great Ferstel Hall with its magnificent chandeliers, parquet flooring and elaborate ceiling murals is one of the most individual and beautiful halls in Vienna. The palace itself is reminiscent of a Venetian palazzo - in the Great Ferstel Hall, the characteristic curved shape of a ship's bow can be seen. Together with the arcade courtyard, this will form the elegant and stylish setting for the ICAVS 8 Conference Dinner.

Dress Code: Cocktail style / business attire

To be dressed appropriately we would suggest for men to wear a suit (tie optional) and for ladies to wear either a long dress or a cocktail dress.

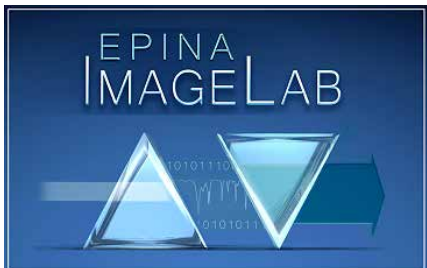
Tickets (€ 80) were available for purchase during the registration process; subject to availability, remaining tickets can be purchased until Monday, July 13, at the registration desk.



# Pre-Conference Workshops

All workshops will be held on Sunday, July 12.

## Short Course on Hyperspectral Imaging



Time: 14:00 - 18:00

Location: Getreidemarkt 9, SEM BA02A

The course combines theoretical explanations with practical applications. It includes a free, time-limited ImageLab license. Topics covered by the course include:

- Essentials of data preprocessing
- Theory behind spectral descriptors
- Multisensor hyperspectral imaging
- Hands-on experience with
  - Principal Component Analysis
  - Vertex Component Analysis
  - Cluster Analysis (HCA and kMeans)
  - Classification (PLS/DA)

## IR & Raman Spectral Identification Workshop

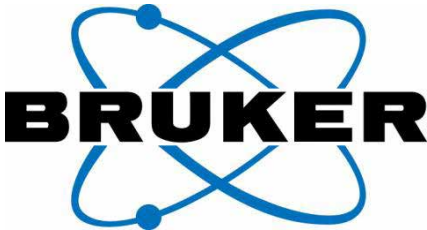


Time: 17:00 – 18:00

Location: Freihaus,  
Computer Room (2<sup>nd</sup> Floor)

This live workshop introduces the latest technology for identifying unknown IR and Raman spectra and the advantages it has over traditional tools like spectral search software and other spectral analysis tools. Real spectral samples including complex mixtures will be used to demonstrate the technology. After a brief presentation, attendees can try the software using their own spectra or those provided by Bio-Rad.

## Workshop on correlative near-field vibrational imaging with <20nm resolution



Time: 14:00 – 18:00

Location: Getreidemarkt 9, SEM BA02C

The workshop will introduce Bruker's Inspire platform that enables imaging of chemical, mechanical and electrical properties with <20nm spatial resolution. We will discuss the technique that is based on a scattering near-field optical microscope, show examples and explain the complete workflow for acquiring these novel, high-resolution correlated data. An interactive demonstration experiment will be performed on the instrument.

## 3D Confocal Raman Imaging - Fundamental Trends and State of the Art Applications



Time: 15:00 – 17:00

Location: Freihaus HS 4

Attendees of this workshop taking place in the course of ICAVS 8 will be informed about our newest technical developments in automated Raman Imaging, correlative RISE (Raman Imaging and Scanning Electron) microscopy and advanced data evaluation of hyperspectral 3D imaging datasets. These talks are given by WITec's staff. An external speaker will report on the current status of Raman Imaging.

## Real-Time Chemical Imaging with Spero, the World's First Laser-Based IR Microscope

DAYLIGHT

SOLUTIONS®



Time: 15:00 – 16:30

Location: Freihaus HS 2

Join the Daylight Solutions team to see how you can use the game-changing real-time discrete frequency imaging capabilities of Spero for rapid chemical identification of biomedical, pharmaceutical, and materials research samples.

The workshop will include a live demo of the Spero microscope and will cover:

- Hardware overview
- Introduction to ChemVision control software
- Live imaging demo
- Discrete frequency imaging demo
- Data collection workflow
- Data visualization and analysis workflow
- Sample images and spectra from various applications

## Latest Developments in FTIR Imaging: Resolution for Every Application



Agilent Technologies

Time: 14:00 – 17:00

Location: Freihaus HS 7

The workshop will consist of presentations by leading academics in FTIR chemical imaging to demonstrate our world-leading imaging system and will cover:

- Latest developments in FTIR Imaging - breaking spatial resolution limits
- FT-IR Imaging in Polymer and Life Science
- The utility of FTIR imaging in the survey of paintings and painted objects and their conservation
- The benefit of FTIR imaging for histopathological diagnosis
- Prognostic subclasses of lung-cancer annotated by FTIR-imaging

## Infrared and Raman tools for measurement of chemical and physical properties - Seeing is believing!

Thermo  
SCIENTIFIC

A Thermo Fisher Scientific Brand

Time: 15:00 – 17:00

Location: Freihaus HS 4

Detailed theoretical and practical knowledge on IR and Raman Spectroscopy is conveyed in our workshop during ICAVS 8, enabling you to conduct qualified measurements and to interpret measuring data. This workshop will benefit beginners, intermediate or professional IR and Raman Spectroscopy users in research and development, or quality control.

- Short theory of Infrared and Raman Spectroscopy
- Infrared spectroscopy
- Step scan and its applications
- Surface analysis, Grazing Angle ATR, PEM-IRRAS
- Optical measurements, measurement of indexes, emissivity
- Raman spectroscopy
- New technologies for Raman Imaging
- AFM and Raman coupling, TERS
- Hands on Session



	SUN	MON	TUE	
08:45-9:00		<b>Opening of ICAVS 8 - HS1</b>		
09:00-10:10		HS1 and video broadcast to HS5	HS1 and video broadcast to HS5	
		<b>Rainer Hillenbrand</b> "Infrared Nanoscopy and nano-FTIR Spectroscopy by Elastic Light Scattering from a Scanning Probe Tip"	<b>Zhenchao Dong</b> "Single-Molecule Raman Spectromicroscopy Down to sub-nm Resolution"	
		<b>Mikhail Belkin</b> "Infrared Vibrational Nanospectroscopy via Molecular Expansion Force Detection"	<b>Nathalie Picqué</b> "Vibrational Spectroscopy with Laser Frequency Combs"	
10:10-10:40	Coffee Break			
10:40-12:00		HS1	HS5	
		<b>Nearfield Infrared Imaging</b> Centrone, Govyadinov, Bechtel, Mastel, Ramer	<b>Material Science 1</b> Pellerin, Enengl, Sturcova, Kozanecski, Marcott	<b>Biomedical Applications 1</b> Popp, Gardner, Mandrile, Gil, Ashton
12:00-13:30		HS6	HS8	
		<b>Portable Raman Systems</b> Ayora-Cañada, Zachhuber, Assi, Carron, Fromm	<b>Appl. in Life Sciences 1</b> eckert-Gaudig, Katz, Höhl, Kaczor, Samek	<b>Material Science 3</b> Furukawa, Jafari, Agresti, Eder, Misra
13:30-14:50		HS5	HS6	
		<b>Nanomaterials 2</b> Ozaki, Kalbac, Spencer, Weselucha-B., López-Lorente	<b>QCL Source Development</b> Wagner, Carras, Szedlak, Müller, Mangold	
Lunch Time				
14:50-15:15		HS1	HS5	
		<b>IR Imaging</b> Martin, Quaroni, Lewin, Rowlette, Kerstan	<b>Material Science 2</b> Gordon, Richard-Lacroix, Nikolaeva, Hikima, Hasegawa	<b>Biomedical Applications 2</b> Nottingher, Dochow, Jeong, El-Mashtoly, Quatela
15:15-16:20		HS6	HS8	
		<b>Environ. and Planetary Sci.</b> Heraud, Wagner, Galvez, Verkaaik, Cinta Pinzaru	<b>Surface Science</b> Erbe, Hore, Warring, Siurdyban, Solovyeva	<b>Material Science 4</b> Kazarian, Vapaavuori, Morita, Shimoaka, Weinberger
Coffee Break				
16:20-18:00		HS1	HS5	
		<b>Nearfield IR Imaging</b> (companies) Boehmler, Wagner, Prater	<b>Nanomaterials 1</b> Zerbi, Zelenovskiy, Jalakanen, Rabolt	<b>Biomed. Applications 3</b> Pastrana-Rios, Mordechai, Liberale, Smith
Evening Program		HS6	HS8	
		<b>Raman Systems</b> (companies) Dieing, Law, Carriere, Kurki	<b>TERS</b> Deckert, Schultz, Lu, Lewis	<b>SERS 1</b> Dluhy, Frøhling, Mahajan, Lopez Ramirez
		HS5	HS6	
		<b>Appl. in Life Sciences 2</b> Heberle, Kötting, Guillon, Melin	<b>QCL Spectrosc. &amp; Imaging</b> Roth, Hugger, Baker, Tittel	
		<b>Poster Session A</b> Microscopy & Imaging, Nearfield Vib. Spec., Biomedical Applications, Fine Arts, Safety Applications, Nanomaterials, Geoscience 1, Portable Raman Systems, Material Science 1		
		<b>Poster Session B</b> MIR Laser Spectroscopy 1, TERS, plasmonics, SERS, SEIRA, Time-Resolved Spectroscopy 1, Life Sciences, Instrumentation (NIR, MIR, THz)		
	Mixer	<b>Shimadzu Young Scientist Event</b>		

----- Workshops (12:00- 18:00) ----- |

WED	THU	FRI
HS1 and video broadcast to HS5 <b>Shigeki Yamamoto</b> "Peptide Conformations and Solvent Environments Obtained from Raman Optical Activity"	HS1 and video broadcast to HS5 <b>Sebastian Schlücker</b> "Surface-Enhanced Raman Spectroscopy and Imaging with Tailor-Made Plasmonic Nanoparticles"	HS1 and video broadcast to HS5 <b>Tahei Tahara</b> "Femtosecond Vibrational Spectroscopy of Simple and Complex Systems"
<b>Klaus Gerwert</b> "Vibrational Imaging Provides Marker-free Annotation of Tissue and Cells in Biomedical Applications"	<b>Rudolf Kessler</b> "Perspectives in Process Analysis: PAT and the Workhorse Vibrational Spectroscopy"	<b>Martin Zanni</b> "From Esoteric to Commonplace: Techn. Advances that are Turning 2D IR Spectroscopy into an Analytical Research"

Coffee Break

Coffee Break

HS1	HS5	HS6	HS8	HS1	HS5	HS6	HS8	HS1
<b>Biomedical Applications 4</b> Bhargava, Malek, Wood, Halamkova, Kuligowski	<b>Material Science 5</b> Casiraghi, Taubner, Mink, Krylova, Kalugin	<b>Vibrational Optical Activity</b> Johannessen, Nafie, Blanch, Oulevey, Kiefer	<b>PAT 1</b> Huck, Wetzel, Chung, Barone, Smith	<b>SERS 2</b> Jamieson, Dugandzic, Tseng, Ozaki, Matejka	<b>Non-linear Techniques</b> Lee, Yui, Ujji, Monfort, Kish	<b>Appl. in Life Sciences 3</b> Lasch, Mezzetti, Nabers, Alves, Mantsch	<b>PAT / imPACTs</b> Golabgir, Mayr, Brandstetter, Kraft, Moser	Julia Davies Kathleen Gough Gottfried Strasser Notburga Gierlinger

Lunch Time / What's hot session HS1

Lunch Time

ICAVS 9 and Closing of ICAVS 8

Excursions	<b>Plasmonics</b> Etezadi, Malš, Osawa, Kielb, Novara	<b>Material Science 6</b> Solonenko, Krylov, Ahlawat, Leonidov, Rao	<b>Time-resolved Spectroscopy</b> Batignani, Simon, Kottke, Iwata, Hauer	<b>PAT 2</b> Lewis, Kemper, Bourson, Artyushenko, Pudney
	<b>SERS 3</b> Ling, Brolo, Zhang, Timmermans	<b>Computational Spectr. 2</b> Andre, Choi, Stavrov, Tandon	<b>Biomedical Applications 5</b> McNaughton, Heise, Huefner, Batista de Carvalho	<b>Advances in IR Detectors</b> Lambrecht, Harter, Ogrodnik, Kunsch
	Coffee Break			
	<b>Poster Session C</b> VOA, PAT, Time-resolved Spectroscopy 2, Non-linear techniques, Material Science 2, Surface Science, MIR Laser Spectroscopy 2, Geoscience 2, Computational Spectroscopy 2			
Heuriger	<b>Conference Dinner</b>			

9:00  
MOPL1 **Infrared Nanoscopy and Nano-FTIR Spectroscopy by Elastic Light Scattering from a Scanning Probe Tip**

Rainer Hillenbrand

With the development of scattering-type scanning near-field optical microscopy (s-SNOM), the analytical power of visible, infrared and THz imaging has been brought to the nanometer scale. The spatial resolution of about 10 - 20 nm opens a new era for modern nano-analytical applications such as chemical identification, free-carrier profiling and plasmon imaging. After a brief overview of fundamentals and applications of s-SNOM, recent achievements such as broadband Fourier transform infrared nanospectroscopy (nano-FTIR) of polymers and proteins will be discussed.



Rainer Hillenbrand is Ikerbasque Research Professor and Nanooptics Group Leader at the nanoscience research center CIC nanoGUNE in San Sebastian (Basque Country, Spain). He is also co-founder of the company Neaspec GmbH (Martinsried, Germany), which develops and manufactures near-field optical microscopes. Hillenbrand's research activities include the development of infrared nanospectroscopy and its applications in nanophotonics, graphene plasmonics, materials sciences and biology, for which he received the Ludwig-Genzel-Price in 2014.

9:35  
MOPL2 **Infrared Vibrational Nanospectroscopy via Molecular Expansion Force Detection**

Mikhail Belkin, Feng Lu, Mingzhou Jin

I will present a technique for very sensitive mid-infrared vibrational nanospectroscopy based on observing a deflection of an atomic force microscope cantilever due to mechanical forces exerted by molecules excited with laser pulses. Spectra are obtained by recording the cantilever deflection amplitude as a function of excitation laser wavelength. Tip-enhancement of light intensity and mechanical cantilever resonance enhancement are used to achieve nanoscale spatial resolution and ultrahigh sensitivity. Non-destructive mid-infrared spectroscopy and imaging of molecular monolayer islands is demonstrated in air with high signal-to-noise ratio and better than 30 nm spatial resolution. Approximately 300 molecules contribute to cantilever deflection in our current experiments and spectra of as few as 30 molecules would be detectable. Recent progress towards extensions of this method to operation in aqueous environment will be discussed as well.



Mikhail A. Belkin is an Associate Professor in the Department of Electrical and Computer Engineering at the University of Texas at Austin. He received his Ph.D. in Physics from the University of California at Berkeley in 2004 and did his postdoctoral work in Prof. Federico Capasso's group in the Harvard School of Engineering and Applied Sciences. Dr. Belkin's research interests focus on novel approaches for mid-infrared and terahertz sub-wavelength resolution microscopy and on-chip chemical sensing as well as on other areas of mid-infrared and terahertz photonics.

## Infrared Nanoscopy and Nano-FTIR Spectroscopy by Elastic Light Scattering from a Scanning Probe Tip

Rainer Hillenbrand<sup>1,2</sup>

<sup>1</sup>CIC nanoGUNE and UPV/EHU, 20018 Donostia-San Sebastián, Spain

<sup>2</sup>IKERBASQUE, Basque Foundation for Science, 48011 Bilbao, Spain

Keywords: infrared near-field microscopy, infrared nano-spectroscopy, nano-FTIR

With the development of scattering-type scanning near-field optical microscopy (s-SNOM)<sup>1</sup>, the analytical power of visible, infrared and THz imaging has been brought to the nanometer scale. The spatial resolution of about 10 - 20 nm opens a new era for modern nano-analytical applications such as chemical identification, free-carrier profiling and plasmonic vector near-field mapping.

s-SNOM is based on elastic light scattering from atomic force microscope

tips. Acting as optical antennas, the tips convert the illuminating light into strongly concentrated near fields at the tip apex (nanofocus) (Figure 1), which provides a means for localized excitation of molecule vibrations, plasmons or phonons in the sample surface. Recording the tip-scattered light as a function of sample position subsequently yields nanoscale resolved optical images, beating the diffraction limit in the infrared spectral range by more than two orders of magnitude.

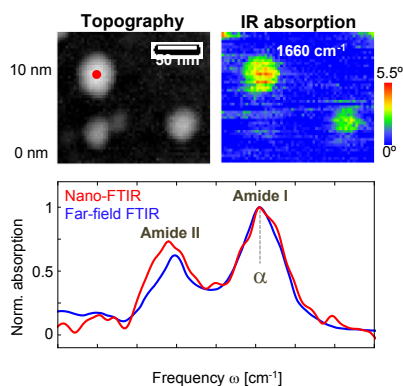
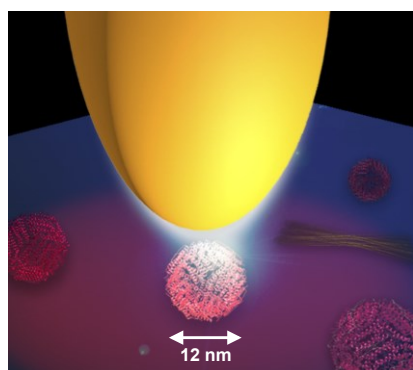


Figure 1. Infrared nanoimaging of a single protein complex (ferritin, 5000 C=O bonds, 1 attogram mass). Left: Illustration of the infrared illuminated tip of a near-field microscope on top of a ferritin complex. Right: Topography and infrared absorption image of three nanoparticles reveals that only two of them are protein complexes. The nano-FTIR spectrum (red) was taken on the complex marked by the red dot in the topography image.

Using broadband IR illumination and Fourier-transform spectroscopy of the tip-scattered light<sup>2,3</sup>, IR spectra with 20 nm spatial resolution can be acquired (nano-FTIR). Near-field images and near-field absorption spectra of molecular vibrations in mid-infrared fingerprint region allow for chemical mapping, identification of polymer<sup>3</sup> and protein<sup>4</sup> nanostructures, and for quantitative measurement of the complex-valued local dielectric function<sup>5</sup>, among others.

<sup>1</sup> F. Keilmann, R. Hillenbrand, *Phil. Trans. R. Soc. Lond. A* 362, 787 (2004)

<sup>2</sup> F. Huth, et al., *Nature Mater.* 10, 352 (2011)

<sup>3</sup> F. Huth, et al., *Nano Lett.* 12, 3973 (2012)

<sup>4</sup> I. Amenabar et al., *Nat. Commun.* 4:2890 doi: 10.1038/ncomms3890 (2013)

<sup>5</sup> A. Govyadinov, et al., *J. Phys. Chem. Lett.* 4, 1526 (2013)

## Infrared Vibrational Nanospectroscopy Via Molecular Expansion Force Detection

Feng Lu, Mingzhou Jin and Mikhail A. Belkin

Department of Electrical and Computer Engineering  
The University of Texas at Austin, Austin, TX 78758, USA

Keywords: Infrared spectroscopy, nanoscale, opto-mechanical

Mid-infrared (mid-IR) vibrational absorption spectroscopy is a universal method to identify chemicals by their molecular absorption fingerprints. There is a growing demand for high precision characterization of materials and biological agents with nanometer spatial resolution and with a sensitivity of only a few molecules.

We report a technique for very sensitive mid-IR nanospectroscopy based on observing a deflection of an atomic force microscope (AFM) cantilever due to mechanical forces exerted by molecules photoexcited with laser pulses on the AFM tip. Spectra are obtained by recording the cantilever deflection amplitude as a function of excitation laser wavelength. Using sample photoexpansion to perform nanoscale molecular spectroscopy was originally suggested by A. Dazzi *et al*<sup>1</sup>. However, to produce detectable cantilever deflection, the original method required high-power laser pulses to induce sample heating by 10-50 degrees and sample thickness of at least ~100 nm. We have dramatically improved the sensitivity of photoexpansion microscopy to work with samples as thin as one molecular monolayer with better than 30 nm spatial resolution<sup>2</sup>. This was achieved sending low-power laser pulses at a repetition frequency that is tuned in resonance with the mechanical vibrational frequency of the AFM cantilever and by employing tip-enhancement of the optical field below a sharp gold-coated AFM tip.

The experimental setup is presented in Fig. 1. Mid-IR laser pulse train from quantum cascade laser (QCL) is focused onto the molecules below a sharp AFM tip. Upon illumination, the molecules absorb radiation energy, rapidly expand and push the tip, which causes periodic displacement of the AFM probe. With the laser trigger as reference signal, we are able to record the AFM cantilever vibration amplitude using a lock-in amplifier. By plotting the lock-in output as a function of QCL emission wavelength, we obtain the molecular expansion force spectrum, which is a proxy for molecular infrared absorption spectrum.

When we tune the QCL repetition frequency to match the cantilever mechanical resonant frequency, the cantilever vibration amplitude is amplified by its Q factor, which can be as high as 5,000 in air. The signal can be increased further using tip-enhancement by employing

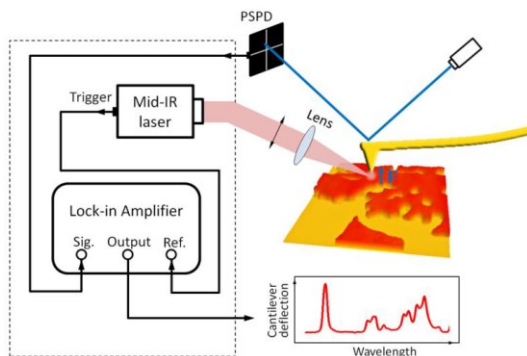


Figure 1. Experimental setup.

sharp gold-coated AFM tips and placing samples on metal substrates. The electromagnetic field intensity under the tip is increased by a factor of  $4 \times 10^5$ , and is spatially localized to a  $\sim 10$  nm-radius region. The combined mechanical and tip enhancement directly translates into very high sensitivity and spatial resolution of our method.

Nanoscale photoexpansion spectra of two self-assembled monolayers (SAMs) on flat gold substrate are shown in Figs. 2(a) and 2(b). The SAM thicknesses are 1.3 nm and 0.5 nm for hydroxyl-terminated hexa (ethylene glycol) thiol (EG6-OH) and 4-nitrothiophenol (NTP), respectively. The photoexpansion spectra (blue circles) match well with the reference macroscopic spectra (red line). To demonstrate high spatial resolution, we used a sample with monolayer islands of poly ethylene glycol thiol (PEG) and took spectra around  $1342 \text{ cm}^{-1}$  absorption peak of PEG at a series of points, separated by 30 nm steps, along the line scan show in the topographic image

in Fig. (c) The results are shown in Fig. 2(d). Absorption peak is seen clearly on top of PEG islands while on the bare gold substrate, the spectra are flat. Chemical mapping shown in Fig. 2(e) is performed by fixing the laser wavenumber at the absorption peak and scanning with cantilever deflection signal.

To sum up, non-destructive mid-IR photoexpansion spectroscopy and imaging technique with monolayer sensitivity and better than 30 nm spatial resolution is demonstrated. We estimate that approximately 300 molecules contribute to cantilever deflection in our current experiments and spectra of as few as 30 molecules would be detectable. Future work towards extensions of this method to operation in aqueous environment will also be discussed.

The authors acknowledge the financial support from the Welch Foundation (grant No. F-1705) and the U.S. Department of Energy STTR program.

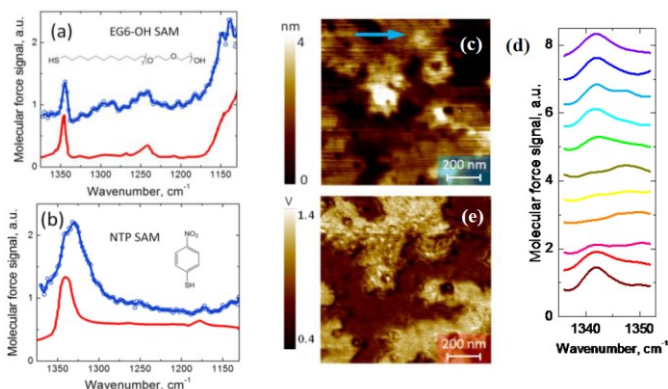


**Figure 2.** Nanoscale photoexpansion spectra (blue circles) compared to macroscopic infrared absorption-reflection spectra (red line) of (a) EG6-OH and (b) NTP. (c) AFM topography of PEG islands on gold. (d) Photoexpansion spectra taken along the blue arrow in (c) with 30 nm steps. (e) Chemical mapping of the area shown in (c).

<sup>1</sup> Dazzi, A., Prazeres, R., Glotin, F. & Ortega, J. M. (2005), “Local infrared microspectroscopy with subwavelength spatial resolution with an atomic force microscope tip used as a photothermal sensor”, *Optics Letters* 30, 2388–2390

<sup>2</sup> Lu, F., Jin, M & Belkin (2014), “Tip-enhanced infrared nanospectroscopy via molecular expansion force detection”, *Nature Photonics* 8, 307-312

# Nearfield Infrared Imaging

Monday, 10:40 - 12:00

HS1

General Information

Program

Exhibition

Author Index

10:40  
MO101-inv **Absorption Spectroscopy and Imaging from the Visible through Mid-IR with 20 nm Resolution Using AFM Probes**

Andrea Centrone

Absorption spectroscopy and mapping from visible (500 nm) through mid-IR wavelengths (16000 nm) has been achieved with spatial resolution exceeding the limit imposed by diffraction, via the photothermal induced resonance technique. Correlated vibrational (chemical), and electronic properties are obtained simultaneously with topography with a wavelength-independent resolution of 20 nm using a single laboratory-scale instrument. After presenting PTIR working principles, recent examples of PTIR characterization from my lab will include: plasmonic nanomaterials, metal organic frameworks and trihalide perovskites.

11:00  
MO102 **Recovery of Permittivity and Depth from Near-Field Data as a Step Toward Infrared Nanotomography**

A.A. Govyadinov, S. Mastel, F. Golmar, A. Chuvillin, P.S. Carney, R. Hillenbrand

The increasing complexity of nanostructured composite materials requires highly sensitive nondestructive analytical tools for nanoscale chemical identification in three dimensions (3D). Infrared near-field microscopy and spectroscopy provide high chemical sensitivity and nanoscopic spatial resolution in two dimensions, however the quantitative extraction of material properties of 3D-structured samples has not been achieved yet. Here we introduce a method and perform the first experimental demonstration of the recovery of thickness and permittivity of thin polymer films and 3D nanostructures from near-field measurements.

11:15  
MO103 **Committing SINS: Broadband Synchrotron Infrared Nano-Spectroscopy**

Hans A. Bechtel, Eric A. Muller, Rob L. Olmon, Michael C. Martin, Markus B. Raschke

By combining s-SNOM with synchrotron infrared radiation, synchrotron infrared nano-spectroscopy (SINS) enables vibrational chemical imaging, spanning the mid- and far-infrared regions with nanoscale spatial resolution. This highly powerful combination provides access to a new form of nano-chemometric analysis with the investigation of nanoscale phenomena that were previously impossible to study with IR techniques. We have installed a SINS end-station at the Advanced Light Source (ALS) at Lawrence Berkeley National Laboratory, making the s-SNOM technique widely available to non-experts.

11:30  
MO104 **Nanoscale Chemical Identification by Infrared Near-Field Spectroscopy (nano-FTIR)**

Stefan Mastel, Alexander A. Govyadinov, Thales V. A. G. de Oliveira, Iban Amenabar, Rainer Hillenbrand

Infrared near-field spectroscopy allows for vibrational spectroscopy, and therefore chemical characterization, with nanoscale resolution, beating common far-field Fourier Transform infrared (FTIR) spectroscopy techniques by about three orders of magnitude. In this study, we establish a solid basis for the interpretation of infrared near-field phase and absorption spectra, both quantities signifying absorption in near-field spectroscopy. Furthermore, we provide guidelines for their straightforward comparison with standard FTIR data, thus enabling infrared characterization and chemical identification of organic samples on the nanometer scale.

11:45  
MO105 **Developments in Mid-Infrared Nanoscopy Instrumentation**

Georg Ramer, Anna Balbekova, Andreas Schwaighofer, Bernhard Lendl

We present our latest results on resonance enhanced atomic force microscopy infrared nanoscopy (RE-AFMIR): the development of a time-resolved RE-AFMIR technique for analyzing spectral changes at nano-scale spatial resolution and an investigation of methods for tracking the contact resonance in RE-AFMIR systems.

10:40 **Orientation and Disentanglement in Electrospun Polystyrene Fibers Using**  
MO501-inv **Vibrational Spectroscopy**

Christian Pellerin, Marie Richard-Lacroix

Electrospun fibers show unusual properties that are poorly understood, such as an exponential increase of their modulus with a decreasing diameter. Here, we demonstrate partial disentanglement in polystyrene fibers using IR spectroscopy. We further show by Raman spectroscopy that disentanglement and molecular orientation are also correlated with fiber diameter. Our results help understanding the properties of electrospun fibers.

11:00 **Different Types of Polaronic Absorptions in Organic Conjugated Polymers Induced**  
MO502 **by Distinct Doping Techniques**

Sandra Engl, Christina Engl, Marek Havlicek, Markus C. Scharber, Helmut Neugebauer, Kurt Hingerl, Eitan Ehrenfreund, Niyazi S. Sariciftci

In this work we focus on in situ doping techniques of the organic conjugated polymer poly(3-hexylthiophene-2,5-diyl) (P3HT). In these experiments a broad absorption band arises in the infrared range with a shift in the absorption maximum due to higher oxidation potentials. At the beginning of the oxidation new infrared active vibration (IRAV) modes appear which hardly change as the oxidation proceeds. Additionally, we connect these data with in situ UV-VIS, cyclic voltammogram and electron paramagnetic resonance (EPR) measurements.

11:15 **The Effect of Chain Length and Non-Covalent Interactions on Blending of Polymers**

MO503 Adriana Šturcová, Jaroslav Kratochvíl, Jiří Dybal, Antonín Sikora

An inter-polymer complex and a soluble blend of two polymers were prepared in one solution as a result of fractionation. Although FTIR spectroscopy and DFT calculations showed two types of H-bonds, the usual assumption that complex has ladder-like co-operating hydrogen-bond network, while blends have loose and random hydrogen bonds was not confirmed. It was concluded that fractionation did not precede complex formation, but was its integral part. It was also suggested that the thermodynamic quality of solvent changed upon complexation.

11:30 **Polymer Hydration in Poly(2-(2-methoxyethoxy)ethyl Methacrylate Hydrogels Differ**  
MO504 **on Network Architecture**

Marcin Kozanecki, Magdalena N. Olejniczak, Jakub Saramak

An influence of the architecture of poly(2-(2-methoxyethoxy)ethyl methacrylate (PMEOMA) network on its hydration is discussed. The Raman spectroscopy showed that the hydration shell around PMEOMA chains contains  $11 \pm 1$  H<sub>2</sub>O molecules/mer unit. An accessibility of C=O groups to water is lower in the cross-linked systems than in linear chain. The number of water molecules influencing the vibrational dynamics of single carbonyl group depends on network architecture. This work was supported by the project: 2013/09/B/ST4/03010 (Polish National Science Centre).

11:45 **Characterization of a Polyethylene - Polyamide Multilayer Film Using Nanoscale**  
MO505 **Infrared Spectroscopy and Imaging**

Curtis Marcott, Mauritz Kelchermans, Michael Lo, Eoghan Dillon, Craig Prater, Kevin Kjoller

Atomic force microscopy (AFM) and infrared (IR) spectroscopy have been combined in a single instrument (AFM-IR) capable of producing IR spectra and absorption images at sub-micrometer spatial resolution. This new device enables cross sections of multilayer films to be spectroscopically characterized at levels not previously possible. In particular, it was possible to observe nanoscale IR spectroscopic differences, as well as thermal and mechanical property differences, in the tie layers located between the individual polyethylene and polyamide layers of a multilayer film of unknown structure. It also appears that a two- $\mu\text{m}$ -thick barrier layer between two polyamide layers near the center of the multilayer film consist of an ethylene (vinyl alcohol) copolymer. Mechanical stiffness and thermal property differences are also observed between the various layers in the film. This powerful capability should prove generally useful for reverse engineering complex unknown multilayer film materials, as well as in aiding the intelligent design of superior multilayer film materials.

10:40 **Medical Raman Spectroscopy**

MO601-inv Juergen Popp

A comprehensive analysis to determine diagnostic, prognostic and predictive factors in a few steps requires the development of new, fast and reliable approaches that support and supplement routine medical diagnostics and therapy. In the past years, Raman spectroscopic approaches have shown their potential to meet these aforementioned challenges. In this contribution, we will summarize our recent results in implementing various Raman-approaches for infectious diseases and cancer, as these types of diseases harbor unmet needs regarding diagnosis and therapy.

11:00 **The Latest Developments and Applications of Spatially Offset Raman Spectroscopy (SORS) and Transmission Raman**

MO602

Benjamin Gardner, Martha Z. Vardaki, Pavel Matousek, Nick Stone

The deep Raman techniques, which include spatially offset Raman spectroscopy (SORS) and transmission Raman allow the collection of molecular signals at depth in a sample. Whereas, conventional Raman spectroscopy is confined to molecular signals at the sample surface. We present here a study of the distribution of deep Raman signals in liquid tissue phantoms, as well as accompanying Monte Carlo (MC) simulation of light propagation. We also present exciting new developments in the application of SORS.

11:15 **Bio-Accumulation of TiO<sub>2</sub> Nanoparticles in *Caenorhabditis Elegans*: an In-Vivo Model for Toxicity Analysis**

MO603

Luca Iannarelli, Andrea Mario Giovannozzi, Luisa Mandrile, Paolo Bigini, Luisa Diomede, Valter Maurino, Letizia Pellutiè, Gianmario Martra, Vasile-Dan Hodoroaba, Erik Ortel, Andrea Mario Rossi

In order to provide robust metrology tools in toxicity analysis, the bio-accumulation of TiO<sub>2</sub> NPs with known shape and composition (Pure Anatase structure) was evaluated in *C. Elegans* worm model organism. *C. Elegans* specimen were fed with three different types of TiO<sub>2</sub> NPs. Preliminary results regarding localization of TiO<sub>2</sub> NPs using Raman imaging technique are presented as well as a confocal depth profile aimed at 3D characterization of TiO<sub>2</sub> agglomerats detected along the digestive system of the worm.

11:30 **Study of Tissue Repair after Surgical Trauma by Raman Microscopy**

MO604

Otávio M. Gil, Michele A. Rocha, Vera R. L. Constantino, Ivan H. J. Koh, Dalva L. A. de Faria

Raman microscopy was used for temporal analysis of inflammatory response of muscle tissue after surgical implantation of a lamellar inorganic material in comparison to the natural processes caused only by the surgical trauma. Through the spectral signatures it was possible to discriminate the biological responses from different periods, identifying important components that restore the physiological functionality to the repaired tissue. The results here reported demonstrated that Raman spectroscopy stands as one of the most powerful techniques in studies of biocompatibility/biointegration.

11:45 **Raman Spectroscopy as a Tool for Bioanalytical Characterisation of Biopharmaceuticals**

MO605

Lorna Ashton, Katherine A. Hollywood, Roy Goodacre

Raman spectroscopy offers vast potential for bioanalytical characterisation at every stage of the biomanufacturing process from protein engineering to protein production to formulation. We have successfully applied Raman Spectroscopy to two of these stages: protein engineering and single cell drug uptake. We have characterised temperature-induced aggregation in antibody variants with differing propensity to aggregate using 2D correlation analysis and by placing a specialized cell incubator within the chamber of the Raman microscope we have monitored drug distribution in live cells.

10:40 MO801-inv **On-site Non-invasive Investigation of Polychrome Decorations Using Raman Spectroscopy: Achievements and Limitations**

María José Ayora-Cañada, María José de la Torre López, Ramón Rubio Domene, Ana Domínguez Vidal

Possibilities and limitations of portable Raman Spectroscopy were explored in the study of the paintings of the stalactite ceilings in the Alhambra. The on-site approach allowed the identification of many pigments and different degradation processes with high representativeness and no damage. Complementary measurements on micro-samples with conventional laboratory instrumentation provided higher sensitivity and spatial resolution allowing the investigation of the stratigraphy. The use of different lasers was relevant for identification of green pigments and their degradation products.

11:00 MO802 **Raman Line Scanner for Automated Explosive Detection on Hand Luggage and Spatially Offset Raman Spectroscopy (SORS) for Threat Detection**

Bernhard Zachhuber, Martin Glimtoft, Mattias Svanqvist, Ola Norberg, Niklas Johansson, Matilda Ågren, Anders Elfving, Henric Östmark

A Raman line scan system for the identification of explosive particles was developed for the analysis of particles on hand luggage. This fully automated system was integrated in the housing of an x-ray scanner common on airports. The autofocus of the system allows single-shot analysis on the luggage as it passes the setup on a conveyor belt. Furthermore, the system was adapted to determine the content in containers which are non-transparent to the human eye, using Spatial Offset Raman Spectroscopy.

11:15 MO803 **On the Quantification of Caffeine, the Major Impurity in Legal-High Stimulants, Using Handheld Raman Spectroscopy and Partial Least Square Regression**

Sulaf Assi, Stuart Preston, David Osselton

Legal-highs represent a major public health threat due to their unpredicted toxicity. This work aims at quantifying caffeine (the major stimulant in legal-high stimulants) using Raman spectroscopy and partial least square regression (PLSR). Three PLSR models were constructed from binary mixtures prepared by diluting caffeine with 2-aminoindan, lidocaine and mephedrone. The models showed acceptable accuracy for powder mixtures. However, when legal high products were predicted, they showed accuracy of 16% which highlights the needs for further work to improve quantification.

11:30 MO804 **Hand Held Off-Axis Raman Spectroscopy for Process Analysis**

Keith Carron

The most common collection geometry for Raman spectroscopy is 180 degrees backscattering collection. This collection geometry overcomes tedious alignment of off-axis excitation and collection. The key to understanding off-axis collection is the spatial filter. A handheld Raman instrument with Off-Axis Raman Scattering (OARS) can easily see into chemical containers to eliminate wasteful, time consuming sampling inside the container. This can be particularly useful to eliminate the handling of hazardous materials.

11:45 MO805 **BRAVO – Advances in Handheld Raman Spectroscopy**

Felix Fromm, Armin Gembus

With BRAVO Bruker introduced a new handheld Raman spectrometer dedicated for material verification. BRAVO overcomes current limitations of handheld Raman spectrometers combining latest technologies as Sequentially Shifted Excitation (SSE TM) and Duo LASER TM for an efficient fluorescence mitigation and the highest sensitivity throughout a large spectral range. This work demonstrates the advances in performance of this next-generation instrument which constitutes new possibilities for handheld Raman spectroscopy.

13:30 **Infrared Spectroscopy in 3D and Nano Scales**

MO106-inv Michael Martin, Hans Bechtel, Dilworth Parkinson, Michael Nasse, Carol Hirschmugl, Eric Muller, Robert Olman, Markus Raschke

Synchrotron infrared beamlines use the diffraction-limited beam properties to enable a variety of cutting edge science at the micron length scale in both reflection and transmission. In this talk, I will explore how can we go further? I will describe two new techniques we have recently developed and demonstrated: 3D FTIR Tomography and Synchrotron Infrared Nano-Spectroscopy.

13:50 **Biochemistry in Single Cells Seen by Infrared Microscopy: From the Study of Molecular Distribution to the Imaging of Metabolic Networks**

MO107

Luca Quaroni

We demonstrate the use of infrared microscopy to characterize the glycolytic network of cancer cells, including detection of relevant metabolites, assignment of sequence of events and measurement of rates of formation. We achieve this objective by providing a protocol to improve the reliability of band assignments in complex reacting systems. We extend the application to the two-dimensional case by describing the spatial distribution of metabolite formation in single cells and cell clusters.

14:05 **Material Contrasts of Layered Phase Change Materials in Infrared s-SNOM**

MO108

Martin Lewin, Benedikt Hauer, Manuel Bornhöfft, Lena Jung, Ann-Katrin U. Michel, Joachim Mayer, Thomas Taubner

We investigate the material contrasts of layered phase change materials using scattering-type scanning near-field optical microscopy. We apply infrared light to address the strong drude contribution of AgInSbTe in the crystalline phase compared to the amorphous phase. By performing correlative TEM studies we could show that it is possible to distinguish both phases even below 100 nm of capping layer. The found complex material contrasts are explained by theoretical calculations taking into account the layered structure of the sample.

14:20 **Laser Based Mid-Infrared Spectroscopic Imaging for Biomedical Research and Clinical Diagnostics**

MO109

Jeremy Rowlette, Miles Weida, Edeline Fotheringham, Matt Barre, David Arnone, Benjamin Bird

Mid-infrared spectroscopic imaging of cells, tissue and biofluids is now a mature science with a wealth of evidence to support its adoption as an adjunctive tool for clinical research and diagnostics. However, instrumentation that provide increased sample throughput, improved image quality, a small footprint, low maintenance, and require minimal expertise are essential for translation. The advent and commercialisation of Quantum Cascade Lasers has allowed the development of new discrete frequency based microscopes that can markedly accelerate IR based spectral pathology.

14:35 **High Spatial Resolution FTIR Imaging of Biomedical Tissue Samples Using a Novel Method of Magnification Enhancement**

MO110

Andreas Kerstan, Mustafa Kansiz, Carol Hirschmugl, Benedict Albensi, Catherine Liao, Kathleen Gough

The Fourier Transform Infrared (FTIR) imaging is a well-established analytical method for obtaining spectral and spatial information simultaneously in the micron-size domain. The technique has been applied across many different application areas, from polymer science to biomedical imaging. Over recent years, interest has increased in pushing the diffraction limited spatial resolution performance of FTIR imaging systems, primarily using synchrotron based systems. In this application note, we present a novel method of magnification enhancement achieved using existing objectives. The result is an FTIR system with high spatial resolution imaging capabilities in the order of  $1 \mu\text{m}/\text{pixel}$ . Uniquely, this configuration conserves the relatively large working distance of regular objectives (21 mm) by not requiring an objective change between magnification settings.

13:30 **Low-Frequency Raman Spectroscopy as a Probe of Order: From Pharmaceuticals to Organic Solar Cells**

MO506-inv

Keith Gordon

The low frequency region of the vibrational spectrum contains a number of interesting spectral features. These include transitions associated with phonon and torsional modes. Phonon modes can be a powerful way to detect crystallization in materials such as amorphous drugs. Torsional and phonon modes can also be used to probe order in plastics such as organic photovoltaic (OPV) cells. We have investigated both types of process with griseofulvin and polythiophene respectively.

13:50 **Orientation Quantification by Confocal Raman Spectroscopy: Improved Methodology and Applications**

MO507

Marie Richard-Lacroix, Christian Pellerin

Molecular orientation profoundly affects most physical properties of polymers but it is often challenging to characterize properly. In this presentation, we first describe our original Raman quantification approach called the 'most probable distribution' (MPD) method. We show that it simplifies the experimental measurement of orientation while improving the accuracy of the results. We then demonstrate its application to more challenging samples, electrospun nanofibers, by studying the impact of electrospinning parameters and the effect of the diameter on their orientation.

14:05 **Regularity Modes in Ethylene and Propylene Copolymers: the Comonomer Content and Temperature Dependences**

MO508

Gulnara Nikolaeva, Kirill Prokhorov, Elena Sagitova, Yury Zavgorodnev, Pavel Pashinin, Polina Nedorezova, Alla Klyamkina, Tatiana Ushakova, Lyudmila Novokshonova, Elena Starchak

In this work, we investigate the behavior of the regularity modes of isotactic polypropylene and polyethylene in the Raman spectra of the neat polymers and of a wide range of recently synthesized random copolymers of propylene or ethylene with olefins. The dependence on both the content and chemical structure of the incorporated monomer as well as on the temperature is analyzed in detail. The comparison with model substances such as n-alkanes and alkylammonium salts is also presented.

14:20 **Investigation of Carbon Dioxide Sorption in Poly(Methyl Methacrylate) Plate by In-Situ Near-Infrared Spectroscopy and FT-IR Imaging**

MO509

Yuta Hikima, Koji Hamada, Masahiro Ohshima

Carbon dioxide (CO<sub>2</sub>) sorption in a poly(methyl methacrylate) (PMMA) plate was investigated by near-infrared spectroscopy (NIR). We found that the appearance of absorption band during CO<sub>2</sub> sorption at isothermal and isobaric conditions, and calculated CO<sub>2</sub> sorption curve in a PMMA plate from this band intensity. CO<sub>2</sub> concentration distributions along the thickness direction in PMMA plates after the sorption were investigated using FT-IR imaging. The CO<sub>2</sub> diffusion front was formed and propagated to the center on the early stage of sorption.

14:35 **The Stratified Dipole-Arrays (SDA) Model Toward Unified Understanding of Bulk Properties of Perfluoroalkyl Compounds Studied by Infrared Spectroscopy**

MO510

Takeshi Hasegawa, Takafumi Shimoaka, Yuki Tanaka, Nobutaka Shioya, Kohei Morita, Masashi Sonoyama, Toshiyuki Takagi, Toshiyuki Kanamori

To reveal the intrinsic chemical property of a perfluoroalkyl compound, a new chemical model is proposed, which is examined by infrared spectroscopy using some model compounds. When the Rf length is (CF<sub>2</sub>)<sub>n</sub>, or longer, the molecules would spontaneously be aggregated to exhibit a Rf-specific character such as water repellency.

13:30 **Selective-sampling Raman Micro-spectroscopy for Tissue Diagnosis**

MO606-inv Ioan Notingher, Kenny Kong, Christopher Rowlands, Faris Sinjab

The problem of establishing an optimal sampling strategy that would ensure accurate estimation of the characteristic of interest is not new to Raman micro-spectroscopy, but it has been encountered in industry, politics, etc: detect reservoirs of oil or ore, estimation the number of animals in certain parts of the globe, election surveys, etc. We will present examples of using Raman micro-spectroscopy based on the adaptive cluster sampling, stratified sampling and multiplex Raman microscopy to diagnose large tissue specimens within minutes.

13:50 **Combined Fiber Probe for Fluorescence Lifetime and Raman Spectroscopy**

MO607 Sebastian Dochow, Dinglong Ma, Ines Latka, Thomas Bocklitz, Brad Hartl, Julien Bec, Sebastian Wachsmann-Hogiu, Michael Schmitt, Laura Marcu, Jürgen Popp

In this presentation a combined fiber probe for Raman spectroscopy and fluorescence lifetime imaging will be presented. The full characterization of the probe, its validation on tissue samples and finally in vivo spectra of a rat's brain are presented.

14:05 **Fluorescence-Raman Dual-Modal Endomicroscopic System for in Vivo Real-Time Multiplexed Molecular Diagnosis**

MO608 Sinyoung Jeong, Yong-il Kim, Homan Kang, Gunsung Kim, Myeong Geun Cha, Hyejin Chang, Yoon-Sik Lee, Dong Soo Lee, Dae Hong Jeong

We developed the fluorescence-Raman endomicroscopic system (FRES) for multiplexed molecular diagnosis with fluorescence-SERS active nanoprobes (F-SERS dots) based on optical fiber bundle probe; it can simultaneously detect the fluorescence and Raman signal using optical fiber bundle. To demonstrate the feasibility of this system for molecular imaging based diagnosis, in vivo and intraoperative targeting in a xenograft tumor model bearing mouse were investigated; it showed that this system can be applied for real-time in vivo molecular diagnosis during clinical endoscopic examinations.

14:20 **Prediction of Poor Prognosis of Targeted Cancer Therapy by Label-free Raman Imaging**

MO609 Samir El-Mashtoly, Hesham Yosef, Laven Mavarani, Dennis Petersen, Carsten Kötting, Klaus Gerwert

Mutational acquired resistance is a major challenge in cancer therapy. Somatic tumors harbouring oncogenic mutations are characterized by poor prognosis and high rate of mortality. In the present study, Raman spectral imaging as an in vitro method is used to emphasize the oncogenic mutation resistance to targeted therapy such as panitumumab and erlotinib. Furthermore, the distribution and metabolism of erlotinib in colon cancer cells is monitored through its strong  $C\equiv C$  stretching vibration at  $2110\text{ cm}^{-1}$ .

14:35 **Studying the Effects of UV Radiation on Human Skin by *In Vivo* Confocal Raman Spectroscopy**

MO610 Alessia Quatela, Ali Tfayli, Lynda Miloudi, Arlette Baillet-Guffroy

We present the effects of UVA and UVB exposure in suberythemal doses and over a relatively short period of time. Twenty females volunteers aged 20–30 years (mean 25 years) with healthy skin were enrolled in the study. Fast in vivo measurements of SC response to UV irradiation were performed by means of a confocal Raman optical microprobe. TEWL, corneometry and temperature measurements were carried out after irradiation and together with Raman sessions, they were held five times weekly.

13:30 **Vibrational Spectroscopy of Southern Ocean Phytoplankton: A New Tool for Understanding Drivers of Primary Productivity**

MO806-inv

Philip Heraud, Olivia Sackett, John Beardall, Katherina Petrou

Each year, marine phytoplankton convert ~50 Tg of inorganic carbon into biomass. Estimations of this oceanic primary productivity are crude lacking definition in quantifying species composition within phytoplankton blooms nor defining the physiological status of different species and how this affects carbon uptake. Infrared spectroscopy is a powerful new tool in this research area having potential for both species identification and characterisation of physiological responses of phytoplankton to the environment in terms of carbon partitioning at the single cell level.

13:50 **Infrared Extinction Spectra of Polar Stratospheric Cloud Constituents: Variation of Particle Phase and Shape with Formation Conditions**

MO807

Robert Wagner, Martin Ebert, Sandy James, Ottmar Möhler, Martin Schnaiter, Ralf Weigel

The homogeneous and heterogeneous nucleation of solid NAX (e.g. NAD = Nitric Acid Dihydrate or NAT = Nitric Acid Trihydrate) particles from supercooled aqueous  $\text{HNO}_3/\text{H}_2\text{O}$  solution droplets at simulated stratospheric conditions was investigated by experiments conducted in the low-temperature aerosol chamber facility AIDA (Aerosol Interactions and Dynamics in the Atmosphere) of the Karlsruhe Institute of Technology. In situ infrared extinction spectroscopy was used to infer the chemical identity and the shape of the nucleated particles.

14:05 **Studies on the Photolysis of Iodate Salts**

MO808-inv

Oscar Galvez, Alfonso Saiz-Lopez

The photolysis of atmospherically relevant frozen iodate salt has been studied experimentally using FTIR spectroscopy. The samples were generated at low temperatures in presence of different amounts of water. The mid-IR spectra have confirmed that under near-UV/Vis radiation iodate is photolyzed. In this work, we have estimated the integrated mid-IR absorption coefficient and the integrated absorption cross section at wavelengths relevant for tropospheric studies for of iodate anion in an ammonium frozen salt. The photolysis of iodate could be an impact in the budget of reactive iodine species in the atmosphere.

14:20 **Raman Spectroscopic Techniques for Planetary Exploration: Detecting Microorganisms Through Minerals**

MO809

Mattheus Verkaaik, Jan-Hein Hooijschuur, Gareth Davies, Freek Ariese

Raman spectroscopy may play a significant role in interplanetary missions, especially for searching life elsewhere in our Solar System. A major challenge will be the unambiguous detection of low levels of biomarkers hidden behind scattering minerals. Here we report the detection of carotenoid-containing microorganisms behind mineral layers using time resolved Raman spectroscopy. The picosecond laser pulses and gated intensified CCD camera provide depth selectivity for the subsurface microorganisms over the mineral surface layer, and also lower the fluorescent background.

14:35 **Noble Metal Nanoparticles in Seawater: Nano Risk Towards Aquatic Organisms Assessed by SERS**

MO810

Simona Cinta Pinzaru, Csilla Müller, Sanja Tomšić, Ivana Ujević, Ana Bratoš Cetinić, Bogdan I. Cozar, Rares Stiuftuc, Monica M. Venter, Branko Glamuzina

Oligotrophic seawater has been assessed concerning the SERS response in the presence of noble metal nanoparticles prepared by various methods. Several examples of SERS signal collected from individual plankton cells are correlated with the overall response of raw seawater revealing the natural defense against nano risk.

## Nearfield Infrared Imaging (commercial)

Monday, 15:20 - 16:05  
Chair: Mikahil Belkin

HS1

15:20  
MO111

### **Nano-FTIR: Imaging and Spectroscopy with 10 nm Spatial Resolution** Miriam Boehmler

The power of Neaspec's near-field optical microscopy and spectroscopy systems (NeaSNOM) to overcome the diffraction limit of light is presented, enabling optical measurements at a spatial resolution of 10nm at vis, IR and THz frequencies. Examples of (i) nanoscale vis, IR, and THz imaging, (ii) nano-FTIR spectroscopy, (iii) THz-TDS nanoscopy, and (iv) time-resolved experiments, enabled by the nano-FTIR NeaSNOM systems, are given. Inorganic, organic and metallic samples can be studied, providing insight to structural, electrical and chemical properties.

15:35  
MO112

### **Nano-Chemical and Nano-Mechanical Imaging of Proteins Using a Novel Combination of Peak-Force Tapping/Near-Field s-SNOM Microscopy** Martin Wagner, Karina Carneiro, Stefan Habelitz, Thomas Mueller

In our paper we investigate the spatial distribution of phosphate in amelogenin protein nanoribbons of a few nanometer height with <20 nm spatial resolution using scattering-type scanning near-field microscopy (s-SNOM) at infrared frequencies. In our novel instrument we combine s-SNOM with peak-force tapping which allows us to extract not only near-field optical information, but also the mechanical properties, in this case in order to study nanocrystal formation in the protein sample.

15:50  
MO113

### **High Speed Infrared Nanospectroscopy with Sub-Monolayer Sensitivity** Craig Prater, Eoghan Dillon, Qichi Hu, Honghua Yang, Curtis Marcott, Feng Lu, Mingzhou Jin, Mikhail Belkin, Kevin Kjoller

This presentation will focus on recent innovations in atomic-force microscope based infrared spectroscopy (AFM-IR), a technique that provides chemical spectroscopy and imaging with nanoscale spatial resolution. Recent innovations that have resulted in dramatic improvements in measurement speed, sensitivity and range of applicable samples. Sub-monolayer sensitivity has been demonstrated on biological membranes and self-assembled monolayers. Interpretable IR absorption spectra from nanoscale regions of a sample can also now be obtained in times as short as a few seconds.

15:15  
MO511 **Resonance Raman Based Cytochrome C Biosensor as a Tool for the Evaluation of the Redox Properties of Carbonaceous Particles**

Giuseppe Zerbi, Andrea Lucotti, Maurizio Gualtieri, Marina Camatini

The danger to human health by inhaled PM (particulate matter) and diesel exhaust particles (DEP) is at present a hot issue worldwide. The redox properties of carbonaceous particles can be probed exploiting the sensitivity to superoxide formation by Cytochrome C. We have developed a Cytochrome C based biosensor based on Resonance Raman Spectroscopy. Particles from PM to nanocarbon through ball milled graphites have been studied. The measured reaction kinetics reveal relevant new information.

15:35  
MO512 **DSC and Raman Study of Phase Transitions in Diphenylalanine Nanotubes**

Pavel Zelenovskiy, Anton Davydov, Semen Vasilev, Alla Nuraeva, Kate Ryan, Alexander Krylov, Maciej Wojtas, Vladimir Shur, Andrei Kholkin

Low and high temperature phase transitions occurred in diphenylalanine nanotubes are investigated by differential scanning calorimetry (DSC) and Raman spectroscopy. The role of water molecules in those low temperature transitions is discussed.

15:50  
MO513 **Helical Structures of Collagen: Relative Stability of Triple and Single Helix Forms Characterized by Vibrational Spectroscopy**

Karl Jalkanen, Michaela Knapp-Mohammady, Kasper Olsen, Jakob Bohr

In this work we present our work on the structure, stability and properties of two helical forms of collagen as modelled by 3.(PPC)<sub>n</sub> mimetics. The structures, relative stabilities, vibrational absorption (VA), vibrational circular dichroism (VCD), Raman scattering, and Raman optical activity (ROA) spectra are all presented. Conformers stabilized in the triple helix are investigated as single chains and the mechanisms of triple helix formation are investigated. Finally the properties of collagen and collagen composites with hydroxyapatite are investigated.

16:05  
MO514 **Investigation of Molecular Structure and Orientation in Thin Films and Electrospun Nanofibers of Poly[(R)-3-hydroxybutyrate-co-(R)-3-hydroxyhexanoate] (PHBHx) Using AFM-IR Spectroscopy and Imaging Techniques**

John Rabolt, Liang Gong, Bruce Chase, Isao Noda, C.J. McBrin, Curt Marcott

The combination of atomic force microscopy (AFM) and infrared (IR) spectroscopy is a powerful tool that provides chemical, conformational and molecular orientation information at a spatial resolution of 50-100 nm. Using an AFM-IR instrument, we have explored the correlation between structure, processing and chain orientation/crystallinity and tested the hypothesis that improved chain orientation in electrospun nanofibers can increase modulus and tenacity even while crystallinity is disrupted by appropriate addition of longer side-chain comonomer compositions. Nanofibers and films of poly[(R)-3-hydroxybutyrate-co-(R)-3-hydroxyhexanoate] (PHBHx) have been produced with a wide range of crystallinity and molecular orientation. They have been characterized using polarized AFM-IR spectroscopy and imaging in order to assess the role of processing on orientation and morphology.

15:15  
MO611-inv **The Use of 2D IR Correlation Spectroscopy in Fragment Based Drug Design and the Identification of Novel Protein-Targets**

Belinda Pastrana-Rios

Centrin-targets have been identified by yeast-two-hybrid assays. Our group has confirmed the interaction of a novel centrin-Prp40A complex. Herein we provide the thermodynamic parameters governing the binding by isothermal titration calorimetry (ITC), its relative dependence on calcium binding affinity and the molecular events that describe complex formation via 2D IR correlation spectroscopy. To our knowledge this is the first time protein-protein interactions (PPI's) have been confirmed in vitro using a unique combination of molecular biophysical techniques such as the one presented.

15:35  
MO612 **Early Detection of Colorectal Cancer Relapse Using Infrared Spectroscopy in Morphologically Normal Anastomosis**

Shaul Mordechai, Ahmad Salman, Gilbert Sebbag, Shmuel Argov, Ranjit Sahu

The potential of infrared spectroscopy in tandem with multivariate analysis PCA-LDA was evaluated to detect and predict whether a patient who undergoes a colonic surgery will experience colorectal cancer recurrence or not. This was done by classifying different crypts measured from longitudinal section obtained from patients into three categories: control, local recurrence, and distant recurrence, based on their IR absorption spectra. Our classification results were eventually compared with the patients' medical files yielding 92% success rate.

15:50  
MO613 **Lipid Droplets: A Raman Signature of Colorectal Cancer Stem Cells**

Carlo Liberale, Luca Tirinato, Simone Di Franco, Vijayakumar Rajamanickam, Jan Paul Medema, Matilde Todaro, Giorgio Stassi, Enzo Di Fabrizio, Patrizio Candeloro

The identification of Cancer Stem Cells (CSCs) in solid tumors has been of paramount importance for cancer eradication as their known chemo- and radio-resistance, and recurrence after therapy. We have shown that Lipid Droplets (LDs) are a distinctive feature of Colorectal CSCs using Raman micro-spectroscopy. In addition, with an *in vivo* tumorigenic assay, we have demonstrated that the Colorectal CSC subpopulation with higher LD content is endowed with the highest tumorigenic potential.

16:05  
MO614 **Multimodal Raman Imaging and a Comparison of Scanning vs Non-Scanning Approaches for Spectral Discrimination of Immune Cells**

Nicholas Smith, Nicolas Pavillon, Alison Hobro

One important application of Raman analysis is the discrimination of cell types. This presentation will discuss our multimodal Raman/phase imaging for cellular analysis. Additionally, the demonstration of a new scanning approach which can be employed when full Raman imaging is not required, results in the improvement of signal to noise and discrimination capabilities. The ability to use the quantitative phase information to guide the Raman targeting areas leads to the possibilities of full automation and high throughput.

15:20  
MO811 **New Generation Raman Imaging: Confocal 3D Raman Imaging Meets Highest Spectral Resolution**

Thomas Dieing, Ute Schmidt, Wolfram Ibach, Olaf Hollricher

In the past decade confocal Raman imaging gained in importance in the characterization of heterogeneous materials. Until recently the acquisition of highest lateral resolution 3D Raman images was limited by the computer memory and data acquisition routines. For high spectral resolution only long focal length spectrographs with low light throughput were available. The aim of this contribution is to present the newest achievements in confocal Raman imaging microscopy. The highlights will be cosigned with examples from various fields of applications.

15:35  
MO812 **Fast, Quantitative Analysis of Large Volume Bulk Mixtures Using Transmission Raman Spectroscopy**

Philippa Law, Tim Smith, David Reece

The uniformity of powder blends has become increasingly important in regulating manufacturing processes. Transmission Raman spectroscopy (TRS) presents significant benefits over the more common backscattered Raman Spectroscopy by providing an average through the entire sample depth, offering fast and effective analysis of content uniformity. In this work, we introduce a novel technique utilising TRS and mapping for the analysis of bulk mixtures far larger than conventional TRS configurations. Multivariate analysis is used to produce a chemical image revealing mixture distribution.

15:50  
MO813 **Structural Analysis of Conjugated Aromatic Compounds Using Low Frequency Raman Spectroscopy**

James Carriere, Anjan Roy, Randy Heyler, Peter Larkin

To better understand the relationship between a material's physical structure and its low vibrational energy modes, we analyzed the polycyclic aromatic hydrocarbon family of materials containing compounds such as Naphthalene, Biphenyl and Anthracene. With increasing molecular complexity, the corresponding measured peak positions for each material are compared with the crystalline structure parameters of the organic molecular crystals and theoretical calculations from the literature. We then differentiate the bands which derive from molecular vibrations and crystalline lattice vibrations and identify trends.

16:05  
MO814 **New Electrically Gated Raman Technique for Fast Mineralogical Analyses**

Mari Tenhunen, Lauri Kurki, Jyrki Savela

Conventional Raman measurements often face the difficulty of fluorescence, which can cover totally the Raman signal. In this presentation, we show the power of new electrically gated Raman spectroscopic technique based on pulsed laser excitation and new SPAD array detector to catch the Raman signal before the fluorescence within a "timegate" of 100 picoseconds. With this technique the Raman signal can be differentiated perfectly from the fluorescence effect, and therefore it is an ideal tool e.g. for fast mineralogical analyses.

## Microspectroscopy & Imaging

- A001 **Three-Dimensional Mid-Infrared Tomographic Imaging of Endogenous and Exogenous Molecules in Intact Cells with Subcellular Resolution**  
Luca Quaroni, Martin Obst, Marcus Nowak, Fabio Zobi  
 We provide a method that allows 3D visualization of subcellular components in a vegetable cell by using tilt-series infrared tomography with a standard benchtop infrared microscope. This approach gives access to the quantitative 3D distribution of molecular components based on the intrinsic contrast provided by the sample. We demonstrate the method by quantifying the distribution of endogenous and exogenous molecules throughout the cell.
- A002 **Ultrafast Confocal and Rayleigh Imaging**  
Sergej Shashkov  
 Some capabilities of ultrafast Raman mapping mode with PMT and a galvanic mirror scanner have been shown. The time of acquisition of each pixel of the image is only 3  $\mu$ s, and the total time for 1000x1000 pixels Raman image may be 3 sec only.
- A003 **Preventing Oil Contamination During Immersion Confocal Raman Microscopy**  
Harald Fitzek, Christian Lembacher, Boril Chernev  
 Oil immersion is necessary for accurate depth profiles using Raman spectroscopy, but the sample contamination by the oil can be an issue. Sample contamination can be prevented by applying a protective film to the sample. We are looking for the best approach to thoroughly apply the protective film and the best film to keep the sample dry when using oil immersion in confocal Raman microscopy.
- A004 **Analysis of Glutamic Acid/Lysine Mixture by Using TLC/FTIR Technique**  
Ye Jiang, Xiaoyan Kang, Yanjun Zhai, Anqi He, Yizhuang Xu, Isao Noda, Jianguang Wu  
 We applied TLC/FTIR coupled with mapping technique to analyze a glutamic acid /lysine mixture. Narrow band TLC plates by using AgI as a stationary phase were used to separate the mixture. Glutamic acid and lysine are successfully separated and the separated glutamic acid and lysine spots can be observed on the 3D chromatogram. Additionally, FTIR spectra of the separated glutamic acid and lysine spots on the narrow band TLC plate are roughly the same as the corresponding reference IR spectra.
- A005 **Polarized Microscopic FT-IR for Molecular Orientation of Chiral Nematic Liquid Crystal**  
Masanori Matsumura, Norihisa Katayama  
 Polarized microscopic FT-IR spectroscopy has been applied for characterization on molecular orientation change in phase transition of chiral nematic liquid crystal (NLC). The band intensity changes of obtained spectra suggest that the helical axis of chiral NLC is inline with respect to the parallel direction on cooling process whereas that had been vertical to substrate before heating.

- A006 **High-Speed Line-Focus Raman Microscopy with MCR-ALS and Decomposition Analysis**  
Oleksii Ilchenko, Yuriy Pilgun, Roman Slipets, Andrii Kutsyk, Denis Slobodianiuk, Andrii Reint, Oleksandr Kolada, Dmitrii Krasnenkov

In order to save the laser power and obtain homogeneous laser power distribution throughout the line in line-focus mode we designed Raman microscope with laser line generator or Powell lens. Quantitative information about spectral and concentration profiles of components was obtained from Raman map using hybrid technique of decomposition via library spectra and MCR-ALS analysis. Described method was realized in Raman line-focus microscope for investigating different types of temperature sensitive biological samples.

- A007 **Comparing HSI-NIR and ATR HSI Mid Infrared for Black Pens Discrimination and Document Forgery Identification**  
José Pereira, Carolina Silva, Fernanda Pimentel, Ricardo Honorato, Celio Pasquini, Peter Wentzell

Middle and near Infrared hyperspectral image and multivariate exploratory analysis are used to evaluate if simulated forged document was produced with different black pens. Two different unsupervised pattern recognition techniques (Principal Component Analysis – PCA and Projection Pursuit – PP) were evaluated. For the 22 pairs of registers tested, 82% were correctly discriminated using HI-NIR (using PCA or PP). For the HI-MIR data set, PCA and PP was able to discriminate 59% and 100% of the samples, respectively.

- A008 **Making Colourful Sense of Raman Images of Single Cells**  
Lorna Ashton, Katherine Hollywood, Roy Goodacre

Raman mapping is a powerful technique for single cell analysis, providing vast amounts of spatially resolved biochemical data. However, there is a risk of undermining the routine use of Raman mapping due to a lack of consistency and transparency in the way false-shaded Raman images are constructed. We highlight the need for a careful shading approach and suggest the use of data distribution plots to aid in shading decisions to avoid ambiguity and potential subjectivity in image interpretation.

- A009 **Infrared Spectroscopy of Surface Moieties on Laser or Rf Plasma Treated Colloidal Diamond Nanoparticles**  
Halyna Kozak, Anna Artemenko, Jan Čermák, Vladimír Švrček, Bohuslav Rezek, Alexander Kromka

We report on a surface modification of colloidal diamond nanoparticles (DNPs) proceeded by two methods: (a) a laser beam to generate a plasma in the colloid; (b) an high frequency microplasma is generated in a quartz capillary and “jetted” out onto the colloid for 15 min. Using grazing angle reflectance Fourier transform infrared spectroscopy, Kelvin force microscopy, and X-ray photoelectron spectroscopy we compare the surface chemistry of two different kinds of DNPs produced either by detonation process or high-pressure high-temperature.

## Nearfield Vibrational Spectroscopy

- A010 **IR Broadband Laser System for Near-Field Spectroscopy of Gallium Nitride**  
Fabian Gaussmann, Jochen Wueppen, Thomas Taubner

In this presentation we will present our results on near-field imaging and near-field spectroscopy of different GaN samples in order to characterize both structural and electrical properties. Therefore we used a self-developed tunable broadband laser system in the infrared spectral range between 9 and 16 microns. Our optical setup is mainly based on a Michelson interferometer which allows for near-field spectroscopy known from conventional Fourier transform infrared spectroscopy.

- A011 **An Inter-Laboratory Comparison on Accurate Measurements of Optical Contrast in Tip-Enhanced Raman Spectroscopy Through Elimination of Far-Field Artefacts**  
Dario Imbraguglio, Debdulal Roy, Andrea Mario Rossi, Naresh Kumar  
The present study is an inter-laboratory comparison on accurate measurements of the optical contrast in tip-enhanced Raman spectroscopy (TERS). The superior accuracy of measurement is achieved by elimination of far-field artefacts through the use of a recently developed bilayer reference sample for TERS.
- A012 **Development of the Ultra-High Vacuum – Low Temperature TERS System and Measurement of the Stable TERS Spectra of 1,2-Di(4-pyridyl)ethylene on Au Substrate**  
Toshiaki Suzuki, Yoshito Tanaka, Tamitake Itoh, Yasutaka Kitahama, Yukihiro Ozaki  
In this work, we develop the ultra-high vacuum and low temperature TERS system by combination of UHV-LT STM system and confocal Raman spectrometer, and we measured TERS to evaluate the system. Under LT condition, stable TERS spectra could be observed because thermal effect of TERS measurement was decreased and movement of molecules should be stopped.
- A013 **Synchrotron Infrared Nano-Spectroscopy (SINS) of Fungal Cell Walls**  
Kathleen Gough, Catherine Findlay, Hans Bechtel, Michael Martin, Robert Johns, Susan Kaminskyj, Tanya Dahms  
Synchrotron infrared nano-spectroscopy (SINS) enables spectrochemical imaging with ~25 nm spatial resolution, hence it is ideally suited to probe the walls (20 to 200 nm thick) that protect fungal cells and control their interactions with their environment. Our SINS data provide the first spectroscopic evidence of radically altered carbohydrate composition in *Aspergillus* strains lacking genes responsible for biosynthesis of critical minor compounds, constituting the first nanoscale FTIR analysis, together with AFM morphological analysis, of fungal cell walls.
- A014 **Tip-Enhanced Raman Spectroscopy Studies of Bradykinin onto Ag Nanowires**  
Dominika Swiech, Yukihiro Ozaki, Dariusz Sobolewski, Adam Prah, Sebastian Mackowski, Edyta Proniewicz  
The main purpose of this work was to define the adsorption mode of bradykinin, physiologically important peptide, obtained by the solid-phase method using the Fmoc-strategy, onto Ag nanowires. Tip-enhanced Raman studies highlight that the C-terminal part of BK plays an important role in the adsorption processes onto Ag surfaces.
- A120-pdp **Limitations in Subsurface Imaging of Small Particles with an Infrared Near-Field Optical Microscope**  
Lena Jung, Benedikt Hauer, Thomas Taubner  
We present a study on subsurface imaging with an infrared near-field microscope (s-SNOM). The depth-limitation for the visibility of gold nanoparticles with 50 nm in diameter under silicon nitride as well as particle-size dependence of resolution and signal strength are investigated. In a spectroscopic investigation a significant influence of the actual value of the dielectric function on the lateral resolution can be shown. The explanation of this observation combines the research areas of subsurface imaging and superlensing.
- A121-pdp **Secondary Structure Transformation of Biopolymer Thin Films Observed by Time Resolved Photothermal Infrared Nanoscopy**  
Anna Balbekova, Georg Ramer, Andreas Schwaighofer, Bernhard Lendl  
In this experimental study dynamic changes in biopolymer thin film were monitored in real-time by photothermal infrared nanoscopy. Spectral changes of the amide I band of Poly-L-lysine film induced by secondary structure transformations were chosen as an object for monitoring the dynamic changes. The utilized setup allows time resolved measurements with a time resolution of 15 ps per spectrum.

## Biomedical Applications

### A015 **Theoretical Prediction of the Molecular Structure of Bradykinin Versus Vibrational Investigation**

Dominika Swiech, Piotr Kubisiak, Marcin Andrzejak, Piotr Borowski, Edyta Proniewicz

We present here the first theoretical Raman and infrared spectra of bradykinin (BK; Arg1-Pro2-Pro3-Gly4-Phe5-Ser6-Pro7-Phe8-Arg9) that is based on the ab initio molecular dynamics (BOMD) calculations in the presence of water molecules that form the first coordination sphere. The simulated BK vibrational spectra are in good agreement with the experimental spectrum. The obtained data indicate that the folded structure of BK is stabilized by the intermolecular interactions and the C-terminal part of the peptide (Phe8-Arg9) remains “exposed”.

### A016 **Rapid Stratified Serum Spectroscopic Diagnostics**

Matthew Baker, James Hands, Graeme Clemens, Robert Lea, Katherine Ashton, Timothy Dawson, Michael Jenkinson, Andrew Brodbelt, Charles Davies, Ryan Stables

Gliomas are the most frequent primary brain tumours in adults, with these intracranial neoplasms accounting for 70% of adult malignant brain tumours. The current diagnostic regime is to some extent subjective, invasive, and may require unnecessary surgery. Studies have shown the potential of ATR-FTIR spectroscopy for diagnostic applications when collecting spectral measurements of human serum to discriminate between healthy and diseased states; studies involve cardiology, ovarian cancer and our previous studies on brain cancer, to name but a few. We built upon our existing spectral dataset to construct 5 models: 1) cancer vs. non-cancer, 2) metastatic brain cancer vs. brain cancer vs. non-cancer, 3) organ of tumour origin, 4) high grade glioma vs. low grade glioma vs. meningioma, 5) subtype of brain cancer. In total our latest research includes 433 patients demonstrating a rapid stratified serum diagnostic process using minimal sample.

### A017 **Mucin Signatures in Mid-IR as a Marker of Colonic Malignancy**

Shaul Mordechai, Ranjit Sahu, Gilbert Sebbag, Shlomo Walfisch, Ahmad Salman

Biomarkers are important in the diagnosis of diseases and often relate biochemical processes with clinical manifestation. In the present study we examined the relevance of mucin absorbance in the mid IR region from human colonic tissues in resection margins. Identifying crypts with a propensity to proliferate and behave as potential foci for relapse is important in designing regimen to decrease the number of surgeries in colon cancer patient and the present investigation highlights this possibility.

### A018 **Rationally Designed Mixed-Monolayer Glyconanoparticles for the Detection of Cholera Toxin by Surface Enhanced Raman Spectroscopy**

Jonathan Simpson, Derek Craig, Karen Faulds, Duncan Graham

We have generated glyconanoparticles which rapidly, specifically and sensitively detect cholera toxin B (CTB) by surface enhanced Raman spectroscopy (SERS). The particles are designed to mimic the cell surface glycan, GM1. This glycolipid is exploited by cholera bacteria for attachment to intestinal cells and establishment in a host. Detection of CTB occurs rapidly (within 5 minutes) and the established limit of detection, of 1 nM (56 ng/mL), is considerably lower than previously achieved with similar techniques including UV-visible extinction spectroscopy.

### A019 **Development of a Non-Bioptic Diagnostic Technique for Eosinophilic Esophagitis Using Raman Spectroscopy**

Tatsuyuki Yamamoto, Hemanth Noothalapati, Suguru Uemura, Naoki Ohshima, Yoshikazu Kinoshita, Masahiro Andou, Hiro-o Hamaguchi

Prevalence of eosinophilic esophagitis with dense eosinophile infiltration is increasing recently. The characteristic property of this disease is that the dense infiltration of eosinophile only in the esophageal mucosa. We have recently applied Raman spectroscopy and succeeded in detecting eosinophils infiltrated in esophageal mucous membrane using eosinophil peroxidase as a marker substance for the disease. Eosinophil peroxidase is only found in granules in eosinophil. We are now working on the development of a new non-bioptic diagnostic technique using this fact.

A020 **In Situ SERS Spectroscopy Explore Intranuclear Molecular Information**  
Lijia Liang, Dianshuai Huang, Hailong Wang, Haibo Li, Shuping Xu, Weiqing Xu

Investigating intranuclear molecular information of cancer cell is crucial for biomedical research because cell nucleus possess almost all the genetic information of a whole cell and controls cell metabolism and genetic expression. SERS spectroscopy as a noninvasive analysis and label-free tool can provide structural information of native biomolecules of cell nucleus. We explored molecular information of cancer cell by SERS spectroscopy.

A021 **Combination of Image Processing and Raman Spectroscopy for Automated White Blood Cell Classification**  
Oleg Ryabchykov, Anuradha Ramoji, Thomas Bocklitz, Ute Neugebauer, Michael Bauer, Michael Kiehntopf, Jürgen Popp

Classification of white blood cell types is a routine method for diagnosis of many diseases such as infection, inflammation, a bone marrow disorder, an autoimmune disease, etc. In this work we propose differentiation between neutrophils and lymphocytes based on coupling of Raman spectroscopy with cell images processing to provide better results than for each of these methods by alone. To transfer the information about cell morphology from images to mathematical classification model we use Pseudo-Zernike moments.

A022 **Enhancing Raman Diffraction to Measure Ketone Bodies in Human Breath**  
Alfredo Marquez, Miguel Orozco, Pedro Piza

Enhancing RAMAN diffraction to measure ketone bodies in human breath. This development is focused on detecting ketone bodies in diabetic breath, those substances are produced by keto acidosis. This condition is characteristic of Type I diabetes, where, in patients in acute impairment of insulin in the blood, present up to 5 ppm of ketone bodies in breath. To measure such a small concentration, Raman gas spectroscopy is an excellent tool, specially employing the Surface Enhanced Raman Spectroscopy (SERS).

A023 **A Comparative Study on the Interaction of tRNA with Chloroethyl Nitrosourea Derivatives; Semustine and Lomustine: Structural-conformational Characterization**  
Shweta Agarwal, Ranjana Mehrotra

We have investigated interaction of 2-chloroethyl nitrosourea (CENUs) derivatives, lomustine and semustine with tRNA using spectroscopic techniques (ATR-FTIR and CD), to explore their possible interaction with RNA as part of their anti-proliferative action. Comparative study on tRNA binding properties of semustine (4-methyl derivative of lomustine) and lomustine is reported that gives glimpse of structure-function-relationship. Spectral outcomes suggest CENUs interaction via guanine and cytosine residues of tRNA by the means of groove-directed-alkylation. CENUs induce no conformational change in A-conformation of biomolecule.

A024 **Characterization of Bone and Bone Graft Substitute by X-Ray Microtomography and Raman Spectroscopy**

Johann Charwat-Pessler, Maurizio Musso, Karl Entacher, Bernhard Plank, Peter Schuller-Götzburg, Stefan Tangl, Alexander Petutschnigg

This study examines the statistical relationship of these two different image information contents, via a pork bone sample comprising the bone graft substitute Bio-Oss®, which was investigated by X-ray microcomputed tomography (μ-CT) and by Raman spectroscopic imaging. A one way ANOVA was carried out in order to find out whether typical gray-level values (and the related histograms) in the μ-CT image can be reliably assigned to segments found in the Raman image resulting from the cluster analysis.

A025 **Infrared Spectroscopic Blood Biomarker Candidates for Urinary Bladder Cancer**

Julian Ollesch, H. Michael Heise, Klaus Gerwert

Infrared absorbance spectra of bodyfluids mirror the biochemical status of a patient. An extendedly automated system for reproducible preparation and analysis of dried bodyfluid films was developed, avoiding commonly observed coffee-ring effects. Blood samples of patients at risk for urinary bladder cancer (UBC) were analysed. Two feature selection algorithms depicted UBC-characteristic patterns in spectra of blood serum and plasma. Two classification algorithms yielded an average prediction accuracy of manifested UBC of up to 92 % in leave-one-third-out Monte Carlo cross-validations.

A026 **FTIR-Spectroscopy of Alpha-Synuclein in Blood Plasma**

Julia Lange, Andreas Nabers, Julian Ollesch, Caroline May, Katrin Marcus, Klaus Gerwert

Parkinson disease (PD) is one of the most common forms of dementia. During PD progression, alpha-Synuclein refolds into oligomers and fibrils. These structures appear involved in neurodegeneration. Here, we demonstrate the application of a novel sensor for protein analysis in complex fluids. Alpha-Synuclein was specifically captured from blood plasma by immuno-ATR-FTIR spectroscopy. A highly specific and sensitive antibody for alpha-Synuclein detection was identified. In preliminary results, we see a clear-cut distinction of ten PD versus ten non-PD cases.

A027 **Use of FTIR In Metabolomics to Assess Sample Preparation**

Guillermo Quintas, Julia Kuligowski, David Pérez-Guaita, Ángel Sánchez-Illana, Daniel Sanjuan-Herraez, Máximo Vento

In this work we show the utility of ATR-FTIR for the evaluation of major trends in the plasma composition due to sample collection and clean-up in terms of e.g. aminoacid, protein, lipid and carbohydrate overall contents. Besides, we show the usefulness of JIVE for an unsupervised integration of LCMS and FTIR metabolomic data leading to a more precise characterization of chemical changes from different anticoagulants and solvents, enriched by removing structured variations that are specific to each data source.

A028 **Imaging the Fatty Acid Distribution Inside Macrophages on Single Cell Level by Raman Micro-Spectroscopy**

Clara Stiebing, Christian Matthäus, Stefan Lorkowski, Jürgen Popp

Raman micro-spectroscopy is a powerful tool to investigate cells on subcellular level. Our research focuses on macrophages and their lipid metabolism, which is interesting for the research of atherosclerotic plaque development. We present results on time-dependent incubation studies of macrophages treated with different deuterated lipids. Through deuterium labels the lipids of interest can be specifically located inside cells due to a Raman band in the normally silent region of biological molecules. We present experiments with fixed and living cells.

A029 **Raman Confocal Micro-Probe for Cosmetic and Medical Applications**

David Catalina

We present here our Raman confocal micro probe which enables in situ and non-invasive chemical analysis of skin. The micro-probe is offering a true confocal performance for optimized depth resolution, allowing superficial human skin layers to be distinguished as well as their behavior to cosmetic and/or pharmaceutical products.

A030 **Lipid Droplets Formation in Human Endothelial Cells in Response to Polyunsaturated Fatty Acids and 1-Methyl-nicotinamide (MNA). Confocal Raman Imaging and Fluorescence**

Katarzyna Majzner, Stefan Chlopicki, Malgorzata Baranska

In this work the formation of lipid droplets (LDs) in human endothelial cells culture in response to the uptake of polyunsaturated fatty acids (PUFAs) was studied. Additionally, an effect of 1-methylnicotinamide on the process of LDs formation was investigated. The incubation of endothelial cells with different polyunsaturated acids (PUFAs) resulted in formation of corresponding LDs. LDs are organelles known to regulate neutrophil, eosinophil, or tumor cell functions but their presence and function in the endothelium is largely unexplored.

**A031 Evaluation of Targeted Cancer Therapy by Raman Spectral Imaging**

Hesham Yosef, Laven Mavarani, Abdelouahid Maghnoij, Stephan Hahn, Samir El-Mashtoly, Klaus Gerwert

Derived by high cancer mortality, extensive research is conducted to optimize the evaluation methods of new anti-cancer drugs. Raman microscopy is an attractive choice. Raman spectra of single cell can reflect its biochemical composition. Moreover, changes in the Raman spectra can be utilized as a marker for cellular response to drug treatment. Therefore, we implement Raman spectral imaging to detect the response of cancer cells to therapy. Even more, we can detect the drug resistance of mutated cancers.

**A032 Alterations in Endothelial Lipid to Protein Ratio in Tumor Metastasis: Raman 3D Imaging of the Vessel Wall in the Murine Model of Metastatic Breast Cancer**

Marta Pacia, Elzbieta Buczek, Stefan Chlopicki, Agnieszka Blazejczak, Joanna Wietrzyk, Malgorzata Baranska, Agnieszka Kaczor

Up to now the impact of cancer on tissues was demonstrated without focusing on the endothelial layer as the barrier of migrating cancer cells. Knowing the link between the endothelium status and migrating cancer cells, we decided to characterize biochemical alterations in endothelium in mice with metastatic breast cancer. The most prominent changes, related mostly with lipid to protein content were observed only for tunica intima layer, while the differences were insignificant for outer vessel wall layers.

**A033 Evaluation of Bacterial Variability in Urinary Tract Infection by Means of Raman Microspectroscopy**

Elias Abdou, Bernd Kampe, Petra Rösch, Jürgen Popp

Urinary tract infections are one of the most commonly occurring infections. Raman microspectroscopy is a novel technique for microbial identification and differentiation. This study investigates the potential of Raman microspectroscopy to detect and differentiate between a pathogen and a contaminant strains in comparison to frequently used techniques. Raman microspectroscopy results were compared to other methods. Raman microspectroscopy can be considered as a reliable method for rapid microbial detection and the differentiation between contaminants and pathogens in the same sample.

**A034 Changes in Infrared Spectral Profile of Plasma due to Progression of Systemic Hypertension**

Emilia Staniszevska-Slezak, Kamilla Malek, Lukasz Mateuszuk, Stefan Chlopicki, Malgorzata Baranska

Infrared spectroscopy is a powerful tool for an analysis and recognition of pathology from blood plasma. Thus, the aim of this work is to investigate whether FTIR technique is capable to recognize an early stage of systemic hypertension. An analysis of FTIR spectra was performed with a support of Principal Component Analysis. Our results show that spectral FTIR profile is sensitive to biochemical changes in plasma and allows discriminating progression of systemic hypertension.

**A035 Following Senescence Progression in Human Primary Fibroblast Cell Lines by Raman Spectroscopy**

Katharina Eberhardt, Shiva Marthandan, Christian Matthäus, Stephan Diekmann, Jürgen Popp

In cell cultivation of isolated primary cells a limited capacity during replication was observed, known as cellular senescence. These state acts as an important tumor suppressor mechanism to limit abnormal cell proliferations. Therefore, a reproducible detection and a better understanding on the molecular level are important. However, many of the existing biomarker detection methods are imprecise. Hence, Raman spectroscopy as a label-free and non-destructive technique was used to investigate cellular senescence progression on the single cell level.

A036

**Human Blood Plasma as a Challenge for Chiroptical Spectroscopy**Lucie Šovičková, Michal Tatarkovič, Alla Synytsya, Lucie Kocourková, Vladimír Setnička

Blood plasma contains many chiral biomolecules, whose structure and conformation play a key role in their correct biological functions. However, the structural analysis of these biomolecules by conventional vibrational spectroscopies is limited. Therefore, we present a novel approach in blood plasma analysis based on chiroptical spectroscopy (ROA, ECD, VCD), which is inherently sensitive to the molecular geometry of chiral compounds. The achieved results suggest a promising perspective of these methods for the identification of disease-induced structural changes within plasmatic biomolecules.

A037

**Spectral Biomarkers of Pancreatic Cancer Using the Combination of Chiroptical and Vibrational Spectroscopy**Lucie Kocourková, Michal Tatarkovič, Alla Synytsya, Lucie Šťovičková, Vladimír Setnička

With the five-year survival rate for only 3% of patients, pancreatic adenocarcinoma is one of the most aggressive cancer types. Moreover, the disease is often misdiagnosed, because the early-stage symptoms are similar to type II diabetes mellitus. The onset of pancreatic cancer is also accompanied with structural changes of plasmatic biomolecules. Based on our results, chiroptical spectroscopy might have a potential to follow these pathological changes during the disease development, and thus become a useful tool for its more reliable diagnosis.

A038

**Optimization of Multimodal Spectral Imaging for Assessment of Resection Margins During Mohs Micrographic Surgery for Basal Cell Carcinoma**Kenny Kong, Sho Takamori, Sandeep Varma, Iain Leach, Hywel Williams, Ioan Notingher

Multimodal spectral imaging (MSI) based on the information of auto-fluorescence of collagen, and Raman micro-spectroscopy to diagnosed basal cell carcinoma (BCC) in tissue specimens excised during Mohs micrographic surgery.

A039

**Raman Imaging of alpha-Synuclein in Mouse Brain Tissue**Clemens Roider, Alexander Jesacher, Nadia Stefanova, Werner Poewe, Gregor K. Wenning, Monika Ritsch-Marte

As people are getting older neurodegenerative disorders like Parkinson's disease are getting more and more attention and massive research efforts are put into finding cures. But up to now there is still no treatment to halt or reverse the progress because we have too little knowledge on a molecular level. alpha-Synuclein seems to play an important role in the process and thus we aim to establish Raman imaging as a standard tool for investigating neurodegenerative disorder.

A040

**Investigation of the Potential Dependent Integration of Alamethicin into Artificial Membrane Systems with Surface-Enhanced Infrared Spectroscopy**Enrico Forbrig, Jacek Kozuch, Peter Hildebrandt

Antimicrobial peptides are powerful endogenous molecules produced by the innate immune system to protect the host from bacterial infections. The pore-forming peptide Alamethicin destabilizes the bacterial cell membrane potential and serves as one example for the development of a new class of future antibiotics. In a spectro-electrochemical approach we combine SEIRA with electrochemical methods to show the incorporation and reorientation of Alamethicin into a tethered bilayer lipid membrane system connected with a self-assembled monolayer to a nanostructured gold electrode.

A041

**Design of Raman Fiber-Optic Probes for *in Vivo* Diagnostics**Iskander Usenov, Taravat Saeb-Gilani, Oliver Lux, Hans Joachim Eichler, Franziska Schulte, Viacheslav Artysushenko

Fiber-optic probes in Raman, MIR and NIR spectroscopy are very useful for non-invasive *in vivo* examinations. This study aims to develop effective fiber-optic probes for Raman spectroscopy. The main advantage of these probes is the direct deposition of the dielectric filters at distal end of the probe. Realized fiber coatings are in good accordance with the previous simulations and the test coatings on substrates. Optical design of the probes is calculated using FRED software.

- A042 **Raman Microimaging of Low-Density Lipoprotein Uptake by Activated Macrophages**  
Krzysztof Czamara, Lukasz Mateuszuk, Gabor Csanyi, Malgorzata Baranska, Stefan Chlopicki, Agnieszka Kaczor

Macrophages are recognized as crucial pathophysiologic agents in chronic diseases associated with inflammation and aging. Thrombospondin 1 (TSP1) seems to activate LDL uptake and cholesterol esterification that may represent an early mechanism of atherogenesis. Raman microimaging was performed to study activated macrophages incubated with LDL cholesterol with or without addition of TSP1 and PMA. The results reveal that 24h stimulation with TSP1 and PMA induced an increase in the content of cholesterol and its esters within macrophages.

- A043 **Warfarin Reduced Gold Nanoparticles: Spectroscopic Characterisation, Cellular Uptake and Cytotoxicity**  
Cristina Coman, Olivia Dumitrita Rugina, Loredana Florina Leopold, Zorita Diaconeasa, Nicolae Leopold, Maria Tofana, Carmen Socaciu

We report the synthesis of colloidal AuNPs using sodium warfarin (3-( $\alpha$ -acetylbenzyl)-4-hydroxycoumarin sodium salt) as reducing agent for the tetrachloroauric acid. The nanoparticles were characterised by UV-Vis, FTIR, and SERS spectroscopies, and transmission electron microscopy. In vitro studies were performed to test the nanoparticles cellular uptake and cellular viability. Two cell lines were used for the study, the human fetal lung fibroblast (HFL-1) and human retinal epithelial (D407). The nanoparticles were internalised in the cell cytoplasm and were not cytotoxic.

- A044 **Comparative Spectral Histopathology Study of Colon Cancer Tissue Sections by Raman Imaging (532 nm) and FTIR Imaging**  
Dennis Petersen, Laven Mavarani, Claus Küpper, Axel Mosig, Erik Freier, Andrea Tannapfel, Klaus Gerwert

Spectral Histopathology (SHP) is an emerging tool for label free annotation of tissue. We used 532 nm excitation to annotate colon tissue by Raman SHP and proceeded on the same slide for FTIR SHP. In Raman SHP we were able to identify cancerous and non-cancerous areas and resolve erythrocytes, lymphocytes and single cell nuclei. The same areas in the FTIR SHP were compared to the Raman SHP concerning accuracy of the classification.

- A045 **Molecular Structural Studies on the Synthesized Eu(III) Complex of Coumarin Hydrazide Ligand and its Potential as a Chemo-Sensor in Determination of Activity of Xanthine Oxidase in Serum Samples**  
Badr Elsayed, Mohamed Attia, Mohamed Elsenety

Eu(III) complex of coumarin hydrazide ligand has been synthesized. The ligand and its complex have been characterized by FTIR, <sup>1</sup>HNMR, and U.V. & Visible spectroscopic techniques. The complex has stoichiometry of the type [Ln(L)<sub>2</sub>(H<sub>2</sub>O)<sub>2</sub>]NO<sub>3</sub>·2H<sub>2</sub>O with molar ratio 2L:1M where the tridentate ligand (HL) coordinates to the lanthanide ion Eu(III) through azomethine nitrogen atom, phenolic oxygen of hydrazide moiety after deprotonation and ketonic oxygen of the amide group. Fluorescence properties of the complex in different organic solvents have been studied. The synthesized complex has been used as a potential chemo-sensor in determination of activity of xanthine oxidase in serum samples using developed spectrofluorimetric method.

- A046 **Raman Spectroscopic Investigation of LPS Induced Murine Inflammation Model: Influence of Biological Heterogeneity on Raman Model**  
Anuradha Ramoji, Robert Requardt, Oleg Ryabchykov, Kerstin Galler, Robby Markwart, Ignacio Rubio, Thomas Bocklitz, Michael Bauer, Jürgen Popp, Ute Neugebauer

This study focuses on the Raman spectroscopic investigation of T-lymphocytes isolated from mouse spleen during systemic inflammation. Lipopolysaccharide (LPS) insulted mice have been used as inflammatory model. Raman spectral data of the T-lymphocytes were collected at different time points: 1, 4, 10 and 30 days after the LPS insult. A support vector machine based Raman differentiation model can distinguish T-lymphocytes from the control group and those from animals 10 days after the LPS insult with an accuracy of 70%. No changes were observed in T-lymphocytes after 30 days of LPS insult, indicating T-lymphocytes recovery process.

A047 **Laser Wavelength Dependence of Transmission Raman Spectroscopy: Exploration of Wavelength Effects on Deep Tissue Detection**

Adrian Ghita

Transmission Raman spectroscopy is a simple non-invasive approach suitable for detection of breast calcifications. With proof of principle being demonstrated by Stone and Matousek in 2008, further research needs to be done to find the optimum laser wavelength for detecting the calcifications located inside a 50 mm thick breast tissue. The results obtained evidence different detection efficiency in respect to sample location within the tissue and laser excitation wavelength.

A048 **Embryo Selection Using Raman Spectra of Day Three Spent Media**

Uğur Parlatan, Nima Bavili, Tugce Ozturk, Gunay Basar, Ercan Bastu, Sibel Bulgurcuoglu, Faruk Buyru

The main issue concerning multiple gestations and in vitro fertilization is the inability to estimate the reproductive potential of an individual embryo. Day three in vitro fertilization spent cultures of 64 samples from 39 patients were investigated using Raman spectroscopy. According to the statistical analysis of the measured Raman spectra 90% prediction rate was achieved. The results will be discussed.

A049 **Testing the Feasibility of Diabetes Mellitus Screening by Non-Invasive Attenuated Total Reflection Spectroscopy of the Stratum Corneum of Human Forearm Skin**

H. Michael Heise, Markus Stücker

The potential of ATR spectroscopy for dermatology is increased by the development of fibre-optic probes from polycrystalline silver halide material, which eases the epidermis characterisation significantly. This non-invasive measurement technique has been applied for various human studies, focusing on normal and diseased skin. Here we studied the variance of the horny layer of human skin on the basis of their infrared keratin spectra with a possible glycation of keratin under the influence of an increased blood glucose level as parameter.

A050 **Monitoring of Interstitial Buffer Systems using Micro-Dialysis and Infrared Spectrometry**

H. Michael Heise, Julian Elm

The human body maintains the blood pH around 7.4, but for severe changes, acidosis or alkalosis, can lead to serious health problems. Three different buffer systems exist: bicarbonate, phosphate and protein buffering systems. The first two buffer systems with their components including pH value can be monitored by infrared spectroscopy in combination with micro-dialysis. By using the dissolved CO<sub>2</sub> and HCO<sub>3</sub><sup>-</sup> bands of the bicarbonate spectra, also the pH of the harvested interstitial fluid is predictable using the Henderson-Hasselbalch equation.

A051 **Raman Mapping and Preliminary Multivariate Curve Resolution (MCR) Analysis of the Chemotherapy Tablet Xeloda**

Aditya Pandya, J. Carl Kumaradas, Alexandre Douplik

The current study utilizes Multivariate Curve Resolution (MCR) method to analyze Raman datasets obtained by spatial mapping of signatures from a chemotherapy tablet. The method was initially tested with a quartz plate drop coated with Polystyrene microspheres to evaluate the efficiency of spectral modeling and obtaining spectral component contribution maps. Distribution maps were formed for the inactive ingredients of the drug. The results qualitatively depict that the method can be used to denoise data and map the mixture of chemical signatures.

A052 **An Automatic Method for Estimation of Background of Raman Spectra**

Crescenzo Gallo, Giuseppe Perna, Maria Lasalvia, Vito Capozzi

A flexible polynomial background construction algorithm has been implemented in order to estimate the background of typical Raman spectra from both inorganic and biological samples. The developed algorithm computes the background in a piecewise manner performing an efficient spline construction region by region of the measured spectrum, by producing a proper polynomial function for each spectral range. This method has been tested with synthetic and experimental spectra.

**A053 Identification of Circulating Tumor Cells for Cancer Diagnostics by Raman Spectroscopy**

Christoph Krafft, Claudia Beleites, Iwan Schie, Jürgen Popp

Circulating tumor cells (CTCs) offer new prospects in cancer diagnostics. They can be extracted from body fluids, and such a liquid biopsy can be performed with fewer risks than collecting a tissue biopsy. Due to their lifetime of just few hours, CTCs represent the current disease status. We initiated a research program to distinguish cancer cells from normal blood cells using Raman-based methodologies. An overview about our achievements is presented.

**A054 A Spotlight on Structure: Pioneering the ROA Analysis of Synthetic Peptide Antibiotics and in Biomembranes**

Maria Giovanna Lizio, Simon J. Webb Webb, Ewan Blanch Blanch, Sarah Pike

Peptaibols represent a type of AMPs produced by fungi characterized by a high content of non-proteinogenic residues, mostly aminoisobutyric acid, a C-terminal 1,2-amino alcohol and usually acetylated or acylated at the N-terminus. Raman Optical Activity (ROA) is a sensitive spectroscopic technique able to detect local conformation of single amino acids. Raman and ROA are both compatible with water so these techniques can potentially be used to obtain information about the conformational changes of these peptides between solution and membrane environments.

**A055 ATR-FTIR Diagnosis of Malaria**

David Perez-Guaita, Phil Heraud, Aazam Khoshmanesh, Patcharee Jearanaikoon, Matthew W. A. Dixon, Leann Tilley, Don McNaughton, Bayden R. Wood

Here we describe our first field study in Thailand for the diagnosis of malaria using direct ATR-FTIR spectroscopy of RBCs fixed in methanol. Spectra of samples from 57 patients (29 positive and 28 negative) were acquired and models based on PLSDA were performed, obtaining classification error rates below 10%. The high sensitivity, low cost, ease of use, portability and robustness of the ATR-FTIR technique could see it become a standard diagnostic tool in both the clinic and remote field locations.

## Fine Arts

**A056 MRS as a Tool for the Study of the Archaeological Heritage of the Iberians in a Multidisciplinary Framework: the Arquiberlab Project**

José Alfonso Tuñón, Alberto Sánchez, David Jesús Parras Guijarro, Manuel Montejo, Carmen Rísquez, Fernando Márquez, Peter Vandenabeele

The ARQUIBERLAB Project represents a multidisciplinary approach to the study of the archaeological heritage of Iberians in Southern Spain. In the frame of the project, MicroRaman Spectroscopy has been extensively used for the determination of the chemical composition of more than 300 samples of different typologies recovered from twelve different archaeological sites.

**A057 Micro-Raman Spectroscopy and SEM/EDS in Investigation of White and Red Painting Layers from Celtic Pottery, Modlniczka Site, Poland**

Joanna Trbska, Aleksandra Weselucha-Birczynska, Barbara Trybalska, Marcin Przybya, Magorzata Byrska-Fudali

Celtic red and white painted pottery from a Modlniczka site, Poland, was investigated with the use of Raman spectroscopy and SEM/EDS. Painting layers were performed very homogeneously for all examined shards, i.e. red layers as thinner, ca. 0,02 mm and white of 0,04 mm. Raman spectroscopy of a red layer revealed the presence of moderately ordered haematite, supposed to have been separately painted extremely thin layer composed of well crystallised raw material. White layers produced no Raman signal.

A058 **On-Site Spectroscopic Investigation of Pigments in Archaeological Egyptian Funerary Artifacts at Qubbet el-Hawa Necropolis (Aswan)**

Maria Jose Ayora-Cañada, Ana Dominguez-Vidal, Yolanda de la Torre, Alejandro Jimenez-Serrano

The study of different funerary objects excavated during the archaeological survey at the Qubbet el-Hawa necropolis by using a portable Raman instrument brought to the excavation site is reported. Funerary artifacts like coffins and cartonnage masks dating from Middle, New Kingdom and Third Intermediated Period were investigated. The main pigments were identified despite the intense fluorescence background found in most of the cases. The pigment palette consisted of hematite, yellow ochre, carbon black, orpiment, calcite, gypsum and Egyptian blue.

A059 **Characterization of Nasrid Polychrome Wood Ceilings Using Raman Spectroscopy**

Ana Dominguez-Vidal, Elena Correa-Gomez, Ramon Rubio-Domene, Maria Jose Ayora-Cañada

A portable Raman spectrometer has been used to study the polychrome decorations of the wooden ceilings in two halls of the Alhambra complex. The wood ceilings were composed of small, geometric pieces richly painted in glowing colors. They were jointed to obtain large wooden surfaces. Raman spectra revealed the use of a protective priming layer of minium. Other pigments identified were lead white, cinnabar, lapis lazuli, carbon black and orpiment.

A060 **Raman Spectroscopy of the Pigments on Korean Traditional Paintings**

In-Sang Yang, Kiok Han, Ji-Yeon Nam, Jeong-Eun Ji, Han-Hyoung Lee, Dai-Il Kang, Yon-Na Song, Gyo-Ho Kim

Vibrational spectroscopy is a useful tool in conservation science as well as many areas of scientific research. In this report, a micro-Raman spectroscopy was applied to identify pigments in several traditional paintings and building decoration of Korean heritage. Korean traditional colors are often represented by five basic colors; blue, white, red, black, and yellow. We report results of Raman spectroscopy of the pigments including the basic Korean traditional colors, especially the mineral pigments found in traditional paintings and building decorations. Raman spectra are used to identify the various components of minerals in the pigments if they are mixtures of several different minerals. As a result, we could distinguish some inorganic materials such as Chinese ink and mixtures of minium and litharge which are very difficult to identify by conventional analytical method such as XRF, SEM-EDX, XRD. Our work would provide a scientific basis for the reconstruction of aged and destroyed Korean traditional heritages.

A122-pdp **Raman Imaging for Cultural Heritage Investigations**

Federica Cappa, Valentina Pintus, Johannes Ofner, Manfred Schreiner, Bernhard Lendl

Raman spectroscopy has been widely used in the field of cultural heritage as it is a non-invasive as well as non-destructive technique for art works. In this study, Raman spectral imaging was applied for the analysis of different materials such as natural and synthetic pigments in paintings as well as parchment and inks of medieval manuscripts. Raman imaging provides useful information for conservation and preservation purposes as well as for historical and curatorial perspectives.

## Safety Applications

A061 **Chloramphenicol Molecularly Imprinted Polymer Synthesis and Application on SERS Detection**

Yunfei Xie, Mengyao Zhao, Qi Hu

This work intends to detect trace antibiotic residues in food by combined SERS and molecular imprinting (MIP) technique.

A062 **Handheld Raman Spectroscopy for Counterfeit Screening at Point of Interception**  
Katherine Bakeev

Counterfeit medicines are a global health hazard and must be countered with rapid analysis tools that can be easily used in the field, thus preventing the flow of such products. Handheld Raman spectroscopy has been used as an easy method to quickly identify counterfeit antimalarial tablets in the case of an absent active ingredient. It is a valuable screening tool for counterfeits and can be used at the point of drug seizure with minimal training of inspectors.

A063 **Evaluation of Vibrational Spectroscopic Methods to Identify and Quantify Adulterants in Weightloss Herbal Medicines**

Jeremy Rooney, Keith Gordon, Clare Strachan, Arlene McDowell

To counter the growth of herbal medicines adulterated with pharmaceuticals crossing borders, three vibrational spectroscopies (MIR, NIR and Raman) are evaluated for adulterant screening and semi-quantification. Multivariate analyses were performed on the spectral and reference data. The performance of these models was then evaluated by independent test set validation.

## Nanomaterials

A064 **Evaluation of Graphene-Substrate Interactions Based on Surface Enhanced Raman Spectroscopy Measurements**

Jana Vejpravova, Martin Kalbac

Graphene on sapphire substrate were studied using the surface enhanced Raman spectroscopy. The enhancement of the signal enabled performing fast Raman mapping on sapphire substrate. The correlation analysis of Raman maps showed relatively homogenous doping of graphene on sapphire. We also show that the G mode split induced by interaction of graphene with its surroundings can be correlated with doping and presence of sp<sup>3</sup> like carbon defects.

A065 **Annealing Effects on (CoFe<sub>2</sub>O<sub>4</sub>)<sub>0.20</sub>+(ZnO)<sub>0.80</sub> Nanocomposites Studied by X-Ray Diffraction and Raman Spectroscopy**

T. J. Castro, S. W. da Silva, F. Nakagomi, N.S. Moura, A. Franco Jr., P. C. Morais

In this study, the effects of varying the annealing temperature (T) on the structural properties of the nanocomposites of type (CoFe<sub>2</sub>O<sub>4</sub>)<sub>0.20</sub>+(ZnO)<sub>0.80</sub> were investigated by means of X-Ray Diffraction (XRD) and Raman Spectroscopy. The samples were prepared by mixing zinc oxide and cobalt ferrite nanoparticles, synthesized by the combustion reaction method previously performed and subsequently annealed at different temperatures. Phonon Confinement Model (PCM) was employed to investigate the level of defects in the nanocomposites.

A066 **Micro-Raman Study of a Single Silicon Nanowire**

Heesuk Rho, Sang-Kwon Lee, Gil-Sung Kim

We report simultaneous studies of Raman scattering and transmission electron micrograph from a single Si nanowire. The Si nanowire exhibited highly faceted and tapered surface. Spatially-resolved Raman spectra along the nanowire long axis revealed variations in the TO phonon energy along the nanowire long axis. Despite the formation of facets and stacking faults, polarized Raman results of the Si nanowire were consistent with the Raman polarization selection rules expected for a cubic crystal.

A067 **Spectroscopic Studies of Phase Behaviour in Nanopores: Toward Supercritical Fluid Electrodeposition**

Ashley Love, Xue Han, Jie Ke, Michael George

Recent developments have led to electrodeposition from supercritical fluids (SCFs). The exact phase behaviour of these fluids within the pores is yet to be fully understood. A grasp of the phase behaviour within a pore will allow the properties of these fluids to be tuned via temperature or pressure changes to deposition conditions and perhaps co-solvent choices, allowing for optimal electrodeposition into a nanochannel. A robust spectroscopic method has been developed to elucidate both the critical temperature shift and composition change of mixtures within nanopores. Both NIR and Raman have been utilised to obtain confined phase properties and corroborate the results obtained from both.

A068

### **Fabrication of Plasmonic Nanoparticle-Decorated 3D Semiconductor Nanostructures as Recyclable SERS Substrates**

Sung-Gyu Park, Jung-Dae Kwon, ChaeWon Mun, Dong-Ho Kim

Highly roughened plasmonic nanoparticle-decorated 3D ZnO inverse nanostructures were prepared using a combination of prism holographic lithography and atomic layer deposition techniques. These metal-semiconductor structures described here offer an alternative to traditional single-use SERS substrates.

A069

### **Attenuated Total Reflection Surface-Enhanced Infrared Absorption Spectroscopy and Surface-Enhanced Raman Spectroscopy for the Analysis of Fatty Acids on Silver Nanoparticles**

Yuichi Kato, Eiichi Sudo

Micro-ATR measurements using Ge crystals were performed for silver nanoparticles modified with fatty acids. The fatty acids coating of the silver nanoparticles could be directly identified by SEIRA enhancement, because both carboxylate symmetric stretching vibration and methylene wagging vibration were strongly detected. ATR-SEIRA would appear to have substantial potential as a technique for identifying the substances coating Ag nanoparticle surfaces.

A070

### **One-Step, Surfactant-Free Synthesis for Controlling Surface Morphology of Silver Nanoshells and Their Enhanced Scattering Properties**

Myeong Geun Cha, Homan Kang, Yoon-Sik Lee, Dae Hong Jeong

Controlling surface morphology of metal nanoshells is one of the key factors to change surface plasmon resonance and scattering properties. However, there are several problems such as using surfactant or stepwise processes. Here, we developed one-step and surfactant-free synthesis for controlling morphology and thickness of silver nanoshells using various kinds of alkylamines as a reductant and capping agent. In addition, their scattering properties were investigated by using surface-enhanced Raman scattering (SERS) technique for using NIR-SERS probe.

A071

### **Raman Mapping of Release Properties for Oil-Filled Nanoparticle Coatings on Packaging Papers**

Pieter Samyn

The hydrophobicity of paper substrates can be controlled by a barrier coating including organic nanoparticles and vegetable oils. To get better insight in the nanoparticle interactions, surface chemistry of coated papers and presentation of oil at the surface by thermal release, the coated papers are further studied by Raman spectroscopy and imaging. Depending on the oil-types, different release profiles have been determined.

A072

### **Raman Spectra of Randomly Oriented Diamondoid Ensembles**

Dominique B. Schuepfer, Andrey A. Fokin, Peter R. Schreiner, Peter J. Klar

Different kinds of diamondoids were prepared by linking the smallest building blocks of diamond, e. g. adamantane and triamantane. These linked blocks show distinct Raman spectra depending on the strength of the coupling and the symmetry reduction of the molecules. We studied the large cages by polarized Raman experiments to obtain information about the similarities between the basic units and the randomly oriented ensemble of coupled diamondoids. The results can further be related to the symmetry type of the vibrations.

A073

### **Microwave Absorption of Electromechanical Nanoresonators**

Ondrej Krivosudský, Michal Cifra

We present the first model of protein structures as mechanical nanoresonators and the coupling of electromagnetic field to vibrational normal modes of protein structures. We analyze conditions for oscillations in Non-Newtonian fluids which influence damping of the mechanical oscillations. Based on this we propose new method considering slip and stick boundary conditions given by nano-scale dimension of the system and oscillation amplitude which could be relevant for tuning oscillation quality factor with relaxation times and is responsible for damping reduction.

**A074 Temperature Induced Strain in Isotope Labeled Mono- and Bilayer Graphene**

Tim Verhagen, Vaclav Vales, Martin Kalbac, Jana Vejpravova

The remarkable range of properties of graphene can be further extended using strain engineering. Using Raman spectroscopy, we investigated in-situ the temperature dependence (4-300K) of strain and doping of isotope labeled mono- and bilayer graphene. Isotope labeling allows us to follow the strain and doping simultaneously and independently in both layers of the bilayer. We find that the strain in the monolayer graphene and both layers of the bilayer graphene is large and follows the thermal expansion of the Si/SiO<sub>x</sub> substrate.

**A075 Investigation of Phonon Behavior in NiFe<sub>0.75</sub>Cr<sub>1.25</sub>O<sub>4</sub> Nanoparticles by Micro-Raman Spectroscopy**

Chun-Rong Lin, Kun-Yauh Shih, Kai-Wen Wu, Hsu-Ming Chung, Jiann-Shing Lee

The Raman spectroscopy has been proven a very successful technique in studying the nanomaterials and nanostructures since it is very sensitive to the structures and symmetry of the system. Moreover, the complex physical properties, such as spin-phonon and magnetoelectric coupling resulted from competing interactions between magnetic (spins), structural (phonons), and polarization (charges) order parameters, can be observed by the temperature-dependent Raman spectra.

**A076 AFM-IR Studies of Single Electrospun Nanofibers of Poly[(R)-3-Hydroxybutyrate-co-(R)-3-Hydroxyhexanoate]**

Liang Gong, D. Bruce Chase, Isao Noda, Curtis Marcott, C.J. McBrin, John Rabolt

AFM-IR was used to investigate the structural details of individual electrospun nanofibers of poly[(R)-3-hydroxybutyrate-co-(R)-3-hydroxyhexanoate] (PHBHx). The IR mappings of a single electrospun PHBHx nanofiber at 1728 cm<sup>-1</sup> and 1740 cm<sup>-1</sup> revealed an interesting core-shell structure with  $\alpha$ -form crystal structure primarily in the core and  $\beta$ -form primarily in the shell, which was further confirmed by the corresponding IR spectra collected in the center and on the edge of the fiber. The thickness of the shell was around 10 nm and independent from fiber size.

**A077 Chemically Modified Flat and Rough Silicon Substrates as Models for Liquid Repellant Surfaces**

Roland Bittner, Helmuth Hoffmann

Flat silicon wafers and rough silicon nanowire surfaces were chemically modified with inert, low surface energy monolayers using a uniform click-chemistry reaction scheme and were analysed by Brewster angle transmission FTIR spectroscopy as well as ellipsometry, SEM (scanning electron microscopy) and contact angle measurements. The roles of chemical composition and surface structure for the wetting properties were investigated, aiming at the design of stable anti-wetting, liquid-repelling surfaces.

**A078 Characterization of Sp<sup>2</sup>-Sp<sup>3</sup> Hybridized Carbon Composites by Raman and FTIR Measurements**

Marian Varga, Tibor Izak, Viliam Vretenar, Viera Skakalova, Halyna Kozak, Anna Artemenko, Alexander Kromka

The proposed contribution will make a comprehensive experimental investigation and characterization of hybrid sp<sup>2</sup>-sp<sup>3</sup> carbon based composites. Main focus will be on fabrication and characterization of different carbon composites by Raman and Fourier transform infrared spectroscopy measurements. A detailed study of deposition processes, and morphological and chemical properties of the carbon composites will be also supported and correlated by scanning electron microscopy and X-ray photoelectron spectroscopy measurements.

A079 **Vibrational Spectroscopy Assessment of Kerogen Maturity in Organic-Rich Source Rocks**

Lucia Bonoldi, Donato Barbieri, Eleonora Di Paola, Lea Di Paolo, Cristina Flego, Elisabetta Previde Massara

Organic matter in sedimentary rocks (kerogen) changes following temperature and pressure conditions over geological time. In this work the maturity of different kerogens, both natural and artificially matured, is studied by Raman and Attenuated Total Reflectance (ATR-IR) spectroscopies. ATR analysis is more suited to describe lower maturity samples, while Raman higher maturity ones. The combination of these two approaches can be successfully used to study the full range of kerogen maturity in geological samples.

A080 **Simultaneous Infrared Detection of the *syn*-ICH<sub>2</sub>OO Radical and the Criegee Intermediate CH<sub>2</sub>OO - the Pressure Dependence of the Yields of CH<sub>2</sub>OO and ICH<sub>2</sub>OO in the Reaction CH<sub>2</sub>I + O<sub>2</sub>**

Yuan-Pern Lee, Li-Wei Chen, Yu-Hsuan Huang

We recorded the IR spectrum of ICH<sub>2</sub>OO in the reaction CH<sub>2</sub>I + O<sub>2</sub> at pressures greater than 100 Torr. Vibrational bands at 1233.8, 1221.0, 1087.0, and 923.0 cm<sup>-1</sup> agrees well with theoretical calculations. With direct detection of formation of CH<sub>2</sub>OO and ICH<sub>2</sub>OO, and destruction of CH<sub>2</sub>I<sub>2</sub>, we determined the accurate yields of CH<sub>2</sub>OO and ICH<sub>2</sub>OO; the former is greater than previous reports and will have a significant impact on atmospheric chemistry. We also recorded high-resolution spectrum of the simplest Criegee intermediate CH<sub>2</sub>OO at 0.25 cm<sup>-1</sup> with partially resolved rotational structure and reassigned the band at 1233.5 cm<sup>-1</sup> as 2v<sub>9</sub> and the band at 1213.0 cm<sup>-1</sup> as v<sub>5</sub>.

A081 **Application of Raman Spectroscopy for Shale Gas Compositions Measurements in Two-Phase Systems**

Tomasz Wlodek, Szymon Kuczynski, Krzysztof Polanski

Currently, top energy companies' R&D centers are interested in new continuous monitoring systems for oil/gas extraction and exploitation processes. Raman spectroscopy allows identification of hydrocarbons and chemicals used in oil/gas recovery and can be very promising for its application in oil/gas industry. Such system can provide quick, non-contact, nondestructive and quantitative analysis. This work present preliminary investigation for both single- and two-phase hydrocarbon systems.

A083 **Nitric Oxide Fractionation Studies and Isotopic Ratiometry Using Time-Multiplexed Dual-Modulation Faraday Rotation Spectroscopy**

Eric Zhang, Stacey Huang, Qixing Ji, Michael Silvernagel, Bess Ward, Daniel Sigman, Gerard Wysocki

We present a transportable dual-modulation Faraday rotation spectrometer for nitric oxide isotopic ratiometry. Noise analysis indicates a minor isotope (<sup>15</sup>NO) detection limit of 0.35 ppb/rt(Hz) at 1.4x the fundamental quantum shot-noise limit, enabling sub-per-mille precision for nitric oxide ratiometry. Time-multiplexed analysis for quasi-simultaneous isotopic measurements demonstrates substantial fractionation effects on the hundreds of per-mille level, indicating the necessity for proper sampling to minimize degradation during the measurement process.

**A084 Chemometric Analysis of Multisensor Hyperspectral Images of Atmospheric Particulate Matter**

Johannes Ofner, Katharina A. Kamilli, Elisabeth Eitenberger, Gernot Friedbacher, Bernhard Lendl, Andreas Held, Hans Lohninger

Multisensor hyperspectral imaging using Raman and energy-dispersive X-ray (EDX) spectroscopy imaging in combination with electron microscopy, allows a combined analysis of vibrational features and elemental compositions of atmospheric particulate matter. By applying chemometric methods like principal component, hierarchical cluster and vertex component analysis, single chemical species of atmospheric aerosols can be unravelled. Multisensor hyperspectral imaging gains access to an understanding of single particle composition, linkage and coverage and will therefore assist source apportionment and chemical analysis on a sub-micron scale.

**A085 Role of Vibrational Progression Seen in Photoelectron Spectrum of PAHs in Astrophysical Environment**

Preeti Mishra, Lorenzo Avaldi, Paola Bolognesi, Kevin Prince, Robert Richter, Sarita Vig, Umesh Kadhane

Experimental (UV photoelectron spectroscopy) and theoretical (Franck-Condon factor calculations for vibrational progression) investigations were performed for two PAH molecules: pyrene and fluorene. The C-C trans-annular stretching in-plane mode around  $1400\text{ cm}^{-1}$  with  $a_g$  symmetry was found to be dominant mode of vibration in both experimental and theoretical spectrum, which is also observed in the infrared emission bands of interstellar medium (ISM). This indicates that vibrationally excited PAH cation due to UV photoionization contributes to the IR bands seen in ISM.

**A086 Vibrational Spectroscopy and Microscopy of Tree Pollen**

Laura Felgitsch, Hinrich Grothe, Bernhard Pummer, Bertrand Chazallon, Sebastien Facq

Pollen grains are covered with many different biochemical compounds, which are only loosely attached to the pollen. This mixture is analyzed by both Raman and infrared spectroscopy. The dominant signals in the pollen grain spectra are those from sporopollenin and carotenoids. The former is high-molecular and tightly bounded while the other compounds are extractable by water, which in turn differ significantly between species. Raman microscopy could dissolve the local distribution of these compounds of the grain surface.

## Portable Raman Systems

**A087 Tapping the Full Potential of Raman Spectroscopy**

Nina Schafroth, Münir Besli

In recent years, the technical development and miniaturisation of handheld Raman systems have carved the way for the then relatively unknown analytical technique: today, handheld Raman spectroscopy stands for fast, easy, and nondestructive analysis or identification of chemical substances. Increasing the interrogation area by implementation of the Orbital-Raster-Scan (ORS) technique, i.e., without compromising spectral resolution, has made it possible even for handheld devices to reliably determine heterogeneous samples in a matter of seconds.

**A088 Non-destructive and On-site Analysis of Lycopene in Intact Tomato Fruits with a Hand-held Raman Spectrometer**

Takuma Genkawa, Risa Hara, Tohru Ariizumi, Norio Yasuda, Kazuki Watanabe, Madahiro Watari, Yukihiro Ozaki

The feasibility of non-destructive, on-site analysis of lycopene in intact tomato fruits was investigated using a small and lightweight hand-held Raman spectrometer (Indicator, Serstech). In the obtained Raman spectra, intense bands at  $1510$  and  $1150\text{ cm}^{-1}$  arising from lycopene in tomato fruits were observed successfully owing to the resonance Raman effect and the baseline correction. In addition, the intensities of these bands from the high-lycopene cultivar were higher than those of the common cultivar bands.

A089 **Investigating the Bioequivalence of Valerian Sleep Aids Using Handheld Raman Spectroscopy**

Stephanie Farrant, Sulaf Assi, David Osselton

Valerian is one of the most commonly used herbal sleep aids. Valerian extract contains a whole range of active pharmaceutical ingredients (APIs) that contribute to its sleeping effect and include valeric acid, isovaleric acid, isovaltrate and valeranone. The bioequivalence of valerian depends on the concentration of valerian extract in different formulations. Therefore, this work aims at predicting the bioequivalence of valerian sleep aids using handheld Raman spectroscopy which is a rapid and non-destructive technique.

A123-pdp **Stand-Off Raman Spectroscopy and the SORS Effect: The Importance of Focus**  
Christopher Gasser, Thomas Aichinger, Bernhard Lendl

Stand-off Raman spectroscopy is a powerful technique in remote sensing applications. Recently, it has been shown that spatially offset Raman spectroscopy and time resolved Raman experiments can also be done at stand-off distances. However, there are several effects that influence all of the aforementioned techniques, like instrumental configuration (e.g. timing of the detector), as well as optical configuration. We present a study on the importance of focus of the telescope on stand-off SORS spectra.

## Material Science 1

A090 **FTIR Spectroscopic Investigation of the Biodegradability of LDPE/PLA Bioblends**  
Naima Belhaneche-Bensemra, Bahia Boubekeur, Valérie Massardier

The present work concerns the study of new biodegradable materials by mixing poly lactic acid (PLA), a biodegradable polymer, with low density polyethylene (LDPE), a current thermoplastic. For that purpose, LDPE/PLA blends of variable composition were prepared. Hydrolysis and soil burial tests were conducted. The weight loss of the samples with time was followed. The structural changes were investigated by FTIR spectroscopy. The two tests evidenced the fact that the studied blends are degradable. These results were confirmed by FTIR spectroscopy.

A091 **Moisture Induced Changes in Secondary Structure and Crystallinity of Human Fibrinogen Powders**

Verena Wahl, Otto Scheibelhofer, Ulrich Rössl, Stefan Leitgeb, Thomas deBeer, Johannes Khinast

The aim of this study was the investigation of protein structural changes upon moisture sorption using Raman and infrared spectroscopy. These changes were correlated with the relative crystallinity of human fibrinogen. A  $R^2$  of 0.953 was generated by correlating combined infrared and Raman data to the solid-state generated by Wide Angle X-ray Scattering (WAXS).

A092 **Vibrational Spectroscopy and Quantum Chemical Calculations Applied to the Study of Fluorinated Polymers**

Stefano Radice, Alberto Milani, Chiara Castiglioni

Fluorinated polymers constitute a performing class of polymers, useful when environmental conditions are demanding in terms of chemical/thermal resistance. Amorphous fluorinated polymers show unique optical properties, being almost totally transparent in a wide range of wavelength. Engineering of polymers requires also the capability to customize and control end groups. This study presents spectral band assignments in TFE based polymers, achieving structural and analytical information. Quantum Chemical Calculations was useful and effective to explore different chemical groups and vibrational eigenvectors.

A093 **Determination of Temperature-Dependent Stress in Semiconductor Power Devices by Raman Spectroscopy**

Ryuichi Sugie, Tomoyuki Uchida, Kenichi Kosaka, Aki Suzuki, Naoki Muraki

A procedure to determine the temperature-dependent stress in silicon carbide (SiC) power devices was developed using Raman spectroscopy. Compressive stress was observed near the interface between the SiC chip and solder. The observed compressive stress increased as temperature decreased. The difference of coefficients of thermal expansion is considered to be the main cause of the stress. These results indicate that this method is effective for determining the thermal stress not only at room temperature but at low and high temperatures.

A094 **Dispersion Analysis of Single Crystal Yttrium Orthosilicate**

Thomas Mayerhöfer, Sonja Höfer, Jürgen Popp

Dispersion analysis was performed on a single crystal of monoclinic yttrium orthosilicate ( $Y_2SiO_5$ ), an important laser material. The spectra have been analyzed by dispersion analysis using Lorentz oscillators as well as a 4 parameter oscillator model, which includes in contrast to the Lorentz oscillator frequency-dependent damping. The results will be presented and compared.

A095 **The Interaction of Polypyrrole with Methyl Orange and its Influence on Polypyrrole Morphology**

Zuzana Morávková, Ivana Šeděnková, Miroslava Trchová, Jaroslav Stejskal

If the oxidation of pyrrole is performed in the presence of methyl orange, the formation of nanotubes is observed instead of the granules. Methyl orange forms needle-like templates in the presence of chloride anions, that later lead the growth of polypyrrole nanotubes. FTIR and resonance Raman spectra were used to assess the molecular structure of polypyrrole and methyl orange. The interaction between the components has the form of protonation, methyl orange is capable of displacing other anions.

A096 **Terahertz Time-Domain and Low-Frequency Raman Spectroscopy of Crystalline and Glassy Pharmaceutical Indapamide**

Tatsuya Mori, Yukiko Kobayashi, Kei Iwamoto, Tomohiko Shibata, Hiroshi Matsui, Seiji Kojima

We investigate THz dynamics of crystalline and glassy pharmaceutical indapamide (IND) by THz time-domain spectroscopy (THz-TDS) and low-frequency Raman scattering (LFRS). Measured temperature range is from 8 K to 300 K. In the glassy IND, we found the obvious discrepancy of spectral shape between THz-TDS and LFRS. It suggests that the glassy IND may have centrosymmetry locally, although single IND molecule has no centrosymmetry.

A097 **Raman Study on Pentacene:  $C_{60}$  Bulk Heterojunction Films**

Yasuhiro Iwasawa, Tomoya Sasaki, Takanori Shibata, Yukio Furukawa

We have measured Raman spectra of bulk heterojunction films of pentacene: $C_{60}$  and pentacene- $d_{14}$ : $C_{60}$  in an organic solar cell. Only the  $C_{60}$  bands showed broadenings in bandwidth and downward shifts in peak frequency, which indicates that  $C_{60}$  is amorphous and pentacene is crystalline. The 514-, 453-, and 253- $cm^{-1}$  bands were attributed to pentacene- $C_{60}$  complex existing at pentacene/ $C_{60}$  interfaces. The relative intensity of the 1596- $cm^{-1}$  band to that of the 1532- $cm^{-1}$  band showed that pentacene molecules take a standing orientation.

A098 **Raman Spectroscopic Investigation of Structural Phase Transition in the Chain Ermanate Series  $CaCu_{1-x}Zn_xGe_2O_6$**

Andreas Hiederer, Andreas Reyer, Reinhard Gratzl, Günther J. Redhammer

The class of pyroxenes, with the general formula  $M_2M_1T_2O_6$ , are chain silicates and germanates. Mineral members of this group are very prevalent constituents of the Earth Crust and upper mantle. The investigated clinopyroxene-type structure of  $CaCu_{1-x}Zn_xGe_2O_6$ , shows a phase transition between  $P21/c$  and  $C2/c$  symmetry by changing Cu content from 0,90 to 0,88 apfu at 298 K. The target of this study is to follow the structural phase transition with confocal Raman spectroscopy as a function of chemistry and temperature.

A099 **Spectroscopic Determination of Compressive Stress of Zircon Inclusions in Gem Corundum From Mercaderes, Cauca, Colombia**

Manuela Zeug, Andrés Ignacio Rodríguez Vargas, Lutz Nasdala

The present study deals with Raman micro-spectroscopy for the non-destructive estimation of the degree of radiation damage of zircon crystals confined within corundum of metamorphic origin, and the determination of pressures acting on such inclusions. Among other inclusion minerals, we have analyzed several zircon inclusions inside seven gem-corundum samples originating from an alluvial deposit from Mercaderes, Cauca, Colombia.

A100 **Structural Characterization of Europium-Activated Zinc Tin Oxide Phosphor**

Tamara Ivetic, Goran Strbac, Bojan Miljevic, Ljubica Dacanin, Dragoslav Petrovic, Svetlana Lukic-Petrovic

Europium-activated ternary zinc tin oxide ( $Zn_2SnO_4$ ) was synthesized by high-energy ball-milling solid-state reaction method. X-ray powder diffraction analysis showed the formation of highly crystalline face-centered cubic  $Zn_2SnO_4$  spinel and the occurrence of three impurity-related diffraction peaks assigned to europium tin oxide ( $Eu_2Sn_2O_7$ ). The increased  $Zn_2SnO_4$  lattice constant means that some of the  $Eu^{3+}$  ions are incorporated in  $Zn_2SnO_4$  matrix. Raman scattering measurements have enabled verification and interpretation of the observed differences in  $Zn_2SnO_4$  structural characteristics induced by doping.

A101 **Crystallization of 1-Butyl-3-Methylimidazolium Chloride/Water Mixtures**

Nikolay Kotov, Adriana Šturcová, Alexander Zhigunov, Vladimír Raus, Jiří Dybal

1-Butyl-3-methylimidazolium chloride (bmimCl) is an ionic liquid (IL), with a mixture of interactions such as Coulombic, electron pair donor acceptor and hydrogen bonds between the ions. Clear understanding of the contribution of each type of interaction has not been fully achieved, but can be inferred by studying the properties of neat ILs or mixtures of ILs with solvents. The work presented here is an attempt to explain the effect of water on crystallization of the hygroscopic imidazolium-based bmimCl.

A102 **Characterization of Tannin-Furanic Rigid Foams by Multi-Wavelength Raman Spectroscopy**

Andreas Reyer, Gianluca Tondi, Alexander Petutschnigg, Maurizio Musso

Tannin-furanic rigid foams are innovative materials made of inexpensive organic ingredients, and are produced via an acid catalyzed polycondensation reaction between furfuryl alcohol and condensed flavonoids. The target of the present study is the characterization of the tannin-based rigid foams by multi-wavelength Raman spectroscopy in order to compare their spectral signature with that of the precursor materials. At present the most interesting information obtained deals with the still preserved organic nature of the tannin-furanic rigid foam compared to carbon materials.

A103 **Stability and Kinetics of Polymorphic Phase Transitions in  $\beta$ -Glycine**

Pavel Zelenovskiy, Timur Khazamov, Semen Vasilev, Daria Vasileva, Alla Nuravaeva, Dmitry Isakov, Vladimir Shur, Andrei Kholkin

Micro-Raman and piezoresponse force microscopy are used in this work to study of and polymorphic phase transitions in organic ferroelectric  $\beta$ -glycine and to establish its stability conditions. Detailed study of kinetics of to phase transition was performed by PFM, whereas Raman measurements allowed us to propose a microscopic description of the transition in the frame of the rigid molecules approximation.

A104 **Residual Stress-Fields Near Fractures in Radiation Damaged Zircon**

Andreas Artac, Lutz Nasdala, Gerlinde Habler, Rainer Abart

We present results of Raman-mapping on a polished section prepared from a heterogeneously radiation-damaged zircon crystal from Plešovice, Czech Republic. Our study focused on the internal stress pattern within a mildly radiation-damaged growth zone located between two strongly damaged zones. Due to strong volume expansion of the latter, the weakly radiation-damaged growth zone under discussion must be affected by tensile stress, which has been partially released by the opening of fractures.

- A105 **Visualisation of the Microstructure of Packaging Laminates by Spectroscopic Imaging Techniques and Chemometric Tools**  
Patricia Heussen, Gerard van Dalen, Robert Hoeve, Petra Groenendijk, Maria Sovago

Packaging laminates are composed of various layers that fulfil different functions. ATR-FTIR-imaging and Raman-imaging in combination with chemometric tools like PCA, K-mean clustering or MCR can be used to analyse the microstructure and result in useful information about the spatial distribution of the chemical compounds, defects and layer thickness of packaging materials. These images can be correlated to the DSC melting pattern and this technique can be used in the future to investigate the quality of these packaging foils.

- A106 **Spectroscopic Correlation of Mechanical Properties of PAM/PEO Polymer Blends**  
Gaurangkumar Patel, M. B. Sureshkumar, Purvi Patel

Dimensionally stable and free standing films of polymer blends' structural and mechanical properties were characterized. Mechanical properties are enhancing due to hydrogen bonding interaction between  $-\text{CONH}_2$  group of PAM and  $-\text{CH}_2\text{OH}$  group of PEO which is also confirmed by FTIR Spectra.

- A107 **Molecular Orientations of Nematic Liquid Crystals on Polar Surface**  
Kigook Song, Youngju Kim, Seungho Han

Orientation of nematic liquid crystal molecules on a polymer substrate depend on various molecular interactions at the interface. The vertical alignment mechanism of liquid crystals was studied on a substrate with different polarity. The planar alignment was obtained for positive LC whereas the vertical alignment for negative LC on the polar substrate. In the present study, relations between the anchoring transition of liquid crystals and the polarity of substrates were studied using polarized microscopy and FTIR spectroscopy.

- A109 **Vibrations and Reorientations of  $\text{H}_2\text{O}$  Molecules and  $\text{ReO}_4^-$  Anions and Phase Transition in  $[\text{Ca}(\text{H}_2\text{O})_2](\text{ReO}_4)_2$**   
Joanna Hetmanczyk, Lukasz Hetmanczyk

The polymorphism of the  $[\text{Ca}(\text{H}_2\text{O})_2](\text{ReO}_4)_2$  compound was investigated by means of differential scanning calorimetry. One reversible phase transition has been found at  $T = 261.6$  K (onset on heating). Vibrational-reorientational dynamics of  $\text{H}_2\text{O}$  ligands and  $\text{ReO}_4^-$  anions in the high- and low-temperature phases of  $[\text{Ca}(\text{H}_2\text{O})_2](\text{ReO}_4)_2$  was investigated by Fourier transform middle and far-infrared spectroscopy (FT-MIR and FT-FIR), Raman Spectroscopy (RS) and quasielastic and inelastic incoherent Neutron Scattering (QENS and IINS) methods.

- A110 **Raman and IR Studies of Niccolite Metal Formate Frameworks  $[(\text{CH}_3)_2\text{NH}_2][\text{Fe}^{\text{III}}\text{M}^{\text{II}}(\text{HCOO})_6]$  (M=Fe, Mg, Zn, Ni, Cu)**  
Mirosław Maczka, Aneta Ciupa, Maciej Ptak

Four novel heterometallic metal formate frameworks,  $[(\text{CH}_3)_2\text{NH}_2][\text{Fe}^{\text{III}}\text{M}^{\text{II}}(\text{HCOO})_6]$  with  $\text{M}^{\text{II}}=\text{Mg}$ , Zn, Ni and Cu, were synthesized. These compounds as well as the known  $[(\text{CH}_3)_2\text{NH}_2][\text{Fe}^{\text{III}}\text{Fe}^{\text{II}}(\text{HCOO})_6]$  formate were studied by Raman and IR spectroscopic methods. The obtained temperature-dependent data were interpreted in terms of structural and magnetic phase transitions in the iron compound as well as evolution of dynamic disorder into a static disorder in the other studied compounds.

- A111 **A Spectroscopic Study of the Hydrogen-Bonded Semiconductor Quinacridone in View of Extended Chemical Stability**  
Christina Enengl, Sandra Enengl, Marek Havlicek, Philipp Stadler, Eric D. Glowacki, Markus Scharber, Kurt Hingerl, Eitan Ehrenfreund, Helmut Neugebauer, Niyazi S. Sariciftci

One major challenge in organic electronics concerns the stability of organic semiconductor materials, thus the operational lifetime of devices. Recent reports have shown that hydrogen-bonded pigments of the indigoid family, like quinacridone, are examples for extraordinary chemical stability. Here, we present in-situ spectroscopic studies on quinacridone as compared to pentacene confirming different spectral response of their radical cations. While in pentacene the barrier between doping and irreversible overoxidation is small, this stability towards overoxidation is increased by the hydrogen-bonded quinacridone.

- A112 **First Order Pressure-induced Amorphization in  $\text{Sm}_2\text{Mo}_4\text{O}_{15}$  System**  
Waldeci Paraguassu, Silvio Domingos Silva Santos, Mirosław Maczka, Paulo de Traso Cavalcante Freire

In this work, high-pressure Raman experiments were performed on  $\text{Sm}_2\text{Mo}_4\text{O}_{15}$  up to 7.9 GPa. the assignment of vibrational modes at ambient pressure was made based on lattice dynamics calculations. A pressure-induced structural phase transition was identified at 4.5 GPa, which results in the change of structure from triclinic, space group  $\bar{1}$ , to most likely monoclinic, space group P2/m. Upon further increase in pressure  $\text{Sm}_2\text{Mo}_4\text{O}_{15}$  exhibits irreversible amorphization at 5.0 GPa. We show that in contrast to previously studied  $\text{Dy}_2\text{Mo}_4\text{O}_{15}$  and many other molybdates and tungstates, the pressure-induced amorphization in  $\text{Sm}_2\text{Mo}_4\text{O}_{15}$  has strongly first-order character. Analysis of the Raman data indicates that the most likely scenario of the amorphization process is chemical decomposition into  $\text{MoO}_3$  and samarium molybdates of unknown chemical composition.

- A113 **Non-destructive Evaluation of Tissue-Engineered Cartilage by THz-TDS**  
Ikuya Moritomo, Ayaka Kamada, Takuma Ota, Seizi Nishizawa, Katsuko Furukawa, Takashi Ushida

We intended to establish a novel non-invasive evaluation method of cartilage tissue with terahertz time-domain spectroscopy (THz-TDS).the purpose of this research was to clarify the correlation between THz spectra and cartilage characteristics. In this paper, we determined water molecular relaxation strength, which parameter corresponds to amount of free water within tissue, thus free/bound water ratio was yielded. We also performed mechanical and biochemical tests and discovered that THz technology could be a promising tissue evaluation method.

- A114 **Temperature and Magnetic Field Dependent Raman Spectroscopy on  $(\text{La}_{0.65}\text{Pr}_{0.45})_{0.7}\text{Ca}_{0.3}\text{MnO}_3$**   
Sebastian Merten, Oleg Shapoval, Bernd Damaschke, Vasily Moshnyaga, Konrad Samwer

Crucial for understanding the physics of the manganites is the strong electron-phonon coupling due to the Jahn-Teller effect. Here we report on a detailed Raman study of  $(\text{La}_{0.65}\text{Pr}_{0.45})_{0.7}\text{Ca}_{0.3}\text{MnO}_3$  thin films. We observed four pronounced modes at  $235\text{ cm}^{-1}$ ,  $434\text{ cm}^{-1}$ ,  $485\text{ cm}^{-1}$  and  $609\text{ cm}^{-1}$  whereupon the last two can be assigned to an anti-stretching and stretching mode, respectively, due to the Jahn-Teller (JT) effect. Furthermore, the temperature as well as magnetic field dependent Raman spectra show a correlation with the metall-insulator transition and the colossal magnetoresistance. Due to the rise of a sharp feature and the disappearance of the broad JT band, the evolution of the spectra suggest a transition from a disordered to a more ordered structure. Financial support from DFG, SFB 1073 (TP B04) is acknowledged.

- A115 **New Advances in Raman Study of Polyvinylchloride Structure**  
Gulnara Nikolaeva, Kirill Prokhorov, Daria Aleksandrova, Elena Sagitova, Tatyana Vlasova, Pavel Pashinin, Colin Jones, Simon Shilton

In this work we present an extensive study of polarized Raman spectra of a number of industrial grades of polyvinylchloride (PVC) powder and films, prepared from solutions of tetrahydrofuran and acetophenone. We determined the number and the spectral characteristics of Raman lines of PVC and residual solvents. these data were used to define more accurately the assignment of PVC Raman lines to particular vibrations.

**A116 Back-Scattering Raman Spectroscopy of Mesoporous Titania Aerogels with Different Hydrolysis Levels**

Sima Sadriyeh, Rasoul Malekfar, Ehsan Talebian

Mesoporous titania aerogels with different hydrolysis levels were prepared by sol-gel method and subsequent drying by supercritical carbon dioxide extraction at 75°C and 220 atmosphere. The samples were calcined for 2 hours at 450°C. Raman scattering spectroscopy was carried out before and after the calcination, the diffraction peaks of anatase were found for the calcined samples while the uncalcined ones were amorphous. The microstructure and total surface area of the aerogels were evaluated by N<sub>2</sub> adsorption and BET.

**A117 Micro-Raman Study of Heterogeneity in Binder-Free Lithium Titanate**

Boris Slautin, Dmitry Pelegov, Pavel Zelenovskiy, Denis Alikin, Eugene Kiselyov, Vadim Gorshkov, Andrei Kholkin

*Not provided*

**A118 Hydrogen Bonding and Its Effect on Alkoxysilane Condensation**

Killian Barton, Brendan Duffy, Brendan Kneafsey, Eimear Fleming, Deirdre Ledwith

Raman and FTIR spectroscopy were used to investigate the condensation behaviour of an alkoxysilane coupling agent. The alkoxysilane coupling agent is used to bind rubber to metal in an industrial injection moulding process. An analogue of the application environment was prepared and Raman and FTIR spectra recorded as a function of temperature. Hydrogen bonding was seen to control the condensation of the alkoxysilane coupling agent.

**A119 Raman Spectroscopy of L-Phenylalanine-L-Phenylalaninium Nitrate Subjected to High Pressure**

Katiane Pereira da Silva, Paulo de Tarso C. Freire, Maciej Ptak, J. Mendes Filho, W. Paraguassu

The L-phenylalanine is an essential amino acid that takes part of several bio chemicals processes related to the production of some human proteins and enzymes. This essential amino acid is converted to the L-tyrosine amino acid by means of the L-phenylalanine hydroxylase. The L-tyrosine plays an important role in the synthesis of different chemicals that transmit signals between the nerve cells and the brain, such as the dopamine, nor-epinephrine and epinephrine. The deficiency of that enzyme lifts the L-phenylalanine concentration in blood what can lead to some diseases like phenylketonuria, where the liver cannot produce enough tyrosine. As a result, the organism cannot produce fundamental substances and this anomaly can yield irreversible neurological illness.

**A124-dpd Vibrational Spectra, First-Order Molecular Hyperpolarizability of a Potential Antihistaminic Drug, Diphenylpyraline Hydrochloride (Di.HCl)**

Seda Sagdinc, Dilek Erdas

Diphenylpyraline hydrochloride (Di.HCl), (4-benzhloxy-1-methylpiperididine) is a kind of antihistamine drug that internationally available. The FT-IR (4000-400 cm<sup>-1</sup>) and FT-Raman (3500-50 cm<sup>-1</sup>) spectra of diphenylpyraline hydrochloride have been recorded and analyzed. The assignment of bands observed in vibrational spectra have been made by comparison of their theoretical vibrational frequencies obtained using a DFT/B3LYP/6-311G++(d,p) method. The calculated first-order molecular hyperpolarizability value is comparable with the reported values and attractive object for future studies of non-linear optics.

9:00  
TUPL1**Single-Molecule Raman Spectromicroscopy Down to Sub-nm Resolution**Zhenchao Dong

The vibrational spectroscopy based on tip-enhanced Raman scattering (TERS) has opened a path to obtain enhanced vibrational signals of molecules thanks to strongly localized plasmonic field originated at the tip. I shall first demonstrate a TERS spatial resolution down to  $\sim 0.5$  nm for a single type of molecules and then use it to chemically distinguish two adjacent but different molecules in real space and address the issue of how close and how similar these different molecules can be.



Dr. Zhen-Chao Dong is currently a full professor at University of Science and Technology of China (USTC). His research interest is in the field of single-molecule optoelectronics and nanoplasmonics, particularly on STM based single-molecule electroluminescence and single-molecule Raman scattering. The aim of his research is to understand the underlying physics that governs the light generation, energy transfer, and molecular plasmonics at the nanoscale, and to explore scientific basis for future technologies related to information, energy, and bio.

9:35  
TUPL2**Vibrational Spectroscopy with Laser Frequency Combs**Nathalie Picqué

New opportunities for Fourier transform spectroscopy are opened up by laser frequency combs. Nonlinear Fourier transform spectroscopy demonstrates an intriguing potential for Doppler-free spectroscopy as well as for Raman hyperspectral imaging.



Nathalie Picqué is a senior permanent research scientist at the Max Planck Institute of Quantum Optics and the Ludwig Maximilian University (Munich, Germany). Her research interests include laser frequency combs and the development of new techniques of molecular spectroscopy. She received her doctor degree in Physics in 1998 from Université Paris-Sud Orsay (France). She has been a permanent scientist with the Centre National de la Recherche Scientifique in France from 2001 until 2011. The awards she received include the 2007 Bronze Medal of the CNRS, the 2008 Jean Jerphagnon Prize of the French Physical Society and the 2013 Coblenz Award.

## Single-Molecule Raman Spectromicroscopy Down to Sub-nm Resolution

Zhenchao Dong

Hefei National Laboratory for Physical Sciences at the Microscale and  
Synergetic Innovation Center of Quantum Information & Quantum Physics,  
University of Science and Technology of China (USTC), Hefei 230026, China

Keywords: Vibrational spectroscopy, tip-enhanced Raman spectroscopy, super-resolution imaging, single-molecule Raman scattering, plasmonics

Visualizing individual molecules with chemical recognition is a longstanding target in catalysis, bio-science, nanotechnology, and materials science. Molecular vibrations provide a valuable “fingerprint” for this identification. The vibrational spectroscopy based on tip-enhanced Raman scattering (TERS) has opened a path to obtain enhanced vibrational signals thanks to the strong localized plasmonic field at the tip apex. In this talk, I shall demonstrate single-molecule Raman spectroscopic imaging with unprecedented sub-nm spatial resolution (figure 1), resolving even the inner structure of a single molecule and its configuration on the surface<sup>1</sup>. This is achieved by a delicate

plasmon enhanced nonlinear TERS technique that invokes a double-resonance process and resultant nonlinear optical effect, thanks to the exquisite tuning capability provided by low-temperature ultrahigh-vacuum scanning tunneling microscopy (STM)<sup>2</sup>. I shall also show the powerful application of this technique for chemically distinguishing adjacent different molecules in real space and address the issue of how close and how similar these different molecules can be. These findings should open up new avenues for probing and controlling nanoscale structures, catalysis, photochemistry, and even DNA sequencing, all at the sub-nm and single-molecule scale.

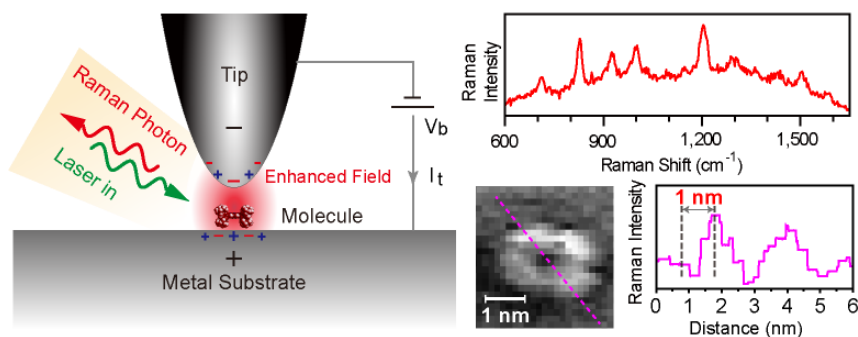


Figure 1. Single-molecule Raman imaging with sub-nm resolution by STM-controlled TERS

<sup>1</sup> R. Zhang, Y. Zhang, Z. C. Dong\*, S. Jiang, C. Zhang, L. G. Chen, L. Zhang, Y. Liao, J. Aizpurua, Y. Luo, J. L. Yang, and J. G. Hou\* (2013). *Nature* 498, 82-86.

<sup>2</sup> Z. C. Dong\*, X. L. Zhang, H. Y. Gao, Y. Luo, C. Zhang, L. G. Chen, R. Zhang, X. Tao, Y. Zhang, J. L. Yang, J. G. Hou\* (2010). *Nature Photonics* 4, 50-54.

## Vibrational Spectroscopy With Laser Frequency Combs

Nathalie Picqué<sup>1,2</sup>

1. Max-Planck-Institut für Quantenoptik, Hans-Kopfermannstr. 1, 85748 Garching, Germany
2. Ludwig-Maximilians-Universität München, Fakultät für Physik, Schellingstr. 4/III, 80799 Munich, Germany  
nathalie.picque@mpq.mpg.de

Keywords: Ultrashort pulse laser, Fourier transform spectroscopy, absorption, Raman, two photon.

Laser frequency combs [1] are coherent sources which spectrum consists of several hundreds thousand sharp and evenly spaced spectral lines. A mode-locked femtosecond laser with a regular pulse train can for instance give rise to a comb spectrum of laser modes with a spacing precisely equal to the pulse repetition frequency. Fifteen years ago, such laser frequency combs have revolutionized the art measuring the frequency of light. The invention of the frequency comb technique has been motivated by precision laser spectroscopy of simple atoms. Today, frequency combs are finding applications far beyond the original purpose. Emerging applications range from fundamental research in astronomy or attosecond science to telecommunications and satellite navigation. Laser combs are becoming powerful instruments for broadband molecular spectroscopy and by creating new opportunities for Fourier transform nonlinear spectroscopy, such as two-photon spectroscopy or coherent Raman spectroscopy.

Recent experiments of multi-heterodyne frequency comb Fourier transform spectroscopy (also called dual-comb spectroscopy) have demonstrated that the precisely spaced spectral lines of a laser frequency comb can be harnessed for new techniques of linear absorption spectroscopy [2-5]. The light from a first comb is superimposed on a second frequency comb

with slightly different repetition frequency. A single fast photodetector then produces an output signal with a comb of radio frequencies due to interference between pairs of optical comb lines. The optical spectrum is thus effectively mapped into the radio frequency regime, where it becomes accessible to fast digital signal processing. The first proof-of-principle experiments have demonstrated a very exciting potential of dual-comb spectroscopy without moving parts for ultra-rapid and ultra-sensitive recording of complex broad spectral bandwidth absorption molecular spectra. Compared to conventional Michelson-based Fourier transform spectroscopy, recording times could be shortened from seconds to microseconds, with intriguing prospects for spectroscopy of short lived transient species. The resolution improves proportionally to the measurement time. Therefore longer recordings allow high resolution spectroscopy of molecules with extreme precision, since the absolute frequency of each laser comb line can be known with the accuracy of an atomic clock.

Ongoing developments will expand the range of applications of this new spectroscopy and thus they hold much promise for new approaches to sensing of gaseous, liquid and solid-state samples. Mid-infrared frequency combs [6-9] will interrogate the fundamental vibrational transitions of molecules resulting in

additional sensitivity. Miniaturized frequency comb generators [7] might even lead to chip-scale sensors.

Moreover, since laser frequency combs involve intense ultrashort laser pulses, nonlinear interactions can be harnessed. Broad spectral bandwidth ultra-rapid nonlinear molecular spectroscopy and imaging with two laser frequency combs is

demonstrated with coherent Raman effects [10,11] and two-photon excitation [12]. Real-time multiplex accessing of hyperspectral images may dramatically expand the range of applications of nonlinear microscopy. Two-photon dual-comb spectroscopy opens up opportunities [13] for Doppler-free spectroscopy of molecules.

- [1] T.W. Hänsch, Nobel Lecture: Passion for Precision, *Rev. Mod. Phys.* **78**, 1297-1309 (2006).
- [2] F. Keilmann, C. Gohle, R. Holzwarth, Time-domain mid-infrared frequency-comb spectrometer, *Opt. Lett.* **29**, 1542-1544 (2004).
- [3] I. Coddington, W.C. Swann, N.R. Newbury, Coherent Multiheterodyne Spectroscopy Using Stabilized Optical Frequency Combs, *Phys. Rev. Lett.* **100**, 013902 (2008).
- [4] B. Bernhardt, A. Ozawa, P. Jacquet, M. Jacquy, Y. Kobayashi, T. Udem, R. Holzwarth, G. Guelachvili, T.W. Hänsch, N. Picqué, Cavity-enhanced dual-comb spectroscopy, *Nature Photonics* **4**, 55-57 (2010).
- [5] T. Ideguchi, A. Poisson, G. Guelachvili, N. Picqué, T.W. Hänsch, Adaptive real-time dual-comb spectroscopy, *Nature Communications* **5**, 3375 (2014).
- [6] A. Schliesser, N. Picqué, T.W. Hänsch, Mid-infrared frequency combs, *Nature Photonics* **6**, 440-449 (2012).
- [7] C.Y. Wang, T. Herr, P. Del'Haye, A. Schliesser, R. Holzwarth, T. W. Hänsch, N. Picqué and T. J. Kippenberg, Mid-infrared optical frequency combs at 2.5  $\mu\text{m}$  based on crystalline microresonators, *Nature Communications* **4**, 1345 (2013).
- [8] S. Chaitanya Kumar, A. Esteban-Martin, T. Ideguchi, M. Yan, S. Holzner, T.W. Hänsch, N. Picqué, M. Ebrahim-Zadeh, Few-cycle broadband mid-infrared optical parametric oscillator pumped by a 20-fs Ti:sapphire laser, *Laser Photonics Rev.* **8**, L86–L91 (2014).
- [9] B. Kuyken, T. Ideguchi, S. Holzner, M. Yan, T.W. Hänsch, J. Van Campenhout, P. Verheyen, S. Coen, F. Leo, R. Baets, G. Roelkens, N. Picqué, An octave-spanning mid-infrared frequency comb generated in a silicon nanophotonic wire waveguide, *Nature Communications* **6**, 6310 (2015).
- [10] T. Ideguchi, S. Holzner, B. Bernhardt, G. Guelachvili, N. Picqué, T.W. Hänsch, Coherent Raman spectro-imaging with laser frequency combs, *Nature* **502**, 355-358 (2013).
- [11] T. Ideguchi, B. Bernhardt, G. Guelachvili, T.W. Hänsch, N. Picqué, Raman-induced Kerr effect dual-comb spectroscopy, *Optics letters* **37**, 4498-4500 (2012).
- [12] A. Hipke, S.A. Meek, T. Ideguchi, T.W. Hänsch, N. Picqué, Broadband Doppler-limited two-photon and stepwise excitation spectroscopy with laser frequency combs, *Phys. Rev. A* **90**, 011805(R) (2014).
- [13] A. Hipke, S. A. Meek, G. Guelachvili, T.W. Hänsch, and N. Picqué, "Doppler-free Broad Spectral Bandwidth Two-Photon Spectroscopy with Two Laser Frequency Combs," in *CLEO: 2013, OSA Technical Digest (online)* (Optical Society of America, 2013), paper CTh5C.8.

# VERTEX



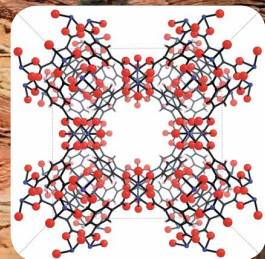
VERTEX 70-70v Fourier Transform  
FIR-MIR Research Functionality

## VERTEX FM Main Application Fields

- Inorganic and organometallic chemistry
- Studies on polymer filler material and color pigments
- Geological and rock analysis
- Pharmaceutical fillers and active agent measurements
- Polymorphs differentiation
- Crystallinity identification (e.g. plastics explosives)
- Semiconductor development and research

VERTEX FM is an FT-IR spectrometer technology capable of covering the FIR/THz and MIR spectral ranges in a single scan. No exchange of optical components or merging of spectra is needed to obtain data from the FIR/THz through the MIR. This innovative and unique development is no longer a dream for many spectroscopists. This new VERTEX FM functionality once again demonstrates Bruker's leadership and expertise in continuing to improve the use of infrared analysis and to meet new challenges in various application fields.

Contact us for more details: [www.bruker.com/vertex](http://www.bruker.com/vertex)



### Bruker Optik GmbH

Rudolf-Plank-Str. 27  
76275 Ettlingen  
Tel. +49 7243 504 2000  
Fax. +49 7243 504 2050  
E-Mail: [info@brukeroptics.de](mailto:info@brukeroptics.de)

10:40  
TU101-inv **Tip-Enhanced Raman Spectroscopy - A Compelling Device for Amyloid Fibril Analysis**

Tanja Deckert-Gaudig, Dmitry Kurouski, Igor Lednev, Volker Deckert

Amyloid fibril analysis is of great interest since such elongated fiber-like protein structures are associated with diseases like Alzheimer disease and diabetes type II. We will show that the specificity, sensitivity and high spatial resolution of tip-enhanced Raman spectroscopy (TERS) qualify this technique to chemically characterize fibrils on the single particle level. The acquired data enable a distinction of chemical composition and peptide secondary structures and might help developing an appropriate reagent for fibril annihilation.

11:00  
TU102 **Resonance Raman Spectroscopy Reveals a Novel Intermediate in the Catalytic Cycle of [FeFe] Hydrogenase**

Sagie Katz, Marius Horch, Jens Noth, Ingo Zebger, Thomas Happe

A combined approach of low-temperature IR and resonance Raman spectroscopy allowed us to experimentally observe a novel metastable intermediate of [FeFe]-hydrogenase, Hred. Based on an unusual electronic configuration, Hred is identified as the missing first intermediate of the catalytic cycle, providing valuable insights into biological hydrogen evolution. This thermodynamically unstable species is induced by the laser probe light and kinetically trapped at cryogenic temperatures, illustrating the capability of low-temperature spectroscopy to capture otherwise inaccessible intermediates in metalloproteins.

11:15  
TU103 **Resonance Raman Spectroscopy for Analysis of Amino Acids**

Martin Höhl, Merve Meinhardt-Wollweber, Uwe Morgner, Heike Schmitt, Thomas Lenarz

The composition of inner ear fluids is an important factor in human hearing and cannot be measured non-invasively so far. We investigate Raman scattering for this purpose. In order to reach physiological concentrations, resonance Raman scattering in the ultraviolet is used to gain a high sensitivity. An optical parametric oscillator is applied for recording the resonance profiles of amino acids.

11:30  
TU104 **Carotenoids, Hemoproteins and the “Life Band” – Raman Microimaging of Live Rhodotorula Mucilaginosa Cells**

Jan Pukalski, Marta Pacia, Katarzyna Turnau, Malgorzata Baranska, Agnieszka Kaczor

“Raman signature of life” is a unique spectroscopic feature related to mitochondria activity, present both in animal and yeast cells. The latter contain also flavohemoglobins and carotenoids playing a role in detoxification and antioxidative mechanisms. Raman imaging of live *Rhodotorula mucilaginosa* cells grown in aerobic, anaerobic conditions and diazinone presence were undertaken. Analysis of differences in cells grown upon various environments and a phenotypic switch due to oxidative phosphorylation recovery enabled to interrelate carotenoids, hemoproteins and “Raman signature of life”.

11:45  
TU105 **Raman Spectroscopy and SEM Study on Microorganisms for Applications in the Field of Biofuels and Biopolymer Production**

Ota Samek, Stanislav Obruèa, Andrea Haroniková, Zdenik Pilát, Silva Bernatová, Kamila Hrubanová, Jan Ježek, Vladislav Krzyžánek, Ivana Márová, Pavel Zemánek

Main aim of our investigations was to study – using Raman spectroscopy and scanning electron microscopy (SEM) – how different cultivation conditions influence production of oil, carotenoids, and biopolymers in selected microorganisms. Thus, all matrix changes within the studied cells introduced by stress response mechanisms can be visualized (SEM) and chemically characterized/monitored (Raman spectroscopy).



10:40  
TU501 **Raman Spectra of Carriers in Ionic-Liquid-Gated Transistors Fabricated with Poly(2,5-bis(3-tetradecylthiophen-2-yl)thieno[3,2-b]thiophene)**

Yukio Furukawa, Kotaro Akiyama, Jun Yamamoto

Raman spectral of an ionic-liquid-gated polymer transistor fabricated with poly(2,5-bis(3-tetradecylthiophen-2-yl)thieno[3,2-b]thiophene) (PBTTT-C<sub>14</sub>) and an ionic liquid [BMIM][TFSI] as a function of the gate voltage with excitation at 785 nm. Positive polarons are generated in the range between 0.0 and -1.4 V, whereas positive bipolarons are generated in the range above -1.2 V. The drain current of the transistor rose at -1.2 V and showed the maximum at -1.9 V. Thus, positive bipolarons are major carriers in the transistor.

11:00  
TU502 **Chemical Mapping in Light-Emitting Electrochemical Cells**

Mohammad Javad Jafari, Jiang Liu, Isak Engquist, Thomas Ederth

We show that infrared microscopy is a robust tool for in-situ monitoring of doping-dedoping reactions and ion diffusion in electroactive polymers. We have studied a light-emitting electrochemical cell with a MEH-PPV/PEO/KCF<sub>3</sub>SO<sub>3</sub> active layer, and successfully monitored time-resolved ion (CF<sub>3</sub>SO<sub>3</sub>) diffusion profiles and polymer (MEH-PPV) doping under forward bias, and subsequent dedoping at zero bias. In conclusion, we demonstrate that infrared microscopy has great potential for monitoring materials reactions in polymer science and organic electronics.

11:15  
TU503 **Investigation onto the Degradation Mechanisms Affecting Long Term Stability of Hybrid and Organic Photovoltaic Devices by Means of Raman Spectroscopy**

Antonio Agresti, Sara Pescetelli, Aldo Di Carlo

Stability of hybrid (dye sensitized solar cell- DSCs) and organic (small molecule solar cell- SMSCs) photovoltaic devices is investigated by means of resonant Raman spectroscopy under real working conditions. When DSC experiences reverse bias condition due to shadowing phenomena in a module, polyiodides formation in electrolyte solution and dye molecule degradation are detected. On the other hand thermal stress (85°C) on donor/ acceptor (ZnPc/C<sub>60</sub>) planar heterojunction based SMSC is discover to be responsible for the coarsening of C<sub>60</sub> grains, likely explaining the decrease in devices performance.

11:30  
TU504 **FTIR-Spectroscopic Investigations on the Absorption of Metamaterial Multi-Arrays Built by Submicron Single-Structures**

Gabriele Eder, Christian Brandl, Boril Chernev, Astrit Shoshi, Hubert Brückl

Metamaterials consist of artificial periodic structures with unusual optical properties. These materials can show a variable/tunable absorption behavior for electromagnetic irradiation (infrared region) in dependence on the dimensions and arrangement of the metallic sub-micron periodic structures applied on the surface. Fourier Transform InfraRed spectroscopic (FTIR) reflection measurements on arrays of absorber elements were performed in order to elaborate their selective absorption behavior.

11:45  
TU505 **Structurally Dissimilar Phase Separation in La<sub>5/8-y</sub>Pr<sub>y</sub>Ca<sub>3/8</sub>MnO<sub>3</sub> Thin Films**

Dileep K. Misra, R. Rawat, V.G. Sathe

Epitaxial La<sub>5/8-y</sub>Pr<sub>y</sub>Ca<sub>3/8</sub>MnO<sub>3</sub> (y = 0.45) thin films on LaAlO<sub>3</sub> substrate are prepared by pulsed laser deposition technique. The strain disorder is incorporated into the films by strain relaxation. Presence of uniform strain is found to stabilize insulating phase while strain disorder favours metallic phase. By low temperature Raman spectroscopy and Raman mapping structural aspect of metallic and insulating phases is investigated and found to be structurally dissimilar having R3-C and P2<sub>1</sub>/m like symmetries respectively.

10:40  
TU601**Tip-Enhanced Raman Scattering Study on the Nanoscale Features of Epitaxial Graphene**Sanpon Vantasin, Toshiaki Suzuki, Yoshito Tanaka, Tamitake Itoh, Tanabe Ichiro, Yasunori Kutsuma, Tadaaki Kaneko, Yukihiro Ozaki

Nanoscale characterization of epitaxial graphene is crucial because of the existence of nanostructure and strain variations, which can affect both physical and electronic attributes of graphene. In this study, these nanoscale features were characterized using tip-enhanced Raman spectroscopy (TERS). For the first time, the relaxation of compressive strain on a single nanoridge of epitaxial graphene was measured spectroscopically. The results confirm many speculations in previous studies about nanoscale effects and origin of the nanostructures.

11:00  
TU602**Application of Raman Spectroscopy and *in Situ* Raman Spectroelectrochemistry in the Studies of Isotopically Labeled Graphene Heterostructures**Martin Kalbac, Johan Ek Weis, Sara Costa, Jana Vejpravova, Mildred Dresselhaus

Recent advances in the growth of graphene by chemical vapor deposition allow preparing isotopically labeled graphene samples. In this study we compare isotopically labeled turbostratic two-layered graphene and graphene–BN–graphene heterostructure. We will review our results obtained on the analysis of Raman features of these low dimensional materials in neutral and doped state.

11:15  
TU603**Resonance Raman Spectroscopy of Extreme Nanowire Systems**Joe Spencer, Liam McDonnell, Reza Kashtiban, Gavin Bell, Eric Faulques, Jeremy Sloan, David Smith

Extreme nanowires are wires at the fundamental limit of the nanoscale, just a few atoms in diameter. These new materials exhibit physics that is not merely further miniaturisation of a larger nanomaterial, but entirely new. We demonstrate new vibrational modes appearing in extreme quantum confined materials and highlight the importance of Resonance Raman spectroscopy in identifying optical and vibrational transitions in extreme nanowires that cannot be as easily achieved by other means.

11:30  
TU604**The Structure of Metal - Carbon Nanotube's Coating Interface, the Effect of Interaction with Albumin**Aleksandra Weselucha-Birczyńska, Ewa Stodolak-Zych, Sylvia Turrell, Franciszek Cios, Magdalena Krzuś, Aleksandra Benko, Wiktor Niemiec, Marta Błażewicz

An analysis of the interface of the titanium support and CNTs layer deposited on the titanium surface was performed. The amount points disorder differentiates the layers of CNTs and phase boundary as well as their bottom and top layers. Depending on the thickness of the CNT layer, the interaction between the CNT and the protein is different, reflected in the albumin conformational changes. The model for the interaction of CNTs with protein was confirmed by spectroscopic, microscopic and physicochemical analyses.

11:45  
TU605**Infrared Attenuated Total Reflection Spectroscopy for the Characterization of Gold Nanoparticles in Solution**Ángela I. López-Lorente, Markus Sieger, Miguel Valcárcel, Boris Mizaikoff

In-situ synthesis of bare gold nanoparticles (AuNPs) mediated by stainless steel was monitored via infrared attenuated total reflection (IR-ATR) spectroscopy. As nanoparticles were formed, a layer of particles was deposited at the SiO<sub>2</sub> ATR waveguide surface and absorption bands of water increased resulting from SEIRA effects arising from the presence of the AuNPs within the evanescent field. The suitability of IR-ATR spectroscopy for investigating changes of nanoparticles in solution including their aggregation and sedimentation process was confirmed.

10:40 **Recent Advances in EC-QCL Technology and Its Use in Spectroscopic Sensing**

TU801-inv Joachim Wagner, Ralf Ostendorf, Jan Grahmann, Andre Merten, Stefan Hugger, Lorenz Butschek, Frank Fuchs, Dusan Boskovic, Harald Schenk

Widely tunable quantum cascade lasers (QCL) are well suited for spectroscopic sensing exploiting characteristic finger print absorption of molecules in the mid-infrared (MIR). This includes on- and in-line MIR spectroscopic sensing which requires analytical data to be taken at high sampling rates. We report on recent advances in broadband-tunable MIR EC-QCL technology as well as their use in spectroscopic analysis. Results are presented on rapid scan EC-QCL, employing a custom-made MEMS scanning grating in Littrow-configuration as wavelength-selective optical feedback element.

11:00 **Monolithic Tunable MIR-Lasers from mirSense**

TU802 Mathieu Carras, Gregory Maisons, Clement Gilles, Mickael Brun

mirSense develops monolithic solutions for tunable MIR-laser sources using the quantum cascade laser technologies, coupled with photonics integrated circuit (PIC) in the mid-infrared. We show the results and performances of different approaches, with either InP or silicon as a substrate for the PIC.

11:15 **Ring Quantum Cascade Lasers for Infrared Spectroscopy**

TU803 Rolf Szedlak, Martin Holzbauer, Donald MacFarland, Tobias Zederbauer, Hermann Detz, Aaron Maxwell Andrews, Werner Schrenk, Gottfried Strasser

Quantum cascade lasers have proven to be powerful and compact devices for infrared spectroscopy. Compared with conventional ridge lasers, ring QCLs provide strongly collimated emission beams. Depending on the grating, the beam can have an intensity minimum or maximum in the center. We show how this light beam can be additionally focused with a gradient index based metamaterial. In addition, we propose a novel laser array design, which makes beam combining optics obsolete.

11:30 **Recent Results on Performance Optimization of QCLs for Spectral Coverage, Heat Dissipation, and Output Power**

TU804 Antoine Müller, Alfredo Bismuto, Stéphane Blaser, Tobias Gresch, Olivier Landry, Richard Maulini, Romain Terazzi

In this presentation the results of recent optimization efforts performed at Alpes Lasers SA will be presented. For applications such as hand held battery powered apparatus, devices with total dissipation lower than one Watt are presented. Focus will also be put on applications related to extended tuning devices, showcasing DFB devices with up to  $10 \text{ cm}^{-1}$  of tuning. Finally watt level output power in the 4 to 5 micron region will be presented.

11:45 **QCL Frequency Comb Technology for Mid-Infrared Sensing**

TU805 Markus Mangold, Andreas Hugi, Markus Geiser, Gustavo Villares, Jérôme Faist, Lukas Emmenegger

At IRsweep, we develop a spectroscopy platform for industrial applications based on semiconductor quantum cascade laser (QCL) frequency combs. The platform's key features will be an unmatched combination of optical bandwidth up to 100 wavenumbers, spectral resolution down to 100 kHz, and acquisition speed of ten to hundreds of  $\mu\text{s}$ . The robust platform opens doors to beforehand unreachable applications.

13:30  
TU106**Oxygen Reduction and Water at the Semiconductor/Solution Interface Probed by Stationary and Time-resolved ATR-IR Spectroscopy Coupled to Electrochemical Experiments and DFT Calculations**Andreas Erbe, Stefanie Pengel, Fang Niu, Simantini Nayak, P. Ulrich Biedermann, Rochus Schmid, Stefan Wippermann, Francois Gygi, Giulia Galli, Stefanie Tecklenburg

Changes at the semiconductor electrode/electrolyte interface are probed in situ and operando during the oxygen reduction reaction (ORR) and during simple electrode polarisation by internal reflection IR absorption spectroscopy. Results gathered by FTIR show intermediate species in the ORR and changes in electrode solvation during polarisation. Using a quantum cascade laser enables high time resolution and insight into the electrode kinetics of intermediate steps in the ORR. Computations of spectra are needed for a full interpretation of the spectra.

13:50  
TU107**Influence of Surface Structure on Biofilm Growth**Dennis Hore, Tasha Jarisz, Sarah Kowallik, Sandra Roy, Paul Covert

The behaviour of bacterial biofilms is critically sensitive to the nature of the surface on which they grow. Nonlinear vibrational spectroscopy monitors the influence of the interfacial environment on the growth of biofilms on silica. Comparing the response of the O-H stretching region to that observed in a study of ionic strength alone, it appears that the cells seek to reduce the salinity of the interfacial region, thereby increasing the penetration of the surface potential into bulk water regions.

14:05  
TU108**Silanol-to-Siloxane Interconversion during Room Temperature Hydration/Dehydration of Amorphous Silica Films as Observed by ATR-IR Spectroscopy**Suzanne Warring, A. James McQuillan

Silica has been frequently studied using infrared and Raman due to its importance as a surface coating on silicon semi-conductors and use in chromatography. However, room temperature hydration and dehydration of thin silica films has not been well characterized. Using ATR-IR spectroscopy spectral features showing the reversible conversion between surface siloxanes and hydrogen-bonded silanols have been observed which suggest porosity changes within the silica films.

14:20  
TU109**Immobilization of Cryptophane Derivatives onto SiO<sub>2</sub>/Au and Au Substrates**Elise Siurdyban, Thierry Brotin, Karine Heuzé, Luc Vellutini, Thierry Bufféteau

Cryptophane derivatives possess a lipophilic cavity suitable to encapsulate neutral molecules or ionic species, such as cesium or thallium cations. The immobilization of cryptophanes onto surfaces is an original approach for the sequestration and extraction of toxic metals. The immobilization of cryptophanes was performed onto silica and gold surfaces considering different ways. PM-IRRAS was used to characterize the immobilization of cryptophanes and surface coverage was estimated by comparing the experimental PM-IRRAS spectrum with that calculated for a compact monolayer.

14:35  
TU110**Versatility of SERS Spectra Potential Dependence to Surface Equilibria**Elena Solovyeva, Assima Rakhimbekova, Lubov Myund, Anna Denisova

This work presents the study of SERS spectra potential dependence for a number of aromatic heterocycles and their derivatives, and shows how to establish the relationship between the molecule structure, type of the SERS spectra potential dependence and the form of adsorbate. In report the unique sensitivity of SERS even to the conformational equilibrium on the surface is demonstrated.

13:30 **Recent Advances in Micro and Macro ATR-FTIR Spectroscopic Imaging**TU506-inv Sergei Kazarian

The most recent developments in ATR-FTIR spectroscopic imaging and its applications will be summarized here. Two complementary approaches have been used, providing flexibility with field of view and spatial resolution: micro ATR-FTIR imaging using a microscope objective with a Ge crystal, and macro ATR-FTIR imaging using a single-reflection ATR accessory, the latter provides many opportunities for studying dynamic chemical systems. Recent advances in ATR-FTIR imaging include control of the angles of incidence for depth profiling.

13:50 **ATR-IR-based Molecular-Scale Thermometer Reflecting Free Volume Changes due to Azobenzene Photoisomerization**

TU507

Jaana Vapaavuori, Audrey Laventure, Jérémie Bourotte, Olivier Lebel,  
C. Geraldine Bazuin, Christian Pellerin

By correlating IR wavenumber shifts upon heating to shifts upon illumination, we show that the free volume created by the photoisomerization of azobenzene derivatives in glassy materials is unevenly distributed. A concept of apparent temperature reflecting the free volume surrounding each molecular group is developed. The gradient-like distribution of the apparent temperature offers a plausible molecular-level explanation for photoinduced diffusion of azobenzenes and helps understanding why photoisomerization renders these materials malleable at the temperatures far below their glass transition.

14:05 **ATR-IR Spectroscopic Observations of Water Structure in Zwitter-Ionic Polymers**

TU508

Shigeaki Morita

Water structure in antithrombogenic biomaterials having zwitter-ionic groups was investigated using ATR-IR spectroscopy. An effect of NaCl addition to the water contacting with the material surface was discussed. Water in the zwitter-ionic polymers hardly dehydrated by the salt addition, while that in neutral polymer easily dehydrated. However, spectral shape variation of the OH stretching band induced by the salt addition was clearly observed. Detailed structure change of water in the polymer matrix will be discussed from the spectral shape variation.

14:20 **Chemical Structural Analysis of an Antifreeze Solution by Using Infrared Spectroscopy with an Aid of Chemometrics**

TU509

Takafumi Shimoaka, Takeshi Hasegawa

To reveal the anti-freezing protection mechanism of an aqueous solution of ethylene glycol (EG) at a molecular level, concentration-dependent infrared spectra are analyzed with an aid of chemometrics. The result indicates that the spectral variation is explained by the quantity changes of three constituents, two of which are the 'bulk water' and the 'bulk EG', and the rest is assigned to a 'complex' of water and EG molecules.

14:35 **Variable Temperature ATR-IR Spectroscopy as a Valuable Tool for the In Situ Spin State Detection of Iron(II) Spin Crossover Complexes**

TU510

Christian Knoll, Marco Seifried, Danny Müller, Peter Weinberger

Variable temperature vibrational spectroscopy has proved a valuable tool for structural characterization of iron(II) coordination compounds undergoing a high-spin (HS) low-spin (LS) transition. MIR- and FIR-spectroscopy of iron(II) compounds allows not only for the observation of the first order structural phase transition, but also concomitant for an in-situ detection of the spin state.

- 13:30  
TU606 **Unraveling the Sum-Frequency Generation Signatures of Functionalized Surfaces using Quantum Chemical Calculations**  
Vincent Liégeois, Conrard Giresse Tetsassi Feugmo, Benoît Champagne  
Sum-frequency generation (SFG) spectroscopy is a widely used tool to determine the structure of the interface. In this contribution, we present our recent developments on the simulation of the sum frequency generation (SFG) spectra. Our methodology combines density functional theory calculations to evaluate the molecular properties with a three-layer approach to determine the macroscopic response of the organic monolayer. In addition to its detailed presentation, the method is illustrated in the case of 1-dodecene covalently bonded to hydrogen-terminated Si(111).
- 13:50  
TU607 **Generalized Dispersion Analysis of Arbitrarily Cut Crystals with Unknown Orientation**  
Sonja Höfer, Jürgen Popp, Thomas G. Mayerhöfer  
Dispersion analysis is the determination of the dielectric tensor function of a material in terms of its oscillator parameters. Based on the scheme for triclinic crystals we modified the formalism to enable performing dispersion analysis for uniaxial, orthorhombic and monoclinic crystals with a priori unknown orientations. A comparison with results obtained from principle cuts and from x-ray analysis proofs that our new formalisms allow to obtain oscillators and, simultaneously, orientations within reasonable margins.
- 14:05  
TU608 **Investigation of Band Gap Effect and Dephasing on Raman Line Broadening for the Highest Ag Mode in Comparison with SrWO<sub>4</sub> and SrMoO<sub>4</sub>**  
Jun Suda, Petr G. Zverev  
Temperature dependence of calculated linewidth of the highest Ag mode well described the observed ones below RT by both the cubic term and the dephasing with band gap effect. The bands for internal mode above band gap in SrWO<sub>4</sub> are broader than those for SrMoO<sub>4</sub>. The number of the up-conversion in SrWO<sub>4</sub> is produced by interaction between higher bands with very lower bands. So the relative ratio of the dephasing in linewidth in SrWO<sub>4</sub> is smaller than that in SrMoO<sub>4</sub>.
- 14:20  
TU609 **General Vibrational Spectroscopies with Wilson**  
Magnus Ringholm, Dan Jonsson, Kenneth Ruud  
The program Wilson, by a recursive and general approach, aims to offer a frequency-domain treatment of any elastic vibrational spectroscopy where incident lasers are either in the infrared or in the ultraviolet/visible range, detuned from electronic resonance, making possible the computational study of a wide range of vibrational spectroscopic phenomena. With molecular response properties from the code OpenRSP, also developed by our group, fully analytic ab initio calculation is possible. We show preliminary results from the program.
- 14:35  
TU610 **Vibrational Spectra of the Isotopic Species of Nitrosyl Halides: A Study Using the U(4) Algebraic Model**  
Nirmal Sarkar  
In this study, a successful application of the U(4) algebraic model has been reported in the vibrational spectral analysis of the isotopic species of nitrosyl halides. With a detail spectral analysis, it has been shown in this study that all the isotopic species of NOF, NOCl, NOBr and NOI can be approximated very well using the U(4) algebraic model.

13:30 **Broadband High-Resolution Multi-Heterodyne Ro-Vibrational Spectroscopy of Gases with Quantum- and Interband Cascade Lasers**

TU806-inv

Gerard Wysocki, Jonas Westberg, Eric Zhang, Andreas Hangauer

This paper discusses performance studies of mid-IR multi-heterodyne spectrometers based on quantum-, and interband cascade lasers (QCLs and ICLs) and their applications to chemical sensing. A general detection performance and the first implementation of wavelength modulation spectroscopy (WMS) technique applied to multi-heterodyne spectral measurement will be demonstrated.

13:50 **Interband Cascade Lasers with Spectrally Single Mode Emission in the Mid-infrared Wavelength Range from 3 to 5 Microns**

TU807

Julian Scheuermann, Michael von Edlinger, Robert Weih, Lars Nähle, Marc Fischer, Johannes Koeth, Martin Kamp, Sven Höfling

Compared to the near-infrared, many technologically and industrially relevant gas species have absorption features in the mid-infrared, with more than an order of magnitude higher absorption strength. Distributed feedback (DFB) interband cascade lasers (ICLs) that can access this wavelength range are a perfect tool for tunable laser absorption spectroscopy and other spectroscopic applications. DFB ICL devices operating continuous above room temperature with low power consumption and tuning ranges above 20 nm are presented in this work.

14:05 **Improvements of a Capillary Raman System for Trace Gas Analysis and Rapid Process Control**

TU808

Simone Rupp, Timothy M. James, Andreas Off, Hendrik Seitz-Moskaliuk, Helmut H. Telle

Highly sensitive Raman systems are required for low-pressure gas analysis applications. A simple and robust approach to enhance the Raman signal makes use of a highly reflective, hollow capillary as the gas cell. However, in standard capillary systems the achievable sensitivity is limited by a fluorescence background due to interactions between the laser and optical components. Therefore, fluorescence reduction measures were investigated and successfully implemented in an optimized setup. This contribution discusses the improvements and quantifies the resulting sensitivity enhancement.

14:20 **Fiber and Cavity Enhanced Raman Spectroscopic Analysis of Breath and Environmental Gases**

TU809

Torsten Frosch, Tobias Jochum, Di Yan, Anne Bachmann, Timea Bögözi, Stefan Hanf, Robert Keiner, Juergen Popp

Fiber-enhanced Raman spectroscopy (FERS) and cavity-enhanced Raman spectroscopy (CERS) were proven as versatile new techniques for online and real-time monitoring of disease markers in exhaled breath and may develop into new point-of-care devices. Biogenic gases play also an important role in the biosphere, the continuous online monitoring of gas compositions and exchanges helps to reveal complex biogeochemical processes and enables the characterization of ecosystems without disturbance. CERS also enabled the contactless and sterile online acquisition of the pH changes.

14:35 **New Developments in THz Quartz-Enhanced Photoacoustic Spectroscopy**

TU810-inv

Vincenzo Spagnolo, Pietro Patimisco, Angelo Sampaolo, Gaetano Scamarcio, Miriam S. Vitiello, Frank K. Tittel

Recent advances in terahertz (THz) photonics and nanotechnology have opened the way to gas sensing applications in an increasingly wide variety of fields. Among trace-gas detection techniques, quartz-enhanced photoacoustic spectroscopy (QEPAS) is capable of record sensitivities using a compact and relatively low-cost acoustic detection module. We will review our recent developments in the realization of THz QEPAS sensors exploiting quartz tuning forks of new geometry and providing an enhancement of photoacoustic transduction efficiency.

15:15 **High Resolution Aspects of AFM Based Tip-Enhanced Raman Scattering**  
TU111 Volker Deckert, Pushkar Singh, Steffen Trautmann

High resolution spectroscopies gained a lot of attention recently. The 2014 Nobel Prize honoring high resolution fluorescence based methods exemplifies this trend. Near-field optics provides another approach towards nanometer resolution. Here, no labels are required if vibrational techniques are utilized. Recent experimental evidence points to surprisingly high spatial resolution, in particular for tip-enhanced Raman scattering (TERS). In this contribution we intend to compare experimental evidence with theoretical modeling approaches to investigate the potential effects leading to such resolution.

15:35 **Selective TERS Detection in Cell Membranes**  
TU112 Zachary Schultz, Hao Wang, Stacey Carrier

We show that a specific protein receptor within a cell membrane can be selectively detected using tip enhanced Raman scattering (TERS). Our results show that the TERS signal obtained from a ligand on a nanoparticle probe interacting with a protein is a statistical match to the SERS signal from the purified protein in SERS experiments. In both cases, the observed signal provides information about the protein receptor. These results provide a selective method to investigate molecular interactions with membrane receptors.

15:50 **AFM-Tip Enhanced Near-Field Raman Imaging Analysis of Single-Molecule and Single-Electron Interfacial Electron Transfer Dynamics at Chemical and Biological Interfaces**  
TU113 H. Peter Lu

To characterize the inhomogeneity and the complex mechanism of interfacial electron transfer at chemical and biological interfaces, we have applied single-molecule spectroscopy and correlated AFM/STM imaging to study the Interfacial ET dynamics of dye molecules adsorbed at the surface of TiO<sub>2</sub> nanoparticles related to solar energy conversion and redox protein reactivity on bacterial surface related to bioremediation.

16:05 **Understanding the TERS Effect with On-line Tunneling and Force Feedback Using Multiprobe AFM/NSOM with Raman Integration**  
TU114 Aaron Lewis, Rimma Dekhter, Patricia Hamra, Yossi Bar-David, Hesham Taha, David Lewis

Tip enhanced Raman scattering (TERS) has evolved in several directions over the past years. The data from this variety of methodologies has now accumulated to the point that there is a reasonable possibility of evolving an understanding of the underlying cause of the resulting effects that could be the origin of the various TERS enhancement processes. This is the objective of our presentation.

15:15 **Detection of Virulence Markers in Highly Pathogenic Influenza by SERS**

TU511

Richard Dluhy

The current work aims to identify potential influenza virulence factors that occur from deletion of amino acid sequences in the NA stalk region using SERS. 5'-thiolated ssDNA oligonucleotides Au nanoparticle substrates. Synthetic RNA sequences corresponding to specific amino acid deletions in the influenza NA stalk region were attached to the AuNPs; two corresponding high virulence sequences, and one to a low virulence sequence. Hybridization of matched and mismatched DNA-RNA complexes were detected based on the intrinsic SERS spectra.

15:35 **Statistical Analysis of Large Areas of Raman Mapped DNA Functionalized Gold Coated Silicon Nanopillar SERS Substrates**

TU512

Kasper Fröhling, Tommy Alstrøm, Michael Bache, Michael Schmidt, Mikkel Schmidt, Jan Larsen, Mogens Jakobsen, Anja Boisen

The amount of data usually published on SERS using nanoparticles offers limited statistical information. By utilizing the emergence of uniform SERS substrates it is possible to generate a tremendous amount of data. We present a way to statistically analyze large area maps of SERS signals using a peak-fitting model. By analyzing the chemical functionalization with DNA and 6-mercapto-1-hexanol it is possible to observe peak creation and shifts. This allows for direct interpretation of the functionalization steps useful for diagnostic assays.

15:50 **Reporter-free Surface-Enhanced Raman Spectroscopy for Studying the Differentiation of Adult Stem Cells**

TU513

Sumeet Mahajan, Anna Huefner, Justyna Smus

Non-invasive and non-destructive identification of the biochemical composition of closely related cells can revolutionize (stem) cell-based therapies and thus the field of regenerative medicine. We have shown that reporter-free intracellular surface-enhanced Raman spectroscopy (SERS) allows distinction of closely related cell types and identifies biochemical changes even inside its nucleus. The application of this strategy to study the differentiation status of cells under different chemical cues and the importance and effect of functionalization of intracellular SERS probes will be described in this work.

16:05 **SERS Study of Thiocarbonyl Compounds Adsorbed on Metal Nanoparticles**

TU514

Maria Rosa Lopez Ramirez

The main objective of this work is focussed on discussing the observed vibrational wavenumber shifts of thiobenzoic acid (TBA) and thiobenzamide (TB) upon adsorption on silver nanoparticles. The analysis of the vibrational wavenumbers shifts of the Raman and SERS spectra allow us to know the adsorption process. The experimental results suggest a unidentate coordination of both adsorbates to the silver surface through the sulfur atom. DFT calculations have been carried out for different silver complexes of TBA and TB confirming the experimental conclusions.

15:15  
TU611-inv **Surface-Enhanced and Near-field IR Spectroscopies to Study Biomembranes and Membrane Proteins**

Joachim Heberle, Kenichi Ataka, Ramona Schlesinger

Optical near-field spectroscopy is a vibrant field to study monolayers of biomembranes. As membrane proteins are vectorial in their functionality, we present a methodology to specifically adhere and orient membrane proteins on a gold surface to finally yield a fully functional reconstituted membrane. Here, we showcase novel opportunities to study the structure, function and folding of membrane proteins by surface-enhanced IR absorption spectroscopy. Near-field IR microscopy is applied to resolve membrane constituents at a lateral resolution of 30 nm.

15:35  
TU612 **New Developments in ATR-FTIR Difference Spectroscopy of Protein Monolayers**

Carsten Kötting, Jonas Schartner, Jörn Güldenhaupt, Klaus Gerwert

We optimized an ATR-FTIR system based on thiol chemistry on germanium crystals to perform stimulus induced difference spectroscopy of monolayers without depending on the surface enhance effect. The great advantage of using thiols is that a huge variety of linker molecules with functional groups for many kinds of protein immobilizations are readily available. In the flow through system protein-ligand, protein-protein and protein-drug interactions can be investigated.

15:50  
TU613 **Infrared Micro-Spectroscopy Combined with Microfluidics is Promising to Monitor in Situ the Enzymatic Degradation of Plant Tissues**

Fabienne Guillon, William Andre, Estelle Bonnin, Brigitte Bouchet, Sylvie Durand, Camille Alvarado, Paul Robert, Luc Saulnier, Frédéric Jamme, Marie-Françoise Devaux

The potential of infrared micro-spectroscopy to monitor in situ the enzymatic degradation of plant tissues was investigated. Cross-sections of maize internode were treated with enzymes exhibiting cellulase and xylanase activities within a fluidic cell and FT-IR spectra were acquired in situ from different cell types taking advantage the spatial resolution offered by the synchrotron source. No spectral changes were observed in sclerenchyma and xylem fibres. Differences in parenchyma were clearly evidenced depending on their localisation in the stem.

16:05  
TU614 **Infrared Spectroscopic and Electrochemical Approaches for the Study of the Reaction Mechanism of Membrane Proteins from the Respiratory Chain Immobilized on Nano Structures**

Frédéric Melin, Sébastien Kriegel, Thomas Meyer, Petra Hellwig

Spectroelectrochemical techniques are developed to study the reaction mechanism of membrane proteins from the respiratory chain immobilized on nanostructured electrodes. Different immobilization techniques for the proteins are compared and electrochemically induced FTIR difference have been successfully obtained from SEIRAs.

15:15 **Biomedical Applications of IR Spectroscopy - from FTIR to QCLs**

TU811-inv Andreas Roth, Werner Mäntele

IR spectroscopy is a very specific technique for qualitative and quantitative determination of ingredients in multi-compound systems. Especially for biomedical applications, the sample interface is of great importance because both in vitro and in vivo samples are normally aqueous solutions with known challenges in IR spectroscopy. We want to present different approaches for biomedical applications such as dialysis or the non-invasive measurement of blood glucose for diabetes patients, starting with ATR-systems ranging to photoacoustic spectroscopy and photothermal deflectometry with QCLs.

15:35 **Active Hyperspectral Imaging Using Broadly Tunable Quantum Cascade Lasers for Standoff Detection of Explosives**

TU812

Stefan Hugger, Frank Fuchs, Jan Jarvis, Quankui Yang, Marcel Rattunde, Ralf Ostendorf, Christian Schilling, Rachid Driad, Wolfgang Bronner, Rolf Aidam

We report on the use of external-cavity quantum cascade lasers for active hyperspectral imaging in the 7.5  $\mu\text{m}$  -10  $\mu\text{m}$  spectral range. This technique is employed for contactless identification of contaminations on surfaces over distances of up to 20 meters. Main purpose of our present system is standoff-detection of explosives. However, due to the spectroscopic nature of the detection scheme, it is easily extended to any substance that exhibits a characteristic reflectance spectrum in the mid-IR.

15:50 **Developing Discriminant Frequency Infrared (DFIR) Diagnostics**

TU813

Matthew Baker, Caryn Hughes, Grame Clemens, Benjamin Bird, Matt Barre, Mile Wieda, Jeremy Rowlette

Mid-infrared spectroscopic imaging is an emerging technique for clinical diagnostics. Spectroscopic analysis allows for the label-free objective classification of biological material on the molecular scale. Recently, broadly tunable mid-infrared quantum cascade lasers (QCLs) have been successfully integrated within a microscope for spectrochemical imaging across the molecular fingerprint region. The combination of a broadly tunable laser source, refractive-based high numerical aperture objectives and a large format detector system has enabled high-definition diffraction-limited resolution, without a trade-off in signal to noise and field of view when compared to FTIR-based microscope systems. In addition, the use of a tunable laser source provides new opportunities for data collection including real-time and data collection for discrete frequency infrared (DFIR) imaging. This paper will discuss recent applications in the development and validation of DFIR with a focus on cancer diagnosis from serum.

16:05 **Recent Advances of Mid-Infrared Semiconductor Laser Based Trace Gas Sensor Technologies for Environmental Monitoring**

TU814

Frank Tittel, Lei Dong, Chunguang Li, Yajun Yu, Pietro Patimisco, Angelo Spagnolo, Gaetano Scamarcio, Vincenzo Spagnolo

Recent advances of sensor systems, based on mid-infrared interband cascade lasers (ICLs) for the detection of trace gas species and their application in atmospheric chemistry, medical diagnostics, life sciences, petrochemical industry, and national security will be reported.

## MIR Laser Spectroscopy 1

### B001 **QCLAS Sensor for Purity Monitoring in Medical Gas Supply Lines**

Henrik Zimmermann

Continuous monitoring on the distribution lines in hospitals could avoid fatal accidents that unfortunately still happen to patients. Concentration limits for harmful compounds are defined for every gas line by local regulatory. Within the scope of the EU funded project MIRIFISENS, which addresses technological issues as specified by a number of selected safety and security applications, the neoplas control GmbH is focusing on the on-site purity monitoring of medical gases used in hospitals. Achievements in related developments are presented.

### B002 **Mid-Infrared Supercontinuum Spectroscopy with a MOEMS-Based Fabry-Perot Microspectrometer**

Jakob Kilgus, Petra Müller, Peter M. Moselund, Markus Brandstetter

Supercontinuum sources (SC) - most recently proceeding into the mid-infrared wavelength region - emerge as promising new light sources for laser-based infrared spectroscopy. We present the combination of a mid-infrared SC laser with a MOEMS-based Fabry-Perot microspectrometer (FPMS) and its application to various analytical tasks. While the SC source features both broadband and high-intensity laser emission, the FPMS acts as fully integrated wavelength-selective element featuring eligible properties for process applications.

### B003 **High Performance Ring Quantum Cascade Laser for Sensing Applications**

Martin Holzbauer, Rolf Szedlak, Donald MacFarland, Tobias Zederbauer, Hermann Detz, Aaron Maxwell Andrews, Werner Schrenk, Gottfried Strasser

Ring quantum cascade lasers are ideal light sources for mid-infrared spectroscopy, due to their compact size, designable wavelength, high output power and collimated light beam. However, high duty-cycle operation at room temperature is a demanding task because of the huge amount of heat generated in the active laser core. Therefore, various techniques for better heat extraction are investigated with a finite element based approach.

## TERS

### B004 **Tip-Enhanced Raman Scattering Spectroscopy of Graphene/SiO<sub>2</sub>: Tip Preparation and Evaluation of Spatial Resolution**

Masamichi Yoshimura, Ryo Uehara, Tomomi Kozu, Mayumi Misawa, Misao Suzuki

We report on the reproducible TERS measurement using the custom-made Ag/Al-coated tips, where 70-80 % of tips show the enhancement. Using this tip we did TERS imaging of the CVD-graphene on SiO<sub>2</sub> substrate, simultaneously with AFM imaging. It is found that the spatial resolution of TERS is ~5 time higher than the normal Raman imaging and that even small fluctuation in the sample was revealed revealed.

B005 **Tip-Enhanced Raman Scattering (TERS) Measurements with AFM Contact Mode Low Force Constant Cantilever**

Tomomi Kozu, Mayumi Misawa, Kyo Uehara, Masamichi Yoshimura, Ken Nishida

Tip-enhanced Raman scattering spectroscopy (TERS) is an important and useful technique for nanotechnology. TERS is a combination technique of surface enhanced Raman scattering and scanning probe microscope, and it has high spatial resolution. To demonstrate TERS measurement, we used low force constant cantilever and AFM contact mode. With this setting, we demonstrated TERS measurement of graphene sample. This will be a good tool for bio samples analysis.

B006 **Instrumentation and Development of Tip Enhanced Raman Imaging Toward Revealing 2D Nanomaterials**

Dung-Sheng Tsai, Chi Chen

In this poster, we present our homemade STM-TERS instruments with improved stability and photon collection efficiency as well as our recent progress in TERS spectral analysis of 2D TDMC materials.

B007 **Tip-Enhanced Raman Spectroscopy of Nucleation-Mode Aerosol: New Frontiers in Image-Based Analysis of Atmospheric Nanoparticles**

Johannes Ofner, Katharina A. Kamilli, Tanja Deckert-Gaudig, Hans Lohninger, Andreas Held, Volker Deckert, Bernhard Lendl

Formation of atmospheric nucleation-mode particles in the nanometer size through homo- or heterogeneous nucleation is a global phenomenon of utmost scientific importance. Secondary organic aerosol (SOA) particles with aerodynamic diameters between 10-100 nm were analysed using TERS. Using hierarchical cluster and vertex component analysis, single Raman spectra could be extracted from the TERS dataset and the chemical formation process of atmospheric nano particles could be unravelled.

## Plasmonics, SERS, SEIRA

B008 **Development of a Simple Approach for Ultrasensitive Detection of Bisphenols by Multiplex Surface-Enhanced Raman Scattering**

Charlotte De Bleye, Elodie Dumont, Lauranne Netchacovitch, Pierre-François Chavez, Pierre-Yves Sacré, Philippe Hubert, Eric Ziemons

A very simple, cheap and fast SERS method using functionalized silver nanoparticles was developed to detect bisphenols. This method was applied for the semi-quantitative detection of bisphenol A (BPA), bisphenol B (BPB) and bisphenol F (BPF) separately. Afterwards, a feasibility study of performing a multiplex SERS detection of BPA, BPB and BPF was successfully carried out. Finally, this developed method was applied on real samples which were solutions comprising cash receipts collected from different stores.

B009 **SERS-Based Determination of the Effects of Radiation Therapy in a Prostate Cancer Model System**

Victoria Camus, Colin Campbell

Worldwide, prostate cancer is the second most common cancer in men, with radiation therapy being a primary form of treatment. The ionising radiation destroys cancerous cells through generation of reactive oxygen species (ROS) which are also implicated in the regulation of intracellular redox state; dysregulation is associated with cancer progression. Using redox-sensitive nanosensors and SERS, we can quantitatively measure cystolic redox potential in 2D and 3D cell systems to model sensor behaviour and generate a prototypical system for radiation treatment.

- B010 Sheath-Flow SERS Detection for Bioanalysis**  
Zachary Schultz, Matthew Bailey, Pierre Negri, Kevin Jacobs, Colleen Riordan, R. Scott Martin  
The confinement of analyte molecules to a planar substrate provides a reproducible and high throughput method of SERS analysis. In this presentation we will demonstrate a sheath-flow SERS detector and illustrate its utility for bioanalysis.
- B011 Label-Free Surface-Enhanced Raman Spectroscopic Detection of Mycobacterium Smegmatis Using Silver Nanoparticles**  
Melisew Alula, Jonathan Blackburn  
The development of surface-enhanced Raman scattering method for the detection of bacteria in different samples has received much attention in recent times. In this work, we present the development of simple, fast, and sensitive surface-enhanced Raman spectroscopy (SERS) for the detection of Mycobacterium smegmatis using silver nanoparticles (AgNPs) that are coated on the surface of the bacteria. The silver mirror reaction was used for coating silver nanoparticles on the cell envelope of the bacteria. The bacteria were initially mixed with AgNO<sub>3</sub> and treated with NaOH after which of ammonium hydroxide was added until the Ag<sub>2</sub>O was completely dissolved. Treatment of the reaction mixture with glucose at 55°C resulted in the formation of AgNPs on the surface of the bacteria. The detection of M.smegmatis is simple and straightforward; 4L of M.smegmatis coated AgNPs (smegmatis@AgNPs) were pipetted on the hydrophobic carbon surface and SERS spectra are collected. Quantitative evaluation of the bacteria was done with the distinguishable strong vibrational band around 735 cm<sup>-1</sup>.
- B012 Enhancing Raman Spectroscopy of Monolayer MoS<sub>2</sub> by Plasmonic Nanopatch Cavity**  
Tian Ming, Shengxi Huang, Xi Ling, Mildred Dresselhaus, Jing Kong  
Two-dimensional molybdenum disulfide (MoS<sub>2</sub>) is promising for optoelectronics due to its extraordinary crystal and electronic structure. We performed Raman spectroscopy of monolayer MoS<sub>2</sub> inside and outside plasmonic nanopatch cavities. Results shown that the cavity induces significant Raman enhancement, as well as significant spectral modification. Vibrational modes that are not Raman active outside the cavity is activated inside the cavity. the cavity is assumed to introduce asymmetry to the three-atomic layer thin MoS<sub>2</sub> lattice, at the same time alter its electronic structure.
- B013 SERS Study of the Hybridization Changes of the Boron Atom of the Ortho-Substituted N-benzylamino(boronphenyl)methylphosphonic Acid under Different pH Conditions**  
Natalia Piergies, Edyta Proniewicz, John R. Lombardi  
Here, we present SERS investigations of the N-benzylamino-(2-boronphenyl)-R-methylphosphonic acid (o-PhR) adsorbed onto the colloidal silver nanoparticles surface under various environmental conditions, including excitation wavelengths (488.0, 632.8, and 785.0 nm), and pH levels of the solutions (from pH=5 to pH=9). The obtained SERS data indicate that at pH equal 5 and 7 the PhB(OH)<sub>2</sub> molecular fragment rather weakly interacts with the silver nanoparticles surface, whereas at pH=9 this interaction (mainly through the -CB(OH)<sub>2</sub> group) is strong.
- B014 The Effect of the Applied Electrode Potential on the Surface Geometry of NPY<sup>24-36</sup> onto the Electrochemically Roughened Ag, Au, and Cu Substrates**  
Helena Domin, Natalia Piergies, Dominika Swiech, Ewa Pieta, Edyta Proniewicz  
Here, we discussed the SERS results for the mutated acetyl-(Leu<sup>28,31</sup>)-NPY<sup>24-36</sup> C-terminal fragment immobilized onto electrochemically roughened Ag, Au, and Cu electrodes under various applied electrodes potentials. This biologically active molecule is an analogue of neuropeptide Y (NPY). The spectral analysis indicates that at positive electrode potential (0.100V) the investigated molecule is moved away from the Ag electrode surface. However, at -1.200 V strong interaction between the Tyr, Arg, and amide bonds of NPY<sup>24-36</sup> and the Ag substrate occurs.

B016 **Single Molecule Level of SER(R)S Spectral Detection of [Ru(bpy)<sub>3</sub>]<sup>2+</sup> Incorporated in Liquid Overlaid Ag Nanosponge Aggregates**

Veronika Sutrová, Ivana Šloufová, Blanka Vlčková

A single 3D nanosponge aggregate with incorporated [Ru(bpy)<sub>3</sub>]<sup>2+</sup> complex dications and overlaid by a thin layer of aqueous phase was prepared and tested as the sample for SERS spectral measurements. The 1x10<sup>-15</sup> M and 1x10<sup>-15</sup> M concentration values of the SERS and SERRS spectral limits of detection limit of incorporated [Ru(bpy)<sub>3</sub>]<sup>2+</sup> into the Ag nanosponge aggregate were determined at 445 and 532 nm excitation wavelengths, respectively. These values correspond to a single molecule level of [Ru(bpy)<sub>3</sub>]<sup>2+</sup> detection.

B017 **Characterization of the Vibrational Structures and Adsorption Geometries of Neuropeptide Y and Its Mutated C-Terminal Fragment onto the Ag and Au Colloidal Nanoparticles Surfaces**

Helena Domin, Dominika Świąch, Ewa Pieta, Natalia Piergies, Edyta Proniewicz

In this study, we present the spectroscopic analysis of neuropeptide Y (NPY) and its mutated acetyl-(Leu<sup>28,31</sup>)-NPY<sup>24-36</sup> C-terminal fragment immobilized onto colloidal Ag and Au nanoparticles surfaces. Some changes in the adsorption geometry of the investigated molecules immobilized onto these two SERS-active substrates are observed. However, the obtained SERS results demonstrated that, for both biologically active molecules, the NPY<sup>32-36</sup> C-terminal part is responsible for the molecule/metal interaction at the Ag nanoparticle/water and Au nanoparticle/water interfaces.

B018 **The Effect of the Surface Roughness of Gold Films on the Adsorption Process of Bombesin and Its Native Fragments. SERS Studies.**

Agnieszka Tąta, Dominika Świąch, Edyta Proniewicz

Bombesin (BN) is an endogenous neurotransmitter. In human BN binds with high affinity to the GRP-preferring bombesin receptor (rGRP-R). Different bombesin subfamily peptides, having from 2 to 9 amino acid of the BN amino acid sequence, show different biological activity. In this work, full length BN and the aforementioned C-terminal fragments were immobilized onto gold film surface with roughness in the range between 80 to 200 nm. Products of these processes have been studied surface-enhanced Raman scattering (SERS).

B019 **Highly Reproducible SERS Substrate Based on Ag Pyramidal Arrays**

Nan Lyu, Yandong Wang, Wentao Wang, Lingxiao Liu, Lei Feng

The close-packed Ag pyramidal arrays were fabricated for achieving plentiful and homogeneous SERS hot spots by taking the inverted pyramidal pits on Si as a template. The sharp nanotip and the four edges of Ag pyramid result in strong electromagnetic field enhancement. Moreover, the feature of the Ag pyramidal array can be well controlled, which allows for achieving SERS substrates with reproducibility. The relative standard deviation is lower than 8.78% across the whole substrate and different batches of substrates.

B020 **What is the Role of Temperature on SEIRA Spectral Features of Nicotinic Acid Adsorbed on Copper Substrate?**

Alzbeta Kokaislova, Pavel Matejka

SEIRA spectra of nicotinic acid, adsorbed on copper substrate, were recorded in the course of gradual heating the substrate from 15 °C to 50 °C and further cooling back to 15 °C. Changes of spectral features, induced by temperature changes, were investigated by simple comparison of band intensities and widths and by applying the Partial Least Squares (PLS) regression in order to distinguish changes which correlate with temperature. The results of both these methods were found to be in accordance.

B021 **Investigation of Cysteine-containing Peptides on Massive Metal Substrates Using Surface-enhanced Vibrational Spectroscopic Techniques**

Tereza Helesicova, Alzbeta Kokaislova, Pavel Matejka

This study utilises SERS and SEIRA spectroscopy for detection and investigation of biologically important peptides (glutathione and Glu Cys) that both contain cysteinyl unit.

**B022 Application of Surface-enhanced Raman Scattering (SERS) for Assessing the Oxidation Degree of Oxo-biodegradable Plastics**

Jesus Salafranca, Magdalena Wrona, Cristian Nerin

The oxidation of an oxo-biodegradable polyethylene film has been assessed by means of SERS. A substrate of silver nanoparticles has been generated in-situ directly on the plastic surface for the first time. Different oxidation agents have been tested: ultraviolet light, heat, chemical oxidants and hydroxyl radicals produced in a home-made set-up. Chemometrics have been applied to get the maximum information. The method is fast, cheap and can be used for screening purposes or as a complement to other analytical techniques.

**B023 Excitation Wavelength Dependent Sers Spectra of Single Layer Graphene Overdeposited by Fused Ag Nanoparticle Aggregates**

Ivana Sloufova, Veronika Sutrova, Blanka Vlckova, Martin Kalbac

Excitation wavelength-dependent SERS spectra of single layer graphene (SLG) deposited on Si/SiO<sub>2</sub> (300nm) substrate, overdeposited by fused aggregates of chloride-modified Ag nanoparticles (NPs) and measured at 780, 633, 532 and 445 nm excitations are reported, and compared to Raman spectra of graphene. Preservation of SLG native structure and achievement of only moderately strong enhancement in SERS of SLG/Ag NP aggregate nanocomposite is attributed to the presence of a very thin AgCl spacer between the SLG and the AgNP aggregate.

**B024 Smart Plasmonic Metal-Dielectric Nanostructures for Surface Enhanced Raman Scattering**

Fabrizio Giorgis, Alessandro Virga, Andrea Lamberti, Alessandro Chiado, Chiara Novara, Paola Rivolo, Stefano Bianco, Francesco Geobaldo

In this work, we present an overview concerning with the SERS analysis and applications of Ag nanoparticles synthesized on different dielectric substrates such as porous silicon, polydimethylsiloxane membranes, titania nanotubes and graphene monolayers. The morphology of all the discussed substrates were optimized in order to achieve the lowest Limit of Detection with probe molecules. Single/few molecule detection regimes were obtained taking advantage of plasmonic and chemical enhancements. The application of such SERS-active substrates for oligonucleotide-based bioassays analysis were critically presented and discussed.

**B025 Detection of CBR Materials by Using SERS**

Yeonju Park, Sila Jin, Jae Hwan Lee, Young Mee Jung

Recently it is important to find better and less expensive method for detecting chemical, biological, radiological (CBR) materials. Device for useful detection of CBR materials must be sensitive, reliable, and rapid. In this study, for successful detection of various chemical threats at very low concentration, we prepared the functionalized silver and gold nanoparticles. Various chemical threats were detected by SERS. Details on SERS spectra of chemical threats and their quantitative analysis will be discussed in this presentation.

**B026 Surface-Enhanced Raman Scattering Probe for DNA Detection Based on Surface Potential Change Using 4-Methoxyphenyl Isocyanide**

Minwoo Lee, Kyung-Hun Kim, Ho-Young Lee, Yoon-Sik Lee, Dae Hong Jeong

SERS is one of DNA detecting methods, but many researches have reported Raman label modified DNA based DNA detection which are time-consuming, expensive and complicated. In this study, we present label-free DNA detection probe based on surface charged changing of metal nanoparticles. Using this probe, after ssDNA binding, isocyanide SERS band was changed about 8 cm<sup>-1</sup> by surface charge changing of nanoparticles. These results demonstrated isocyanide SERS probe showed the potential of ssDNA detection based on surface charge changing.

B027

### **Preparation of SERS-Active Substrates and its Applications in Quantitative Detection of L-Amino Acids**

Raju Botta, A. Rajanikanth, C. Bansal

Novel SERS-active substrates were prepared using cluster deposition system. Ag nanocluster (AgNC) films were deposited on glass substrates and annealed these substrates for tuning the surface plasmon resonance peak of AgNC which is close to wavelength of excitation laser source. All characteristic Raman lines of analyte molecules were presented even at the low concentration. Highly reproducible SERS spectra were obtained from this technique and we used this technique to quantify the SERS detection of amino acids.

B028

### **Surface Enhanced Raman Spectroscopy Application on Aflatoxin (B1) Detection Using Colloidal Silver Nanoparticles**

Reza Mohammadigol, Rasoul Malekfar, Ehsan Talebian

Regarding the upcoming issues of laboratory methods to detection/quantify Aflatoxins, this study focuses on the possibility of detecting B1 Aflatoxin by SERS technique using Ag nanoparticles as a substrate. By comparing the corresponding Raman shift peaks of the B1 Aflatoxin Raman spectrum with the values reported from computational method (DFT), peaks in 945, 1048, 1148, 1252, 1390, 1527, 1583, 1658  $\text{cm}^{-1}$  were confirmed as the fingerprints of B1 Aflatoxin Raman spectrum. The results reveal that Ag nanoparticles substrate has the potential to detect B1 Aflatoxin.

B030

### **Molecular Selectivity of Graphene-Enhanced Raman Scattering**

Shengxi Huang, Xi Ling, Liangbo Liang, Jing Kong, Vincent Meunier, Mildred Dresselhaus

Graphene-enhanced Raman scattering (GERS) uses graphene as the substrate for enhancing Raman signals of adsorbed molecules. GERS obtains the unique molecular selectivity--the enhancement factors of different molecules can range from ~1 to almost 100. In this work, we measured and discussed the main factors of molecular selectivity--molecular energy levels and molecular structures. This work is important for the fundamental study of molecule-graphene coupling and the chemical mechanism in Raman enhancement, as well as the applications in chemical detection.

B031

### **3D SERS Imaging Using Highly Symmetric Nanoporous Silver Microparticles**

Sanpon Vantasin, Wei Ji, Yoshito Tanaka, Harnchana Gatemala, Kanet Wongravee, Sanong Ekgasit, Yukihiko Ozaki

Highly symmetric nanoporous silver microparticles were synthesized by galvanic replacement of AgCl. the shape and porosity of the particles can be finely controlled. 3D SERS imaging using these particles as a substrate show a predictable symmetric enhancement pattern. with a predictable shape and SERS enhancement, it is very possible that these particles can be embedded into solutions or polymers and being used to detect the concentration gradient of target molecules.

B032

### **Study of Human Saliva by Surface-Enhanced Vibrational Spectroscopic Techniques**

Michaela Grafova, Pavel Matejka

Human saliva is an important, easy accessible body fluid. Different approaches of saliva collection were tested, namely the use of an absorbent device Salivette (a plain cotton swab) and a passive drooling to deposit them on Ag, Au and Cu SEVS substrates. Both SERS and SEIRA spectra were collected and chemometrically evaluated. The study is focused mainly on monitoring of the spectral changes caused by the temperature variation of deposited human salivary sample in the range 10°C to 45°C.

B033

### **DSP Marine Algal Biotoxins Interaction with Silver Nanoparticles**

Müller Csilla, Glamuzina Branko, Ujevic Ivana, Vasile Chiş, Simona Cîntă-Pânzaru

Diarrhetic shellfish poisoning (DSP) is a severe gastrointestinal illness caused by consumption of shellfish containing DSP toxins that are originally produced by Dinoflagellates. Aiming to translate SERS technique to the specific monitoring programs in the aquaculture sector, we investigated the SERS response with AgNPs of three related DSP toxins, okadaic acid and dinophysistoxins (DTX-1 and DTX-2) at extremely low concentrations. SERS achieved detection at 0.6523  $\mu\text{g/mL}$ . Challenging results revealed SERS signal of toxins similar with those of natural, oligotrophic seawater.

**B034 Crumpled Thin Gold Layer: An Ultra-Simple and Reliable Substrate for Reproducible SERS Detection**

Lucie Štolcová, Jan Proška, Marek Procházka, Martin Petrevec

The crumpled thin gold layer, prepared by a straightforward compression of a flat gold layer, is a SERS-active substrate with high density of hot spots providing high, homogeneous and reproducible enhancement of Raman signals. The preparation technique is very simple, low cost and does not contaminate the gold surface. The compression, which results in 'trapping' analyte molecules into nanometre-sized gaps, can be performed directly before SERS measurements to subdue problems caused by aging of the SERS-active substrates.

**B035 Correlative SEM-SERS Imaging of Morphologically Complex SERS-active Substrates**

Lucie Štolcová, Rostislav Váňa, Jan Proška

Raman imaging and scanning electron (RISE) microscopy is a novel imaging technique combining confocal Raman microscopy and SEM within one instrument. The high resolution of RISE microscopy is well suited for experiments on SERS-active substrates aiming to understand the structure-activity relationship. We show the direct correlation of SERS intensity maps obtained from silver nanostructures with highly complex morphology with their SEM images. RISE appears to be a very effective method in probing the location of hot spots at SERS-active substrates.

**B036 Versatile Templates for Ad-hoc SERS-active Substrate Preparation**

Jan Proška, Lucie Štolcová, Maria Domonkos, Tibor Izák, Marek Procházka, Alexander Kromka

Morphology of metal nanostructures have been proved to play a crucial role in achieving the high enhancement of local electromagnetic field in their vicinity. Here we report on plasma treatment as a versatile technique for a production of large area (ready-made) templates designed for a subsequent ad-hoc metalization and eventual functionalization procedure.

**B039 Detection of Low-concentration Contaminants in Solution by Exploiting Chemical Derivatization in Surface Enhanced Raman Spectroscopy**

Mike Hardy, Matthew Doherty, Igor Krstev, Konrad Maier, Torgny Möller, Gerhard Müller, Paul Dawson

A simple derivatization methodology extends the application of surface enhanced Raman spectroscopy (SERS) to the detection of trace concentration of contaminants in liquid form, where techniques such as chemisorption or drop-casting and subsequent solvent evaporation are not always effective. The detection of nitric acid is demonstrated down to 100 ppb via reaction with ammonium hydroxide to produce the corresponding ammonium salt. This yields an improvement of 4 orders of magnitude in the low-concentration detection limit compared with liquid phase detection.

**B040 Surface Enhanced Raman Scattering Spectra of Extracellular and Intercellular Components of Microorganisms**

Tibebe Lemma, Jussi Toppari, Vesa Hytönen

The intercellular and extracellular biochemical components of microorganisms and their structural features such as bacteria have been investigated using SERS. The structural differences of components reside in the cell envelope are manifest in their Raman spectra: e.g. lysis vs non-lysis cell. Silver nano-aggregate particles have been used as SERS substrate exploiting the existence of hot spots, which is due to the electromagnetic field produced from the aggregation of silver nanoparticles induced by the chloride ions. The SERS spectra display various cellular macromolecules, such as proteins, polysaccharides, lipids and nucleic acids with excellent structural-spectra correlations. The SERS spectra associated with these features give rise to intense bands that provide very useful information on the complex chemical composition and low concentration compounds of bacteria cells envelope.

B041 **Determining the Trace Concentration of Compounds Using Surface Enhanced Raman Spectroscopy**

Shekhar Sharma, Eugene Carmichael, David McCall

SERS was evaluated to investigate its lower detection limits of a model compound, Rhodamine 6G (R6G). Measured volumes of R6G concentrations were dried down, onto a substrate consisting of copper loaded with silver nanostructures. SERS was able to detect R6G down to a concentration of 0.5 μM. The substrate performance was then tested for its ability to detect melamine, and glyphosate. The SERS technique enhancement factor was determined and averaged at about 105 over conventional Raman spectroscopy.

B042 **Surface-Enhanced Raman Spectroscopy of Simulants of Bacillus Anthracis Spores. A Fast and Reliable Technique for Early Warning of Biological Threats**

Salvatore Almagusa, Antonia Lai, Antonio Palucci, Valeria Spizzichino, Alessandro Rufoloni, Domenico Luciani, Roberto Viola

Raman Spectroscopy is a fast tool for the detection of molecular species, capable of sensing also microorganisms. Its branch Surface-Enhanced Raman Spectroscopy (SERS) strongly increase Raman sensitivity and selectivity. We present our SERS results on the characterization of Bacillus Thuringiensis and bacillus atrophaeus spores, as simulants of the deadly Bacillus anthracis, as part of the RAMBO project (Rapid Air particle Monitoring against BiOlogical threats) whose goal is developing a sensor capable of detecting few spores with good selectivity and sensitivity.

B043 **Versatile Fabrication of Nanofluidic Devices on CaF<sub>2</sub> Substrate for Ultra-Sensitive Infrared Spectroscopic Applications**

Thu Le, Takuo Tanaka

This paper reports a versatile process to fabricate nanofluidic devices on infrared (IR)-transparent calcium fluoride substrates for IR-spectroscopic applications. It includes the fabrication of guiding microchannels and nanochannels, following by the bonding of two substrates by chemical bonding. The direct fabrication on calcium fluoride substrates allows not only the construction of fluidic channels with fine nanostructures, but also the integration of nanostructures to utilize the localized surface plasmon effects. This method is promising to open a new perspective of IR-spectroscopies in nanofluidics for label-free bioanalysis.

B044 **Highly SERS Active Gold Nanoparticle Assemblies of Controllable Size Obtained by Hydroxylamine Reduction at Room Temperature**

István Todor, László Szabó, Oana Marișca, Vasile Chiș, Nicolae Leopold

In this study, colloidal nanoparticle assemblies (NPAs) were obtained in a one step procedure, by reduction of HAuCl<sub>4</sub> by hydroxylamine hydrochloride, at room temperature, without the use of any additional nucleating agent. By changing the order of the reactants, nanoparticle assemblies with mean size of ~20 nm and ~120 nm were obtained. The here proposed NPAs were assessed as surface-enhanced Raman scattering (SERS) substrate and found to provide a higher enhancement compared to conventional citrate reduced nanoparticles.

B045 **SEIRA Measurements on Gold Stars**

Joyce Ibrahim, Christians Huck, Anne-Marie Pucci, Gilles Lerondel, Timothée Toury

Metallic nanoparticles display a collective resonance of free confined electrons. They can be used to enhance the IR vibrational signal of absorbed molecules on the sample surface. Nanostars have already shown an increase in the enhancement in extinction measurement in the visible. In this work we demonstrate the fabrication of stars by a new approach, three coplanar beam interferential lithography, their optical resonance in IR and SEIRA measurements of CBP.

**B046 Tools for Identification of Biofilm Layer Fouling, Measured with Real-Time Raman Kinetics**

Martin Kögler, Bifeng Zhang, Yunjie Shi, Li Cui, Marjo Yliperttula, Tapani Viitala, Kaisong Zhang

Biofilm-fouling of membrane surfaces causes a significant challenge for the filtration of drinking water. The observation of the real time changes of fouling using a proof of concept experimental set-up is explored. A custom designed cross-flow cell replicating a membrane-filtration system with the possibility to measure Surface Enhanced Raman Scattering (SERS), using colloidal golden nanoparticles in real-time from changes of surface-foulants, such bacteria and adenine under similar conditions as in industrial filtration systems was realized as a proof-of-concept.

**B047 Detection of Pesticide with Plasmonic Nanoparticles Functionalized with Humic Substances of Different Origins Giving Rise to Huge Surface-Enhanced Raman Signals**  
Rafael Jesus Gonçalves Rubira, Carlos José Leopoldo Constantino, Santiago Sanchez-Cortes

In this work we report the functionalization of AgNPs with the shape of nanospheres and nanostars with standard humic substances (HS) extracted from soils and from leonardite. The amount of immobilized HS was increased by a previous functionalization of NPs with aliphatic diamines with variable length. These substrates were employed to detect atrazine and prometryn, two of the most used triazine pesticides used in agricultural practices in order to increase the sensitivity and selectivity of the SERS analysis.

## Time-Resolved Spectroscopy 1

**B037 Single-Molecule Interfacial Electron Transfer Dynamics of Porphyrin on TiO<sub>2</sub> Nanoparticles: Dissecting the Complex Electronic Coupling and Driving Force Dependent Dynamics**

H. Peter Lu, Vishal Rao, Bharat Dhital, Yufan He

The photosensitized interfacial electron transfer (ET) dynamics of Zn(II)-5,10,15,20-tetra (3-carboxyphenyl) porphyrin (m-ZnTCPP)-TiO<sub>2</sub> nanoparticle (NP) system has been studied using single-molecule photon stamping spectroscopy. The single-molecule fluorescence intensity trajectories of m-ZnTCPP on TiO<sub>2</sub> NP surface show fluctuation and blinking between bright and dark states, which are attributed to the variation in the reactivity fluctuation of interfacial ET, i.e., intermittent interfacial electron transfer dynamics.

**B038 Time-Resolved Raman Spectroscopy**  
Jouni Takalo, Lauri Kurki, Mari Tenhunen, Jyrki Savela

This presentation focuses on data processing of timegated Raman data. Raman spectra of several samples were obtained by rejecting the fluorescence using electrically gated technique. The results clearly show that this Real Fluorescence Rejection technique can capture the Raman signal before fluorescence background starts to dominate spectra. The relative peak intensities can be calculated as projections in wavenumber-count cross-section or as peak volumes including the time delay axis. Additional mathematical algorithms are used for baseline correction to remove the residual fluorescence background.

## Computational Spectroscopy 1

**B048 Electrodynamical Forbiddance of the Quadrupole Light-Molecule Interaction and Some Features of the SERS, SEHS and SEIRA Spectra in Molecules with Cubic Symmetry Groups**

Aleksey Polubotko, Vladimir Chelibanov

The report presents some features of a strong quadrupole light-molecule interaction in molecules with cubic symmetry groups. It is demonstrated that this interaction is forbidden due to peculiarities of the quadrupole light-molecule interaction and the law of electrodynamics. This forbiddance results in the absence of the lines caused by totally symmetric vibrations in SEIRA, slight enhancement of such lines in SEHS and lower enhancement of the SERS spectra in such molecules, with respect to the spectra of usual Raman scattering.

B049 **The Theory of SERS, SEHRS and SEIRA Based on the Conception of a Strong Quadrupole Light-Molecule Interaction**

Aleksey Polubotko, Vladimir Chelibanov

The report presents dipole-quadrupole theory of SERS, SEHRS and SEIRA, which is based on the phenomenon of a huge enhancement of the quadrupole interaction in surface fields strongly varying in space near rough metal surface. This approach allows to explain appearance of forbidden lines in all the spectra of SERS, SEHRS and SEIRA, which are observed in molecules with sufficiently high symmetry and all other features of these enhanced optical processes.

B050 **FT-IR and Raman Spectra Vibrational Assignments and Density Functional Calculation of 2-Pyridinecarboxaldehyde**

Srinivasaiyah Seshadri

The vibrational spectra of 2-pyridinecarboxaldehyde (2PCE) have been computed using B3LYP methodology and 6-31G\* basis set. The liquid phase FTIR and FT-Raman spectra were recorded in the region 4000-400cm<sup>-1</sup> and 3500-100cm<sup>-1</sup> respectively. A close agreement was achieved between the observed and calculated frequencies by employing normal coordinate calculations. The observed and simulated spectra were found to be well comparable.

B051 **Complete Dispersion Analysis of Single Crystal Neodymium Gallate**

Sonja Höfer, Jürgen Popp, Thomas G. Mayerhöfer

A single crystal of neodymium gallate was investigated by FTIR-spectroscopy in the reststrahlen region between 100 - 1000 cm<sup>-1</sup>. The three spectra of the crystal in principal orientations were analyzed by dispersion analysis employing different dispersion relations and the corresponding dispersion parameters and dielectric tensor functions were obtained. This allows to properly characterize and quantitatively analyze films of this important substrate material by IR-optical methods.

B052 **Interpretation of Vibrational Spectra (FT-IR, FT-Raman) of 2-Thiohydantoin Derivatives: on Evidence for Hydrogen Bonding**

Archana Gupta, Vipin Deval, Poonam Tandon, Ko-Ki Kunitomo

In the present work the structural and spectral characteristics of 5-benzyl-2-thiohydantoin (5-BTH) have been studied by methods of infrared, Raman spectroscopy and quantum chemistry. Stability of the molecule arising from hyperconjugative interactions has been analyzed using NBO analysis. Vibrational analysis supports the hydrogen bonding pattern reported by crystalline structure. TD-DFT calculations have been performed to explore the electronic absorption spectra in the gas phase, as well as in solution environment using PCM model.

B053 **Quantum Chemical DFT Studies of 1,4-bis(4-formylphenyl)anthraquinone**

Renjith Raveendran Pillai, Yohannan Panicker

Anthraquinones or anthracene-9,10-diones are essential chemical constituents of fungi, lichens and higher plants which are known for their anti-inflammatory, analgesic, antimicrobial and other medicinal properties, which makes them a natural target for the pharmaceutical industry. In the present work, FT-IR and FT-Raman spectra of title compound are reported, both experimentally and theoretically. HOMO and LUMO analysis have been used to elucidate information regarding charge transfer within the molecule. Nonlinear optics is one of a few research frontiers where tremendous interest arises not only from the request for understanding of new physical phenomena but also from the potential technological applications. In this context, the hyperpolarizability of the title compound has been calculated in the present study.

B054 **Anharmonic Effects in Vibrational Light-Scattering Phenomena**

Yann Cornaton, Magnus Ringholm, Kenneth Ruud

Vibrational light-scattering phenomena are used to get information about the structure of molecular systems through spectroscopies as Raman or hyper-Raman scattering. A computational treatment of these spectroscopies requires the calculation of high-order molecular properties, and more so if anharmonic effects are to be taken into account. In this contribution, we present examples of our recent work on the treatment of such effects using our recently developed response-theory program OpenRSP for the analytic calculation of high-order properties.

- B055**      **Vibrational Study of Riluzole Hydrochloride, a Drug Used for the Treatment of Amyotrophic Lateral Sclerosis (ALS) by Using DFT Calculations and SQM Methodology**  
María Ladetto, Maximiliano Iramain, Elida Romano, Silvia Brandán  
In this work, we have presented the complete assignment of the bands observed in the infrared spectrum by combining the available experimental infrared spectrum of riluzole hydrochloride with density functional theory calculations, the internal symmetry coordinates and a generalized valence force field. The comparisons between the experimental infrared spectra with the corresponding theoretical show a reasonable agreement. In addition, the force constants of riluzole hydrochloride were also reported together with the predicted Raman spectrum at the same level of theory.
- B056**      **Modeling the Vibrational Properties of Single Crystals: Case of CaCO<sub>3</sub> Polymorphs**  
Erwan Andre, Marco De La Pierre, Roberto Dovesi, Cedric Carteret  
On the condition to work on single crystals (which is per se not so easy to achieve), polarized Infrared and Raman spectroscopies are powerful tools to explore vibrational, optical and dielectric properties of solid state samples. The aim of this work is to show how simulated spectrum, generated by quantum mechanical calculations, can dramatically reduce the risk of erroneous attributions or artefacts. To illustrate this procedure calcium carbonate will be used as an example.
- B057**      **Prediction of the Vibrational Frequencies for Adamantane via Computational Approach**  
Ehsan Talebian, Rasoul Malekfar, Reza Mohammadigol, Sima Sadriyeh, Hamid Motahari  
The aim of this study is to analysis vibrational modes of adamantane using theoretical prediction of vibrational frequencies. The chosen calculated technique is based on DFT/B3LYP. The obtained results show all major peaks on adamantane and confirmed by the experimental measurements and other selected theoretical simulation. The achieved vibrational frequencies were at 759, 981, 1088, 1227, 1443 and 2925 cm<sup>-1</sup> regarded to CC stretch, CCC bend/CC stretch, CH<sub>2</sub> wag/CH rock, CH<sub>2</sub> twist, CH<sub>2</sub> scissor, CH stretching modes respectively.
- B058**      **Inter-Molecular and Low-Frequency Vibrational Modes in N-Methylacetamide Dimer Studied Beyond the Harmonic Approximation**  
Václav Parchanský, Petr Bour, Josef Kapitán  
Low-frequency modes (approx. 0-300 cm<sup>-1</sup>) of the molecules bring down about unique information about molecular structure and interactions. Experimental techniques, allowing study those modes as far-infrared and terahertz spectroscopy are available. Computational models (e.g. DFT with harmonic approximation) commonly used to aid spectral interpretation aren't very accurate in this frequency domain. Models going beyond harmonic approximation are tested in this study on a model system of N-methylacetamide. The models exhibit more consistent results which are closer to the experiment.
- B059**      **Molecular Structure, Conformation, Vibrational and Electronic Spectra of Methyl 3-Cyano-2-Propenoate**  
Ajit Viridi  
Ab initio studies of molecular structure, conformation, Vibrational and electronic spectra of methyl 3-cyano-2-propenoate.

B060 **Raman, Resonance Raman and Car-Parrinello Molecular Dynamics of Flavonoids. Study of the Molecular Basis of Their Photoprotective, Fluorescence and Antioxidant Properties**

Alberto Mezzetti, Carla Marrassini, Alexandre Barras, Abdenacer Idrissi, Stefano Protti, Ari P. Seitsonen

We have applied Raman and Resonance Raman spectroscopy coupled to quantum chemistry calculations to study how the microenvironment modifies the chemical and photochemical properties of a series of flavonoids (3-hydroxyflavone, 5-hydroxyflavone, quercetin, luteolin, apigenin, chrysin). Events like solvent-induced formation/disruption of intramolecular hydrogen bonds, or deprotonation of OH groups could be investigated. Car-Parrinello Molecular Dynamics simulations allow rationalizing the dynamics of the solute-solvent interactions. The results make it possible to understand how the microenvironment influences the flavonoid photochemistry and antioxidant role.

B061 **Vibrational Spectroscopy and DFT Calculations of Bisoprolol**

Anca Farcas, Cristian Iacovita, Rares Stiufiuc, Constantin M. Lucaciu, Emil Vinteler

In this paper we investigate the vibrational properties of bisoprolol, using both experimental and theoretical methods. Density functional theory (DFT) calculations were performed with Gaussian 09W software package and were based on hybrid functional methods like B3LYP/6-31+G(d, p) and B3LYP/6-311+G(d, p). Infrared spectroscopy (IR), Raman spectroscopy and Surface Enhanced Raman Spectroscopy (SERS) were employed in order to obtain the vibrational bands of the molecule and to establish the geometry of bisoprolol interaction with gold and silver nanoparticles, respectively.

B062 **Large Scale Variational Calculations on the Vibrational Level Structure of  $S_0$  Thiophosgene**

Svetoslav Slavov, David Moule

In this work, using our recently developed vibrational variational method, we carry out a detailed theoretical study on the vibrational level structure and IVR characteristics of  $S_0$  thiophosgene ( $Cl_2CS$ ). We provide a detailed description of our method of calculations and the associated programming code, called TPG\_vibcalc. Using our method, we determine a refined set of force constants for the molecular potential energy surface, that gives a good coincidence of the calculated with the experimentally measured vibrational frequencies.

B063 **Temperature and Pressure Dependence of the Raman Frequency Shifts in Anthracene**

Hilal Özdemir, Hamit Yurtseven

Raman frequency shifts of the phonons and vibrons of crystalline anthracene are calculated as functions of temperature (zero pressure) and pressure (ambient temperature) up to 3.1 GPa. This calculation is performed for six phonons and nine vibrons of anthracene using the volume data from the literature. Mode Grüneisen parameters are determined and the frequency shifts of the Raman phonons and vibrons are predicted as a function of temperature ( $P=0$ ), which can be compared with the observed data for anthracene.

B064 **Infra-red, Far-Infrared and Raman Spectroscopic and Theoretical Studies of  $LiP_{15}$  Polyphosphides**

Janos Mink, Nadine Eckstein, Laura-Alice Jantke, Thomas F. Faessler, Markus Drees, Tom Nilges

The large structural diversity of polyphosphides is continued in the chemistry.  $LiP_{15}$  polyphosphide has been studied by far-infrared and Raman spectroscopy and by DFT calculations.  $LiP_{15}$  crystallizes triclinic, in space group  $P$ , with  $Z = 2$  and exhibit 96 total modes. From these 78 will be internal modes, so called intra-tube vibrations. Thus 18 external (libration and translation) inter-tube modes are predicted. The way of the assignments of internal and external vibrations will be discussed and the structural results will be analysed.

- B015 Functional Polymeric Supports for Biocatalysts for the Enzymatic Hydrolysis of Cellulose**  
Katarzyna Sokołowska, Ewa Witek, Agnieszka Tata, Anna Konieczny-Molenda, Edyta Proniewicz, Natalia Pierges, Joanna Świdér
- In the present study cellulose enzyme was immobilized onto three of the polymeric carriers. The first carrier is based on N-vinylformamide and styrene with divinylbenzene. The second had the same based monomer and ethylene glycol dimethacrylate, whereas the third consisted of polyvinylamine, N-vinylformamide and ethylene glycol dimethacrylate. The FT-Raman and FT-IR spectroscopies were used to characterize the obtained catalytic polymer-carrier systems. Received systems were used in the test reactions of hydrolysis of paper and wood pulp.
- B029 Raman Spectroscopy Combined with Linear Discriminant Analysis for Detection of Pistachio Aflatoxins**  
Reza Mohammadigol, Rasoul Malekfar, Ehsan Talebian, Mahdi Ghahghaei Nezamabadi
- Raman spectroscopy combined with linear discriminant analysis technique was used to classify intact and aflatoxins (B1+B2+G1+G2) contaminated pistachio samples (100 and 20 ng/g). Raman spectra were analyzed in the spectral region of 848-2000  $\text{cm}^{-1}$ . The effect of the preprocessing methods such as smoothing, normalization, the first and second derivatives, standard normal variate and multiplicative scatter correction and their combination on classification results was studied. All preprocessing methods reduced the average of F, except Savitzky-Golay (SG) smoothing method (F= 0.73).
- B065 ATR-FTIR: A Simple and Rapid Tool for Detection of Bacterial Resistance**  
Mohsen Golabi, Mohammad Javad Jafari, Edwin Jager, Anthony Turner, Thomas Ederth
- We demonstrate that ATR-FTIR can be used for rapid and accurate quantitative assessment of bacterial resistance against antibiotics. The obtained results are in good agreement with conventional antibiogram tests. We also demonstrate the ability of our approach as a rapid method (less than 1 hour) for antibiotic susceptibility tests, and of its suitability for translation into the clinical environment.
- B066 Modular Multi-Level DNA Logic Gates Based on Surface Enhanced Raman Scattering (SERS) for Construction of DNA Half-Adder**  
Zitong Wu, Yizhen Liu, Aiguo Shen, Xiaodong Zhou, Jiming Hu
- Herein, we present a novel optical output based on SERS where molecular Raman spectra were collected from magnetic beads concentrated oligonucleotides-modified AuNPs through strand displacement reactions. We also demonstrated for the first time the SERS-based half-adder by immobilizing logic gates and reactions on magnetic beads.
- B067 Using Synchrotron Radiation Infrared Microspectroscopy as a Novel Approach to Study Interrelationship between Molecular Structure Features and Metabolic Characteristics**  
Peiqiang Yu, Ling Yang, David A. Christensen, John J. McKinnon, Aaron D. Beattie
- The objectives of this study were to (1) apply the Synchrotron-based Fourier Transform Infrared Microspectroscopy as a novel approach to reveal molecular structures of the four hullless barley varieties, and then (2) quantify molecular structural features in relation to rumen degradation kinetics, intestinal nutrient digestion and potential protein supply.
- B068 Using NIR and FTIR as Rapid Methods to Determine Nutritional and Structural Features Among Different Varieties of Forage Corn Grown in Dry Land and Irrigated Land**  
Peiqiang Yu, Hangshu Xin, David A. Christensen, Samen Abeysekera, Xuewei Zhang
- In this study, eight varieties of corn forage grown in semi-arid Western Canada were selected to explore the effect of irrigation implementation in comparison with non-irrigation on 1) agronomic characteristics; 2) basic chemical profile explored by using Near Infrared Reflectance (NIR) system; and 3) protein and carbohydrate internal structural parameters revealed by Attenuated Total Reflectance - Fourier Transform Infrared Spectroscopy (ATR-FTIR) system.

B069

### Characterization of Carotenoids in Soil Bacteria and Investigation of Their Photodegradation by UVA Radiation via Resonance Raman Spectroscopy

Vinay Kumar BN, Bernd Kampe, Petra Rösch, Jürgen Popp

Resonance Raman spectroscopy is a sensitive and powerful technique used to detect and characterize carotenoids and also monitor processes associated with it in its native system at a single cell resolution. Here, we devise a method to overcome the current limitations of this approach by monitoring the photodegradation of the carotenoids by UVA radiation. We have applied this method to characterize the carotenoids in five species of pigmented soil bacteria. Our results show that the monitoring of the carotenoid photodegradation profile might be extremely useful in resonance Raman spectroscopy based carotenoid characterization and analysis.

B070

### In Situ Determination of Phosphatase Activity in Osteoblasts by IR Spectra Using Natural Substrates

Yuqing Wu, Zhongyuan Ren, Le Duy Do, Géraldine Bechhoff, Saida Mebarek, Rene Buchet

We developed an infrared assay which can determine simultaneously protein concentration (using the amide-II band located at  $1550\text{ cm}^{-1}$  with a concentration absorption coefficient of  $3.6\text{ mg}\cdot\text{mL cm}^{-1}$ ) as well as substrate concentration (using the substrate band whenever possible) and phosphate concentration (using phosphate bands located at  $990\text{ cm}^{-1}$  with  $\epsilon = 443 \pm 50\text{ M}^{-1}\text{ cm}^{-1}$  and at  $1080\text{ cm}^{-1}$  with  $\epsilon = 1215 \pm 131\text{ M}^{-1}\text{ cm}^{-1}$ ) in Saos-2 cells as well as in primary osteoblasts.

B071

### Automated Recognition of Subcellular Organelles by Coherent Anti-Stokes Raman Scattering

Daniel Niedieker, Samir F. El-Mashtoly, Dennis Petersen, Sascha Krauss, Erik Freier, Abdelouahid Maghnoij, Stephan Hahn, Carsten Kötting, Klaus Gerwert

Label-free methods are an emerging topic in the Raman community. Since the sometimes long measurement times hinder its wide use, effort was undertaken to overcome this. One recent possibility is the use of non-linear techniques like Coherent Anti-Stokes Raman Scattering (CARS). Here, we combined this method with a supervised learning algorithm, Random Forest, to automatically identify subcellular components like nucleus, nucleolus, lipid droplets and endomembrane systems, and validated our results via fluorescence.

B072

### What Vibrations Tell Us About GTPases

Carsten Kötting, Klaus Gerwert

Time-resolved Fourier transform infrared (FTIR) spectroscopy is used to understand how GTP hydrolysis is catalyzed by small GTPases and their cognate GTPase-activating proteins (GAPs). By interaction with small GTPases, GAPs regulate important signal transduction pathways and transport mechanisms in cells. The GTPase reaction terminates signaling and controls transport. Dysfunctions of GTP hydrolysis in these proteins are linked to serious diseases including cancer. We utilize transmission FTIR spectroscopy with caged compounds and ATR-FTIR spectroscopy of membrane anchored GTPases.

B073

### Effects of Plant Cryopreservation on the Structure of Genomic DNA from Leaf Tissues: a SERS Assessment

Cristina Muntean, Nicolae Leopold, Carmen Tripon, Ana Coste, Adela Halmagy

In this work, SERS spectra of genomic DNAs isolated from leaves of different in vitro grown plant cultivars, in non-cryopreserved control plants, respectively, have been studied. Structural changes induced in genomic DNAs upon liquid nitrogen treatment of shoot apices were also discussed in detail for some cases. SERS signatures, spectroscopic band assignments and structural interpretations for these plant genomic DNAs are reported. Proposed SERS band assignments found in the literature for similar compounds are also included.

**B074 Influence of Microwaves on the Structure of Genomic DNA from Leaf Tissues Monitored by Vibrational Spectroscopy**

Carmen Tripon, Cristina Muntean, Emanoil Surducan, Ana Coste, Adela Halmagyi, Nicoleta Dina

Untreated and microwaves irradiated DNAs were analyzed by FT-IR spectroscopy, in order to investigate their screening characteristic features and their structural tolerance at microwaves irradiation. FT-IR wavenumbers are reported here for all types of vibrations of genomic DNAs, including bands assigned to localized modes of purine and pyrimidine residues, localized vibrations of the deoxyribose-phosphate moiety, etc. Proposed IR band assignments found in the literature for similar compounds were given.

**B075 Towards On-Site Applications: Employing SERS in Drug Monitoring and Food Analysis**  
Dana Cialla-May, Karina Weber, Jürgen Popp

To establish detection schemes in life sciences such as drug monitoring or food analysis, specific and sensitive methods allowing for fast detection times are required. Surface-enhanced Raman spectroscopy became a very powerful analytical tool due to its molecular specificity and high sensitivity. The capability of SERS in combination with microfluidic systems is demonstrated for drug monitoring detection schemes investigating methotrexate and levofloxacin. Furthermore, SERS is applied to detect Sudan III in paprika extracts and E122 in commercial available beverages.

**B076 Potential of Light-Induced Mid-Infrared Emission Spectroscopy to in Situ Analysis of Plants**

Evgeny Terpugov, Olga Degtyareva, Valerie Savranskie, Sofia Terpugova

We are developing the light-induced mid-IR emission spectroscopy (LIMIRES), which allows in situ investigations of chromophore included in a complex biological medium. In this study we show that by using a low intense visible light and a high sensitive FT-IR technique, it is possible to obtain high-quality IR-emission spectra of intact leaf samples. In vivo LIMIRES measurements can be successfully applied to characterize key constituents of the leaf samples of wild-type and transgenic *Nicotiana tabacum* plants.

**B077 The Raman Examination of a Healthy Rat's Brain Tissue**

Julia Sacharz, Janina Zięba-Palus, Aleksandra Weselucha-Birczyńska, Łukasz Chrobok, Mariam H. Lewandowski, Rafał Kowalski, Katarzyna Palus, Agnieszka Sozańska

Three areas of the healthy tissue of rat's brain: the somatosensory cortex (Sc), the dorsal lateral geniculate nucleus of the thalamus (DLG) and the cerebellar cortex (Cc) were tested using Raman spectroscopy. Examined fragments revealed differences in Raman spectra. Analysis showed differences in the bands of amide I, lipids ( $1660\text{ cm}^{-1}$  and  $1440\text{ cm}^{-1}$ ) and  $\text{CH}_2$  and  $\text{CH}_3$  vibrations of proteins and lipids in the  $3000\text{-}2800\text{ cm}^{-1}$  region. Data reduction technique (PCA) was applied to extract and verified obtained information.

**B078 The Application TLC/FTIR Technique in Analysis of a Caffeine/Theophylline Mixture**  
Yizhuang Xu, Danqing Gao, Ye Jiang, Tingguo Kang, Anqi He, Isao Noda, Jinguang Wu

A caffeine/theophylline mixture was analyzed by using TLC/FTIR method developed in our lab. The mixture was developed on a narrow band TLC plate whose stationary phase was AgI. FTIR analysis by using mapping technique was performed on the narrow band TLC plate. Caffeine/theophylline can be successfully separated and the distribution of caffeine and theophylline spots was manifested via a 3D chromatogram generated from the IR mapping data. FTIR spectra of caffeine/theophylline spots are the same as the corresponding reference spectra.

**B079 Combined Experimental and Theoretical Characterization of Naratriptan Hydrochloride**

Judyta Cielecka-Piontek, Mikoaj Mizera, Alicja Talaczyńska, Magdalena Paczkowska, Kornelia Lewandowska, Mirosaw Szybowicz, Anna Krause

The work focused on investigation of the impact of the type of diffusion basis functions relating to different hybrid models (B3LYP, CAM3LYP, MO6, PBE1PBE, RHF) on the optimization of naratriptan hydrochloride molecule geometry. The confirmation of identification of naratriptan hydrochloride by using experimental spectra: UV, Raman and FT-IR was supported by the density functional theory with the B3LYP hybrid functional and 6-31G(d,p) basis set. The HOMO and LUMO orbitals and molecular electrostatic potential were also determined.

B080 **Vibrational Spectroscopy (FT-IR, Raman) Investigations and DFT Analysis on the Structure of Crystalline Form Tebipenem and its Ester. An Application for Identification of Labile Drugs**

Judyta Cielecka-Piontek, Magdalena Paczkowska, Kornelia Lewandowska, Bolesaw Barszcz

The current work was aimed at a comparative analysis of the application of FT-IR and Raman spectroscopies for a quality control study of tebipenem and its ester form – the first oral  $\beta$ -lactam antibiotic from carbapenem group. The analysis of experimental spectra was supported by quantum-chemical calculations performed with the use of B3LYP functional and 6-31G(d,p) as a basis set. In addition, the optimized geometry, the frontier molecular orbitals and the molecular electrostatic potential were established for tebipenem and tebipenem pivoxyl.

B081 **Application of FT-IR and Raman Spectroscopy for Study of Impurities of Tedizoid Enantiomers**

Judyta Cielecka-Piontek, Katarzyna Michalska, Kornelia Lewandowska, Mikoaj Mizera

The aim of this work was to assess the possibility of applying classical spectral methods such as FT-IR and Raman spectroscopy for studies of the chiral purity of tedizoid enantiomers, with UV-CD spectroscopy used as a reference method. The analysis of the purity of tedizoid enantiomers, both R and S were conducted in combination with experimental and theoretical studies of vibrational spectra (FT-IR and Raman spectra, UV-CD). The calculations were made using the density functional theory.

B082 **Observation of Effect on Cellulose Derivative against a Pseudo-polymorphism Conversion and Dehydration in Pharmaceutical Granules by Using a Terahertz Spectroscopy and Near-Infrared Chemical Imaging**

Tomoaki Sakamoto, Tetsuo Sasaki, Noriko Katori, Yukihiro Goda

We examine an effect on viscosity of a binder against pseudo-polymorphism conversion of theophylline in pharmaceutical granules. the conversion from the amorphous to the anhydride were analysed using a terahertz spectroscopy. It is predicted that an intermolecular interaction between a binder and theophylline would affect about a delay of the conversion rate. Moreover, the conversion rate increased with depending on its viscosity. Moreover, distribution of pseudo-polymorphs of theophylline and water on the tablet were monitored using a near-infrared chemical imaging.

B083 **Raman Resonance Effect in Water Solutions of Selected Inorganic Salts**

Marcin Kozanecki, Paulina Filipczak

Raman resonance effect in liquid water was demonstrated by Pastorczak et al. in 2008. An increase of intensity of the component related to structured water ( $3200\text{ cm}^{-1}$ ) with increase of used excitation line wavelength was observed. In this work we studied the impact of selected inorganic salts (KCl, NaCl and LiCl) on Raman resonance effect in liquid water. the effect of the cation size will be discussed. This work was financially supported from grant no. 2013/09/B/ST4/03010.

B084 **Following Lignification in-Situ by Confocal Raman Microscopy**

Batirtze Prats Mateu, Notburga Gierlinger

Wood is of high importance as raw material for paper and construction industries and also of potential interest for biofuel industry. It is essential to know how it is composed and the nature of its single elements. Here we present multivariate analysis to follow in situ lignification in wood: Non-negative matrix factorization (NMF) and Vertex Component analysis (VCA) for the analysis of the hyperspectral data generated by non-destructive Raman Imaging on the differentiating area of the stem of a 7-years old Spruce (*Picea abies* L.).

- B085**     **Military Incapacitating Agent 3-Quinuclidinyl Benzilate: Raman and SERS Spectral Analysis and DFT Calculations**  
Václav Profant, Lucie Štolcová, Marek Procházka, Vladimír Baumruk, Jan Proška, Kamil Kuča  
3-Quinuclidinyl benzilate (QNB) is a very potent competitive antagonist at all subtypes of muscarinic acetylcholine receptors causing stupor, confusion, hallucinations, etc. Owing to those effects, QNB has been deployed as an incapacitating chemical warfare agent. Recently, the new low concentration detection method based on SERS has been suggested exploiting the novel Au surfaces (see contribution by L. Štolcová, et al.). In our contribution we focus on the Raman and SERS spectral characterization of QNB accompanied by the theoretical DFT calculations.
- B086**     **Absolute Configuration Determination of Key Precursor in Synthesis of Cytostatic Medicament Paclitaxel**  
Václav Profant, Alexandr Jegorov, Vladimír Baumruk  
Paclitaxel, also known as Taxol, is currently one of the best-selling cancer medicament used in the treatment of ovarian, lung and breast cancer as well as Kaposi's sarcoma. One of semi-synthetic Paclitaxel production approaches is based on utilization of baccatin III. The key agent used for the baccatin III functionalization is the synthetic compound 1-t-butoxycarbonyl-3-triethylsilyloxy-4-phenyl-2-azetidinone (I) possessing two chiral centers. In our study we focus on the determination of absolute configuration of (I) via spectroscopic measurements and DFT simulations.
- B087**     **Label-free Identification, Differentiation and Imaging of Bacteria and Biofilms**  
Branko Vukosavljevic, Maike Windbergs  
We identified four different planktonic microorganisms (*S.carnosus*, *P.stutzeri*, *P.anomala* and *E.coli*) based on their Raman spectra and differentiated them in the co-culture. Furthermore, *E.coli* biofilms were investigated with Raman imaging in order to detect differences in the spatiotemporal organization of the bacteria as well as EPS secretion after formation of the biofilm. Confocal Raman microscopy is a valuable tool in the analysis of bacteria, ranging from label-free differentiation of individual strains, up to advanced 3D imaging of bacterial biofilms.
- B088**     **Differentiation of Carotenoids by Surface Enhanced Raman Spectroscopy (SERS)**  
Andreea Radu, Martin Jahn, Uwe Huebner, Karina Weber, Dana Cialla-May, Jürgen Popp  
Surface enhanced Raman spectroscopy (SERS) offers the possibility of performing fast and cost effective analyses of trace amount of analytes by measuring its molecular fingerprint. We present here the application of a SERS substrate, namely a silver deposited micro fabricated quartz arrays produced by electron beam lithography (EBL) for the detection and differentiation of two carotenoids:  $\beta$ -carotene (important vitamin A precursor) and lycopene (strong antioxidant having an important role as an inhibitor of cancer cell proliferation).
- B089**     **Vibrational Spectroscopic Investigations of Alpha/Gamma Hybrid Peptide Organogels**  
Muruga Poopathi Raja Karuppiah, Kanaga Vidhya Ilangovan, Rajkumar Misra, Rahi M Reja, Hosahudya N Gopi  
In this work, we investigated the formation of organogels by short alpha/gamma hybrid peptide in various aromatic solvents. Detailed vibrational spectroscopic investigations by ATR-FTIR exhibited distinct Amide fingerprint spectral signatures, confirming their secondary structure conformations and self-assembly. The peptide yielding organogels in aromatic solvents indicated the predominant beta-sheet and/or extended conformations, whereas peptide in non-aromatic solvents showed multiple conformations failing to gelation, which is clearly characterized by Amide I, II and A vibrational bands.

B090 **Infrared Spectroscopy for Fast Characterization of Fungal Plant Pathogens Using Micro-Techniques**

H. Michael Heise, Christoph Nagel, Arne Ükermann, Roderich Garmeister

For this investigation, Fourier transform infrared spectroscopy (FTIR) was used to identify fungal plant pathogens, which in contrast to conventional species identification, is less time-consuming and more objective. The measurements were performed either in the attenuated total reflection (ATR) mode or using transmission with the potassium bromide micro-pellet method. For determination of the fungi genera, infrared bands, which differ in position, intensity and line shape among the species, were analyzed. Discrimination results are presented using cluster analysis.

B091 **DMSO Addition to Model Membranes: Effects on the Gel to Liquid Crystal Phase Transition**

Paola Sassi, Maria Ricci, Beatrice Gironi, Marco Paolantoni, Alessandra Giugliarelli, Assunta Morresi

Notwithstanding the large use of DMSO as a permeable cryosolvent, the type of interaction with the plasmatic membrane is far from being understood. In the present work the DMSO addition to model membranes (liposomes and ghosts of erythrocyte cells) was followed by IR and Raman spectroscopies to evidence the effects on the thermal stability of the lipid bilayer. Indeed, in the presence of DMSO, the thermotropic behavior of the lipid bilayer is altered and the transition temperature increases.

B092 **Vibrational Features of Dacarbazine and Deticene Revealed by Raman, SERS, THz-Raman and DFT Methods**

Alexandra Falams, Mihaela Chis, Calin Cainap, Nicolae Leopold, Vasile Chis

Raman, THz-Raman and SERS techniques have been coupled to DFT methods and applied for studying the molecular species of Dacarbazine (DTIC) and Deticene (DET) at different pH values. By using the SERS technique we derived the limit of detection of  $9.1 \times 10^{-7}$  M for DTIC in water. THz-Raman spectra of DTIC and DET have shown that the same polymorphic form is present both in the chemical compound (DTIC) and the administered drug (DET).

B093 **Discrimination of Haloarchaeal Genera Using Raman Spectroscopy and PCA**

Anda Leş, Nicoleta E. Dina, Andreea Baricz, Horia L. Banciu, Nicolae Leopold

Raman microspectroscopy in combination with Principal Component Analysis (PCA) was employed for discrimination of Haloferax, Halobacterium and Halorubrum haloarchaeal strains. Spectra pre-treatment is an important factor which influences dramatically the PCA results. Thus, the grouping of haloarchaeal genera after Raman spectra pre-treatment, using scattering and baseline corrections as well as different types of normalization, is presented.

B094 **2D Raman Correlation Spectroscopy for Study of Alpha-Lactalbumin/Oleic Acid Complex**

Yeseul Kim, Yeonju Park, Bogusława Czarnik-Matusiewicz, Young Mee Jung

The ALA can bind to OA the resulting complex possesses cytotoxic activity with respect to tumor cells, which is called HAMLET. However, the actual molar ratio of OA over protein in the complex is not completely understood yet. In this study, to investigate structural changes of ALA/OA complex having different molar ratio, PCA and 2D correlation spectroscopy were applied to the pH-dependent Raman spectra of ALA/OA complex. Details of PCA and 2D correlation spectra will be discussed in this presentation.

B095 **Surface-Enhanced Raman Scattering Characteristics of Cholesterol Oxidase Enzyme Bonded with Gold Nanoparticles**

Renata Wojnarowska, Eugeniusz M. Sheregii, Mykhailo Gonchar, Jacek Polit

Surface-enhanced Raman spectroscopy (SERS), is optimal method for observation of the oscillation spectra in case of biomolecules. The SERS effect was obtained for the protein, which is important in the clinical diagnosis. On the surface of gold nanoparticles, the cholesterol oxidase enzyme was immobilized. The vibrational lines attributed to functional groups existing in the enzyme and linker have been identified. Besides typical functional groups of proteins, the vibration lines associated with the flavin adenine dinucleotide prosthetic group have been observed.

- B096 Raman Spectroscopy Studies of Race B Botryococenes**  
Mehmet Tatli, Hye Jin Chun, Shigeru Okada, Jaan Laane, Timothy P. Devarenne  
*Botryococcus braunii* is a green colonial microalga which produces up to 86 % hydrocarbons, known as *botryococenes* that can be used as combustion engine fuel. It has been shown that there are several identified isomers of *botryococenes* based on C31, C32, and C34 structures. In vitro Raman analysis and DFT calculations have shown that C30, C31, C32 isomers have several significant spectral differences in the region from 200-1700 cm<sup>-1</sup>, and these will be discussed.
- B097 Sound Speed Dispersion and Compressibility of Aqueous Lysozyme Solutions**  
Augustinus Asenbaum, Christian Pruner, Emmerich Wilhelm, Alfons Schulte  
Compared to pure liquid water, aqueous protein solutions show a larger sound speed and a smaller isentropic compressibility, which is interpreted to be due to protein-solvent interaction and the corresponding formation of a hydration shell. We have investigated aqueous lysozyme solutions at ambient pressure over the temperature range 275<T/K<335 by Brillouin spectroscopy and have also measured density, refractive index (at = 514.5 nm) and ultrasonic speed (at 3 MHz). A significant dispersion of the sound speed in the lysozyme solutions was observed corresponding to a smaller compressibility at higher frequencies indicating relaxation processes which have not been seen in pure bulk water.
- B098 Effect of the Ribose Versus 2'-Deoxyribose Residue in Guanosine-5'-Monophosphates on the Formation of G-quartets Stabilized by K<sup>+</sup> and Na<sup>+</sup>**  
Kateřina Mudroňová, Václav Římal, Peter Mojžeš  
The effect of the ribose versus 2'-deoxyribose on the 5'-GMP self-assembling in the presence of Na<sup>+</sup> and K<sup>+</sup> ions was studied by means of Raman and <sup>1</sup>H and <sup>31</sup>P NMR spectroscopy. It was found that ability of 5'-dGMP to constitute G-quartets and supramolecular structures resembling G-quadruplexes strongly depends on the nature of stabilizing alkali cation and is substantially lower than that of 5'-rGMP. Possible consequences for different polymorphism of DNA and RNA G-quadruplexes will be discussed.
- B099 Variation of Near-Infrared Spectrum of Water with Dissolved Salt**  
Naruya Uchida, Norio Yoshimura, Masao Takayanagi  
We analyzed in detail the variations of near-infrared (NIR) spectrum of water upon the dissolution of various salts with principal component analysis (PCA) to get the clue for the microscopic elucidation of the variation of the hydrogen-bond network. Two different type variations were found to be induced by anions, while all cations examined were found to cause a similar type variation.
- B115-pdp Vibrational and Structural Study of Solid State and Aqueous Solution of N-Acetyl-L-Cysteine**  
María Eugenia Tuttolomondo, R. A. Cobos Picot, C. Contreras, S. B. Diaz, M. Puiatti, A. Ben Altabef  
The aim of this work is to evaluate the vibrational and structural properties of N-Acetyl-L-cysteine (NAC), and its electronic behavior mainly in relation to the action of the S-H and C=O groups at different degrees of solvation. Its Raman spectrum was measured in solid state and aqueous solution. Additionally, the UV and circular dichroism spectra of NAC in aqueous solution were measured. The influence of an aqueous environment on the NAC spectra was simulated by means of implicit and explicit solvent models.
- B116-pdp Fluorescence for Monitoring the Degradation of Polypropylene in Consumer Product**  
Marion Egelkraut-Holtus, Yasushi Suzuki  
Polymers are used in many fields because of workability and good lightweight properties, it has become part of modern life. Meanwhile, depending on the material the ageing of the polymer product needs evaluation. Composition Change, structural change and other characteristics are represented by a number of indicators such as change in intensity, fluorescence and chemiluminescence. These effects due to structural changes due to deterioration can be effectively evaluated by the fluorescence technique as a non-destructive measurement method.

B117-pdp **Raman Imaging of Photosynthetic and Photoprotective Pigments in Biological Tissues**  
Petr Vitek, Carmen Ascaso, Karel Klem, Jacek Wierzchos

High resolution Raman images are presented showing distribution of pigments in different kinds of phototrophic biota, from microorganisms to higher plants. Pigments of endolithic algae and cyanobacteria from the Atacama Desert were mapped "in-situ" in the rock habitat showing distribution of carotenoids and scytonemin as a response to high dose of solar radiation. Secondly, carotenoid depletion within leaves of sunflower and cleavers treated by carotenoid biosynthesis inhibitors is presented in the form of Raman images.

## Instrumentation (NIR, MIR, THz)

B100 **UHV FT-IR Spectroscopy: An Instrumental Contribution for Fundamental Research**  
Xia Stammer, Anders Nilsson, Mathias Kessler

In the interdisciplinary research work the demand grows to adapt to the FT-IR spectrometer optics a large gas phase measurement cell, an ultra-high vacuum (UHV) chamber or a plasma reaction chamber. The combination of the FT-IR technique and the external reaction chambers enables in-situ monitoring of reaction processes from fundamentals to applications. Bruker provides multiple innovative adaptation solutions of external chambers to vacuum FT-IR spectrometers.

B101 **MIR-FIR Spectroscopy by a Single Step Data Acquisition**  
Mathias Kessler, Xia Stammer, Günter Zachmann, Anders Nilsson

The newly announced VERTEX FM wide range infrared technology offers the measurement of the whole MIR-FIR infrared region in one single step. This allows for easy and fast infrared analysis and is especially useful for inorganic or organometallic compounds which show low energy vibrations in the far infrared and for the differentiation of polymorphs.

B102 **Reflectance Spectroscopy for Sample Identification: Considerations for Quantitative Library Results at Infrared Wavelengths**

Tim Johnson, Thomas Blake, Carolyn Brauer, Yin-Fong Su, Bruce Bernacki, Tanya Myers, Russell Tonkyn, Brenda Kunkel, Alyssa Ertel

We discuss protocols and instrumentation to make quantitative hemispherical reflectance measurements in the infrared. The data are ideally portable to any instrument, including for "point and shoot" detection. Special sample effects such as particle size and surface scattering will also be discussed.

B103 **Influence of Enflurane, Halothane, Isoflurane and Sevoflurane on the Chain-melting Phase Transition of DPPC Liposomes. Near-infrared Spectroscopy Studies Supported by PCA Analysis**

Katarzyna Cieřlik-Boczula, Marta Kuć, Maria Rospenk, Bogusława Czarnik-Matusiewicz

The effect of four inhalation anesthetics on the chain-melting phase behavior of dipalmitoylphosphatidylcholine (DPPC) liposomes was studied using Near-infrared spectroscopy (NIR). The PCA analysis was applied to regions of NIR spectra associated with the first overtones of the symmetric and antisymmetric stretching vibrations of CH<sub>2</sub> groups of lipid aliphatic chains. All anesthetics significantly reduced temperature of lipid chain-melting phase transition accompanied by an increase in gauche conformers of lipid CH<sub>2</sub> groups and by a formation of the interdigitated lipid phase.

B104 **Investigation of Molecular Processes in Inactive Liquid Hydrogen Isotopologues via Infrared Absorption Spectroscopy**

Sebastian Mirz, Robin Größle, Sebastian Wozniewski

The Tritium Absorption Infrared Spectroscopy Experiment at the Tritium Laboratory Karlsruhe investigates liquid inactive hydrogen isotopologues via IR absorption spectroscopy. This contribution gives an overview of measurements on liquid H<sub>2</sub>, HD and D<sub>2</sub>. Besides a calibration of IR absorption versus isotopologic concentration, results of a study of ortho/para conversion and the measurement of this process via IR and Raman spectroscopy is presented. Moreover the assignment of calculated positions of molecular transitions to visible lines in spectra of the 2nd vibrational branch will be illustrated.

**B105**      **Effect of Intermolecular Interactions on Absorption Intensities of the First and Second Overtones of OH and NH Stretching Vibrations Studied by Near-Infrared Spectroscopy**  
Yusuke Morisawa, Misaki Tatsumi, Yukihiko Ozaki

In the present study we have investigated effects of intermolecular interactions on absorption intensities of the OH and NH the first and second overtones of 1-octanol, and pyrrole in none polar solvent by using NIR spectroscopy. We selected these molecules because they easily form hydrogen-bonding aggregates while in enough dilute solutions they do not form hydrogen-bonding species and have an intermolecular interaction with a solvent (solvent effect). We investigated higher order overtones than previous work.

**B106**      **Poly(Vinyl Alcohol) Coating as Protection Layer for Spectroelectrochemical Characterization of Soluble Organic Semiconductors**

Sandra Enengl, Christina Enengl, Philipp Stadler, Helmut Neugebauer, Niyazi S. Sariciftci

In this work we perform electrochemical and in situ spectroelectrochemical measurements on hydrogen bonded organic semiconductors, among others quinacridone, which normally dissolve in the oxidized or reduced form. By using a thin layer of poly(vinyl alcohol) on top of our studied material, electrochemistry becomes possible. In addition, we demonstrate that this protection layer has no significant influence on the spectroelectrochemical measurement itself.

**B107**      **Sensitivity of Pairs of ro-Vibrational Transitions to a Variation of Electron-to-Proton Mass Ratio**

Florin Lucian Constantin

A mechanism to increase the sensitivity of rovibrational spectra to a possible variation of  $\mu$  is discussed. Pairs of near-resonant transitions from different isotopomers or vibrational bands in the ground state electronic level are considered. The variation of their frequency splitting with the variation of  $\mu$  can be large relative to the frequency splitting or to the variation of one transition. Comparison of isotopic acetylene frequency standards at 1.5  $\mu\text{m}$  is promising for the search of variation of  $\mu$ .

**B108**      **Strong Light-Matter Coupling Exhibited in Mid-IR FTIR Measurements of a PMMA Film Situated Inside a Resonantly Tuned Microcavity**

Merav Muallem, Alex Palatnik, Gilbert D. Nessim, Yaakov R. Tischler

We present a microcavity phonon-polariton system that is derived from coupling cavity-confined mid-IR photons to the vibronic transitions of an organic material. To achieve strong phonon-photon coupling, we use a low-loss resonant optical microcavity that contains a thin film of PMMA, which possesses a suitably absorptive dipole-allowed vibronic transition. Spectroscopy measurements were performed in transmission mode on an FTIR system and show two distinct transmission peaks that are energetically shifted by the Rabi-splitting from the bare phonon and cavity resonance.

**B109**      **Non-Destructive Identification of Contaminated Cosmetics Using Palm-Sized Near-Infrared Spectroscopy**

Jordan Thomas, Sulaf Assi, David Osselton

Contaminated cosmetics can cause many unwanted side effects, including flushing and irritation. Such contamination can be encountered at any stage of the product preparation or even during storage, and can be caused by a range of factors, including changes in humidity or temperature, where subsequently, changes in water content can be observed. The aim of this work was to identify contaminants in cosmetic products using palm-sized near-infrared spectroscopy, a non-destructive and rapid detection method of physicochemical properties.

B110 **Diamond Coatings for Improving Molecular and Nanoparticle Sensitivity of Reflectance-Based IR Spectroscopy**

Alexander Kromka, Halyna Kozak, Oleg Babchenko, Tibor Izak, Bohuslav Rezek

Diamond coated grazing angle reflectance (GAR) Au mirrors and ATR prism were used as optical elements for infrared spectroscopy of proteins adsorbed from FBS solution. The measured IR spectra revealed fingerprints of proteins adsorbed on the hydrophilic diamond surface. For the ATR prisms, the spectral range was limited by the prism material (silicon versus germanium) and no optical interference from the diamond coating was observed. Advance properties of the diamond coated GAR and ATR elements are pointed out.

B111 **Miniaturized Preconcentrator (iPRECON) for Breath Diagnostics Using Substrate-Integrated Hollow Waveguide (iHWG) Mid-Infrared Sensors**

Vjekoslav Kokoric, Andreas Wilk, Boris Mizaikoff

A new generation of integrated preconcentrators particularly suited for exhaled breath gas analysis using mid-infrared (MIR; 2-20  $\mu\text{m}$ ) absorption spectroscopic techniques is described. The developed analyzer system comprises a compact preconcentrator (iPRECON) exemplarily tested for sampling isoprene, which readily couples to substrate-integrated hollow waveguides (iHWGs) of the same footprint, the latter serving simultaneously as highly miniaturized gas cell and photon conduit.

B112 **An Automated Sample Compartment Accessory for Infrared Multiple Angle Incidence Resolution Spectroscopy**

David Drapcho

Multiple Angle Incidence Resolution Spectroscopy (MAIRS) has proven useful for characterization of the in-plane (IP) and out of plane (OP) vibrations of thin films on solid substrates. The MAIRS technique computes the IP and OP spectra by a regression analysis on a series of oblique-incidence transmission spectra of a thin film mounted on a transparent substrate. This paper presents an automated accessory for collection of the spectra, followed by automated processing to compute the IP and OP spectra.

B113 **Near-Infrared Spectroscopy Using a Supercontinuum Laser. Application to Long-Wavelength Transmission Spectra of Barley Seeds**

Tine Ringsted, Sune Dupont, Jacob Ramsay, Søren Rud Keiding, Søren Balling Engelsen

A novel spectrometer for long wavelength NIR using a supercontinuum laser was developed and for the first time tested for transmission analysis of the barley seeds and extracted barley oil from different barley genotypes.

B114 **Application of Tunable Fabry-Pérot Filters to MIR Spectroscopy for Qualitative and Quantitative Analysis of Gas Mixtures**

Christoph Gasser, Andreas Genner, Harald Moser, Johannes Ofner, Bernhard Lendl

Monitoring of chemical processes in a variety of industrial applications is desirable for economic and ecological reasons. This requires a manifold of sensors with adequate selectivity and sensitivity. Tunable Fabry-Pérot interferometers in the mid IR region combined with adequate light sources and detectors allows for construction of small, rugged and powerful sensors for chemical analysis. Here, we show the application of such a device on gas monitoring, simultaneously observing three components.

B118 **Vibrational Spectroscopy in the Cloud: Simple, Web Based Applications**

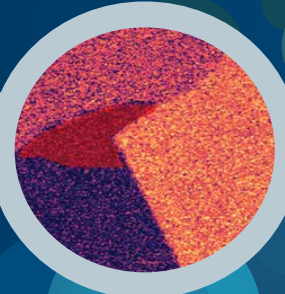
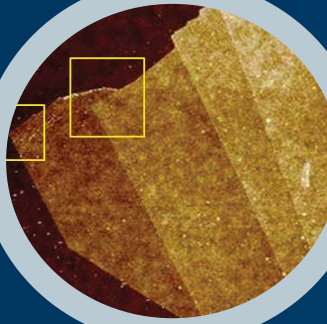
Maren Fiege, Klaus Schürmann, Alexander Holland-Moritz

Web based spectroscopy software offer new possibilities of addressing current problems. Based on a flexible database storing spectral data and additional information, this kind of software can serve as a platform for dedicated “apps”, making spectrum search, mathematical processing, and chemometrics accessible to both expert and novice users. At the same time, the web based approach makes these apps available not only on a PC, but also on mobile devices such as tablet computers or even smartphones.

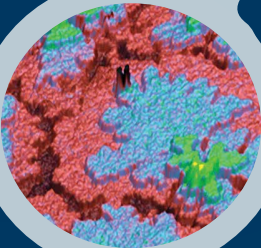
# Integrated AFM & Infrared Nanocharacterisation



PS-PMMA  
Nanochemistry



Graphene Defects  
& Plasmonics



IR Mapping:  
Pentacene Monolayers



## Inspire

PeakForce IR

- Highest-resolution chemical & topographic mapping
- Correlated chemical, mechanical & electrical properties
- Characterises previously impossible samples with PeakForce IR™
- Unmatched productivity with ScanAsyst® automation

What problem do you need to solve? Please visit [www.bruker.com/inspire](http://www.bruker.com/inspire) or email [productinfo.europe@bruker-nano.com](mailto:productinfo.europe@bruker-nano.com) for more information today.

Innovation with Integrity

Atomic Force Microscopy

9:00  
WEPL1 **Peptide Conformations and Solvent Environments Obtained from Raman Optical Activity**

Shigeki Yamamoto

Conformations of peptides and its surrounding solvent environments can be elicited from Raman optical activity (ROA) spectra. We present here our ROA studies on peptides and a small protein by comparisons of the experimental spectra to quantum-mechanically calculated ones which can give information about structures of conformers, conformer populations and also solvent permittivity. A new assignment on extended amide III ROA bands is proposed based on good theoretical reproductions of the experimental spectra.



Assistant professor, Osaka University, Japan. Ph.D. from Osaka University in 2009. After post-doc experiences at IOCB in Czech and Kwansai Gakuin University in Japan, from 2013 at the present position. Current research interests are in chiral spectroscopies especially in Raman Optical Activity (ROA), solution structures of peptides and chiral polymers, instrumentation of ROA, and theoretical simulation of vibrational spectra.

9:35  
WEPL2 **Vibrational Imaging Provides Marker-Free Annotation of Tissue and Cells in Biomedical Applications**

Klaus Gerwert

Infrared, Raman and CARS are emerging tools for label-free, non-invasive characterization of tissue, cells and body fluids. Thereby the pathological annotation of tissue and liquid biopsies maybe performed in automated workflow with high sensitivity and specificity. Vibrational spectra are used as fingerprints to identify and annotate cancer in tissue, living cells and body fluids. The approach is applied to fresh frozen and formalin fixed paraffin embedded tissue samples, small biopsies and blood-plasma. A similar approach is used for neurodegenerative diseases.



Klaus Gerwert studied physics in Muenster, received his Ph.D. in biophysical chemistry in Freiburg, Heisenberg-fellow of the DFG at the Scripps Research Institute, La Jolla, USA and Max-Planck-Institute, Dortmund, since 1993 full professor at the Ruhr-University Bochum, chair of the biophysics department; since 2009 "Max-Planck-fellow" and 2009-2013 director (dual appointment) at the Max-Planck-CAS partner-institute in Shanghai, 2010 founder of PURE. He contributed to the detailed understanding of molecular reaction mechanisms of proteins with focus on the functional role of protein bound water molecules, especially in the membrane proteins bacteriorhodopsin and channelrhodopsin. Recently, he focuses on novel vibrational imaging techniques of cells and tissues in spectral histopathology and spectral cytopathology to improve molecular diagnostics in personalized medicine.

## Peptide Conformations and Solvent Environments Obtained from Raman Optical Activity

Shigeki Yamamoto<sup>1</sup>

<sup>1</sup>Department of Chemistry, Graduate School of Science, Osaka University  
Machiakaneyama 1-1, Toyonaka, Osaka 560-0043, Japan

Keywords: ROA, Vibrational optical activity, Quantum mechanical calculation.

Conformations of peptides and its surrounding solvent environments can be elicited from Raman optical activity (ROA) spectra. We present here our ROA studies<sup>1-7</sup> on peptides and a small protein by comparisons of the experimental spectra to quantum-mechanically calculated ones which can give information about structures of conformers, conformer populations and also solvent permittivity. A new assignment on extended amide III ROA bands is proposed based on good theoretical reproductions of the experimental spectra<sup>1</sup>.

ROA spectra of isotropic solutions may be measured as small differences in Raman scattering intensities corresponding to right and left circularly polarized light.<sup>8</sup> Applications of ROA have been expanded to include the structural analyses of peptides and proteins in solutions, especially denaturing or unfolding proteins and their intermediates which are difficult to analyze by the other measurement techniques<sup>3</sup>. However, some important spectral features of peptide ROA spectra are still not fully understood. For example, as will be discussed in this lecture, extended amide III ROA bands of  $\alpha$ -helical structure seems not well-explained by a conventional explanation<sup>9</sup>, a geometrical change of helices between solvated and unsolvated  $\alpha$ -helical structures.

The most effective way to interpret the ROA spectra is its comparisons to quantum-mechanically simulated ones. Owing to the

developments of the software and the hardware, nowadays it is possible to calculate reliable ROA spectra of small- and medium-sized molecules in an acceptable time. However, for bigger and flexible molecules, it is still difficult to calculate the spectra with high accuracy because of the high cost. We successfully applied the quantum mechanical calculations of ROA of peptides and a small protein, insulin, with the aid of the Cartesian-coordinate tensor transfer (CCT) method<sup>10-12</sup> which can dramatically reduce computational time with retaining nearly ab-initio accuracy.

By applying this method, the experimental ROA pattern in the extended amide III region of PLA was successfully reproduced at the first time<sup>1</sup>. Our calculations on the PLA indicate that the change in dielectric constant of the surrounding solvent is the main factor to change the spectral intensity ratio, whereas the conformational change is a minor one.

The ability of the ROA bands to distinguish solvent dielectric constant around  $\alpha$ -helix will be valuable to study proteins in solutions as they often undergo conversion of hydrated  $\alpha$ -helices during their denaturation. The secondary-structural changes of the amyloid fibril of insulin and its naturing intermediates were explored based on the experimental ROA spectra with the empirical assignments<sup>3</sup>. The vanishing of the hydrated  $\alpha$ -helical ROA band at  $\sim 1340$   $\text{cm}^{-1}$  in unfolding processes of proteins can

be interpreted in terms of the solvent-exposure.

We also successfully applied the ROA calculation with the CCT method to the native insulin molecule<sup>2</sup> (insulin contains about 1600 atoms in its dimer state) in order to verify the assignments of the ROA bands and to know the details of the signal generation of ROA. The CCT methodology yielded spectra of insulin monomer and dimer with nearly ab initio quality, while at the same time reproducing the experiment very well. The link between the spectra and the protein structure could thus be studied in detail. Spectral contributions from the peptide backbone and the amino acid side chains were calculated. Besides, specific

intensity features originating from the  $\alpha$ -helical, coil,  $\beta$ -sheet, and  $3_{10}$ -helical parts of the protein could be assigned. The assignment of the Raman and ROA bands to intrinsic molecular coordinates revealed their origin and degree of locality. Alternatively, the relation of the structural flexibility of insulin to the smoothing of spectral bands was studied by a combination of CCT and molecular dynamics.

The work was partly supported by the JSPS Grants-in-Aid for Young Scientists (A) (26708017), that for Scientific Research (A) (26246037), and Yamada Science Foundation.

- <sup>1</sup> S. Yamamoto, T. Furukawa, P. Bouř, and Y. Ozaki, *J. Phys. Chem. A*, 2014, *118*, 3655-3662
- <sup>2</sup> S. Yamamoto, J. Kaminsky, and P. Bouř, *Anal. Chem.*, 2012, *84*, 2440-2451
- <sup>3</sup> S. Yamamoto, H. Watarai, *Chirality*, 2012, *24*, 97-103
- <sup>4</sup> S. Yamamoto, J. Kaminský, P. Bouř, *ChemPhysChem*, 2011, *12*, 1509-1518
- <sup>5</sup> S. Yamamoto, M. Straka, H. Watarai, P. Bouř, *Phys. Chem. Chem. Phys.*, 2010, *12*, 11021-11032
- <sup>6</sup> S. Yamamoto, H. Watarai, *J. Raman Spectrosc.* 2010, *41*, 1664-1669
- <sup>7</sup> S. Yamamoto, *Anal. Bioanal. Chem.*, 2012, *403*, 2203-2212
- <sup>8</sup> L.D. Barron. 2014, *Molecular light scattering and optical activity*, 2nd ed., Cambridge University Press: Cambridge.
- <sup>9</sup> I.H. McColl, E.W. Blanch, L. Hecht, L.D. Barron, *J. Ame. Chem. Soc.*, 2004, *126*, 8181-8188
- <sup>10</sup> P. Bouř. T.A. Keiderling, *J. Chem. Phys.* 2002, *117*, 4126-4132
- <sup>11</sup> P. Bouř. J. Sopková, L. Bednářová. P. Maloň, T.A. Keiderling, *J. Comput. Chem.* 1997, *18*, 646-659
- <sup>12</sup> S. Yamamoto, X. Li, K. Ruud, P. Bouř. *J. Chem. Theory Comput.*, 2012, *8*, 977-985

## Vibrational Imaging Provides Marker-Free Annotation of Tissue and Cells in Biomedical Applications

Klaus Gerwert<sup>1</sup>

<sup>1</sup>Department of Biophysics, Ruhr-University Bochum, 44801, Bochum, Germany

Keywords: FTIR imaging, Raman imaging, CARS, spectral histopathology, cancer

Infrared, Raman and CARS are emerging tools for label-free, non-invasive characterization of tissue, cells and body fluids.<sup>1</sup> Thereby the pathological annotation of tissue and liquid biopsies maybe performed in automated workflow with high sensitivity and specificity over 95% respectively.

Vibrational spectra are used as fingerprints to identify and annotate cancer in tissue, living cells and body fluids. The approach is applied to fresh frozen and formalin fixed paraffin embedded tissue samples. For the entities colon, bladder and lung, data bases are established to characterize tissue in an automated way with sensitivity and specificity of over 90%.<sup>2-3</sup> A bioinformatics workflow and a corresponding power-full computer cluster is established.<sup>4</sup> While IR provides fast annotation of larger tissue sections,<sup>3</sup> Raman is slower but allows a 10 times higher spatial resolution as compared to IR. This leads to resolve erythrocytes, lymphocytes and single cell nuclei in tissue sections by Raman imaging.<sup>2</sup>

The approach is extended for IR and Raman from tissue to small biopsies using thin fiber optics. Thereby, the measuring time is reduced to few seconds and can be used to annotate not only at the bench but now also at the bedside.

We have used furthermore a combination of CARS, fluorescence, and multivariate analysis to identify in living cells automatically the nuclei, nucleoli, lipid droplets, endoplasmic reticulum, Golgi apparatus, and mitochondria in an automated way in short measuring time.<sup>5</sup>

In addition in blood-plasma the approach was able to distinguish between the inflammation and bladder cancer with sensitivity and specificity over 90%.<sup>6-7</sup>

In a hypothesis driven approach using the conformation of the a-beta protein as biomarker we were able to distinguish between Alzheimer and non-Alzheimer diseased patients. An ATR-based sensor with functionalized surface is developed. The patent application is submitted (EP14155138) and will be published.<sup>8</sup>

<sup>1</sup> Gerwert K., Großerüschkamp F., Ollesch J. (2014), *SPIE Newsroom*, DOI: 10.1117/2.1201-312.005297.

<sup>2</sup> Mavarani L., Petersen D., El-Mashtoly S.F., Mosig A., Tannapfel A., Kötting C., Gerwert K. (2013), *Analyst*, 138(14), 4035-9.

<sup>3</sup> Kallenbach-Thieltges A., Großerüschkamp F., Mosig A., Diem M., Tannapfel A., Gerwert K. (2013), *J. Biophotonics*, 6(1), 88-100.

<sup>4</sup> Zhong Q., Yang C., Großerüschkamp F., Kallenbach-Thieltges A., Serocka P., Gerwert K., Mosig A. (2013), *BMC Bioinformatics*, 14, 333.

## Plenary Wednesday WEPL2

- <sup>5</sup> El-Mashtoly S.F., Niedieker D., Petersen D., Krauss S.D., Freier E., Mosig A., Kötting C., Hahn S., Gerwert K. (2014), *Biophys J.*, 106(9), 1910-20.
- <sup>6</sup> Ollesch J., Drees S.L., Heise H.M., Behrens T., Brüning T., Gerwert K. (2013), *Analyst*, 138(14), 4092-102.
- <sup>7</sup> Ollesch J., Heinze M., Heise H.M., Behrens T., Brüning T., Gerwert K. (2014), *J. Biophotonics*, 7(3-4), 210-21.
- <sup>8</sup> Nabers A., Ollesch J., Schartner J., Kötting C., Haußmann U., Klafki H., Wiltfang J., Gerwert K. (2015), *Journal of Biophotonics*, accepted.

- 10:40  
WE101-inv **Practical Cancer Histopathology by Advancing Spectroscopic Imaging Instrumentation and Analytical Methods**  
Rohit Bhargava, Kevin Yeh, Andre Balla, Shachi Mittal, Saumya Towari, Tomasz Wrobel, Suzanne Leslie, David Mayerich
- Modern IR spectroscopic imaging can become a more useful tool for biomedical tissue analysis with many recent innovations in instrumentation and methods. In particular, the analysis of cancer in complex tissue is an active and potentially very rewarding area. Here, we show the development of new technology guided by optical theory and the use of IR imaging in providing a solution to two problems of biomedical interest.
- 11:00  
WE102 **Can We Image Platelets by Means of FTIR Spectroscopy?**  
Kamilla Malek, Ewelina Wiercigroch, Aleksandra Krawczyk, Emilia Staniszevska-Slezak, Andrzej Fedorowicz, Stefan Chlopicki, Malgorzata Baranska
- FTIR spectroscopy imaging is employed to characterize spectrally platelet rich plasma (prp). the aim of this study was to optimize the sample preparation and then the comparison of FTIR profile of prp in a mice model of pulmonary arterial hypertension at an early and advanced stages. Platelet activation is specific for this disease. We show an effect of fixation methods on FTIR features of prp and discuss spectral changes appearing in the progression of hypertension.
- 11:15  
WE103 **Analysis of DNA Conformation and Nuclear Ultrastructure with Synchrotron FTIR, Soft X-Ray Tomography, NanoIR and TERS**  
Bayden Wood, Phil Heraud, Donna Whelan, Jason Zhang, Dilworth Parkinson, Don McNaughton
- The combination of S-FTIR, X-ray tomographic, nanoIR and TERS was used to investigate the DNA conformation and ultrafine structure in fixed and living cells.
- 11:30  
WE104 **Raman Spectroscopy of Blood Serum for Differential Diagnosis of Alzheimer's Disease**  
Lenka Halamkova, Elena Ryzhikova, Oleksandr Kazakov, Earl A. Zimmerman, Igor K. Lednev
- Alzheimer's disease (AD) is a progressive and incurable neurodegenerative disease, and is the most widespread type of dementia. This study was carried out to explore the potential applicability of near infrared (NIR) Raman microspectroscopy in detecting disease-related perturbations in serum of AD as well as reference subjects and subjects with other types of dementia. The proposed method has shown that Raman spectroscopy can be used to provide diagnosis of subtle changes in serum with high accuracy.
- 11:45  
WE105 **Direct Determination of Low Molecular Weight Biothiols in Umbilical Cord Whole Blood Employing Surface Enhanced Raman Spectroscopy**  
Julia Kuligowski, Marwa R. EL-Zahry, Ángel Sánchez-Illana, Guillermo Quintás, Máximo Vento, Bernhard Lendl
- Monitoring of the redox status in newborns is of key importance for the diagnosis and treatment of diseases associated with oxidative stress. This study shows the feasibility of Surface Enhanced Raman Spectroscopy (SERS) using a silver colloid as SERS substrate for the quantification of thiols in whole blood samples after a simple precipitation step for protein removal. A strong correlation between the SERS signals and thiol concentration could be demonstrated in blood samples as compared to a chromatographic reference method.

10:40 **Raman Spectroscopy of Graphene**WE501-inv Cinzia Casiraghi

Raman spectroscopy is the most common and informative characterization technique in graphene science and technology. In this talk I will discuss the use of Raman spectroscopy to determine the number of layers, doping, strain, defects, and functional groups in graphene. I will also present recent results on Raman spectroscopy of atomically precise and narrow graphene nanoribbons.

11:00 **Hyperbolic Phonon Polaritons in hBN for Near-Field Optical Imaging, Focusing and Waveguiding**

WE502

Peining Li, Martin Lewin, Andrey Kretinin, Joshua Caldwell, Kostya Novoselov, Takashi Taniguchi, Kenji Watanabe, Fabian Gaussmann, Thomas Taubner

Natural hyperbolic materials (NHMs) exhibit sub-diffractive, highly directional, volume-confined polariton modes. Here we report that hyperbolic phonon polaritons (HPs) allow for a flat slab of hexagonal boron nitride (hBN) to enable novel near-field optical applications, including unusual imaging phenomenon (such as an enlarged reconstruction of investigated objects) and sub-diffractive focusing. Both the enlarged imaging and the super-resolution focusing are explained based on the volume-confined, wavelength dependent propagation angle of HPs. With infrared scattering-type scanning optical microscope (s-SNOM) and state-of-art mid-infrared laser sources, we demonstrated and visualized these unexpected phenomena for the first time in both Type I and Type II hyperbolic conditions, with both occurring naturally within hBN. These efforts have provided a full and intuitive physical picture for the understanding of the role of HPs in near-field optical imaging, guiding, and focusing applications.

11:15 **Inelastic Neutron Scattering (INS) and Raman Spectroscopic Study of Lattice Modes for  $\text{KSiH}_3$  and  $\text{RbSiH}_3$  and Their Deuterated Analogues**

WE503

Janos Mink, Yuan-Chih Lin, Maths Karlsson, Carin Österberg, Henrich Fahlquist, Ulrich Häussermann

The alkali metal silyl hydrides  $\text{ASiH}_3$  (A = K, Rb, Cs) show reversible H storage capability near ambient conditions. At temperatures below 200 K  $\text{ASiH}_3$  exists as ordered low-temperature modifications. In this work analysis of external (lattice) modes have been performed based on Raman and INS (at 4 K) spectra of  $\text{KSiH}_3$  ( $Pnma$ ,  $Z=4$ ) and  $\text{RbSiH}_3$  ( $P2_1/m$ ,  $Z=2$ ) and their deuterated analogues. Results of DFT calculations were also used in interpretation of lattice modes.

11:30 **Phase Transitions in Fluorides with Elpasolite Structure**

WE504

Svetlana Krylova, Alexander Krylov, Alexander Vtyurin, Sergey Goryainov, Vladimir Voronov

This work shows the possibilities of Raman spectroscopy with reference to the phase transition investigations of some perovskite-like fluorides. It is shown that Raman spectroscopy provides the opportunity for understanding the phase transition mechanisms and estimating the behavior of ion groups at phase transition. It is shown by Raman spectroscopy that the temperature and pressure transitions from cubic into low symmetry phases in  $\text{Rb}_2\text{KScF}_6$ ,  $\text{Rb}_2\text{KInF}_6$ ,  $\text{Rb}_2\text{NaYF}_6$  crystals result from the lattice instability caused by the  $\text{MeF}_6^{3+}$  octahedral ion tilting.

11:45 **Complementarity of Raman Spectroscopy and Quantum Chemical Calculations in the Interpretation of Interparticle Interactions in Mixtures of 1-N-Butyl-3-methylimidazolium**

WE505

Oleg Kalugin, Bogdan Marekha, Volodymyr Koverga, Abdenacer Idrissi

By means of Raman spectroscopy coupled with DFT calculations and perturbation correlation moving window two-dimensional correlation spectroscopy intermolecular interactions were assessed in mixtures of ionic liquid 1-n-butyl-3-methylimidazolium hexafluorophosphate ( $\text{BmimPF}_6$ ) with polar aprotic solvent-butylolactone (-BL) over the entire range of compositions.

# Vibrational Optical Activity

Wednesday, 10:40 - 12:00  
Chair: Peter Weinberger

HS6

General Information

Program

Exhibition

Author Index

- 10:40 **Towards a Standardized Characterization of Solution Phase Protein Structure Using Raman Optical Activity: Implementation of Comprehensive Structural Databases**  
WE601-inv Carl Mensch, [Christian Johannessen](#)

While experimental Raman optical activity (ROA) spectroscopy long has shown great potential in studying large biomacromolecules in solution, a detailed fundamental understanding of which normal modes give rise to specific ROA band signatures has been limited by algorithmic and computer power restraints. As progress wins over these restraints, performing ROA calculations on biologically relevant models has become possible. Here, we present the outline of the first large scale systematic study of ROA protein spectral signatures related to protein conformation.

- 11:00 **Vibrational Optical Activity: Chirality in Molecular Vibrations**  
WE602 [Laurence Nafie](#)

Vibrational optical activity, as both vibrational circular dichroism (VCD) and Raman optical activity (ROA) has evolved over the past 40 years from discovery to a mature field encompassing a wide range of applications. Instrumentation for VCD and ROA measurements and software for VCD and ROA calculations is commercially available opening research in both academia and principally the pharmaceutical industry where VCD is now used routinely for the determination of the absolute configuration of new chiral drug substances. VCD also shows unusual sensitivity to the formation, development and supramolecular chirality of protein fibrils. ROA is now being used widely in the biopharmaceutical industry as a sensitive determinant of change in higher-order structure. These applications will be highlighted and discussed.

- 11:15 **Surface Enhanced Resonance ROA (SERROA) as a Novel Probe of Chirality Transfer**  
WE603 [Ewan Blanch](#), Saeideh Ostovar Pour, Louise Rocks, Karen Faulds, Duncan Graham, Vaclav Parchansky, Petr Bour

We demonstrate that single nanoparticle plasmonic reporters can enable a stereochemical response to be transmitted from a chiral analyte to an achiral benzotriazole dye molecule in the vicinity of a plasmon resonance generated by an achiral metallic nanostructure. This is the first report of colloidal metal nanoparticles in the form of single plasmonic substrates displaying an intrinsic chiral sensitivity once attached to a chiral molecule. Furthermore, the observed mechanism of chirality transfer is an original and remarkable fundamental effect which can provide a new route for engineering chiral plasmonic nanomaterials based upon vibrational optical activity.

- 11:30 **Raman Optical Activity and Vibrational Circular Dichroism of Amino Acid Based Chiral Ionic Liquids (CILs)**  
WE604 [Patric Oulevey](#), Birte Varnholt, Sandra Luber, Thomas Bürgi

Ionic liquids (ILs) experience an increased interest in recent years, especially because of their favorable application as green solvents and electrolyte materials. Representing the molecular building blocks of life, scientists have always been fascinated by amino acids, which can be used as anions for chiral ionic liquids (CILs). We have synthesized Emim-based CILs for the L-/D-pairs of alanine, valine, and leucine and their ROA and VCD spectra were measured. Computations helped to analyze the recorded spectra.

- 11:45 **Determining the Enantiomeric Ratio by Raman Spectroscopy**  
WE605 [Johannes Kiefer](#)

An experimental Raman technique for enantioselective discrimination is presented. The approach is taken further in order to facilitate quantitative measurements of the enantiomeric ratio. A detailed analysis of the key experimental parameters is carried out in order to allow identification of optimized settings.

**10:40 Recent Advances in Infrared Spectroscopic Natural Product Analysis**WE801-inv Christian Huck

Natural product's properties are related to certain classes of compounds such as alkaloids, flavonoids and others. Infrared spectroscopic techniques enjoy a good reputation, because of the fast and non-invasive analysis enabling the measurement of physicochemical parameters simultaneously. Near infrared (NIR) and attenuated total reflection (ATR) spectroscopy are suitable tools for the determination of a natural products provenience and species in parallel to a simultaneous measurement of parameters being important for quality reasons. Imaging methods give insights into the molecular composition.

**11:00 Direct Quantitative Chemical Imaging of Mixtures of Irregular Solids**WE802 David Wetzel, Mark Boatwright

Heterogeneous mixtures of irregular solids have heretofore been an unaddressed analytical challenge. At long last, quantitative chemical imaging with an array of 81,920 individual spectra enables not only identification, but presently a quantitative dimension of the prevalent chemical species has been superimposed for each x, y coordinate (pixel) of the image. A weighted summation of analyte numerical values enables calculation of percent within the FOV. Comparing the efficiency of sequential industrial unit processes with different settings illustrates the practical utility.

**11:15 Raman Spectra of Samples with Different Particle Sizes and Influence on Particle Size on Accuracy of Quantitative Analysis**WE803 Hoeil Chung, Duy Pham Khac

We have evaluated the variation of accuracy for the determination of ambroxol concentrations (binary mixtures of ambroxol and lactose) when the particle size of samples changes. The magnitude of baseline offset became larger with the increase of particle size due to the greater degree of Mie scattering. When the particle size was larger, uncertainty of photon propagation in a sample increased. So, it degraded accuracy of quantitative representation of sample composition as well as reproducibility of measurement.

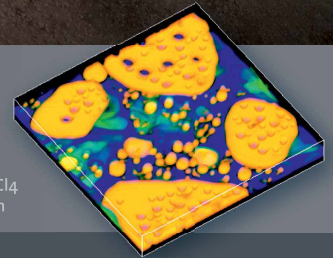
**11:30 Optimisation of Mixing Time in Powder Blending Processes Using Near-Infrared Spectroscopy**WE804 Angela Barone, Gary Montague, Jarka Glassey, Simon Dawson

Near-infrared (NIR) spectroscopy is employed as an in-line control system to continuously monitor the blending of powder products and optimise blending time. A non-contact NIR fiber-optic probe is installed in a conical screw mixer and spectra are collected every few seconds. Data are first cut and pre-treated, then analysed using standard deviation of the Moving Block Standard Deviation and dissimilarity. Homogeneity is reached when no more variations in composition are observed, as indicated by a flat line for both techniques.

**11:45 Imaging the Desolate Microscopic Landscape of Processed Cheese Using Raman Microscopy**WE805 Geoffrey Smith, Keith Gordon, Steve Holroyd

Imaging the microstructure of cheese can be difficult using a light microscope as the structure appears to be homogeneous with minor topographical changes. The use of dyes is not ideal because carbohydrates are challenging to stain and may alter the microstructure in unforeseen ways. Raman microscopy has not only demonstrated its ability to image the typical components of cheese but also some of the additives which are commonly incorporated into processed cheese.

# PIONEERS BY PROFESSION



3D confocal Raman image of  $\text{CCl}_4$  in an oil-water-alkane emulsion

*The WITec apyron Raman system automates the exploration of sample surfaces and chemical components. Software controlled, self-adjusting measurement routines along with TruePower\* and motorization bring a revelation in user-friendliness to cutting edge Raman imaging.*

\*TruePower: Absolute laser power determination in 0.1 mW steps.

*Feel the spirit of exploration, automatically.  
WITec apyron – convenience meets performance*



**alpha500 AR**  
First automated Raman/AFM system for large samples



**alpha300 SR**  
First SNOM system using patented cantilever sensors



**alpha300 AR+**  
First fully integrated Raman Imaging/AFM combination



**apyron**  
First fully-automated high-performance Raman Imaging system

9:00  
THPL1 **Surface-Enhanced Raman Spectroscopy and Imaging with Tailor-Made Plasmonic Nanoparticles**

Sebastian Schlücker, Yuying Zhang, Mohammad Salehi

This lecture gives an overview on the rational design and synthesis of functionalized noble metal colloids for chemical and bioanalytical applications of SERS. After a brief introduction on the theoretical foundations of SERS, two different topics from the chemical sciences with results from our group will be covered:

- 1) Immuno-SERS microscopy (iSERS) for tissue-based cancer diagnostics
- 2) Label-free monitoring of chemical reactions in heterogeneous catalysis.

In both cases plasmonic nanostructures with tailor-made physical and chemical properties play a key role.



Sebastian Schlücker received his Dr. rer. nat. (PhD) in physical chemistry from Würzburg University in 2002. After postdoctoral studies at NIH in Bethesda and his Habilitation, he became Associate Professor of Experimental Physics at Osnabrück University in 2008. Since 2012 he has been Professor of Physical Chemistry at the University Duisburg-Essen. His field of research is nanobiophotonics, in particular the physics and chemistry of molecularly functionalized plasmonic nanostructures and their application in biomedicine, catalysis and ultrasensitive chemical analysis.

9:35  
THPL2 **Perspectives in Process Analysis - PAT and the Workhorse Vibrational Spectroscopy**

Rudolf Kessler

Process analysis is a holistic approach where different disciplines and technologies must be integrated. Spectroscopy will play a major role in the future for knowledge based production as it provides simultaneously information on the morphological and chemical features of the sample. Vibrational spectroscopy offers a versatile tool for inline measurements and can also be used for spectral imaging. The paper will discuss the sensitivity, selectivity and robustness of the techniques together with several industrial applications.



Dr. Rudolf W. Kessler is a Professor emeritus of Chemistry at Reutlingen University/D. After his studies in Chemistry and a PhD in Physical Chemistry at the University of Tübingen/D and in Norwich/UK on spectroscopy, he worked for some years with Mercedes Benz at the basic research department in Stuttgart, Germany. His main research areas are in process analysis by optical and spectroscopic methods in combination with multivariate data analysis. Another focus is on chemical imaging and near field spectroscopy.

## Surface-Enhanced Raman Spectroscopy and Imaging with Tailor-Made Plasmonic Nanoparticles

Wei Xie, Yuying Zhang, Mohammad Salehi, Bernd Walkenfort, Sebastian Schlücker

Physical Chemistry I, Faculty of Chemistry, University of Duisburg-Essen, 45141 Essen,  
Germany

Keywords: SERS, cancer diagnostics, tissue imaging, heterogeneous catalysis, reaction kinetics

Surface-enhanced Raman scattering (SERS) has become a mature vibrational spectroscopic technique during the last decades and the number of applications in the chemical, material, and in particular life sciences is rapidly increasing.<sup>1</sup>

In addition to normal Raman spectroscopy, SERS requires plasmonically active materials, for instance noble metal colloids, which support localized surface plasmon resonances.

This lecture gives an overview on the rational design and synthesis of functionalized noble metal colloids for chemical and bioanalytical applications of SERS. After a brief introduction on the theoretical foundations of SERS, two different topics from the chemical sciences with results from our group will be covered. In both cases plasmonic nanostructures with tailor-made physical and chemical properties play a key role.

Immuno-SERS microscopy (iSERS) for tissue-based cancer diagnostics employs target-specific colloidal SERS probes in combination with Raman microspectroscopy. SERS-labeled antibodies allow the selective and sensitive localization of the corresponding antigen in tissue specimens. The properties of the colloidal SERS probes<sup>2</sup> (Figure 1) are crucial for the success of iSERS experiments. Signal brightness, stability and robustness as well as steric accessibility for bioconjugation are few very important aspects. For instance,

small Raman reporter-functionalized clusters of noble metal nanoparticles (NPs) are very bright SERS labels due to plasmonic coupling. Small clusters of AuNPs were further used for iSERS imaging on prostate biopsies. Current work in our laboratories and future developments of this innovative iSERS imaging approach will be discussed.

The second part of the lecture covers label-free monitoring of chemical reactions catalyzed by Pt, Au and Ag nanoparticles. Bifunctional nanoparticles exhibiting both high plasmonic and catalytic activity are required, but not routinely available. We designed and synthesized Au/Pt nanoraspberries as well as Au/Au and Ag/Ag core/satellite superstructures for this purpose (Figure 2).<sup>3-4</sup> Electron microscopy demonstrates the high uniformity of the particles. Computer simulations predict very high plasmonic activity due to plasmonic coupling, resulting in several hot spots. For proof-of-concept studies 4-nitrothiophenol, which is present as a self-assembled monolayer on Au and Ag surfaces, was chosen. The reduction to 4-aminothiophenol can be achieved either by chemical hydride agents or by a combination of hot electrons and protons. Current work from our group on temperature-controlled microfluidics for kinetic reaction monitoring as well as future directions for the use of hot electrons for driving chemical reactions will be discussed.

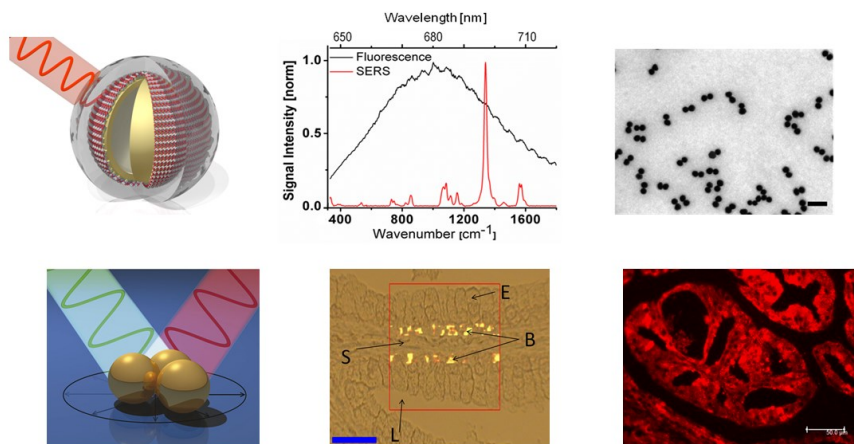


Figure 1. SERS nanoparticle labels for use in immuno-SERS (iSERS) microscopy for tissue-based cancer diagnostics. Spectral multiplexing is possible due to the small linewidth of vibrational Raman bands compared to fluorescent dyes. Correlative SEM/SERS experiments on single small AuNP clusters demonstrate their high SERS signal strength.

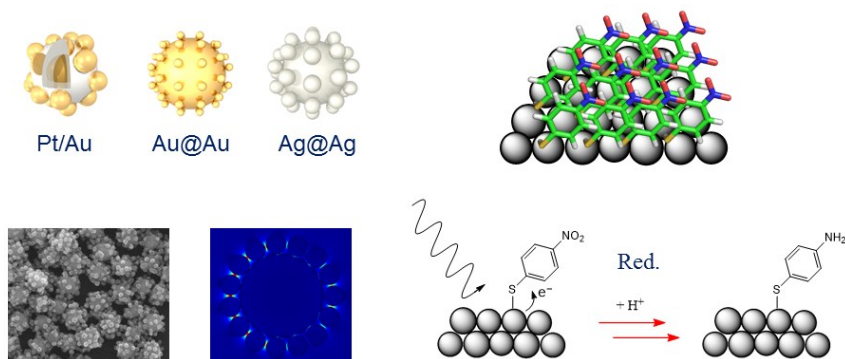


Figure 2 Bifunctional noble metal nanoparticles with plasmonic and catalytic activity (left). Self-assembled monolayer of 4-nitrothiophenol on a metal surface for reduction to 4-aminothiophenol either by chemical hydride agents or by hot electrons and protons (right).

<sup>1</sup> S. Schlücker, *Angew. Chem. Int. Ed.*, **2014**, 53, 4756-4795.

<sup>2</sup> B. Küstner, M. Gellner, M. Schütz, F. Schöppler, A. Marx, P. Ströbel, P. Adam, C. Schmuck, S. Schlücker, *Angew. Chem. Int. Ed.* **2009**, 48, 1950-1953.

<sup>3</sup> W. Xie, C. Herrmann, K. Kömpe, M. Haase, S. Schlücker, *J. Am. Chem. Soc.* **2011**, 133, 19302-19305.

<sup>4</sup> W. Xie, B. Walkenfort, S. Schlücker, **2013**, *J. Am. Chem. Soc.*, 135, 1657-1660.

## Perspectives in Process Analysis: PAT and the Workhorse Vibrational Spectroscopy

Rudolf W. Kessler

STZ Process Control and Data Analysis, Herderstr. 47, 72762 Reutlingen, Germany

Keywords: Process Analytical Technology (PAT), spectroscopy, sensitivity, spectral imaging,

Process analysis is a transdisciplinary technology. Process chemists, process engineers, chemometricians, and many other technologists must work together. Process Analysis includes process design (Quality by Design (QbD)) of the used technology, process analytics (Process Analytical Technology (PAT)), process control units as well as the economic evaluation of the process including supply chain management. Optical spectroscopy together with chemometrics will play an important role in the transition of a re-active industrial production into a pro-active industrial system<sup>1</sup>. As spectroscopic techniques can simultaneously detect all morphological and chemical features, the complete fundamental functionality of a compound is inherent in every spectrum.

Sensitivity, selectivity and robustness of each individual technology in combination with the used wavelength range has its limitations due to the structure of the measured specie and the used optical configuration. In any application, a key issue is to find the causal link between the measured spectral features and the final target quality. In spectral imaging the spatial distribution in the x-, y- and possibly z-direction may be also of interest<sup>2</sup>.

Optical spectroscopy covers a broad wavelength range with different sensitivities and selectivities. The major advantage of near infrared spectroscopy (NIR) is that the absorption cross sections are lower in comparison to the mid infrared (MIR) and therefore the penetration depth of the

photons are higher in particulate systems. As a result, the technique can be used to analyse components even at high concentrations in an industrial environment without the need of pre-processing the sample. The typical detection limits in NIR spectroscopy lie in the lower percentage region, 0.1 % (esp. water) up to 5. In contrast to NIR, MIR spectroscopy enables the analysis of concentrations as low as 0.01%, standard detection limits can be as low as 0.001%. Due to the high absorption cross sections, special arrangements like Attenuated Total Reflectance (ATR) are developed to lower the pathlengths at higher concentrations or to use lasers with a high photon flux. The strength of the water absorption in the NIR and MIR may limit the broad use in many biotechnological applications. Although Raman absorption cross sections lie typically around 10 orders (or more) of magnitude lower than in the MIR, due to recent development of extraordinarily sensitive detection systems and its high selectivity and robustness, Raman spectroscopy may approach the performance of FTIR spectrometers in the near future, especially in aqueous systems<sup>3</sup>.

Ultraviolet-, and visible (UV/VIS) spectroscopy as well as fluorescence spectroscopy are highly sensitive techniques to measure electronic transitions, but lack selectivity. Table 1 shows a rough qualification of the used techniques in PAT with respect to sensitivity, selectivity, robustness and their general suitability for inline control.

Special emphasis in the future will be given to measure not only the chemical entities but also their lateral distribution in an object. Spectral Imaging, or also called Chemical Imaging, is an emerging field with applications ranging e.g. to find biomarkers in a tissue but also to control and qualify 100% of tablets or food<sup>2</sup>. Pushbroom Imaging systems are ideally suited for inline control and in the meantime they are available in almost every wavelength range. A pushbroom imager is a line scanning system and acquires the full spectral information for all lateral x-coordinates simultaneously in a single line, often of several thousand pixels.

Process analysis together with spectroscopy and intelligent data analysis

will play a more important role in the future of the processing industry than it has in the past. According to the Industry 4.0 concept of the German government, the future of industrial automation will be “arbitrarily modifiable and expandable (flexible), connect arbitrary components of multiple producers (networked), enabling its components to perform tasks related to its context independently (self-organizational) and emphasizes ease of use (user-oriented)”<sup>3</sup>. Spectroscopy and its “workhorse” vibrational spectroscopy will be an important toolbox and enabling technology to realize this concept.

Table 1. Qualification of the different techniques for their suitability in PAT-applications

	UV/VIS/	NIR	MIR	Fluorescence	Raman
Selectivity	+	++	+++	++	+++
Sensitivity	+++	+(+)	+++	+++(+)	++(+)
Sampling	+++	+++	+	++	+++
Working in aqueous media	+++	+	+	++	+++
Applicability	+++	++	+	+	+
Process analytical tool	+++	+++	+	+	+++
Light guide glass	+++	+++	(+)	+++	+++
Signal	Absorption	Absorption	Absorption	Emission	Scattering
Sampling online/inline	s, l, g	s, l	s, l, g	s, l (g)	s, l, (g)
Techniques	Transmittance Reflectance ATR	Transmittance Reflectance ATR	ATR (Transmittance)	Reflectance Transmittance	Reflectance Transmittance
Relative costs	1	3 - 5	6 - 10	4 - 6	8 - 12

<sup>1</sup> Bakeev K A. (Ed.), Process Analytical Technology, (2nd edn) Wiley: 2010.

<sup>2</sup> B. Boldrini, W. Kessler, K. Rebner and R. W. Kessler, Hyperspectral imaging: a review of best practice, performance and pitfalls for inline and online applications, Journal of Near Infrared Spectroscopy 2012, 20, 438–508, doi: 10.1255/jnirs.1003.

<sup>3</sup> R. W. Kessler, Perspectives in process analysis. J. Chemometrics, 2013, 27: 369–378. doi: 10.1002/cem.2549.

- 10:40  
TH101 **Multiplexing Cellular Redox Potential and pH Measurements in 3D Breast Cancer Tumour Models Using SERS Nanosensors**  
Lauren Jamieson, Aleksandra Jaworska, Pierre Bagnaninchi, Kate Fisher, Jing Jiang, David Harrison, Colin Campbell
- Cellular redox potential is a highly regulated characteristic and when the redox balance is disturbed disease can progress. My research focuses on the redox gradient in cancer tumours, modeled using multicellular tumor spheroids. SERS is used to map cellular redox potential by delivering nanoshells functionalised with redox active molecules to cells. Cellular redox and pH measurements using SERS have been successfully multiplexed and photothermal OCT has been investigated as a tool for visualising the 3D distribution of nanoshells in MTS.
- 11:00  
TH102 **In Situ Hydrazine Reduced Silver Colloid Synthesis for Reproducible SERS Measurements**  
Vera Dugandžić, Izabella Jolan Hidi, Karina Weber, Dana Cialla-May, Jürgen Popp
- A novel in situ approach for colloid synthesis in LOC-SERS devices was developed. Nanoparticles were produced in a microfluidic chip by hydrazine reduction of  $\text{Ag}^+$  in ammoniacal solution using citrate as a protective agent. The SERS activity and day-to-day reproducibility was tested using adenine as model analyte. The results indicate that measurements performed with in situ synthesized colloids present lower standard deviation as well as a better day-to-day reproducibility as compared to measurements performed with colloids prepared by conventional strategies.
- 11:15  
TH103 **Ultrahigh Sensitivity of Quasi-Three-Dimensional Paper-based SERS Substrates Prepared by Single-Shot Laser Treatment**  
Yi-Chuan Tseng, Chen-Chieh Yu, Sin-Yi Chou, Shao-Chin Tseng, Yu-Ting Yen, Hsuen-Li Chen
- In this study, by exploiting the laser-induced photothermal effect, after single-shot laser treatment, an eco-friendly and ultrasensitive paper substrates are developed for surface-enhanced Raman scattering with performance approaching single molecule detection. Moreover, the quasi-3D distribution of NPs on the SERS paper greatly enhances the SERS signals within the effective collection volume of a Raman microscope. The limits of detection when using the paper substrates reach the attomolar level, thereby approaching single molecule detection.
- 11:30  
TH104 **Semiconductor-Enhanced Raman Scattering for Detection of Small Inorganic Molecules and Ions**  
Wei Ji, Wei Song, Ichiro Tanabe, Yue Wang, Bing Zhao, Yukihiro Ozaki
- Recent advances in semiconductor-enhanced Raman scattering have endowed semiconductor materials as promising candidates for developing SERS sensors. In spite of their lower sensitivity as compared to noble metal substrates, many semiconductor substrates are much more stable as well as reproducible. Here, we present a "turn-off" strategy and demonstrate that this strategy can be used as an efficient methodology to realize semiconductor-based SERS sensing for quantitative analysis of small inorganic molecules and ions.
- 11:45  
TH105 **Variability of Surface-Enhanced Vibrational Spectra: Profits and Drawbacks**  
Pavel Matejka, Alzbeta Kokaislova, Marcela Dendisova, Michaela Grafova, Marie Svecova, Tereza Helesicova
- Large data sets of SERS and SEIRA spectra recorded in our laboratory on plasmonic Ag, Au and Cu substrates (mostly electrodes and nanoparticles) for various molecules (predominantly natural products) during last decade (aimed recently at the elucidation of the effects of variable or stabilized (i) temperature and (ii) electrode potential) represent a substantial experimental basis to discuss the relevance of SEVS data from both physico-chemical and analytical point of view, to draw general conclusions and to suggest future perspectives.

10:40  
TH501

## Coherent Raman Imaging Measurement of Stem Cell Differentiation

Young Jong Lee, Sebastián Vega, Parth Patel, Khaled Amer, Prabhas Moghe, Marcus Cicerone

Broadband coherent anti-Stokes Raman scattering (BCARS) microscopy is used to characterize lineage commitment of individual human mesenchymal stem cells cultured in adipogenic, osteogenic, and basal culture media. We demonstrate robust metrics for differentiation by statistical analysis of functional markers (lipids and minerals) observed in hyperspectral BCARS images. The high speed of BCARS imaging allows us to chemically map a large number of cells, revealing not only phenotype of individual cells, but population heterogeneity in the degree of phenotype commitment.

11:00  
TH502

## Differential Interference Contrast Stimulated Raman Scattering Microscope

Hiroharu Yui, Motohiro Banno, Takayuki Kondo

A new type of stimulated Raman scattering microscope based on differential interference optical configuration is developed, named differential interference contrast stimulated Raman scattering microscope. It enables us to measure chemical contrast topographic images with spatial precision resolution with sub-micrometer in depth direction by an interferometric image construction technique. Differential interference contrast stimulated Raman scattering microscope will be a useful tool for measuring buried layers and interfaces of multi-layered materials and biological tissues in industrial and biomedical applications.

11:15  
TH503

## Spectral Processing Challenges in Coherent Raman Spectroscopy and Microscopy with Applications

Laszlo Ujj

Phase recovery is a critical procedure in broadband nonlinear optical spectroscopy, e.g. polarization sensitive coherent Raman frequency domain spectroscopy and microscopy. A firm mathematical comparison of the methods and their applications will be presented. Phase retrieval examples are taken from vibrational spectra recorded under electronic resonance enhanced conditions of highly fluorescent samples.

11:30  
TH504

## Insights into Health and Disease Using Coherent Raman Imaging

Sumeet Mahajan, Tual Monfort, Justyna Smus

I will describe our work to develop and apply multiphoton label-free bio-imaging techniques. Microscopic techniques based on coherent anti-Stokes Raman scattering (CARS) and second harmonic generation (SHG) are chemically and structurally selective and can be used to rapidly image cells in their native state without any fluorescent labelling or staining. We have applied these techniques to cells and tissues to develop assays for determining the efficacy of drugs and studying differentiation behaviour of stem cells. Recent studies have been on live organisms to correlate metabolic processes to behaviour and on ex vivo tissue samples to track development of respiratory diseases. The ultimate aim is to develop 'imaging diagnostics' for use in clinical and healthcare settings.

11:45  
TH505

## Resonance Raman Spectroscopy for Probing Carotene-Porphyrin Triplet States

Elizabeth Kish, Katherine Wong Carter, Smitha Pillai, Dalvin Mandez-Hernandez, Junming Ho, Victor Batista, Ana Moore, Thomas Moore, Devens Gust, Bruno Robert

Here we present some artificial systems, used to mimic energy transfer in photosynthesis (specifically triplet quenching by carotenoids), studied with resonance Raman spectroscopy. Depending on the relative orientation of the carotenoid to the porphyrin, the triplet-triplet energy transfer triggers changes in bands of the RRS spectra. Specifically, the C=C stretching moiety noticeably downshifts when associated with a more delocalized triplet (and consequently more efficient triplet-triplet energy transfer). We have done extensive modelling to corroborate our experimental results with calculations.

10:40 **FTIR Hyperspectral Imaging for Rapid Identification of Pathogenic Microorganisms**

TH601-inv Peter Lasch

The combination of mid-IR microspectroscopic imaging and neural network analysis has great potentials in microbiological diagnostics. In this presentation we exemplarily show how optimized neural networks can be utilized to reassemble false color images from hyperspectral images of microcolony specimens and to visualize the spatial distribution of taxon-specific spectral fingerprints. Our results suggest that this combination of IR microspectroscopy and machine learning is suitable for rapid, objective and cost effective identification of pathogenic microorganisms down to the species level.

11:00 **Solute-Solvent and Pigment-Protein Interactions in Carotenoids. A Combined Resonance Raman, Step-Scan FTIR, DFT/COSMO and QM/MM Study of Peridinin**

TH602

Alberto Mezzetti, Elizabeth Kish, Daniele Bovi, Riccardo Spezia, Bruno Robert, Rodolphe Vuilleumier, Marie-Pierre Gaigeot, Leonardo Guidoni

Peridinin is a carotenoid involved in light harvesting of dinoflagellates. We studied its vibrational properties in protein and solvents through Resonance Raman, Step-scan FTIR and QM/MM calculations. the lactonic C=O stretching was found to be sensitive to I) H bonding dynamics; II) solvent polarity; III) Fermi resonance coupling. the lactonic C=O becomes therefore a tool to distinguish among different Pers in proteins where up to 8 different Pers are present. We have investigated the photophysics of these proteins by step-scan FTIR.

11:15 **An Infrared Sensor Analysing Label-Free the Secondary Structure of the Abeta Peptide in Presence of Complex Fluids**

TH603

Andreas Nabers, Julian Ollesch, Jonas Schartner, Carsten Kötting, Klaus Gerwert

The secondary structure change of the Abeta peptide to beta-sheet was proposed as an early event in Alzheimer's disease and may be used for diagnostics of this disease. We present an Attenuated Total Reflection (ATR) sensor modified with a specific antibody to extract minute amounts of Abeta out of a complex fluid. Thereby, the Abeta peptide secondary structure was determined in its physiological aqueous environment by FTIR-difference-spectroscopy. This open the door for label-free Alzheimer diagnostics in cerebrospinal fluid or blood.

11:30 **Using IR and Raman Spectra to Explain the Catalytic Activity of the Fe(II)/Fe(III) Pair Toward the Cleavage of Peptide Bonds**

TH604

Wagner Alves, Felipe Camacho

The spectral pattern of an amide solution containing Fe(II) differs from that exhibited by Fe(III). For the former, CO is downshifted whereas CN is upshifted, stabilizing an ionic amide structure, whose O atom is the only coordination site. For the second, upshifts of both CO and CN stabilize a neutral amide structure, in which both O and N atoms are now involved. Both ionic and neutral structures may also coexist in oxidative cleavage processes of polypeptides.

11:45 **A Vibrational Spectroscopic Approach to the Human Mind**

TH605

Henry Mantsch

While today's applications of vibrational spectroscopy in medicine all refer to the human body I will address the human mind as an immaterial construct, a form of electromagnetic or hitherto unknown energy. Being all familiar with the expression of "having good vibrations" when meeting another person, can we envision a link between the human mind and our familiar vibrational frequencies? My short answer is "yes". This presentation is food for thought and aims to stimulate the imagination of young scientists.

10:40  
TH801-inv **Real-Time Physiological Characterization of Bioprocesses Using in-Situ Spectroscopy and Soft-Sensors**

Aydin Golabgir, Christoph Herwig

Bioprocesses are used for the production of a wide range of value-added products, including therapeutics and renewable energy sources. Implementation of advanced bioprocess monitoring and control strategies is hindered by the lack of availability of analytical methods that are capable of measuring physiological and morphological characteristics directly and in a timely manner. In this contribution, the utility of first-principle soft-sensors for estimating inaccessible bioprocess variables (such as biomass) using more accessible measurements provided by in-situ spectroscopic devices is addressed.

11:00  
TH802 **Characterisation of Viscose Fibre Spin Bath by FTNIR-Spectroscopy and Its Implementation for Process Control**

Georg Mayr, Peter Hintenaus, Wolfgang Märzinger, Thomas Röder

FTNIR spectroscopy is a proven analytical method for process analysis. Due to its technological preferences it can be easily implemented in production environment. The application of a FTNIR analytical method for the characterisation of viscose fibre spin bath and its implementation for process control are presented. We discuss possible calibration strategies as well as the issue of appropriate reference selection for the current application as example. The performance of different options for implementation will be judged in terms of RMSEP-values.

11:15  
TH803 **Quantum Cascade Laser Based Photoacoustic Spectroscopy with Remote Optical Detection**

Markus Brandstetter, Armin Hochreiner, Elisabeth Leiss-Holzinger, Gregor Langer, Peter Burgholzer, Christian Kristament, Bernhard Lendl, Thomas Berer

We demonstrate remote absorption spectroscopy based on the photoacoustic effect. In the presented concept a tunable mid-infrared External-Cavity Quantum Cascade Laser serves as excitation source for generation of acoustic waves within the sample. In order to achieve remote detection of the photoacoustic effect the sample surface's deformation is measured with a laser vibrometer, which is based on a fibre-optic Mach-Zehnder interferometer. The theoretical background and practical measurements of various samples are presented.

11:30  
TH804 **In-Line Raman Analysis of Ethylene Vinyl Acetate Curing for and in Industrial PV Module Manufacturing**

Christina Hirschl, Martin De Biasio, Lukas Neumaier, Raimund Leitner, Gabriele Eder, Siegfried Seufzer, Martin Kraft

Raman spectrometry was applied to an urgent problem in industrial process control of renewable energy system manufacturing. A ratiometric approach evaluating the relative  $\text{CH}_2/\text{CH}_3$  intensities proved a reliable measurand for determining the degree of crosslinking of ethylene/vinyl acetate non-destructively in-situ inside assembled PV modules. After extensive validation, the method was adapted to industrial application. Using a specially developed prototype setup incorporating a commercial real-time Raman spectrometer, the method was successfully deployed and used in an industrial PV module manufacturing line.

11:45  
TH805 **Development and Implementation of a QCL Based Gas Sensor for Sub-ppm  $\text{H}_2\text{S}$  Measurements in Petrochemical Process Gas Streams**

Harald Moser, Johannes Ofner, Bernhard Lendl

A sensitive, selective and industrial fit gas sensor based on second harmonic wavelength modulation spectroscopy (2f-WMS) employing a 8  $\mu\text{m}$  continuous wave distributed feedback quantum cascade laser (CW-DFB-QCL) was developed for detecting hydrogen sulfide ( $\text{H}_2\text{S}$ ) at sub-ppm levels in petrochemical process gas streams. The sensor platform has been able to provide sensitive and selective measurements of hydrogen sulfide in petrochemical process gas streams with fast detector response while performing under the imperative on-site safety regulations for hazardous and explosive environments.

13:30  
TH106

## Plasmonic Nanoantennas on Nanopedestals for Ultra-Sensitive Vibrational IR-Spectroscopy

Dordaneh Etezadi, Arif Cetin, Hatice Altug

We experimentally demonstrate that elevating polarization-insensitive nanoring antennas fabricated on dielectric nanopedestals enables high surface enhanced infrared absorption (SEIRA) signals in biomolecular applications. This is due to larger and highly accessible nearfields offering better overlap with biomolecules.

13:45  
TH107

## Angle-Tuning of Antenna Arrays for Optimization and Flexible Application in Surface Enhanced Infrared Absorption Spectroscopy

Tobias Maß, Thomas Taubner

Metallic antenna arrays can efficiently couple light into a region of subwavelength size and enable an increased absorption of molecules which are placed in these so called 'hot spots'. In our work, we use the angular range of a Schwarzschild-objective for a tuning of the antenna array performance in order to optimize the enhancement of C-H vibrational bands of a self-assembled monolayer of 13-MHDA.

14:00  
TH108

## In Situ SEIRAS Study of Cinchonidine Adsorbed on Platinum in Organic Solvents, a Model Enantioselective Hydrogenation Catalyst

Kenta Motobayashi, Ryota Tomioka, Taro Uchida, Masatoshi Osawa

The orientation of cinchonidine (CD) adsorbed on Pt is studied in 1,2-dichloroethane by in situ surface-enhanced infrared absorption spectroscopy to clarify the origin of enantioselective hydrogenation reactions on CD-modified Pt catalysts. CD is shown to be reoriented from a p-bonded parallel orientation to an N-bonded upright one by bubbling the solution with H<sub>2</sub>. The origin of the reorientation is ascribed to the repulsive interaction of the p-orbital of QN with the negatively charged surface induced by the dissociative adsorption of H<sub>2</sub> and hydrogenation of the vinyl moiety.

14:15  
TH109

## Combined SERR, SEIRA and Electrochemistry to Study the Influence of Calcium on Catalysis of Cellobiose Dehydrogenase Immobilized on Electrode

Patrycja Kielb, Lo Gorton, Roland Ludwig, Ingo Zebger, Inez M. Weidinger

Cellobiose dehydrogenase is an enzyme that catalyzes the oxidation of sugars and is considered as an excellent candidate for novel class of biosensors and biofuel cells. In presence of Ca<sup>2+</sup> ions, catalytic activity is significantly increases. We employed for the first time combined electrochemical methods with surface enhanced vibrational (SERR and SEIRA) spectroscopic methods to study in detail the catalytic performance of CDH immobilized on nanostructured noble metal electrodes in presence of Na<sup>+</sup> and Ca<sup>2+</sup> ions.

14:30  
TH110

## Optofluidic Chip Integrating Silvered Porous Silicon Membranes for Multianalyte Surface Enhanced Raman Spectroscopy

Chiara Novara, Andrea Lamberti, Paola Rivolo, Alessandro Virga, Alessandro Chiadò, Francesco Geobaldo, Fabrizio Giorgis

A flexible and transparent multichamber PDMS optofluidic chip is developed for multianalyte Surface Enhanced Raman Spectroscopy (SERS). Patterned porous silicon membranes are integrated as highly efficient SERS active elements, whose SERS enhancement is found higher than 10 orders of magnitude when the samples are tested with Rh6G in molecular resonance conditions. Applicability in biological assays is also demonstrated by detecting model oligonucleotides in the different microfluidic chambers.

13:30  
TH506

## In Situ Raman Study of Silicene: From Monolayer to Multilayers

Dmytro Solonenko, Patrick Vogt, Ovidiu Gordan, Dietrich Zahn

Systematic in situ Raman study of silicene was carried out. We monitored the growth of multilayer silicene starting from one monolayer in ultra-high vacuum chamber. We show that Raman spectra of silicene structures possess their own fingerprint features, unlike the ones of bulk Si, indicating the distinct nature of two-dimensional Si atoms arrangement. The heating of multilayer silicene results in an irreversible phase transition to the bulk-like structure.

13:45  
TH507

## Raman Spectroscopic Study of Phase Transitions in Rare Earth Ferroborate Multiferroic Crystals under Temperature and High-Pressure

Alexander Krylov, Svetlana Sofronova, Irina Gudim, Svetlana Krylova, Alexander Vtyurin

Crystals of the  $(\text{Ho-Nd})\text{Fe}_3(\text{BO}_3)_4$  were reported to possess multiferroic features, demonstrating both structural and magnetic phase transitions, where transition points may be varied by rare earth composition. In this work we used Raman spectroscopy to study  $\text{Ho}_{1-x}\text{Nd}_x\text{Fe}_3(\text{BO}_3)_4$  single crystals. The aim of this study is to investigate possible existence of a soft mode related to structural order parameter and effects of magnetic transitions on Raman spectra under temperature and high-pressure.

14:00  
TH508

## Probing Structural Phase Transformation in $\text{BiFeO}_3$ Thin Films by Polarized Micro Raman Spectroscopy

Anju Ahlawat, Srinibas Satapathy, P.K Gupta, Vasant Sathe

We demonstrate structural phase transition in La and Nd co doped  $\text{BiFeO}_3$  thin films using micro Raman spectroscopy. Based on group theoretical analysis of the number and symmetry of Raman lines, we provide strong experimental evidence that the structure has been transformed from rhombohedral to monoclinic due to co-doping in  $\text{BiFeO}_3$ . Doped films exhibit enhanced ferromagnetic and electric properties compared to pure bulk  $\text{BiFeO}_3$ . These enhanced multifunctional properties highlight the potential applications of doped  $\text{BiFeO}_3$  thin film for smart devices.

14:15  
TH509

## New Insights into the Crystal Structures and Vibrational Properties of Germanates Comprising $[\text{Ge}_3\text{O}_{10}]^{8-}$ and $[\text{Ge}_4\text{O}_{12}]^{8-}$ Anions from Raman Microscopy and Periodic ab Initio Calculations

Ivan Leonidov, Vladislav Petrov, Vladimir Chernyshev, Olga Lipina, Ludmila Surat, Alexander Tyutyunnik, Emma Vovkotrub, Anatoliy Nikiforov, Vladimir Zubkov

Raman microscopy, FTIR spectroscopy and DFT calculations with LDA, GGA and hybrid functionals employed with the CRYSTAL code have been performed to describe the crystal structure and vibrational spectra of  $\text{CaY}_2\text{Ge}_2\text{O}_{12}$ ,  $\text{Ca}_2\text{Ge}_7\text{O}_{16}$  and  $\text{CaRE}_2\text{Ge}_3\text{O}_{10}$  (RE = Y, La-Yb) which represent the promising hosts for lanthanide-doped phosphors. Accurate assignments of the observed bands to vibrational modes are given. The relationship between selected infrared bands and Raman lines, internal vibrations of the anionic units and external modes is discussed in detail.

14:30  
TH510

## Raman Spectroscopic Investigation of $\text{CuGaTe}_2$ at High Pressures

Rekha Rao, Swayam Kesari, Nilesh Salke

Vibrational properties of ternary chalcopyrite semiconductor  $\text{CuGaTe}_2$  has been studied using Raman spectroscopy at high pressures upto 24 GPa. Pressure dependent softening is observed for a few low frequency modes, which has been correlated with instability in the system leading to structural transition around 9 GPa in disordered simple cubic phase. Beyond 11.5 GPa, no Raman spectrum could be observed. This is possibly due to second phase transition which could have accompanied by reduction in band gap.

# Time-Resolved Spectroscopy

Thursday, 13:30 - 14:45  
Chair: Mike George

HS6

General Information

Program

Exhibition

Author Index

13:30  
TH606 **Snapshots of Ultrafast Dynamics in Neuroglobin Captured by Femtosecond Stimulated Raman Scattering**

Giovanni Batignani, Carino Ferrante, Emanuele Pontecorvo, Tullio Scopigno

The reaction pathway in photoexcited Neuroglobin (ligand dissociation, energy redistribution and structural dynamics) has been unraveled by Femtosecond Stimulated Raman Scattering. The possible existence of short living intermediates as opposed to vibrational relaxation is discussed.

13:45  
TH607 **The Reinvention of Interleaved Time-Resolved FT-IR Spectroscopy**

Arno Simon, Michael Jörger, Günter Zachmann

Interleaved FT-IR spectroscopy is a time-resolved technique for particular repeatable kinetics, using measurement time much more efficiently than step-scan spectroscopy. Indeed when the interleaved approach originally emerged in the last millennium, the technology of commercial FT-IRs may still have been too limited to really utilize this benefit. In our contribution we will introduce interleaved spectroscopy for modern VERTEX series FT-IR spectrometers and demonstrate its distinct advantages by means of time-resolved emission spectra of a pulsed infrared LED.

14:00  
TH608 **Time-Resolved FTIR Spectroscopy with Sub-Microsecond Resolution Probes the Blue Light Sensor Cryptochrome**

Christian Thöing, Sabine Oldemeyer, Tilman Kottke

Cryptochromes act as central blue light sensors in animals, plants, fungi, and bacteria. We investigated the photoreaction of the light-sensitive domain of a plant cryptochrome by step-scan and rapid-scan FTIR spectroscopy with a time resolution of 500 ns. The proton transfer to the chromophore within few microseconds was shown to originate from a nearby aspartic acid. A pronounced change in beta-sheet structure was resolved within hundreds of microseconds, which takes place in a subdomain previously not associated with signaling.

14:15  
TH609 **Energy Transfer Mechanism in Liposome Lipid Bilayers Studied with Picosecond Time-Resolved Raman Spectroscopy**

Yuki Nojima, Sho Kitamura, Tomohisa Takaya, Koichi Iwata

We estimate the thermal diffusivity inside the lipid bilayer membranes with picosecond time-resolved Raman spectroscopy. The cooling kinetics of S1 trans-stilbene is measured in liposome lipid bilayers formed by six different phosphatidylcholines. The observed cooling rate constants for the LC phase lipid bilayers from DOPC, DMPC, DLPC, and egg-PC are larger than the rate constants for the gel phase lipid bilayers from DSPC and DPPC. Presence of water accounts for the difference observed between the two phases.

14:30  
TH610 **Two Dimensional Electronic Spectroscopy for Analyzing Ultrafast Vibrational Wavepacket Dynamics and Electron-Phonon Coupling**

Juergen Hauer

Two dimensional electronic spectroscopy (2D-ES) with ultrabroadband pulses lets us study vibrational as well as electronic dynamics and the coupling between them. In a solvated monomer, we demonstrate that vibrational oscillations are stronger in 2D-ES than in related ultrafast techniques. In a molecular J-aggregate, 2D-ES is used to study the effects of vibrational-excitonic coupling. We show how these effects influence and steer the supramolecular aggregation process.

13:30 **Industrial Raman Spectroscopy: Beyond the Analytical Laboratory Setting**

TH806

Ian Lewis, Alexander Pitters, Carsten Uerpmann, Herve Lucas, Bruno Lenain, Maryann Cuellar, David Strachan, Pat Wiegand, Sean Gilliam, Joe Slater

The flexibility to configure an optical in-situ interface allows Raman to be integrated into reactors and processing equipment. Raman spectroscopy offers a number of attractive features to the process control engineer for on-line characterization including a relatively fast response time, chemical functional specificity, and applicability to a wide variety of chemistries and materials. A secondary benefit when selecting Raman is that the analytical approach can be developed in the laboratory and accompany promising chemistries into manufacturing and throughout their lifecycle.

13:45 **Improved Potential for the Use of Process Raman Spectroscopy to Enhance Process Understanding**

TH807

Mark Kemper, Yusuf Bismilla

The application of Raman spectroscopy to process analysis has been active for at least three decades now. One of the most recent innovations with Raman is the High Throughput Virtual Slit (HTVS). This has allowed more efficient photon management and this, in turn, means greatly improved throughput. This is significant for a low signal technique such as Raman as it can improve detection limits or time resolution significantly leading to better process control opportunities.

14:00 **Real Time Measurements of Polymer Properties by Raman Spectroscopy**

TH808

Patrice Bourson, Marie Veitmann, Elise Dropsit, David Chapron, Alain Durand, Sandrine Hoppe, Jean Guilment

Raman spectroscopy is a technique particularly rapidly evolving in spectral qualities, quality of instruments ... and transportability of the new equipment. This allows uses in-situ or real time using of these devices and the possibility of their use for monitoring response and industrial flows directly into the plant or reactor. We show, in this presentation, two examples of real-time monitoring by Raman spectroscopy. The first one is the control in real time of industrial flows using Raman spectroscopy combined with chemometrics to monitor very effectively an industrial polymer production. The second example is an original coupling of a Raman spectrometer with a rheometer for monitoring in real time of the polymerization of acrylic acid.

14:15 **Fiber Optics in Vibrational Spectroscopy for Process Control and Biomedical Diagnostics**

TH809

Viacheslav Artyushenko

Fiber spectrometers and sensors using vibrational spectroscopy methods will be compared for applications in remote reaction monitoring or in-vivo biomedical diagnostics. Pro & contra for one method selection (or combinations) will be provided for diffuse reflection in Near IR, evanescent Mid IR-absorption and Raman scattering spectroscopy. Special focus will be done on development of spectral fiber sensors. In contrast with a broad band spectrometers they can be small and price effective because of customization to a distinct process control or diagnostics by an optimal selection of a few specific spectral bands.

14:30 **Using Raman Spectroscopy to Show How You 'Personally Care' for Your Body**

TH810

Paul Pudney, Eleanor Bonnist, Lynette Weddell, Fiona Baines, Sarah Paterson, Jane Matheson, Andrew Jones, Richard Evans, Susan Bates, Antony Dadd

This paper describes how Raman spectroscopy can be used in the personnel care industry. In particular using in vivo Raman probe that allows investigation of areas of the body that are otherwise difficult to get access to but are where we apply products we buy in the supermarket every day. These areas include the underarm (axilla) and the scalp. Results from these areas of the body that have been very difficult to study before are described, including how they are different, how active molecules are delivered and what effect they have on the skin.

15:15  
TH111**Lighting up the Raman Signal of Molecules in the Vicinity of Graphene Related Materials**Xi Ling, Shengxi Huang, Shibin Deng, Nannao Mao, Jing Kong, Mildred Dresselhaus, Jin Zhang

Recently, graphene, as well as the other two dimensional (2D) materials, were developed to be used as a Raman enhancement substrate, which can light up the Raman signals of molecules, and these substrates were demonstrated to be a promising for micro/trace species detection. This effect was named as “graphene enhanced Raman scattering (GERS)”. GERS technique offers significant advantages for studying molecular vibrations due to the ultraflat and chemically inert 2D surfaces, which are newly available, especially in developing a quantitative and repeatable signal enhancement technique, complementary to SERS. Moreover, GERS is a chemical mechanism dominated effect, which offers a valuable model to study the details of the chemical mechanism. As a practical technique, the combination of GERS with a metal substrate incorporates the advantages from both the conventional SERS and GERS. The introduction of graphene to the Raman enhancement substrate extended SERS applications in a more controllable and quantitative way. In this talk, I will introduce this novel technique and our recent progress on GERS.

15:35  
TH112**Probing the Properties of Random Nanometric Systems by Single-Molecule Surface-Enhanced Raman Scattering**Alexandre Brolo, Marcia Temperini, Diego dos Santos

Single molecule SERS of crystal violet and brilliant green were recorded in different conditions for roughened electrode surfaces and silver colloids. An analysis of the SERS intensities fluctuations observed in single molecule regime, including preferential strong anti-Stokes enhancement, led to fundamental information about the nano-environment that originated the enhanced SERS signal. These information included the resonance energy and the shape and geometry of aggregates.

15:50  
TH113**Localized Plasmonic Catalysis by SERS and TERS**Zhenglong Zhang, Volker Deckert

Our recent research indicates that plasmonic catalysis opens a route to concentrate and direct the energy of visible light to adsorbed molecules, hence, enhancing the rate of chemical reactions and offering a pathway to control reaction selectivity.

16:05  
TH114**Investigating SERS Particles with Integrated Correlative Raman Electron Microscopy**Frank Timmermans, Aufried Lenferink, Henk van Wolferen, Cees Otto

We present a system employing an integrated commercial Raman microscope in a dual beam FIB - SEM. Correlative SEM and Raman analysis enables an accurate analysis of nanometer - sub-micrometer particles. Using SEM particles of interest can be located and identified for subsequent Raman analysis. This method is very promising in the analysis of SERS nanoparticles. SERS particles of different sizes and shapes are located in clusters or as single particles with the SEM before Raman analysis.

15:15  
TH511 **Synergy Between Theory and Experiment for an In-Depth Analysis of the Layered Double Hydroxides Vibrational Properties**

Erwan Andre, Jean Fahel, Arnaud Di Bitteto, Cedric Carteret

The aim of this work is to show how quantum mechanical calculations, realized on periodic systems at DFT level, can be used in synergy with experimental data (XRD, Infrared and Raman) to rationalize the vibrational properties of complex chemical systems. As an illustration, a focus will be made on Layered Double Hydroxides (LDH), a group of lamellar compounds whose chemical properties are closely related to the interactions between their different components: Cationic couple, hydroxide sheets, anion and interlayer domain.

15:35  
TH512 **Computational Vibrational Spectroscopy for Various IR Probes**

Jun-Ho Choi, Minhaeng Cho

A systematic way to numerically simulate linear and nonlinear vibrational spectrum is presented. Using the hybrid method combining electronic structure calculation, molecular dynamics (MD) simulation, and theoretical models for vibrational solvatochromism, the IR and 2D IR spectra for various IR probes can be numerically described directly comparing to experimentally measured ones.

15:50  
TH513 **The C-O Vibrational Frequency as a Measure of the Protein Electric Field in the Heme Pocket of Carbonmonoxy Heme Proteins**

Solomon Stavrov

It is shown that the Stark-effect approach cannot describe reliably the dependence of vibrational frequency of the iron coordinated CO on the protein electric field in heme proteins. This approach fails because the electron density transfer between the porphyrin, the iron and CO mainly affects the frequency. The quantum chemical computations must be used to study this effect. It is shown that spectroscopically observed conformational substates of myoglobin-CO correspond to the X-ray observed different positions of the distal histidine.

16:05  
TH514 **Vibrational Spectroscopic Analysis of Levosimendan Using Experimental and Quantum Chemical Approach**

Poonam Tandon, Vineet Gupta, Marco Reuter, Martin Koch

In the present work we report a combined experimental and theoretical study on the vibrational spectra of Levosimendan (LVM). FT-IR and FT-Raman spectra of LVM have been recorded. DFT calculations have been done at B3LYP/6-311++G(d,p) level using Gaussian 09 software in order to derive the optimized geometry. Molecular electrostatic potential surface has been mapped for predicting reactive sites towards electrophilic and nucleophilic attack. To discuss the biological activity of molecule lipophilicity and aqueous solubility has been calculated.

15:15 **Red Blood Cell Resonators: The Hyper-Enhanced Overtone Modes of Hemoglobin**

TH611

Donald McNaughton, Katarzyna Marzec, David Perez-Guaita, Marlene de Veij, Malgorzata Baranska, Matthew Dixon, Leann Tilley, Bayden Wood

We report on a series of hyper-enhanced non-fundamental bands in resonance Raman spectra of Hb inside the highly concentrated heme environment of the red blood cell by using a 514.5 nm laser line. Using malaria diagnosis we demonstrate that combining the non-fundamental and fundamental regions of the resonance Raman spectrum in a Partial Least Square Discriminate Analysis (PLS-DA) model improves the sensitivity and diagnostic capability of the technique compared to analysis using the fundamental region alone.

15:35 **Reliable Blood Glucose Monitoring for Intensive Care Patients Using Micro-Dialysis and Infrared Spectrometry with On-Line Recovery Rate Determination**

TH612

H. Michael Heise, Thorsten Vahlsing, Sven Delbeck, Janpeter Budde, Dieter Ihrig

Micro-dialysis can be used for continuously harvesting body fluids under variable recovery rates. Perfusates with either acetate or mannitol have been investigated as recovery markers. Despite the overlap of mannitol and glucose infrared spectra, their simultaneous quantification was successful. By investigating the depletion of the marker substances from the perfusates using different micro-dialysis catheters, theoretical relationships between the respective dialysate marker concentration and glucose recovery rate were confirmed, rendering a basis for reliable blood glucose monitoring for intensive care patients.

15:50 **Sensing Molecular Changes Due to Protein Translation Inside Cells Using Surface-Enhanced Raman Spectroscopy**

TH613

Anna Huefner, Wei-Li Kuan, Roger Barker, Sumeet Mahajan

We report the use of intracellular SERS sensors delivered to the cytoplasm in neuronal cells for biosensing molecular interactions and changes induced by the cellular expression of a specific protein. Expression of alpha synuclein and its aggregates, involved in the pathogenesis of Parkinson's disease, is triggered in cells. Combining the intracellular SERS nanoprobe approach with chemometric methods, we are able to detect modifications in the protein-to-lipid content in cells as well as to identify specific molecules interacting with alpha synuclein.

16:05 **Microraman Spectroscopic Signature of Drug Action Pd-based Anticancer Agents Against Human Breast Cancer**

TH614

Ana Batista de Carvalho, Luís Batista de Carvalho, Gianfelice Cinque, Chris Kelley, Peter Gardner, James Doherty, Mike Pilling, Maria Marques

This study aims to apply Raman confocal microspectroscopy for probing the cellular response to a dinuclear Pd(II)-spermine complex, in an estrogen-independent human breast adenocarcinoma (MDA-MB-231). Distinct drug concentrations were tested (4,8 M), at 48 h exposure time (using cisplatin as reference). A clear differentiation was observed between the control and the drug-treated cells, as well as between the two different Pd2Spm dosages. PCA analysis allowed to unveil a major metabolic impact of this drug on the lipids and DNA.

15:15 **MWIR Upconversion Detection for Infrared Gas Spectroscopy**

TH811-inv Armin Lambrecht, Sebastian Wolf, Johannes Herbst, Frank Kühnemann

Upconversion of infrared photons for fast and sensitive MWIR detection without cryogenic cooling has gained new interest by recent progress in solid state lasers and nonlinear optical materials. Results on laser based gas spectroscopy indicate a high potential for many mid-infrared spectroscopy applications.

15:35 **Quantum Cascade Detectors for Sensing Applications**

TH812 Andreas Harrer, Peter Reininger, Benedikt Schwarz, Donald MacFarland, Hermann Detz, Tobias Zederbauer, Werner Schrenk, Gottfried Strasser

A key aspect for integrated sensing is room temperature operation of the sources and detectors with sufficient performance. We demonstrate two approaches to enhance the room temperature responsivity and detectivity for mid-infrared Quantum Cascade Detectors (QCD). First a diagonal transition QCD design with the active transition between two neighboring active wells with a peak responsivity of 16.9mA/W. Second a plasmonic lens enhanced QCD with enhanced light collection and focusing, reporting a factor of 6 photocurrent increase.

15:50 **Room Temperature MCT Detectors for FTIR Spectroscopy**

TH813 Karolina Ogrodnik, Jaroslaw Pawluczyk, Mariusz Romanis, Jozef Piotrowski

We present detection modules for sensitive and wide bandwidth detection of MWIR and LWIR radiation, that are optimized for operation at frequency bandwidth from DC to GHz range. IR detectors with improved performance and high frequency response utilizing optical immersion are reported. Recent efforts concentrated on the extension of useful spectrum range above 13 micrometers for FTIR spectrometer applications is presented.

16:05 **Optimum Drive Conditions for DLaTGS Pyroelectric Detectors in FTIR Applications and Its Impact on Performance**

TH814 Johannes Kunsch, Alan Doctor

Pyroelectric DLaTGS detectors are the workhorse detectors in FTIR instruments. Detector improvements will directly result in instrument improvements. We are investigating the "ideal pyroelectric FTIR detector". Due to basic considerations, current mode operation at appr. 45°C should yield best performance. Furthermore, we developed a unique connection scheme (patent pending) that increases the signal to noise of any pyroelectric detector by a factor of about 1.4. We intend to combine both approaches in order to make the "ideal" DLaTGS detector.

## Vibrational Optical Activity

- C001 (+)-Ketopinic Acid Dimerization in Solution State: a VCD and DFT Study**  
Manuel Montejo, Pilar Gema Rodríguez Ortega, Juan Jesús López González  
 The influence of the polarity of the surrounding media and concentration in the persistence of dimers of (+)-ketopinic acid in solution state is analysed by means of a theoretical-experimental approach. For this task, theoretical models of monomers and H-bonded dimers of the species have been used for a correct interpretation of experimental features in the VCD and FTIR spectra recorded in different solvents and at different concentrations.
- C002 Anomeric Effect in Chiral 1,4-Cioxanes by VCD and IR Spectroscopies and Quantum Chemistry Calculations**  
Pilar Rodríguez Ortega, Manuel Montejo, Juan Jesús López González  
 The physical origin of the anomeric effect (AE) has remained unclear since its first observation and, still up to day, is source of scientific debate. Two distinct mechanisms are widely accepted: (1) the hyperconjugative and (2) the electrostatic model. The current work undertake the study of the the conformational equilibrium and the effect of solvent polarity in the anomeric preference of two AE-archetypical systems using VA and VCD spectroscopies aimed to clarify the nature of the AE in the selected species.
- C003 Conformational Equilibrium in Tobacco Alkaloids: a Combined VCD and DFT Study**  
Pilar Rodríguez Ortega, Manuel Montejo, Fernando Márquez, Juan Jesús López González  
 The known dependence between conformational preference and biological role in alkaloids has motivated the study of the structural preference and associated barrier heights of a set of biochemically relevant tobacco alkaloids, i.e. (-)-S-nicotine, (-)-S-cotinine and (-)-S-anabasine. We implemented a multidisciplinary approach comprising the use of FTIR and VCD, supported by quantum chemistry calculations. Our results provide further evidence of the known hypersensitivity of VCD when studying relatively flexible chiral samples in solution.
- C004 Single Excited State Resonance ROA Spectra of Chiral Single Walled Carbon Nanotubes**  
Martin Magg, Yara Kadria-Yili, Sandra Lubner, R. Bruce Weisman, Thomas Bürgi  
 Raman optical activity (ROA) is a powerful technique to determine the absolute configuration of a chiral molecule. However, ROA is usually limited to highly concentrated or neat samples. In this study we present experimental ROA of chiral (6,5)-SWCNTs using 532 nm as the excitation wavelength. The two enantiomers of (6,5)-SWCNTs were separated by density ultracentrifugation on a micrograms scale. The single excited state ROA spectrum shows a strong enhancement of the tangential G-band. The experimental results are further compared to DFT calculations.
- C005 Raman Optical Activity of Carbohydrates**  
Shaun Mutter, Francois Zielinski, Paul Popelier, Ewan Blanch  
 Raman optical activity (ROA) is a powerful analytical technique that measures small intensity differences in the Raman scattering of chiral molecules using circularly polarized light. We present a combined molecular dynamics quantum chemical approach for the calculation of ROA spectra of carbohydrates. This approach has given excellent results when compared to experiment for several monosaccharides and allows for vibrational analysis at the atomistic level to give otherwise unobtainable vibrational peak assignments.

- C006 **The Secondary Structure of Agarose Derivatives, Analyzed with Vibrational Raman Optical Activity**  
Anja R  ther, Aurelien Forget, Anjan Roy, Rina Dukor, Laurence Nafie, Prasad Shastri, Steffen L  deke

It has been shown that hydrogels formed from the algal polysaccharide agarose, which has helical secondary structure in its canonical form, switches to a  $\beta$ -sheet-like secondary structure after carboxylation in position C6. Raman optical activity is perfectly suited for studies on the secondary structure of polysaccharides. The spectral patterns observed in the region between 990 and 1200  $\text{cm}^{-1}$  show significant changes depending on the degree of carboxylation indicating a transition from helix to a different kind of secondary structure.

- C008 **Raman Non-Coincidence in the Study of the Self-Association and Solvation in Dimethyl Sulfoxide (DMSO)**  
Jocasta de Avila, Paulo S  rgio Santos

The main objective of this work is to study intermolecular interactions using S=O mode of DMSO molecule as probe, and the main technique is the non-coincidence effect (NCE). This effect is consequence of intermolecular coupling of the electric dipole transition moments of neighboring molecules in the liquid and depends critically on other species involved in interactions with the DMSO, as electrolytes. This affects not only the NCR but also your line shape, which implies significant changes in molecular dynamics.

- C009 **Chiroptical Properties of the Antimicrobial Peptide Lasiocepsin and Its Analogs**  
Petr Malon, Mark  ta Pazderkov  , V  clav Profan, Vladim  r Baumruk, Lucie Bedn  rov  

We investigate the effect of disulfide bridges on the structure of lasiocepsin (AMP) and compare them to known NMR based results.

- C010 **Modelling of Vibrational Optical Activity of Protein Systems**  
Jiri Kessler, Josef Kapitan, Shigeki Yamamoto, Timothy A. Keiderling, Petr Bour

Vibrational spectroscopy provides useful information about the structure of protein systems in order to interpret its vibrational spectra and to provide a link between geometry and spectral properties. In this work we firstly focus on poly-L-glutamic acid or insulin fibrils. Secondly, we aim our attention to series of Globular proteins. We simulate the vibrational and vibrational optical activity spectra by means of molecular dynamic combined with quantum chemical calculations. The obtained Spectra are compared with experiment.

## PAT

- C011 **Study of Polymorphism in Pharmaceutical Compounds Using Vibrational Spectroscopic Approach and Quantum Chemical Methods**  
Poonam Tandon

Solids provide a convenient form to deliver active pharmaceutical ingredients (APIs) as part of a formulated product. However, pharmaceuticals may exist in numerous solid forms, which may feature different physical and chemical properties. These solid forms include 'true' polymorphs, solvates (pseudopolymorphs), co-crystals and amorphous solids. Polymorphism is often characterized as the ability of a drug substance to exist as two or more crystalline phases that have different arrangements and/or conformations of the molecules in the crystal lattice. In this presentation, we will review the main applications of the vibrational spectroscopy techniques in the characterization of the solid forms of pharmaceutical substances. Specific examples of qualitative and quantitative investigations of raw materials and formulated products will be discussed and correlated with the results of other experimental techniques and quantum mechanical calculations.

- C012 **Application of Global and Synchrotron Infrared and X-Ray Spectroscopy as Rapid, Direct, Non-Destructive and Bioanalytical Techniques in Feed and Nutrition Science**  
Peiqiang Yu  
Application of global and synchrotron infrared and X-ray spectroscopy as rapid, direct, non-destructive and bioanalytical techniques in feed and nutrition science.
- C013 **Infrared (IR) Monitoring of Photo-Fries Rearrangement**  
Hideyuki Shinzawa  
Photo-Fries rearrangement of phenyl salicylate was examined by real-time IR monitoring. The change in the spectral feature was readily captured during the photo-induced chemical reaction. The obvious variations of spectral intensities due to the production of 2,2'-dihydroxybenzophenone and 2,4'-dihydroxybenzophenone are clearly identified to provide in-depth understanding to the photo-Fries rearrangement.
- C014 **Fourier Transform Infrared Spectroscopy and Chemometrics for Authentication of Canned Fish Packing Oils**  
Ana Dominguez-Vidal, Jaime Pantoja de la Rosa, Luis Cuadros-Rodriguez, Maria Jose Ayora-Cañada  
The authentication of the packing oil media from commercial canned tuna and other tuna-like fish species has been approached using ATR-FTIR and chemometrics. PCA of the spectra clearly distinguishes between oils rich in monounsaturated fatty acids and oils rich in polyunsaturated fatty acids. Using PLS-DA it was possible to differentiate accurately all the different types of oil employed except in the case of packing oils labeled as sunflower oil and with the generic term vegetable oil which were virtually undistinguishable.
- C015 **Determination of the Storage Stability of Melamine-Formaldehyde (MF) Resin by Raman and ATR-MIR Spectroscopy**  
Marcin Pawliczek, Thomas Reischer, Wolfgang Kantner, Markus Brandstetter  
In this work a method for prediction of the storage stability of industrially produced melamine-formaldehyde (MF) resin was developed using Raman and ATR-MIR spectroscopy in combination with spectral analysis and chemometrics. The results indicate that both Raman and ATR-MIR spectra in combination with chemometric modelling can be used for practical determination of storage stability of MF resin right at the beginning of the storage period with satisfactory precision.
- C016 **Rapid Spectroscopic Quantification of Quality in Beer-Mix Beverages Using FTIR Spectroscopy**  
Marcin Pawliczek, Helmut Klein, Clemens Foster, Markus Brandstetter  
In this work methods for the quantification of the most relevant quality parameters of beer-mix beverages were developed using FTIR spectroscopy in combination with spectral analysis and chemometrics. Eventually, these methods shall replace a number of time consuming off-line analyses in the beer-production process. The results indicate that MIR spectra in combination with spectral analysis and chemometric modelling can be used to replace six different analytical methods currently used in off-line analysis.
- C017 **Molecular Localization of Lipids in Emulsions Using Vibrational Micro Spectroscopy**  
Maria Sovago, Patricia Heussen, Gerard van Dalen, Ewoud van Velzen, Eric T Garbaciak, Herman L Offerhaus, John van Duynhoven  
Lipids are one of the major constituents of food products, like margarine. Raman Imaging is a molecular specific technique useful for identifying the phase of the lipids (liquid versus solid) in a label-free manner. Chemometric analysis such as Multivariate Curve Resolution (MCR) of the Raman-images are used to extract concentration maps of all components. Raman Imaging proves to be an attractive technique that can be further implemented for localization of other food ingredients, such as proteins and carbohydrates.

C018 **Blueberries: An Experimental Study of Their Ripening Using Raman Spectroscopy at 1064 nm and a Model for Predicting Anthocyanin Content**

Leonardo Ciaccheri, Belén Gordillo Arrobas, Andrea A. Mencaglia, Francisco J. Rodríguez-Pulido, Carla Stinco, Maria Lourdes González-Miret, Francisco J. Heredia, Anna G. Mignani

A set of lyophilized blueberry samples was measured by means of Raman spectroscopy, making use of excitation at 1064 nm and a dispersive detection scheme. These samples had three different ripening stages: unripe, medium, and mature. The concentration of total anthocyanins, delphinidins, cyanidins, petunidins, and malvidins was available, which was previously measured by standard analytical techniques. The data set was processed by means of multivariate analysis, thus achieving qualitative assessment of ripening, and quantitative information about concentration of anthocyanins.

C019 **Analysis of Clay Smoking Pipes from Archeological Sites in the Region of the Guanabara Bay (Rio De Janeiro, Brazil) by FT-IR**

Renato Freitas

In this study twenty samples of clay smoking pipes excavated in the Guanabara Bay region (Rio de Janeiro, Brazil) were analyzed by infrared spectroscopy. The FT-IR spectra of all the samples show great similarities with the same absorption bands. However, statistical comparison tests (PCA) with FT-IR data indicate, that the samples can be classified into different groups and have confluence in one of the archaeological sites of that region.

C020 **Non-Destructive Detection of Contamination in Foods by NIR and Hyperspectral Imaging**

Norihisa Katayama, Hikaru Kobori, Te Ma, Satoru Tsuchikawa

Non-destructive detection of contamination in foods has been investigated by NIR spectroscopy including hyperspectral imaging system. The contaminated chocolate samples of insects, pieces of plastic or human hairs are prepared. The NIR imaging is effective for investigating of contaminations by insects and plastics inside of chocolate. The hyperspectral imaging measurements and chemometrics analyses enable us to inspect of contaminations in foods, even some ordinary solid contents are comprised.

C021 **Raman Microspectroscopy for Beta-Carotene Partitioning in Oil/Water Protein-Based Emulsions**

Wan Anwar Fahmi Wan Mohamad, Don McNaughton, Mary A. Augustin, Roman Buckow

Confocal Raman microspectroscopy was used to determine partitioning characteristics of  $\beta$ -carotene within O/W emulsions (10 w/w% oil) stabilized by whey protein isolate (WPI), to assist in formulating more effective emulsion-based carrier systems for bioactive. Coupled with the conventional extraction-spectrophotometric method, the effects of varying the  $\beta$ -carotene and WPI concentrations on the partitioning were observed. Increasing the  $\beta$ -carotene or decreasing the WPI concentration, decrease the percentage concentration of carotene in oil droplets, thus increasing the partitioning of carotene into the aqueous phase of emulsion.

C022 **Quantitative Analysis of Polymorphic Forms of Mebendazole in Raw Materials by Terahertz Time-Domain Spectroscopy (THz-TDS)**

Vitor Silva, Francisco Vieira, Jacqueline Gonçalves, Fernanda Pimentel, Celio Pasquini, Claudete Pereira

Terahertz time-domain (THz-TD) spectroscopy with Partial Least Square (PLS) regression was used to quantify three polymorphic forms (A, B and C) of mebendazole (MBZ) in raw materials. The THz-TD spectra for all polymorphic forms showed distinct spectral profiles. PLS models with derivative spectra and variable selection presented the best predictive ability for all polymorphic forms of MBZ. The results obtained demonstrated that the proposed methodology is a powerful method for quantifying polymorphic forms of MBZ in raw materials.

**C023 Quantification of Biodiesel and Adulteration with Vegetable Oils in Diesel/Biodiesel Blends Using a Portable Near-Infrared Spectrometer**

Eduardo Paiva, Fernanda Pimentel, Jarbas Rohwedder, Celio Pasquini, Claudete Pereira

Determination of biodiesel and vegetable oil content in diesel was performed using a portable NIR spectrophotometer with transmittance measurements and multivariate calibration models (PLS and MLR). The RMSEP values were below 0.3% and 0.5% for biodiesel and vegetable oil content, respectively. These results are comparable to those obtained with a benchtop instrument FT-NIR. Therefore, the proposed method can be used to monitor the quality of diesel blends in field, since it employs a compact system of measurements.

**C024 Classification of Brazilian and Foreign Gasolines Adulterated with Ethanol Using Middle Infrared Spectroscopy**

Fernanda Honorato, Neirivaldo Silva, Fernanda Pimentel, Ricardo Honorato, Adriano Maldaner, Marcio Talhavini

Illicit trade of fuel from neighboring countries is a problem in Brazil. Federal Police needs to safely attest the origin of seized gasoline. A rapid and nondestructive method to classify gasoline according to its origin (Brazil and Venezuela), using infrared spectroscopy, multivariate classification and calibration transfer techniques, was established. After standardization of the spectra, a 100% correct classification was achieved using SIMCA or PLS-DA models.

**C025 Fiber-Enhanced Resonance Raman Sensing of Pharmaceutical Drugs in Aqueous Environment**

Di Yan, Juergen Popp, Torsten Frosch

In this work we report the experimental combination of the fiber enhanced Raman sensing (FERS) and UV resonance Raman sensing (UV-RRS) on pharmaceutical drugs. The results show that the sensitivity is highly improved and at the same time the sample volume is reduced compared to conventional measurements. Low limits of detection (LOD) has been achieved, and the enhanced Raman signal has an excellent linear relationship with the concentration of the analyte. Therefore, it has great potential for quantitative analysis of low-concentrated pharmaceuticals.

**C026 Screening of Sugars and Sweeteners by Terahertz Time Domain Spectroscopy**

Igor da Silva, Ivo Raimundo, Jarbas Rohwedder, Celio Pasquini, Pei Wang, Boris Mizaikoff

This study had the objective of testing the potential for screening sugars and sweeteners via Terahertz Time Domain Spectroscopy for potential applications in food quality control. After the preparation of pellets, i.e., individual constituents and mixtures of fructose, glucose, lactose, sucrose, sucralose, and saccharin in PTFE, the obtained transmission absorption spectra in the range of 0-3 THz evidenced characteristic peaks for each analyte, thereby facilitating uni- and multivariate quantitative calibration models in the concentration range of 0-20% (w/w).

**C027 Improving the Precision of Terahertz Time-Domain Spectroscopy for Quantitative Applications**

Rafael Fernandes, Ivo Raimundo, Celio Pasquini, Jarbas Rohwedder

This work is aimed at evaluating the effect of rotating the sample pellet on the precision of measurements performed in THz-TDS spectroscopy. Mixtures of glucose and fructose prepared in PTFE pellets were employed as a model. Quantitative analysis based on PLS calibration employing two strategies, e.g., (a) static pellets and (b) rotating pellets were performed, demonstrating that rotation of the pellets decreases by a factor of two the errors of prediction calculated by means of full cross-validation approach.

**C028 Raman Measurements of the Rate of Saponification of Ethyl Acetate**

Irina Shpachenko, Nikolai Brandt, Andrey Chikishev

The reaction rate is the main characteristic of any chemical process. We apply Raman spectroscopy in the measurements of the rate of the saponification of ethyl acetate. To the best of our knowledge, Raman spectroscopy has not been employed in such measurements. Raman measurements can also be used to measure the kinetic characteristics of the hydrolysis catalyzed by chymotrypsin. Low sensitivity of the Raman spectroscopy is partly compensated for by the uniqueness of the Raman spectrum of the given substance.

- C029 **FT-NIR Spectrometric Determination of Moisture Content of Lyophilized Biopharmaceutical Formulations/Raman Spectroscopic Characterization of API**  
Karl Jalkanen, Biranchi Patra, Linda Soohoo, Claudia De Novaes Davidson, Gerard Jensen

In this work we have combined FT-NIR spectroscopy, Karl-Fischer Coulometric titration, and multivariate spectral analysis to develop a nondestructive chemometric method to determine the moisture content of lyophilized pharmaceutical products. The advantage of this method is that one can determine the moisture content of the lyophilized product in its vial. We also use Raman spectroscopy to identify and characterize the polymorphic form of an active pharmaceutical ingredient; formerly characterized by FTIR which required removal of sample from hicoflex bag.

- C030 **Infrared Reflection Absorption Spectroscopy for Online Monitoring of Industrial Manufacturing Processes**

Julian Haas, Isabell Buresch, Claudia Mader, Boris Mizaikoff

Infrared reflection absorption spectroscopy (IRRAS) was used to investigate the surface of rolled strips of copper and copper alloys in order to determine lubricant residues. Exploiting the exquisite surface sensitivity at grazing incidence along with polarized IR radiation lead to limits of quantification in the range of  $0.04 \text{ mg dm}^{-2}$  depending on the hydrocarbon content of the particular lubricant. Operation at ambient conditions promises facile and rapid operation for routine analysis and quality control in industrial manufacturing environments.

- C031 **Filling the Gap of Pre-Processing in MVDA Analysis**

Thomas Zahel, Patrick Sagmeister, Christoph Herwig

Many manufacturing industries, including the biopharmaceutical domain, use multivariate data analysis (MVDA) to optimize and analyse their manufacturing processes based on complex and often unstructured process data. However, it is still unclear how this data should be pre-processed in order to obtain clear and interpretable results from subsequently applied MVDA tools. We present different workflows for pre-processing and filtering strategies in order to overcome classical problems of real manufacturing data such as data misalignment or statistical and systematic noise.

- C032 **Near-Infrared Imaging Using a High-Speed Monitoring Near Infrared Hyperspectral Camera (Compovision)**

Yukihiro Ozaki, Daitaro Ishikawa, Asako Motomura, Yoko Igarashi

NIR imaging has several superior features such as suitability for nondestructive and in-situ analysis, transmission ability, availability of optical fibers, high-speed monitoring and stability. In the last 10 years or so, novel NIR imaging systems have been developed. We have also been involved in the development of new NIR imaging system based on novel NIR camera named Compovision (Sumitomo Electric. Co. in Japan). Its notable features are the performance of high speed and high sensitivity and wide area monitoring.

- C034 **New Technology for Finding Optimal Spectral Matches in Reference Databases**

Karl Nedwed

Optimized Curve Matching and Display is a novel and valuable curve matching and visualization methodology. It allows users to identify optimal spectral matches within reference databases and visualize the comparative results in a way that is more discernible to the human eye. We will discuss multiple corrections that can be applied automatically to compensate for differences between spectral instruments, environmental conditions, sample concentration, ATR correction, and others to optimize the match between spectral curves.

**C035 Rapid and Non-Destructive Identification of Counterfeit Viagra Tablets Using Dual Laser Handheld Raman Spectroscopy**Sulaf Assi

Counterfeit medicines represent a global health threat and could be encountered anywhere over the wholesale supply-chain. This work aims at developing a rapid method for the identification of counterfeit Viagra tablets using dual laser handheld Raman spectroscopy. A library was constructed using 30 authentic tablets. Five Authentic and 27 counterfeit tablets were tested against the library using the HQI algorithm. Raman spectroscopy and HQI algorithm were able to classify authentic and counterfeit tablets without type I or type II errors.

**C036 Advances in in-Situ Analysis for Low Volume Liquid-Phase Reactors Using Raman Spectroscopy**Ian Lewis, Lisa Ganster, Alexander Pitters

In this presentation example of improvements in sampling for in-situ liquid-phase Raman applications will be shown as well as applications of Raman spectroscopy for the study and control of small reactor systems including sealed microwave systems, continuous flow reactors, NeSSITM platform devices, and small volume thermal reactors.

**C037 Fast Determination of Lignin Content in Feedstock Material for Pulping Process Monitoring and Optimization**Jan Skvaril, Konstantinos Kyprianidis, Anders Avelin, Monica Odlare, Erik Dahlquist

Pulping process is a long residence time process which is fed with highly variable feedstock material in the form of wood chips and corresponding amount of cooking chemicals. Process requires appropriate application of chemicals in order to maintain desired product quality while considering environmental impact. Near infrared spectroscopy is used for rapid determination of lignin content in feedstock material and demonstrates promising results. Better knowledge of the feedstock material enables significant improvements in process monitoring, control and optimization.

**C038 Vibrational Spectroscopy of Fresh and Aged Olive Oil**Gianfranco Giubileo, Adriana Puiu, Stella Nunziante Cesaro, Gabriele Tarquini

The infrared spectroscopy was applied to study changes occurring during the olive oil ageing. Measurements have been performed on commercial olive oil samples. Samples of olive oils were artificially weathered by a weatherometer and the changes in the spectroscopic behavior were carefully examined. Continuous spectra were realized by the FTIR technique, while high resolution line spectra were recorded by the LPAS technique, based on a CO<sub>2</sub> laser source. Changes have been observed around 1000 cm<sup>-1</sup> in the laser emission region.

**C103-pdp Biopolymer Interactions with Ice and Water**Calum Welsh, Paul Pudney, Julian Bent, Mike George

This work explores the interactions of carrageenan, a high molecular weight sulphated polysaccharide extracted from red seaweeds, with water and ice using vibrational spectroscopy. A low temperature ATR-FTIR setup is used to monitor the structural changes of carrageenan occurring as a function of temperature. Deconvolution of the resultant spectra is aided by the use of 2D correlation spectroscopy and principle component analysis.

**C104-pdp Three-Dimensional Analysis of Fluorescent Probes Used for DNA Detection**Marion Egelkraut-Holtus, Kiyoshi Wada, Mikio Sugioka

DNA probes labeled with fluorescent dye are used extensively to detect and identify specific DNA when conducting life science studies. The mechanism involves the selective binding of the probe to specific DNA, thereby permitting the detection of that DNA. However, due to the wide variety of fluorescent dyes, it is important to know the exact wavelength at which the probe fluoresces to ensure DNA detection. Using the three-dimensional spectral measurement it is to identify exact wavelength Position of the fluorescence Peak.

## Time-Resolved Spectroscopy 2

- C039** **Analysis of Molecular Interactions in Polymer Systems by Using a Pulsed Compression ATR Dynamic Infrared Linear Dichroism Step Scan Time Resolved FT-IR/2D-IR. - Generation of Ring Down Compression Pulses**  
Yuji Nishikawa, Hiroto Itoh, Isao Noda
- A rheo-optical method, based on pulsed compression ATR dynamic infrared linear dichroism (DIRLD) step scan time-resolved-FT-IR/2D-IR spectroscopy, is further improved. By inserting a tungsten-carbide block with massive weight between a film sample and a piezo electric actuator, a ring-down response was successfully generated according to the inertial effect. As a result, it became possible to generate the multiplexed compression stress, which has a broad frequency distribution according to the viscoelasticity characteristic of polymer films.
- C040** **Ultrafast Time-Resolved Infrared Spectroscopic Investigation of C-H Activation at Rhodium**  
Alisdair Wriglesworth, Mike George
- We report the use of ultrafast time-resolved infrared (TRIR) spectroscopy to probe the C-H activation of a range of linear and cyclic alkanes at rhodium centres. The nature of the alkane has been observed to play a crucial role in determining the rate of activation. Small changes in the ligand environment also appear to have a very significant influence on the rate of activation.
- C041** **Coupling Between Excited States in Pyridyl Triazole Complexes**  
Gregory Huff
- Complexes of pyridyl 1,2,3-triazole ligands containing d6 and d8 metals have been synthesized and studied with resonance Raman spectroscopy. The Re(I) and Pt(II) complexes are found to behave similarly to analogous bipyridine complexes. The Ru(II) complexes have much shorter excited state lifetimes than the analogous bpy complex and quickly eject the ligand via a metal-centered triplet state. Substitution of the ligand with triphenylamine enhances visible light absorption by the complexes and drastic changes in the photophysics.
- C042** **Facility Development Update: The Kerr-Gated Raman/ Ultrafast Time-Resolved Fluorescence Instrument**  
Igor Sazanovich, Gregory Greetham, Pierre Burgos, Benjamin Coles, Anthony Parker, Michael Towrie
- In this contribution we provide an update on a Kerr-gated Raman/time-resolved fluorescence facility upgraded to 10 kHz repetition rate. the setup demonstrates 4 ps temporal response (carbon disulfide is used as a Kerr medium) at 15 wavenumbers spectral resolution, enabling to study liquid sample solutions and shall also allow work with solid samples such as monitoring catalysis reactions in-situ. More instrument performance specifications along with the experimental results will be presented, including planned time-resolved resonance Raman experiments.
- C043** **Intramolecular Proton Transfer Studied by Femtosecond Stimulated Raman and Transient Absorption Spectroscopy**  
Yoonsoo Pang, Sebok Lee, Myungsam Jen
- Intramolecular proton transfer of alizarin was investigated by time-resolved electronic and vibrational spectroscopy. Proton transfer in neat ethanol and ethanol-water mixture would provide more details about the intramolecular and intermolecular hydrogen bond formations. Lifetimes of locally excited and proton transferred tautomers will be sought in addition to the exact molecular geometries.

## Non-linear Techniques

C044 **Light-Induced Mid-IR Emission Effect as a New Probe for the Vibrationally-excited Species**

Evgeny Terpugov, Olga Degtyareva

Light-induced mid-IR emission spectroscopy is being tested as a technique for the studying of vibrationally-excited molecules of amino acids in liquid and solid states. By varying the excitation conditions, we had tried understand some of the physical phenomena that can drive emission in mid-IR. Our results suggest that the visible light is the source of the nonlinear response and is producing the vibration excitation as well as photostimulated transformations of the molecules possessing the high activity for the nonlinear response.

C045 **CARS Imaging Fiber Probe for Nonlinear Endoscopic Applications**

Aleksandar Lukic, Sebastian Dochow, Olga Chernavskaia, Ines Latka, Christian Matthäus, Anka Schwuchow, Michael Schmitt, Jürgen Popp

Within the last years coherent anti-Stokes Raman scattering (CARS) microscopy has shown its large potential towards a label free in-vivo chemical contrast imaging method for optical pathology. In order to improve the applicability under in-vivo conditions, that is to also reach difficult to access body regions optical fiber based CARS probes are required. In this contribution we will present a novel CARS imaging fiber probe consisting of 10,000 light guiding elements. With this imaging fiber probe scanning, which is necessary for imaging, is shifted from the distal to the proximal end of the fiber probe.

C046 **Probing the Chain-Length Dependency of an Organic Self-Assembled Monolayer by Sum Frequency Generation Spectroscopy**

Cornelia Reitböck, Eric Gowacki, Niyazi Serdar Sariciftci, David Stifter

In this work we present monolayer sensitive and non-destructive probing of n-alkyl phosphonic acids by Sum-Frequency Generation Vibrational Spectroscopy. This nonlinear technique enables in-situ characterisation (e.g. during heating and cooling cycles) of the molecular arrangement and allows an investigation of the orientation of molecules by measuring under different polarisation conditions. The focus of our work is on chain-length dependencies and heat induced ordering effects within the self-assembled monolayers, being relevant components for advanced organic field effect transistors.

C047 **Water Structure at the TiO<sub>2</sub>/Water Interface Probed by Vibrational Sum Frequency Spectroscopy**

Saman Hosseinpour, Simon Schmitt, Fenglong Wang, Ellen Backus

Photocatalytic splitting of water using sun light for production of hydrogen as an environmentally-friendly, storable, and abundant energy source has received much attention in the last decades. In this study we utilized the inherently surface sensitive technique, sum frequency generation spectroscopy, to determine the structure and conformation of interfacial water molecules at the TiO<sub>2</sub>/bulk water interface. We compared the structure of water molecules adsorbed on the TiO<sub>2</sub> surfaces prepared with different methods to that of the single crystalline TiO<sub>2</sub>.

C048 **Comparison of CARS and Raman Spectra of Silicon Carbide Polytypes**

Christian T. Reindl, Detlev M. Hofmann, Sangam Chatterjee, Toni Beckmann, Peter J. Klar

The hydrophobicity of paper substrates can be controlled by a barrier coating including organic nanoparticles and vegetable oils. To get better insight in the nanoparticle interactions, surface chemistry of coated papers and presentation of oil at the surface by thermal release, the coated papers are further studied by Raman spectroscopy and imaging. Depending on the oil-types, different release profiles have been determined.

C049 **CARS Molecular Fingerprinting of iPS Cells - Toward Visualizing Pluripotency**

Hiroaki Yoneyama, Hiroki Segawa, Ken Nishimura, Aya Fukuda, Koji Hisatake, Hideaki Kano

Induced pluripotent stem cells (iPS cells) have potential to differentiate variety of tissues and organs. Recently, various kinds of studies have been carried out in order to apply iPS cells to tissue engineering and regenerative medicine. However, it is still difficult to find pluripotency of living iPS cells without staining or molecular tagging. In the present study, we have performed molecular vibrational imaging of iPS cells using coherent anti-Stokes Raman scattering (CARS) microscopy to explore the spectroscopic signatures of pluripotency.

C050 **Ultra-Broadband Two Beam CARS using Femtosecond Laser Pulses**

Gabor Matthäus, Stefan Demmler, Jens Limpert, andreas Tünnermann, Stefan Nolte, Roland Ackermann

Femtosecond (fs-)CARS has been proven to be a suitable for applications in gas spectroscopy. In particular, the use of ultra-broadband pulses allows the simultaneous detection of multiple species. Here, we present an alternative approach suitable for high-pressure applications, which uses an ultra-broadband pump/Stokes pulse and a femtosecond probe pulse.

C051 **Mode Specific Excited State Dynamics of Bis(phenylethynyl)benzene Using Ultrafast Raman Loss Spectroscopy**

Khokan Roy, Siva Umapathy, Freek Ariese

Femtosecond transient absorption (TA) and Ultrafast Raman Loss Spectroscopy (URLS) was applied to a linear pi-conjugated molecule bis(phenylethynyl)benzene (BPEB), a model system for one-dimensional molecular wires. In the ground state BPEB has a low torsional barrier, and thus will consist of a population of rotamers at room temperature. Femtosecond TA and URLS measurements show multi-exponential behavior related to the structural dynamics in the excited electronic state. Frequency shifts indicate the extent of conjugation during different phases of excited state relaxation (planarization).

## Material Science 2

C052 **Raman Light Scattering, Infrared Absorption and Neutron Scattering Studies of the Phase Transition and Reorientational Dynamics of H<sub>2</sub>O Ligands and ClO<sub>4</sub><sup>-</sup> Anions in [Ca(H<sub>2</sub>O)<sub>4</sub>](ClO<sub>4</sub>)<sub>2</sub>**

Joanna Hetmanczyk, Lukasz Hetmanczyk, Anna Migdal-Mikul

We have performed infrared (FT-MIR), Raman (RS) and neutron scattering (IINS/QENS) measurements in order to establish relationship between the observed phase transition and reorientational motions of the H<sub>2</sub>O ligands ClO<sub>4</sub><sup>-</sup> anions. All experimental facts show distinct changes in FWHM of some bands connected with vibrational modes. The density functional theory plane wave calculations of the normal modes within the periodic boundary conditions (CASTEP code) were performed. We have obtained good agreement between calculated and experimental data (IR, RS, IINS spectra).

C053 **In Situ Confocal Raman Microscopy Observation of Ferroelectric Domain Wall Motion Induced by Polarized Light**

Adolfo Del Campo, Fernando Rubio-Marcos, Pascal Marchet, Jose Francisco Fernandez

Here we show the surprising ability to move ferroelectric domain walls of a BaTiO<sub>3</sub> single crystal by varying the polarization angle of a coherent light source. This unexpected coupling between polarized light and ferroelectric polarization modifies the stress induced in the BaTiO<sub>3</sub> at the domain wall, which is demonstrated for the first time by using in situ Confocal Raman Microscopy. This effect potentially leads to the non-contact remote control of ferroelectric domain walls by light.

C054 **Garnet-Like Structured Solid Solutions  $\text{Li}_{7-x}\text{La}_3\text{Zr}_{2-x}\text{M}_x\text{O}_{12}$  ( $\text{M} = \text{Nb}, \text{Ta}; 0 \leq x \leq 2$ ) for All-Solid-State Li-Ion Batteries - Characterisation via Raman Spectroscopy**

Maria E. Maier, Maurizio Musso, Daniel Rettenwander, Reinhard Wagner, Georg Amthauer

Cubic garnet-like structured Li-ion conductors  $\text{Li}_{7-x}\text{La}_3\text{Zr}_{2-x}\text{M}_x\text{O}_{12}$  ( $\text{M} = \text{Nb}, \text{Ta}; 0 \leq x \leq 2$ ) are promising materials for solid-state electrolytes. Raman spectroscopy is a powerful, non-destructive tool for the characterisation of these materials, e.g. pure-phase determination, highly disordered Li-ion distribution for high ion conductivity (liquid-like Li-sublattice), structural and compositional (in)homogeneity, luminescence/defect structure, effects of synthesis conditions and routes, etc.

C055 **Comparison of IR- and Raman Spectroscopy for a Rapid Characterization of Methylmelamine, Vinylmelamine to the Final Vinylmelamine-Ethylene-Copolymer**  
Manuela List

A method for increasing the flame resistance of polymers is to add nitrogen compounds (e.g. melamine, melamine-cyanurate, trihydrazinotriazine etc.). We have tried to incorporate a melamine based flame retardant via copolymerization, thus affording a chemically homogeneous system. We have found that methylmelamines can readily be vinylated and thus can be used as monomers in several polymerization and copolymerization reactions. A selection of these, especially pentamethylvinylmelamine (PMMV), tetramethyldivinylmelamine (TMMV), and trimethyltrivinylmelamine (TriMMV), were prepared with very high purity to be used in the copolymerization with ethylene. Different methods for the characterization of these new polymer products were applied. Remaining methods such as FTIR, Raman spectroscopy, solid state NMR, and analytical pyrolysis were applied and the results are presented.

C056 **Raman and Photoluminescence Spectroscopy of Cementitious Materials**  
Takafumi Takahashi, Kana Kimura

The aim of this study is to collect Raman spectra of synthetic hydrated minerals with assignment of the observed bands, and furthermore to get Raman images of hydrated minerals in cement pastes. Raman images of cement pastes clarified that finer  $\text{Ca}(\text{OH})_2$  aggregates formed with increasing an aging time. Furthermore, weak photoluminescence signals for synthetic hydrated minerals could be detected by Raman microscope.

C057 **Structural, Magnetic and Vibrational Properties of Metal-Organic Frameworks with the Perovskite and Nicolite Architecture**  
Aneta Ciupa, Mirosław Mączka, Maciej Ptak, Anna Gaġor, Adam Sieradzki

We will present temperature-dependent Raman and IR spectra for novel chromium- and aluminium-based metal-organic frameworks. We will also discuss influence of chromium doping on mechanism of a structural phase transition in the perovskite dimethylammonium manganese formate.

C058 **Micro-Raman Scattering Investigations of CVD Diamond Film**  
Hamid Motahari, Rasoul Malekfar, Ehsan Talebian

Nowadays, the Chemical Vapor Deposition (CVD) techniques are used to produce diamond films. The outstanding properties of diamond films have made it a material of considerable scientific research. Also diamond films have the high applications and commercial potential in many fields. On the other hand, micro Raman spectroscopy is a nondestructive method for the characterization of carbon based materials. In this study, we used CVD diamond films produced by a horizontal quartz tube CVD reactor. Then, the quality of the diamond has been characterized by Raman spectroscopy.

C059 **Enhancement of Structural Phase Transition Temperature in  $\text{BaTiO}_3$  Films Probed by Raman Spectroscopy**

Satish Kumar, Dharendra Kumar, Ajay K Rathore, Vasant Sathe

$\text{BaTiO}_3$  films (~400 nm thickness) have been grown on  $\text{LaAlO}_3$  substrate using pulsed laser deposition technique. The films are highly oriented and single phase in nature. The substrate induced strain in BTO films enhances tetragonal distortions in films. The strain induced distortions in films leads to the enhancement of ferroelectric transition temperature (accompanied by structural transition from tetragonal to cubic) by ~100 K as compared to bulk compound, which is probed by using high temperature Raman spectroscopy.

C060 **Two-Dimensional Raman Correlation Spectroscopy Study of Aggregation Process in Ionic Liquid Systems**

Jonas Kausteklis, Valdemaras Aleksa, Vytautas Balevičius

Phase behavior of the imidazolium-based room temperature ionic liquids (RTIL) 1-decyl-3-methyl-imidazolium bromide and chloride were studied by 2D Raman correlation spectroscopy and principal component analysis. These techniques indicate RTIL imidazolium ring vibration modes sensitive for additional water in the RTIL/H<sub>2</sub>O system. The borders of liquid crystalline ionogel phase have been specified using the concentration dependence of imidazolium ring  $\nu_{C_2-H}$  and  $\nu_{C_{4,5}-H}$  Raman bands chemical shifts and the scores on PC1. Liquid crystalline behavior are comparable with results get using other techniques.

C061 **Further Insights into the Thermal Behavior of Biodegradable P(HB-co-HHx)/PEG Blend**

Yujing Chen, Yeonju Park, Isao Noda, Young Mee Jung

In the present study, thermal behavior of the blend system of P(HB-co-HHx) (HHx = 6.9 mol%) and polyethylene glycol with molecular weight of 400 (PEG 400) upon heating process were investigated by infrared reflection absorption spectroscopy. 2D correlation analysis was performed to explore more deeply the thermal behavior of P(HB-co-HHx) with the addition of PEG 400.

C062 **Understanding the Changes in the Mechanical Behaviour of Hair with Humidity Using Raman Spectroscopy**

Paul Pudney, David Tiemessen, Christopher Marsh

Water is a fundamental component of hair and affects its physical and mechanical properties. Changes in humidity cause changes in the hair water content and hence the mechanical behaviour and can consequently cause drop out of style. There are a number of different models that attempt to explain this behaviour that imply different changes to the hair structure during mechanical change. Here we use a confocal Raman spectrometer with a microscope stress-strain cell within which the humidity can be controlled to investigate and probe changes within hair. Then we use 2DCOS and PCMW analysis to show the molecular transitions. These give new insights to the mechanical transitions.

C063 **Low-Frequency Vibrational Motion of Nylon 6 Studied by Raman and Terahertz Spectroscopies Combined with Quantum Mechanical Simulations**

Shigeki Yamamoto, Erika Onishi, Harumi Sato, Hiromichi Hoshina, Yukihiko Ozaki

Insight into intermolecular interactions including hydrogen bonds among polymer chains can be achieved based on low-frequency Raman and terahertz spectroscopies which can be sensitive to higher-order structural changes of polymers. Nylon 6 is one of the most widely used synthetic fibers, and its phase behavior and crystal structures have extensively been studied by various methods. However, assignments of low-frequency vibrational bands and their correlated intermolecular interactions are still not fully understood. We present our experimental and theoretical studies on them.

C064 **Characterization of Structure and Microstructure Properties Glass-Ceramic Glazes from SiO<sub>2</sub>-Al<sub>2</sub>O<sub>3</sub>-K<sub>2</sub>O-Na<sub>2</sub>O-CaO System by Variable Molar Ratio of the SiO<sub>2</sub>/Al<sub>2</sub>O<sub>3</sub> Using Infrared and Raman Spectroscopy**

Magdalena Lesniak, Janusz Partyka, Maciej Sitarz

IGlazes are thin (0,5-1 mm) glassy or glass-ceramics coverings applied on different ceramic substrates. This study has been carried out verifying how various molar ratio of the SiO<sub>2</sub>/Al<sub>2</sub>O<sub>3</sub> influence on the structure and microstructure properties of glass-ceramic glazes from SiO<sub>2</sub>-Al<sub>2</sub>O<sub>3</sub>-Na<sub>2</sub>O-K<sub>2</sub>O-CaO system. Pseudowollastonite, anorthite and glassy phase were identified after heat-treatment. In order to determine the state of the surface (microstructure) research on the scanning electron microscope (SEM) with EDS were done. For structural studies X-ray diffraction (XRD), Raman spectroscopy and MIR and far FIR spectroscopic studies were performed.

- C065 Studying the Morphology of Polypropylene Extruded Materials Using Raman Microscopy**  
Abhishek Sanoria  
Processing of Polypropylene, infers anisotropies in crystallinity, chain orientation or polymorphic composition. Nucleating agents are widely used to tune the polymer morphology but due to their size, being the order of a few  $\mu\text{m}$ , it is difficult to analyze their distribution and impact on the spherulite size. In this study Raman microscopy has been utilized as a tool to monitor the spatial distribution in the morphology and of the nucleating agent in PP at a high resolution ( $\sim 0.3 \mu\text{m}$ ).
- C066 Investigation of Catalytic Reactions on ALD Model Catalysts and Perovskites with Sum Frequency Generation Spectroscopy**  
Verena Pramhaas, Matteo Roiaz, Christoph Rameshan, Günther Rupprechter  
Platinum is well known for its catalytic activity concerning waste gas reduction and oxygen reduction reaction. We investigate thin films and nanoparticles of Pt on oxides and perovskites with sum frequency generation spectroscopy. This technique allows measuring under high gas pressures.
- C067 Hydrogen Bonding Interactions Between  $[\text{C}_2\text{OHmim}][\text{BF}_4]$  and Acetonitrile**  
Jing Xu, Yu Zhan, Yan-Zhen Zheng, Zhi-Wu Yu  
Recently, functionalized ionic liquids (ILs) have been designed and synthesized for specific purpose. The mixture of alcohol-functionalized ILs and acetonitrile has been used in ionic-liquids-supported-synthesis. In this work, we use experiment and theoretical calculation to investigate the interactions between alcohol-functionalized ILs 1-hydroxyethyl-3-methylimidazolium tetrafluoroborate ( $[\text{C}_2\text{OHmim}][\text{BF}_4]$ ) and acetonitrile ( $\text{CH}_3\text{CN}$ ). With the help of excess spectra, we are able to identify new interactive species during the dilution process and unveil microscopic information on molecular interactions.
- C068 Evaluation of Mechanical Property of Hydrolyzed Polylactide from NIR Spectroscopy**  
Shun Muroga, Yuta Hikima, Masahiro Ohshima  
The aim of this study was to develop non-destructive measuring techniques for polylactide (PLA) processing. Near-infrared spectroscopy was applied to evaluate the effects of crystallinity and hydrolysis on mechanical properties. Crystallized PLA indicated a decrease of flexural strength and increases of PLA crystalline bands. Hydrolyzed PLA showed a sharp drop of the flexural strength and a slight increases of OH group band. Applying discriminant analysis with PLA crystalline and OH group bands to PLA samples, hydrolytic deterioration of the flexural strength was detected considering the effect of crystallinity on the flexural strength.
- C069 Time-Domain THz Imaging as a Flexible Metrology Tool for Characterising Thin Wafers in Semiconductor Manufacturing**  
Thomas Arnold, Christina Hirschl, Johannes Schicker, Germar Schneider, Martin Kraft  
Time-domain THz imaging was evaluated as a metrology tool to measure the 3D shape of warped Si thin wafers nowadays routinely used in semiconductor manufacturing. The method proved to be accurate, reliable and largely immune to most of the interference limiting the practical applicability of alternative methods. While presently still limited to the laboratory, the results achieved provided vital input and now offer a new characterisation tool for various ongoing semiconductor research activities, from materials science to improved handling logistics.
- C070 Terahertz Dynamics of Polymethyl Methacrylate**  
Tatsuya Mori, Yusuke Hashimoto, Kei Iwamoto, Hiroshi Matsui, Seiji Kojima  
We performed terahertz time-domain spectroscopy and low-frequency Raman scattering measurements for Polymethyl methacrylate (PMMA). We determined the complex dielectric constants and imaginary part of Raman susceptibility, and calculated far-infrared and Raman coupling constants of PMMA.

C071 **Polymorphs of Industrial Drugs Monitored by THz-TDS Spectroscopy**

Eugene Morita, Yusuke Suzuki, Seizi Nishizawa

We intended to establish a rapid and cheap analytical method to identify the polymorphs of synthetic drugs with terahertz wave. The purpose of this research was to clarify the correlation between Terahertz Time-Domain (THz-TDS) spectra and the polymorphs of chemicals. In this paper, we measured the THz-TDS and other spectra of several chemicals those have polymorphs. Compared with these spectra, we have found that THz-TDS spectroscopy must be a promising method to evaluate the polymorphic purities of chemicals.

C072 **Matrix Isolation FTIR Studies of Structure and Stability of 1,1,3,3-Tetrachloro-1,3-disilacyclopentane**

Valdas Sablinskas, Valdemaras Aleksa, Justinas Ceponkus, Gamil Guirgis, Milda Pucetaite, Colin Cotter

Spatial structure and stability of a newly synthesized derivative of disilacyclopentane - 1,1,3,3-tetrachloro-1,3-disilacyclopentane was studied by means of vibrational spectroscopy, including matrix isolation technique. It was found that chlorine atoms in the radical of the five membered organosilicon compounds determines flattening of the ring and such flattening can increase adsorption properties of the chlorinated silacyclopentane. On the other hand, replacement of fluorine by chlorine atoms in 1,1,3,3-tetrachloro-1,3-disilacyclopentane decrease stability of TCDCSP, what makes this newly synthesized compound hardly usable for the surface coating purposes.

C073 **Comparing the Proton Dynamics in KDP Type Crystals, in H<sub>2</sub>O and in Pressurized Ice VII**

Raymond Moreh, Yacov Finkelstein, Yaroslav Shchur

The mean atomic kinetic energies of the proton and deuteron were calculated semi-empirically in hydrogen bonded systems including water, pressurized ice VII and KDP type ferro-electric crystals. The calculations utilize the harmonic approximation and assume decoupled modes of motions. Ice/water literature input experimental data were taken from Raman/IR and inelastic neutron scattering. In the case of KDP crystals, Ke(H,D) were calculated using the vibrational density of states deduced from a lattice dynamical model. Good agreement with neutron Compton scattering measurements were obtained.

C074 **Raman Micro-Spectrometry as a Key Tool for Development and Process Control in Modern Semiconductor Manufacturing**

Martin De Biasio, Lukas Neumaier, Eduard Geier, Michael Rösner, Christina Hirschl, Martin Kraft

With a strong industrial trend towards using thin silicon in semiconductor devices, process induced stresses are matter of increasing importance. A key problem here is a lack of suitable metrology equipment for measuring inherent substrate material stresses. To overcome this, the use of Raman microspectrometry as a tool for measuring stress levels was researched. Combining theoretical considerations and real-world samples, it could be shown that Raman can provide the necessary analytical accuracy to measure stress states in silicon wafers.

C075 **Vibrational Properties of Boron-Ion Implanted Polymethylmethacrylate**

Jakub Nowak, Taras S. Kavetsky, Agnieszka Sozańska, Mariusz Trzcinski, Andrzej Marek, Alexander V. Kukhta, Yuri G. Galyametdinov, Andrey L. Stepanov

In the present work the vibrational properties of boron-ion implanted polymethylmethacrylate with the energy of 40 keV, ion doses from 6.251014 to 5.01016 ions/cm<sup>2</sup>, and current density of 2 A/cm<sup>2</sup> are studied by Raman spectroscopy in the 400-3800 cm<sup>-1</sup> range with a Renishaw Raman inVia Reflex spectrometer. The detail analysis of Raman spectra of the B:PMMA samples excited by laser wavelength of 514 nm and 785 nm is performed in dependence on ion dose.

C076 **The Interpretation of Experimental Spectroscopic Data in Coordination Chemistry Using High Performance Computing**

Christian Knoll, Danny Müller, Peter Weinberger

Vibrational and optical spectroscopy are well known as very useful tool for the characterization of inorganic coordination compounds. With the program suite Gaussian09 rev.C using VSC-1 and VSC-3 theoretical molecular spectroscopy is carried out and compared to experimental data in the field of small molecule organic chemistry and coordination chemistry. Within our contribution some of these applications of high performance computing in inorganic coordination chemistry are presented.

C092-pdp **Investigating the Excited State Photophysical Properties of Re(I) Complexes of Hexaazatrinaphthylene with Alkyl and Thioether Substituents Using Time Resolved Vibrational Spectroscopic Techniques**

Raphael Horvath, Holly van der Salm, Jack Turner, Michael Fraser, Charlotte Clark, Samuel Lind, Xue-Zhong Sun, Keith Gordon, Michael George

Mono, bis, and tris-metallic Re(I) complexes of hexaazatrinaphthylene (HATN) with methyl substituents (HATN-Me) and thioalkyl-substituents (HATN-S) are investigated. The initially excited state is probed using resonance Raman and density functional theory calculations and the triplet excited state is probed with time resolved IR spectroscopy. The inclusion of electron-donating thioalkyl chains was found to significantly perturb the initial excitation and reduce charge-transfer in the triplet state.

## Surface Science

C077 **Localization of Phase Transformation Processes in Zirconia-Based Ceramics by Topography-Based Confocal Raman Imaging**

Arne Ziebell, Johannes Ofner, Bernhard Lendl, Michael Konegger

In the past three decades, zirconia (ZrO<sub>2</sub>)-based ceramics have been successfully established as standard structural materials for a wide variety of high-performance applications. As a model system, a tetragonal zirconia polycrystalline surface with a surface defect induced by mechanical impact was used. The objective of this work is the demonstration of the applicability of confocal Raman imaging for the differentiation between ZrO<sub>2</sub> modifications on a microstructural level, taking into account topographical features of a ZrO<sub>2</sub> surface after damage-induced failure.

C078 **In Situ Raman Spectroscopy Studies on Plasmon-Catalyzed Charge Transfer Reaction: From TCNQF<sub>4</sub><sup>-</sup> to TCNQF<sub>4</sub><sup>2-</sup>**

Shuping Xu, Jing Wang, Weiqing Xu

We employed the Raman spectroscopy to investigate the charge transfer reaction of Ag-TCNQF<sub>4</sub> under the plasmonic catalysis.

C079 **Change in the Surface Geometry of the N-benzylamino(boronphenyl)methylphosphonic Acid Analogues Adsorbed onto Silver Nanoparticles in Alkaline Medium: SERS Studies**

Natalia Piergies, Edyta Proniewicz, John R. Lombardi

Here we present the SERS investigations of the selected group of boron analogues of aminophosphonic acids immobilized onto colloidal silver nanoparticles at the alkaline medium. These molecules are considered as potential kinase and protease inhibitors. The presented results indicate time-dependent changes in the adsorption geometry of the molecules. Briefly, within the first 15 minutes the interaction between the molecules and the colloidal silver nanoparticles, through the boronphenyl ring and the B-O bond, is observed. In time, this interaction becomes stronger.

C080 **Potential-Dependent SERS Investigation of the Adsorption of (Diphenylphosphoryl)(pyridin-2-yl)methanol on Ag, Au, and Cu Electrodes**

Ewa Pieta, [Natalia Piergies](#), Bogdan Boduszek, Tomasz K. Olszewski, Malgorzata Nattich-Rak, Edyta Proniewicz

Here we discussed the adsorption geometry of (diphenylphosphoryl)(pyridin-2-yl)methanol ( $\alpha$ -Py) using the potential-dependent surface enhanced Raman scattering (SERS) and two-dimensional correlation analysis (G2DCA) methods. The investigated molecule was adsorbed onto Ag, Au and Cu electrodes under different applied electrode potential. Moreover, we presented the atomic force microscopy (AFM) images of the Ag, Au and Cu substrates morphology. We observed some differences in the arrangement of the molecular fragments with changes of the metal substrate and applied electrode potential.

C081 **The SERS Study of the Structure and Adsorption Mode of Pyridine- $\alpha$ -Hydroxymethyl Biphenyl Phosphine Oxide Isomers onto Colloidal and Electrochemically Roughened Ag Surfaces**

Ewa Pieta, [Dominika Swiech](#), Bogdan Boduszek, Tomasz K. Olszewski, Edyta Proniewicz

Here we investigated three pyridine- $\alpha$ -hydroxymethyl biphenyl phosphine oxide isomers ( $\alpha$ -Py,  $\beta$ -Py and  $\gamma$ -Py) adsorbed onto colloidal and electrochemically roughened silver substrates by surface-enhanced Raman scattering (SERS) technique. We focused on the spectral changes related to the type of the silver substrate and the different position of the substituent with respect to the pyridine nitrogen atom. The obtained results allowed us to discuss the adsorption modes of the  $\alpha$ -Py,  $\beta$ -Py, and  $\gamma$ -Py isomers.

C082 **Study of Molecular Structural Control in an Organic Semiconductor Thin Film by Using IR pMAIRS**

[Nobutaka Shioya](#), Takafumi Shimoaka, Takeshi Hasegawa

Poly(3-hexylthiophene) (P3HT) is employed as an active material in an organic photovoltaic device due to the high carrier mobility in the thin film. The device performance strongly depends on the molecular aggregation structure represented by the molecular orientation and the crystallinity in the thin film. The chemical mechanism is, however, still remained within a speculation. In the present study, the chemical mechanism to control the molecular orientation has been revealed by using IR pMAIRS.

C083 **Immobilization of Cryptophane Derivatives onto  $\gamma$ -Fe<sub>2</sub>O<sub>3</sub> Core-Shell Magnetic Nanoparticles**

[Elise Siurdyban](#), Thierry Brotin, Karine Heuzé, Luc Vellutini, Thierry Buffeteau

Cryptophane derivatives possess a lipophilic cavity suitable to encapsulate neutral molecules or ionic species, such as cesium or thallium cations. The immobilization of cryptophanes onto  $\gamma$ -Fe<sub>2</sub>O<sub>3</sub> core-shell magnetic nanoparticles (MNPs) is an original and clever approach for the sequestration and the extraction of these toxic metals. Different grafting strategies were considered for the immobilization of cryptophanes onto MNPs covered by silica or gold shells. DRIFTS and TEM methods were used to characterize the functionalized MNPs.

C084 **Spectroscopic Study of Perfluoroalkyl Compounds Involving a Normal Alkyl Group**  
[Yuki Tanaka](#), Takafumi Shimoaka, Nobutaka Shioya, Kohei Morita, Masashi Sonoyama, Toshiyuki Takagi, Toshiyuki Kanamori, Takeshi Hasegawa

To reveal the mechanism of the highly complicated C-F stretching vibration band of perfluoroalkyl (Rf) compounds involving a normal alkyl group, the IR p-polarized multiple-angle incidence resolution spectrometry (pMAIRS) is employed to measure a monolayer of Rf-containing myristic acid. The result indicates that the complexity of this band is due to the normal alkyl part directly connected to the Rf group and the oscillation of the alkyl part propagates to the Rf part along the molecular axis.

- C085 **FTIR and Raman: Two Spectroscopies Compared for Surface Contamination Analysis**  
Luisa Mandrile, Andrea Mario Giovannozzi, Saverino Antonio, Cesare Lobascio,  
Francesca Pennechi, Andrea Mario Rossi

Raman spectrometer is metrologically calibrated for quantitative surface contamination analysis and the uncertainty budget of the entire procedure is addressed. The performances of the FTIR and Raman techniques in molecular contamination analysis at industrial critical surfaces are compared. Raman spectroscopy turns out to be more versatile and particularly suitable for punctual contamination detection. A real case study is presented: 2D Raman imaging is used for detecting and quantifying molecular contamination on several surfaces of industrial and biomedical interest.

- C086 **Surface-Enhanced Raman Selection Rules Derived from Plasmon-like Resonances**  
Juan Otero, Jéssica Román-Pérez, Isabel López-Tocón, Juan Soto

DFT calculations predict plasmon-like excitations in small metal clusters able to selectively modify the relative intensities of specific SERS bands of adsorbed molecules. These electronic resonances provide a new kind of SERS selection rules which allow to explain the huge enhancement of mode 9a of pyridine in the spectra recorded at negative electrode potentials.

- C087 **Monitoring Tribological Mechanisms of Polymer Composites Reinforced with Woven Fabric by Raman Microscopy**  
Pieter Samyn

The wear mechanisms of thermoset polyester composites with a polyester fiber fabric reinforcement were assessed by evaluation of the worn surfaces by Raman microscopy. Depending on the fiber orientation and sliding conditions, the Raman images show that wear mechanisms are located near the fibers along oriented parallel to the sliding direction, while the damage is mainly located in the polymer matrix with fibers oriented perpendicular to the sliding plane. Otherwise, the increase in normal loads during sliding progressively increase the modified surface area: it is visualized how the PTFE powder as internal solid lubricant is distributed on the surface.

- C088 **Molecular Level Investigation of the Order-Order Transition in Langmuir-Blodgett Films of a Block Copolymer Supramolecular Complex**  
Marie Richard-Lacroix, Kateryna Borozenko, C. Geraldine Bazuin, Christian Pellerin

Self-assembly of block copolymers attracts much interest due to their ability to generate highly ordered materials. Langmuir-Blodgett (LB) ultra-thin films of polystyrene-*b*-poly(4-vinyl pyridine) (PS-P4VP) and their complexes with 3-*n*-pentadecylphenol (PDP) were studied in a composition where the dot morphology is observed. AFM shows that the system exhibits a macroscopic transition from hexagonal to a square arrangement with increasing surface pressure. Attenuated total reflection infrared spectroscopy reveals the molecular changes (molecular orientation and interaction strength) leading to this order-order transition.

- C089 **Hydrogen Bonding Interactions Between Amides and Dimethylsulfoxide**  
Yu Zhou, Jing Xu, Zhi Wu Yu

Interactions between proteins and the aprotic solvent DMSO are of importance. In this work, threeamide group-bearing molecules, *N*-methylformamide, *N*-methylacetamide, and *N,N*-dimethylformamide, are taken as model protein molecules. Attenuated total reflection (ATR) infrared spectroscopy, excess infrared spectroscopy, and density functional theory calculations have been employed to study the hydrogen bonding interactions.

- C090 **ATR-IR Spectroelectrochemical Studies of Aqueous Solutions at Hydrogen-Terminated Silicon Single Crystals as a Model System for Interfacial Water**  
Stefanie Tecklenburg, Andreas Erbe

Water at interfaces is involved in a wide range of processes both in biological systems and technical applications. The direct experimental accessibility of these interfaces is rather limited. Thus, the molecular structure and behavior of the interfacial water is not fully understood. In this work, hydrogen-terminated silicon single crystals in contact with aqueous solutions are chosen as a model system for interfacial water. The silicon/electrolyte interface is studied via attenuated total reflection spectroscopy while its electrode potential is controlled.

- C091 **Probing Reaction Intermediates Using Matrix Isolation with Supported Model Catalysts**  
Charlotte Pearson, Andrew J. Davies, Xue-Zhong Sun, Paul B. Webb, Robert P. Tooze, Michael W. George  
*Not provided.*

## MIR Laser Spectroscopy 2

- C093 **A Mid-Infrared Sulfur Dioxide Sensor for In-Situ Industrial Applications**  
Peter Geiser, Peter Kaspersen  
A mid-infrared sensor for sulfur dioxide in emission monitoring applications using a monomode DFB ICL at 4  $\mu\text{m}$  and second harmonic detection has been developed. The detection limit of the sensor is below 10 ppm and the measurement is interference-free from all relevant gases at typical emission concentration levels. Results from a first field-test will be presented.
- C094 **Mid-IR Photoacoustic Spectroscopy on Different Skin Locations for Non-Invasive Blood Glucose Measurements**  
Alexander Bauer, Otto Hertzberg, Miguel Pleitez, Arne Küderle, Hermann von Lilienfeld-Toal, Andreas Roth, Werner Mäntele  
Pulsed photoacoustics in the mid-infrared offers the possibility to correlate glucose in the interstitial fluid from spectra of skin with enzymatically measured blood glucose levels non invasively. However, the nature of skin as an in-vivo sample leads to the question which location is most suitable for measurements. In order to determine this we investigated different locations on their suitability for future calibration.
- C095 **Mid-IR Photothermal Deflection Spectroscopy Enhanced by Total Internal Reflection for Non Invasive Glucose Monitoring as Medical Application**  
Otto Hertzberg, Alexander Bauer, Arne Küderle, Miguel Pleitez, Andreas Roth, Werner Mäntele  
IR spectroscopy with detection by photothermal deflection avoids the limitations of transmission and ATR methods. We present here photothermal deflection enhanced by total internal reflection. A tunable quantum cascade laser is utilized to generate a thermal field within the sample, which then deflects a probe beam. The principle, the validation, and applications in skin spectroscopy in vivo to monitor glucose concentration non-invasively are presented.
- C096 **Octave Spanning Mid-IR Quantum Cascade Laser**  
Loan Le, Xiaojun Wang, Jenyu Fan, Mariano Troccoli, Deborah Sivco, Claire Gmachl  
Electroluminescence with a full width half maximum of 4  $\mu\text{m}$  (spanning 3.3  $\mu\text{m}$  to 12.5  $\mu\text{m}$ ) is achieved with a single stack quantum cascade gain medium. A free-running laser of that gain medium emits from 6.2  $\mu\text{m}$  to 12.5  $\mu\text{m}$ .

- C097 **EC-QC Laser Spectroscopy for Mid-IR Transmission Measurements of Proteins in Aqueous Solution**  
Mirta R. Alcaráz, Andreas Schwaighofer, Christian Kristament, Markus Brandstetter, Héctor Goicoechea, Bernhard Lendl

We introduce a rugged setup for mid-IR transmission measurements of the protein amide I band in aqueous solution at large optical paths using an EC-QCL operated in pulsed mode combined with an advanced data processing protocol to overcome non-random fluctuations in single beam spectra inherent to EC-QCL emission curves. A custom-made temperature-controlled flow cell was designed to provide temperature stability. Characteristic spectral features of proteins with different secondary structures have been elucidated at concentrations as low as 2.5 mg mL<sup>-1</sup>.

- C098 **Quartz-Enhanced Photoacoustic Spectroscopy Sensor System for Industrial Application**  
Johannes P. Waclawek, Bernhard Lendl

A compact gas sensor system based on quartz-enhanced photoacoustic spectroscopy (QEPAS) employing a mid-infrared continuous wave distributed feedback quantum cascade laser (DFB-QCL) was developed for detection of carbon disulfide (CS<sub>2</sub>) at sub-ppmv concentration levels. The work reports the suitability of the sensor system for process monitoring at rayon industry, where CS<sub>2</sub> is used in big amounts to produce regenerated cellulose fibers.

- C099 **EC-QC Laser Mid-IR Transmission Spectroscopy for Monitoring Beta-Aggregation in Alcohol-Denaturated Proteins**  
Andreas Schwaighofer, Mirta R. Alcaráz, Christian Kristament, Héctor Goicoechea, Bernhard Lendl

A rugged setup for mid-IR transmission measurements at large optical paths using an EC-QCL was employed for monitoring  $\beta$ -aggregation in alcohol-denaturated proteins. Exposure of  $\beta$ -rich  $\alpha$ -chymotrypsin to 2,2,2-trifluoroethanol leads to immediate formation of nonnative  $\alpha$ -helices. The subsequent gradual transition to intermolecular  $\beta$ -sheet aggregates was monitored by mid-IR laser transmission spectroscopy. Multivariate curve resolution (MCR) was employed for analysis of spectral and concentration profiles of the temporal transition between  $\alpha$ -helices and intermolecular  $\beta$ -sheets.

## Geoscience 2

- C100 **Comparison of Bulk and Imaging-Based Analysis of Aerosol Particles, Collected at the Sonnblick Observatory in Austria: First Attempts Towards Image-Based Quantification**  
Johannes Ofner, Magdalena Kistler, Julia Matzl, Eylem Can Centintas, Elisabeth Schreiner, Gerhard Schauer, Regina Hitzenberger, Elisabeth Eitenberger, Gernot Friedbacher, Bernhard Lendl, Hans Lohninger, Anne Kasper-Giebl

Size classified aerosol samples were collected in July 2013 at the high alpine background site Sonnblick. Classical bulk analysis and imaged-based analysis by Raman and energy-dispersive X-ray (EDX) spectroscopy were compared. First attempts towards image-based quantification of precipitated particulate matter were done by analysing the combined Raman and EDX hyperspectral dataset. Image based quantification of atmospheric particulate matter gains access to a significantly lower required sample amount as well as additional information on species and their linkage to each other.

- C101 **Inclusion Assemblages in Topaz from Serrinha Pegmatite (Medina Batholith, Minas Gerais State, Eastern Brazil)**  
Magdalena Dumańska-Słowik, Tomasz Tobiła, Lucyna Natkaniec-Nowak, Antonio Pedrosa-Soares

The colourless topaz from Serrinha pegmatite contains both mineral and fluid inclusions. Solid inclusions are represented by feldspars (microcline and labite), topaz, quartz, rutile, and uranophane. Fluid inclusions are mainly gaseous or gas-liquid, which contain CO<sub>2</sub> (1285 cm<sup>-1</sup> and 1388 cm<sup>-1</sup>). Occasionally traces of hydrocarbons (mainly CH<sub>4</sub>) are also found. Their presence are manifested by microthermometric measurements (the CO<sub>2</sub> ice melting temperature below -56,6°C) and Raman band at 2917 cm<sup>-1</sup>.

- C102 **An Efficient FTIR Spectroscopic Study of the Solubility of Water in CO<sub>2</sub>-Rich Mixtures for Carbon Capture and Storage (CCS) Technology**  
Norhidayah Suleiman, Stéphanie Foltran, Jie Ke  
*Not provided*

## Computational Spectroscopy 2

- C105 **A Review of the Temperature-Dependent Raman-Line Broadening Due to Anharmonicity**  
Hasim Güven, Riza Demirbilek

There are two different equations used in the last three decades in the literature about temperature-dependent line broadening of the Raman scattering due to the anharmonicity. For the understanding of the reason of this difference, we reviewed the models that explain Raman scattering due to the anharmonicity. We realized that one of these equations has superfluous term that causes some errors in low temperature when evaluating the experimental data. Detailed results will be presented.

- C106 **Conformational Analysis, Spectroscopic Characterization and Molecular Docking Studies on the Potential Anticancer Drug “Busulfan”**  
Karthick Thangavel, Poonam Tandon, Parag Agarwal

Cancer disease is continuously to be a major threat among the peoples since 1930's. The investigation of conformational analysis, spectroscopic characterization, the interactions of anti-cancer drug with various proteins, enzymes which involved in cancerous activity is essential in order to find the similar kind of drugs without any side effects. In the present study, the multiple coordinates scan has been performed to find the stable conformer of busulfan. The FT-IR and FT-Raman spectra of busulfan have been recorded. Vibrational assignments of entire vibrational modes have been reported based on Gar2ped results. The presence of inter- and intramolecular hydrogen bonding interactions have been predicted using NBO and AIM analysis. To enumerate the activity of busulfan against various proteins and enzymes, molecular docking studies have been performed by SwissDock web server. Docking results revealed that busulfan is active with protein targets such as; 2V7A, 3AYU, 12CA, 1Z93, 3D2N.

# AGILENT FTIR MICROSCOPE RESOLUTION FOR EVERY APPLICATION

## NEW AGILENT FTIR ENHANCEMENTS:

- Resolve micron sized features within your larger sample without compromising data quality
- Measure samples that are centimeters in area in minutes
- Simplify data collection with NEW point and click software
- Eliminate sample preparation
- Accelerate product development

The Measure of Confidence

**WITNESS SPATIAL RESOLUTION NEVER THOUGHT POSSIBLE!  
VISIT AGILENT AT ICAVS ON BOOTH #G8**



© Agilent Technologies, Inc. 2015



Agilent Technologies

## Kaiser Raman: Optimized Solutions from the Research Lab to the Process Line

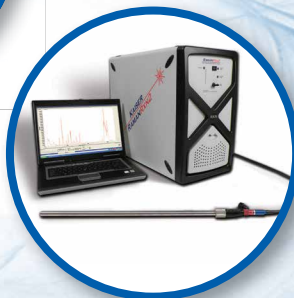


**RAMANRXN4™**  
Multi-channel

Pilot Plant / Manufacturing



**RAMAN  
WORKSTATION™**  
Transmission Raman,  
Microscopy, Imaging, or  
P<sup>AT</sup> for Research



**RAMANRXN2™ 1000**

Development, Monitoring,  
& Control Platform for Highly  
Fluorescent Material



**RAMANRXN2™**  
**HYBRID** with P<sup>AT</sup>  
or Multi-channel  
Development &  
Monitoring Platform



**KAISER  
OPTICAL SYSTEMS, INC.**

An Endress+Hauser Company



WWW.KOSI.COM

9.00 **Femtosecond Vibrational Spectroscopy of Simple and Complex Systems**

FRPL1

Tahei Tahara

With an ultrashort optical pulse that has a duration shorter than the vibrational period, we can induce coherent nuclear motion of the molecule and observe Raman-active vibrations directly in the time domain. By combining this time-domain Raman measurement with the pump pulse that starts chemical reactions, we realized time-resolved impulsive stimulated Raman spectroscopy (TR-ISRS) that provides femtosecond time-resolved Raman spectra. We report our recent TR-ISRS studies, in particular, the study of a photoreceptor protein, photoactive yellow protein.



Tahei Tahara obtained the D. Sc. degree in 1989 from the University of Tokyo. After working at the University of Tokyo and the Kanagawa Academy of Science and Technology, he started his own research group at the Institute for Molecular Science (IMS) in 1995 as an associate professor. He became Chief Scientist of RIKEN in 2001 and has been the Director of the Molecular Spectroscopy Laboratory. His interests are ultrafast spectroscopy, nonlinear spectroscopy and single molecule spectroscopy.

9.35 **From Esoteric to Commonplace: Technological Advances That Have Turned 2D IR Spectroscopy into a Robust Research Tool**

FRPL2

Martin Zanni

This talk will outline some recent developments in the technology of 2D IR spectroscopy that have enabled turn-key instruments and new scientific experiments. Mid-IR pulse shaping has enabled us to design a more accurate and more sophisticated 2D IR spectrometer that is user-friendly and robust. As an example, experiments will be reported in which we have studied the aggregation of the polypeptide associated with type 2 diabetes and discovered a structural intermediate that appears to explain the lack of diabetes in many species, such as rats and dogs.



Martin Zanni is the Meloche-Bascom Professor of Chemistry at the University of Wisconsin-Madison. He is an expert in femtosecond 2D spectroscopies and has helped pioneer the development of 2D IR spectroscopy and its application to protein structures and dynamics. He also studies semiconducting carbon nanotubes and other topics in material science using 2D White-Light spectroscopy, another new 2D technique. He has received many recognitions for his work, including the International Raymond and Beverly Sackler Prize in the Physical Sciences and the National Academy of Sciences Research Initiatives Award.

## Femtosecond Vibrational Spectroscopy of Simple and Complex Systems

Tahei Tahara<sup>1,2</sup>

<sup>1</sup>Molecular Spectroscopy Laboratory, RIKEN, 2-1 Hirosawa, Wako, Saitama 351-0198, Japan

<sup>2</sup>Ultrafast Spectroscopy Research Team, RIKEN Center for Advanced Photonics (RAP),  
2-1 Hirosawa, Wako, Saitama 351-0198, Japan

Keywords: femtosecond, time-resolved, Raman, photochemistry, photoreceptor protein

Raman spectroscopy is one of the most important optical spectroscopies and has been extensively utilized in a variety of fields of science and technology. In ordinary Raman spectroscopy, we measure energetically-shifted inelastic light scattering, and the energy shift from the excitation light provides information about the vibrational energy of the molecule. On the other hand, by using an ultrashort optical pulse that has a duration shorter than the vibrational period, we can induce coherent nuclear motion of the molecule by the impulsive Raman process and observe Raman-active vibrations directly in the time domain [1]. This way of observing molecular vibrations is called time-domain Raman spectroscopy. In principle, the information obtained by time-domain Raman spectroscopy is equivalent to that obtained by the ordinary frequency-domain Raman spectroscopy. However, because time-domain Raman spectroscopy is performed using only femtosecond pulses, we can trace the temporal change of the Raman spectrum with a femtosecond accuracy by combining it with a femtosecond pump pulse that excites the sample to start chemical reactions.

For investigating ultrafast dynamics by Raman spectroscopy, we developed time-resolved impulsive stimulated Raman spectroscopy (TR-ISRS) and demonstrated its high potential by applying it to simple molecules in solution [2, 3]. In this method,

we use three femtosecond pulses: The first pulse (P1) photoexcites molecules to start chemical reactions. After a certain delay time ( $\Delta T$ ), the second pulse (P2) is irradiated to induce coherent nuclear wavepacket motion in the transient species, and the third pulse (P3) measures the wavepacket motion through the oscillation of the transient absorption and/or stimulated emission. The Fourier transform of the observed oscillation corresponds to the time-resolved Raman spectrum at the time delay at  $\Delta T$ . Because we use only femtosecond pulses in the TR-ISRS measurements, we can change the delay time with a femtosecond accuracy. Therefore, we can trace the temporal change of the sample through the evolution of femtosecond time-resolved Raman spectra. Using sub-7-fs pulses for the ISRS measurement, we are now able to obtain time-resolved Raman spectra of the transient in the all the fundamental frequency region from terahertz to over  $3000\text{ cm}^{-1}$  by this time-domain approach.

In this presentation, we report on our recent TR-ISRS studies for simple and complex molecular systems, in particular, the study on a photoreceptor protein, photoactive yellow protein (PYP). PYP is a water-soluble, phototrophic bacterium, which was discovered in a halophilic purple phototrophic bacterium, *Halorhodospira halophila*. PYP is considered to function as a blue-light photoreceptor for negative phototactic response of this organism. The

function of PYP is realized by a photocycle, which is triggered by the photo-induced trans-to-cis isomerization of the chromophore, p-coumaric acid (pCA). The isomerization reaction has been considered to occur on the femto-to-picosecond time scale, and it gives rise to the formation of the first ground-state intermediate called the  $I_0$  state. We excited PYP with 450 nm (P1), and carried out TR-ISRS measurements with broadband 500-700 nm sub-7-fs pulses (P2 and P3) (Fig. 1). The P2 and P3 pulses are in resonance with the stimulated emission of the first excited  $pG^*$  state as well as the transient absorption of the first ground-state intermediate,  $I_0$ . The obtained time-resolved

Raman spectra indicated that the chromophore (p-coumaric acid) retains a trans-configuration in the  $pG^*$  state while the surrounding hydrogen-bonding structure changes in a few hundred femtoseconds after photoexcitation. Time-resolved Raman spectra of the  $I_0$  state have also been measured with very high S/N. The comparison between the obtained Raman spectrum and DFT calculation indicates that the chromophore in the  $I_0$  state has a highly distorted cis-form. This study clearly demonstrate that TR-ISRS is highly capable of clarifying the ultrafast structural change of the complex systems such as photoreceptor proteins.

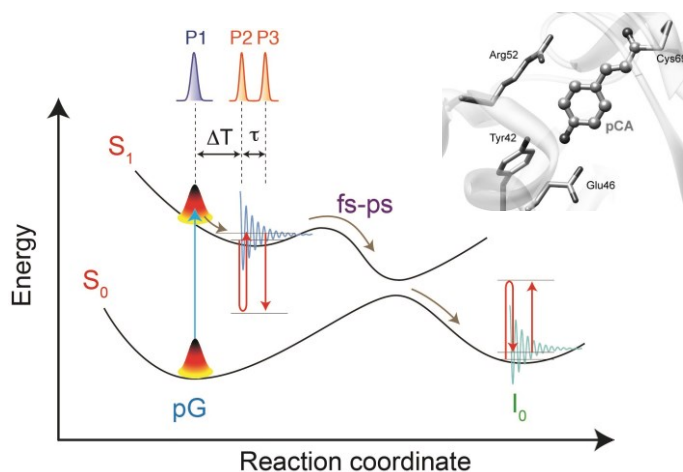


Figure 1. Experimental scheme of TR-ISRS for PYP.

<sup>1</sup> For example, Matsuo S., Tahara, T. (1997), *Chem. Phys. Lett.*, 264, 636-642.

<sup>2</sup> Fujiyoshi, S., Takeuchi, S., Tahara, T. (2003), *J. Phys. Chem. A*, 107, 494-500.

<sup>3</sup> Takeuchi, S., Ruhman, S., Tsuneda, T., Chiba, M., Taketsugu, T., Tahara, T. (2008), *Science*, 322, 1073-1077.

<sup>4</sup> Kuramochi, H., Takeuchi, S., Yonezawa, K., Kamikubo, H., Kataoka, M. Tahara, (2015), T. in preparation.

## From Esoteric to Commonplace: Technological Advances that have Turned 2D IR Spectroscopy into a Robust Research Tool

Martin T. Zanni

Department of Chemistry, University of Wisconsin-Madison, Madison WI 53706 USA

Keywords: femtosecond, 2D infrared, vibrational, spectroscopy

The field of femtosecond 2D IR spectroscopy is at a turning point, both intellectually and technologically. Researchers in the field now understand the nuances behind the technique. We now know how to interpret 2D lineshapes, the intensities of cross peaks, and the polarization dependence of the spectra. From the spectra, we can now reliably obtain dynamical parameters, bond angles, coupling strengths, and many other structural constraints. In parallel to the interpretation have been developments in quantitatively simulating 2D IR spectra. Molecular dynamics simulations of proteins can now be routinely converted to very accurate 2D IR spectra. Technological advances have improved the signal strengths, accuracy, and ease of which 2D IR spectra can now be collected. And the range of applications is now very broad, encompassing chemical reactions, electron transfer, peptide and protein structures, materials research, the energy sciences and more. As a result, the field of 2D IR spectroscopy is pivoting from that of an untested and poorly understood technique to a versatile and widely applied research tool.

This talk will cover recent technological advances that have made 2D IR spectroscopy as easy to implement as common transient absorption spectroscopy.<sup>1</sup> And, having explained this technology, a scientific example will be given in which we have uncovered an explanation for why some species, like humans and cats, develop

type 2 diabetes while other species, like rats and dogs, do not.<sup>2</sup>

Regarding the technology, I will explain how a pump-probe spectrometer can be converted into a 2D IR spectrometer by adding a mid-infrared pulse shaper. Prior to our work, the most common place design for a 2D IR spectrometer has 4 overlapping laser beams, which made experiments extremely difficult. Our pulse shaper approach enables very accurate spectra to be collected very rapidly. It also enables pulse sequences to be generated that were difficult or impossible to make previously. For example, the phases of the pulses can now be rotated in order to subtract the background without chopping the beam and decreasing the repetition rate. Most importantly, it is now a 2 beam experiment with an easily measured signal.

In a similar manner, sum-frequency generation (SFG) spectrometers can also be converted into 2D SFG spectrometers by the addition of a mid-IR pulse shaper. 2D SFG spectra collected in this manner will be shown briefly.

We have been using our pulse shaping 2D IR spectroscopy to study the aggregation of the human islet amyloid polypeptide (hIAPP or amylin) that is associated with type 2 diabetes. Not all mammals contract type 2 diabetes even though all species contain a very similar peptide. 25 years ago it was postulated that the amino acids in the central region of peptide containing the FGAIL sequence in humans formed the beta-sheets that were the core of the amyloid

fibers. This hypothesis was based on many experiments showing that peptides with mutations in this region to amino acids that could not form beta-sheets did not aggregate. That hypothesis stood the test of time until the fiber structure was solved and the FGAIL region turned out to be a disordered loop instead.

Using 2D IR spectroscopy, we have monitored the formation of amyloid fibers made from hIAPP. We have used isotope labels to monitor individual residues during aggregation. The vibrational coupling between isotope labeled residues that form parallel beta-sheets is very strong and so have a characteristic frequency shift and cross peaks. From our experiments, we discovered that the FGAIL sequence adopts a parallel beta-sheet prior to rearranging into the structure of the fiber. This intermediate appears to explain many of the prior experiments and resolves the contradiction of the 25 year old hypothesis with the structure of the fibers.

This example is very apt for describing the technology of pulse shaping 2D IR spectroscopy, because the measurements are done at low protein concentrations, utilize phase cycling to remove background scatter, and must be acquired very quickly to monitor kinetics on-the-fly. Because it deals with aggregates and kinetics, it is unlikely that this information could be obtained by any other technique. It exemplifies the transition that 2D IR spectroscopy has undergone to become a sophisticated research tool for probing cutting-edge topics in the life sciences.

Acknowledgements: This work was funded in part by the NIH NIDDK 79895 and the NSF CHEM-1266422. Zanni is co-founder of PhaseTech Spectroscopy, Inc., which manufactures commercial 2D IR spectrometers.

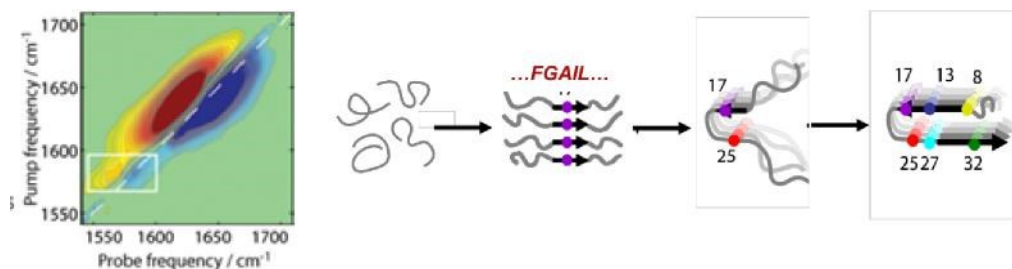


Figure 1. (left) 2D IR spectrum of the human islet amyloid polypeptide (hIAPP or amylin) showing an isotope labeled peak created by a beta-sheet secondary structure. (right) Schematic for the structural changes that hIAPP undergoes as it aggregates into amyloid fibers.

- 1 Middleton, C.T., Woys, A.M., Mukherjee, S. S., Zanni, M. T., “Residue-Specific Structural Kinetics of Proteins through the Union of Isotope Labeling, Mid-IR Pulse Shaping, and Coherent 2D IR Spectroscopy,” *Methods*, 52, 12 (2010).
- 2 Lauren E. Buchanan, Emily B. Dunkelberger, Huang Q. Tran, Pin-Nan Cheng, Chi-Cheng Chiu, Ping Cao, Daniel P. Raleigh, Juan J. de Pablo, James S. Nowick, Martin T. Zanni, “Mechanism of IAPP amyloid fibril formation involves an intermediate with a transient  $\beta$ -sheet,” *PNAS*, 110, 19285 (2013).

## Friday Invited

Friday, 10:40 - 12:00  
Chair: Jim de Haseth

HS1

10:40  
FR101

### Investigating the Binding of Metal Ion to Peptides and Inhibitors to Proteins Using Two-dimensional Infrared Spectroscopy

Julia Davies, Hugh Sowley, Keith Willison, David Klug

A variant of two-dimensional infrared (2DIR) spectroscopy has been used to investigate several biological systems of interest. The first is the chelation of zinc ions to histidine residues in the amyloid beta peptide, which is of relevance to the formation of senile plaques in Alzheimer's Disease. The second system is the binding of an inhibitor to the tyrosine kinase domain of a fibroblast growth factor receptor, FGFR1, which is of therapeutic significance for a number of growth disorders and cancers.

11:00  
FR102-inv

### High Resolution FTIR Tomographic Imaging of Single Cells

Kathleen Gough, Catherine Findlay

Tomographic imaging of single cells is achievable with a thermal source FTIR microscope. Diffraction-limited spatial resolution ( $\sim 1.1 \mu\text{m}$  pixel edge) with focal plane array detection enables rapid 2D imaging, comparable to the best synchrotron source FTIR microscopic imaging capability. Our new tomography accessory allows full positioning, alignment and focussing of any microsample. Automated rotation facilitates collection of projections at sufficient non-redundant angles to create the 3D reconstruction by back-projection of infrared images using modified CT and voxelated display algorithms (Matlab).

11:20  
FR103-inv

### A Mid-Infrared On-Chip Sensor Array Based on Bi-functional Quantum Cascade Structures and Plasmonics

Gottfried Strasser, Daniela Ristanic, Benedict Schwarz, Peter Reininger, Hermann Detz, Aaron M. Andrews, Tobias Zeerbauer, Donald MacFarland, Werner Schrenk

Quantum cascade lasers have proven to be powerful and compact devices for infrared spectroscopy. By the use of a bi-functional quantum cascade structure material for the generation and detection of light the realization of mid infrared on-chip sensors is possible. A specially designed intersubband material is working as QC laser for a given bias voltage and as a QC detector without any external bias. This concept allows liquid sensing at room temperature with a monolithically integrated sensor by a QC laser, a dielectrically loaded surface plasmon polariton waveguide as interaction section of the infrared light with the liquid, and a QC detector. Using DFB lasers allow the realization of a sensor array.

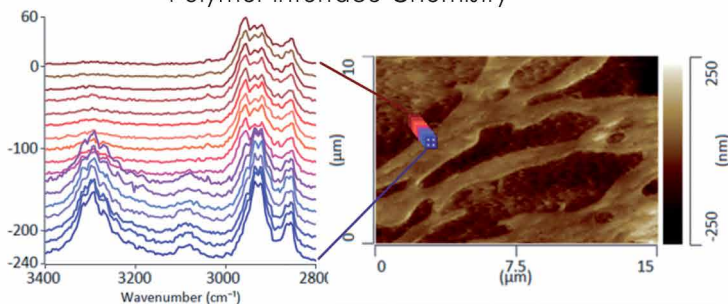
11:40  
FR104-inv

### Imaging Molecular Structure of Plant Cells by Confocal Raman Microscopy

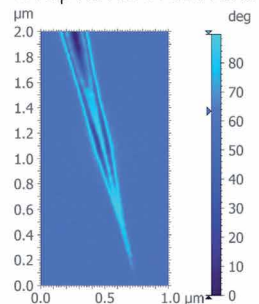
Notburga Gierlinger

During the last years Confocal Raman microscopy evolved as a powerful method to get insights into chemistry and structure of plant cells and cell walls with a spatial resolution of around 300 nm. Two-dimensional spectral maps can be acquired of selected areas and Raman images calculated by integrating the intensity of characteristic spectral bands or by using multivariate data analysis methods. This enables direct visualization of changes in the molecular structure and analyzing the spectra laying behind the chemical images reveals detailed insights into cell wall chemistry and structure.

Polymer Interface Chemistry



Graphene Plasmons



**AFM-IR**

Proven, easy to use IR spectroscopy  
(model free, reference-free)



**s-SNOM**

Nanoscale optical constants

Protein Secondary Structure

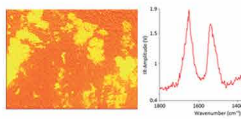
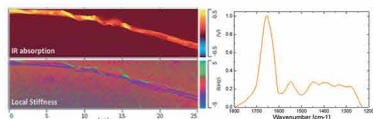
Sub-cellular Composition

Monolayer Spectroscopy

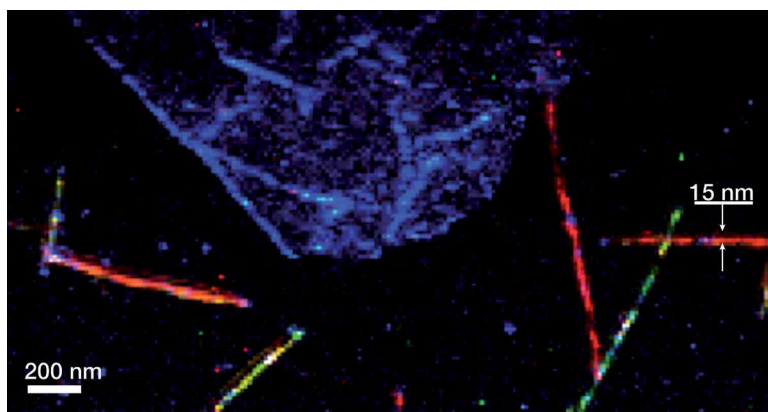
Semiconductors



**nanoIR2-s**



**Can Your Raman Do This?**



**High Speed &  
High Resolution  
Label-free  
Chemical Imaging**

**NanoRaman  
Made Easy!**



Titration



Ion Chromatography



Electrochemistry



Spectroscopy



Laboratory



Process

## Your partner for chemical analysis

Metrohm is a leading manufacturer of high-precision instruments for chemical analysis.

We offer a complete line of analytical laboratory and process systems for titration, ion chromatography, spectroscopy, and electrochemistry. [metrohm.com](http://metrohm.com)



Excellence in Science

Particle Size Analysis Impact Universal Hardness

High-Speed Video Camera Material Testing & Inspection Fatigue

FTIR NIR Fluorescence Energy Dispersive X-ray Fluorescence/EDX

AAS / Atomic Absorption Spectroscopy

UV-VIS Protein Sequencing ICP-OES Data Management & Software

Bio Pharmaceutical Life Sciences Electrophoresis LabSolutions

Total Organic Carbon Sum Parameter Laboratory Analyzers Gas Chromatography

Sum Parameter Process Analyzers Comprehensive GCxGC GCMS

Online Sample Preparation TOX.I.S. UHPLC iPad-Control UFLC MALDI

Method Scouting UFMS Comprehensive LCxLC Compact HPLC

Liquid Chromatography LCMS

Mass Spectrometry

[www.shimadzu.eu](http://www.shimadzu.eu)

## Booth P1



WITec is the leading manufacturer of confocal and scanning-probe microscopes for outstanding Raman, Atomic Force (AFM), and Scanning Near-Field Optical Microscopy (SNOM). From the company's founding in 1997, WITec has been distinguished by its innovative product portfolio and a microscope design that enables combinations of the various imaging techniques within one system. An exemplar of the company's breakthrough development is the world's first integrated Raman-AFM microscope. To this day, WITec's confocal microscopes are unrivaled in sensitivity, resolution and imaging capabilities. Significant innovation awards document WITec's enduring success and innovative strength.

## Booth P2



Renishaw's inVia confocal Raman microscope Study the widest range of samples, using the broadest range of Raman imaging techniques, with Renishaw's inVia confocal Raman microscope. The addition of transmission Raman to Renishaw's unique suite of complementary imaging options makes it easy to identify and characterise the chemistry and structure of materials. Use these options to study both large and small features simultaneously and produce high definition 2D and 3D chemical images.

## Booth P3



**Bruker Nano Surfaces**  
AFM-Based IR Nanocharacterization System: Providing highest resolution nanochemical and properties mapping  
Bruker's Inspire™ delivers, for the first time, highest-resolution nanoscale chemical and property mapping combining FTIR with uncompromised Atomic Force Microscope (AFM) performance. The integrated, self-optimizing system acquires nanoscale infrared absorption and reflection maps at regular AFM imaging speeds, without added complexity for the user. Taking full advantage of Bruker's exclusive PeakForce Tapping® technology, Inspire's new approach to infrared scattering scanning near-field optical microscopy (sSNOM) extends its capability to nanoscale chemical mapping of a wide variety of samples. The new technique, PeakForce IR™ also simultaneously maps nanomechanical properties, surface potential and 3D surface topography providing the full combined set of information at the same time.

Bruker Nano Surfaces additionally have a range of AFM systems that simultaneously deliver co-localised and Tip Enhanced Raman Spectroscopy (TERS). Bruker is the only major AFM manufacturer with a state-of-the-art probes nanofabrication facility. Bruker provides our users with world-wide, application specific customer support and is uniquely positioned to deliver the equipment, guidance, and support for all their nanoscale research needs.

## Booth P3



**Bruker Optics**  
Bruker Optics, part of the Bruker Corporation (NASDAQ:BRKR) is one of the world's leading manufacturer and worldwide supplier of Fourier Transform Infrared, Near Infrared and Raman spectrometers.

Bruker entered the field of FT-IR spectroscopy in 1974. The early instruments set new standards in research FT-IR with evacuable optics, high resolution and automatic range change. Since then, the product line has been continuously expanding with instruments suitable for both analytical and research applications with exceptional performance characteristics.

Today, Bruker Optics offers complete technical solutions for various markets which cover a broad range of applications in all fields of research and development as well as industrial production processes for the purpose of ensuring quality and process reliability.

Bruker Optics has a R&D and manufacturing center in Ettlingen, Germany, technical support centers and sales offices throughout Europe, North and South America, Asia, India, Middle East and Africa.

## Booth G3



From cutting edge scientific research to routine surface investigations, NT-MDT has a unique portfolio of scanning probe microscopes. Our application-focused instruments provide you with a full range of capabilities in AFM-Raman, high-resolution, multi-frequency measurements, and AFM based nanomechanics. NT-MDT has a specialized unique high-performance solution for your research needs.

## Booth G4



A Thermo Fisher Scientific Brand

Thermo Fisher Scientific is the world leader in serving science, with revenues of \$17 billion and approx. 50,000 employees in 50 countries. Our mission is to enable our customers to make the world healthier, cleaner and safer. We accelerate research from pharmaceutical formulation and life sciences to semiconductor manufacturing or geology with our innovative molecular spectroscopy solutions. From NIR, FT-IR and Fluorescence, to Raman and UV-Vis, we deliver a full spectrum of answers with instruments and user-friendly software - in real-time and at reduced costs due to autofocus and automatic feature identification. For more information, please visit [www.thermoscientific.com/spectroscopy](http://www.thermoscientific.com/spectroscopy).

## Booth G5



Excellence in Science

Shimadzu as a worldwide leading manufacturer of analytical instrumentation provides essential tools for quality control of consumer goods and articles of daily use, in health care as well as in all areas of environmental and consumer protection. Since 140 years, Shimadzu has been at the service of science ensuring precise, reliable diagnoses and analyses in food, chemistry, pharmacy and medicine. Shimadzu's innovative solutions in field of atomic- and molecular spectroscopy, chromatography, mass spectrometry and material testing ensure the highest level of analysis. <http://www.shimadzu.eu/analytics>

## Booth G6



Metrohm is a leading manufacturer of high-precision instruments for chemical analysis. We offer a complete line of analytical laboratory and process systems for titration, ion chromatography, spectroscopy, and electrochemistry. From the beginning, our sales engineers guide you through the instrument purchasing process. Together with our team of application chemists we create unique solutions for your laboratory needs. From installation to routine preventative maintenance, our global team of certified service professionals ensures ongoing performance and reliability of your Metrohm instrument. Our local presence, with offices or subsidiaries in over 120 countries, makes Metrohm your neighbor.

## Booth G7



HORIBA Scientific is a worldwide leader in development and production of analytical measurement equipment for research, laboratories, and quality control. We offer instrumentation for Fluorescence- and Raman-Spectroscopy and Ellipsometry, as well as components for optical spectroscopy including OEM applications. In addition, measurement techniques like ICP- and GD-OES, Particle analysis, sulfur-in-oil-Analysis and methods for the determination of water quality and SPRi (surface plasmon resonance imaging) belong to our expertise. These instruments can be used not only for macroscopic analysis, but also for micro-measuring techniques - often in a non-destructive manner, which is a major advantage over many other analytical methods.

## Booth G8



Agilent is a leader in life sciences, diagnostics and applied chemical markets. The company provides laboratories worldwide with instruments, services, consumables, applications and expertise, enabling customers to gain the insights they seek. Agilent's expertise and trusted collaboration give them the highest confidence in our solutions. To learn more on Agilent: [www.agilent.com/chem](http://www.agilent.com/chem) Discover our Molecular Spectroscopy Portfolio: [www.agilent.com/chem/molecularspec](http://www.agilent.com/chem/molecularspec).

Booth G9



Kaiser Optical Systems, an Endress+Hauser company, is recognized as a world leader in the field of Raman for its Raman analyzers, phase-optimized Raman probes, and components for spectroscopy. Kaiser's Raman products can be found in Research, Analytical, and Process settings including R&D, Lab, and Manufacturing, and are used for analysis, (in-situ, at-line, & off-line), monitoring, and control.

Raman fields benefitting from Kaiser's products include gas-phase, ROA, standoff, transmission, in situ and process Raman, deep ocean exploration, and space chemistry including GeoRaman. Application areas include biopharmaceutical, biotech, forensics, hydrocarbons, nanotechnology, olefins, petrochemical, pharmaceutical, polymers, semiconductors, and specialty chemical.

Booth G10



We are the nanoscale analysis company. Our tools reveal hidden chemical and mechanical characteristics of materials through spectroscopy and thermal analysis at nanometer scales. With a researcher's productivity always in mind, we deliver integrated hardware and software solutions that clear the path to your next discovery. Infrared spectroscopy, thermal and mechanical analysis combined add a special dimension to AFM imaging.

Our product platforms include the nanoIR2-s; nanoIR2; afm+ and nanoTA2

Booth S1



Thorlabs (www.thorlabs.com), a vertically integrated photonics products manufacturer, was founded in 1989 to serve the laser and electro-optics research market. As that market has spawned a multitude of technical innovations, Thorlabs has extended its core competencies in an effort to play an ever increasing role serving the Photonics Industry at the research end, as well as the industrial, life science, medical, and defense segments. The organization's highly integrated and diverse manufacturing assets include semiconductor fabrication of Fabry-Perot, DFB, and MEMS-VCSEL lasers, fiber towers for drawing specialty glass optical fibers (silica, fluoride, rare earth doped, and microstructured), MBE/MOCVD crystal growth, extensive glass and metal fabrication facilities, advanced thin film deposition capabilities, and optomechanical and optoelectronic shops.

Booth S2



Die Soliton Laser und Messtechnik GmbH ist ein 1990 in München gegründetes, mittelständisches Unternehmen, welches sich auf den Vertrieb und die Entwicklung von Hightech Produkten aus dem Laserbereich spezialisiert hat. Unsere Produktpalette umfasst neben Laserquellen auch analytische Instrumente, welche für die verschiedensten Messaufgaben zum Einsatz kommen. So gehören diverse Spektrometer ebenso zu unserem Portfolio, wie Partikelmessgeräte auf Laserbasis oder 3D Mikroskope.

Wir sind auf allen wichtigen Messen der jeweiligen Branchen vertreten und sind kontinuierlich dabei unser erfahrenes Team zu erweitern.

Seit 2008 ist unser Team nach ISO 9001 zertifiziert.

Booth S3



www.mgopticalsolutions.com

Daylight Solutions' molecular detection and imaging products consist primarily of lasers, sensors, and imaging systems, all of which leverage the company's mid-infrared, quantum cascade laser (QCL) technology. This core technology provides a versatile platform from which new products are developed. Spero™, the world's first laser-based infrared microscope will be showcased at ICAVS 8. Daylight Solutions will be exhibiting jointly with MGO Optical Solutions, who provide excellent local sales and technical support for Daylight Solutions products in Austria, Germany, and Switzerland. Established in 2007, MGO Optical Solutions provides a unique portfolio of high quality products dedicated to mid-infrared laser spectroscopy and hyperspectral imaging.

## Booth S4



Princeton Instruments designs and manufactures high-performance CCD, ICCD, EMCCD, emICCD, and InGaAs cameras; spectrographs; and optics-based solutions for the scientific research, industrial imaging, and OEM communities. We take pride in partnering with our customers to solve their most challenging problems in unique, innovative ways. We will be featuring our award-winning IsoPlane family of aberration-corrected spectrographs at ICAVS 2015. These spectrographs are currently used in a variety of applications including micro-spectroscopy, Raman scattering, LIBS, biomedical imaging, and many more. Princeton Instruments is a registered ISO 9001:2008 company. Please visit [www.princetoninstruments.com](http://www.princetoninstruments.com) for more information.

## Booth S5



B&W Tek is an advanced instrumentation company that delivers lab quality Raman spectroscopy solutions through user-friendly mobile platforms. B&W Tek provides solutions for the pharmaceutical, biomedical, physical, chemical, security and research communities. B&W Tek is the worldwide leader in Raman spectrometer manufacturing with over 10,000 spectroscopy solutions delivered. Our complete line of high performance portable and handheld Raman spectrometers sets us apart with solutions for the classroom, lab and field. Our extensive knowledge and cutting edge technology has allowed us to focus on solution-oriented products that are designed for non-specialists and provide easy, rapid measurements in a matter of minutes.

## Booth S6



TimeGate Instruments was founded in spring 2014. Despite its young age it enjoys strong scientific background. TimeGated® technology is based on years of research in several Finnish research institutes and it is utilizing the patent pending technologies from that work.

We provide TimeGated® Raman spectrometers with a picosecond laser excitation source and new, time resolved single photon counting array detector solution. This is a totally new type of Raman spectrometer which achieves Real Fluorescence Rejection and Time Resolved Fluorescence Data. The system gives valuable new information in several different application fields.

## Booth S7



Neaspec is dedicated to delivering innovative solutions for nanoscale optical imaging & spectroscopy for researchers in industry and academic institutions.

We are proud to introduce NeaSNOM - the ultimate nanoanalytic microscopy platform for materials research and photonics. NeaSNOM enables nanoscale infrared imaging & spectroscopy at about 1000-times better spatial resolution of 10 nm when compared to conventional infrared spectroscopy. It even allows to utilize the visible & terahertz spectral region at the same high resolution enabling additional material characterization applications.

## Booth S8



Molecular Vista manufactures VistaScope featuring photo-induced force microscopy (PiFM), which concurrently measures sample's topography and polarizability with sub 10 nm spatial resolution. PiFM is a near-field excitation and near-field detection technique, which completely removes far-field background signal. When coupled with a tunable (CW or pulsed) laser, PiFM generates superb spectral images associated with molecules' electronic, plasmonic, and vibrational resonances. When coupled with ultrafast lasers, time-resolved pump-probe PiFM enables studies of molecular dynamics with ultrashort time scale and nanoscale spatial resolution. VistaScope's flexible optical platform also supports other concurrent detector based tip-enhanced near-field techniques such as TERS and scattering SNOM.

## Booth S9



Newport Corporation is a leading global supplier of advanced technology products and solutions for Scientific Research, Life & Health Science, Aerospace & Defense, Photovoltaics, Industrial Manufacturing, Semiconductors, and Micro-electronics markets. Newport has over 40 years of industry knowledge and expertise across a broad range of technologies allowing the company to continually deliver innovative products in the areas lasers, photonics instrumentation, sub-micron positioning systems, vibration isolation, optical components and subsystems and precision automation to enhance the capabilities and productivity of its customers' manufacturing, engineering and research applications.

## Booth S10



Enhanced Spectrometry, Inc. develops portable Raman and/or luminescent spectrometry solutions for advanced substances control, quality inspection, real-time testing and innovative brand protection based on proprietary technology of substances detection, recognition and coding of information.

We sell EnSpectr® instruments, accessories, professional software and services for identification of illicit substances, inspection of raw materials, consumer goods, pharmaceutical supplies, gemstones and minerals, water and beverages. EnSpectr® spectrometers perform highly efficient real-time analysis providing hyper-sensitive methods of substance detection.

We are proud to offer EnSpectr® powerful and price-efficient spectrometry solutions worldwide.

[www.enspectr.com](http://www.enspectr.com)

## Booth S11



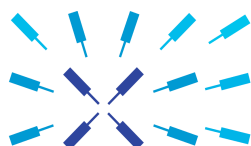
Bio-Rad Laboratories specializes in Spectroscopy Databases & Software Solutions (IR, Raman, NMR, MS, UV-Vis). They are a leading producer of spectral databases with over 1.4 million spectra including Sadtler™ Data. Their KnowItAll® Spectroscopy Software offers a range of solutions including: spectral search, spectral data management, spectral identification, quality control, mixture analysis, polymer analysis, chemometrics, etc. This unique combination of spectral software with a vast collection high-quality spectral reference data gives KnowItAll users a distinct advantage when it comes to spectral analysis.

## Booth S12



BioTools is pleased to announce disruptive new products: 1) the first portable Raman microscope – Mobile  $\mu$ -RAMAN - offering resolution and specifications of a bench-top Raman system with portability. 2) MANTIS – a DualPEM VCD accessory for Thermo FT-IR; 3) RAMAN spectrometer that provides measurements of four forms of ROA, Raman microscopy / imaging and AFM. With these introductions, BioTools continues tradition developing innovative and unique vibrational spectroscopy products. BioTools was the first to introduce VCD & ROA– the ChiralIR-2X™ & ChiralRAMAN-2X™. Our PROTA-3S for measurements and analysis of FT-IR spectra of biologics is the number one choice of bioscientists. We also offer software for calculations, databases and unique cells and accessories.

## Booth S13



Zurich  
Instruments

Zurich Instruments makes lock-in amplifiers, phase-locked loops, and impedance spectroscopes that have revolutionized instrumentation in the high-frequency (HF) and ultra-high-frequency (UHF) ranges by combining frequency-domain tools and time-domain tools within each product. This reduces the complexity of laboratory setups, removes sources of problems and provides new measurement approaches that support the progress of research.

## Booth S14



Ondax, Inc. is the market leader and largest volume manufacturer of high-performance Volume Holographic Gratings (VHG/VBGs), Wavelength-stabilized Laser Sources, and high-performance, THz-Raman® Low-frequency (Low-wavenumber) Raman Spectroscopy Systems for a wide range of industrial, medical, defense, and scientific applications. THz-Raman® extends the range of the standard Raman “chemical fingerprint” spectra to include low-frequency/THz-regime spectra that reveal important structural information about compounds, enabling fast, real-time monitoring and analysis of polymorphs, cocrystals, amorphous/crystalline transitions, and other molecular structural characteristics. This new “structural fingerprint” provides for in-situ monitoring of structure, improved forensic analysis and determination of synthetic pathways.

## Booth S15



TOPTICA Photonics AG develops, manufactures, services and distributes technology-leading diode and fiber lasers and laser systems for scientific and industrial applications. Sales and service is offered worldwide through TOPTICA Germany and its subsidiary TOPTICA USA, as well as through 14 distributors. A key point of the company philosophy is the close cooperation between development and research to meet our customers’ demanding requirements for sophisticated customized system solutions and their subsequent commercialization.

## Booth S16



LASER COMPONENTS is specialized in the development, manufacture, and sale of components and services for the laser and opto-electronics industries. In-house production includes products such as IR detectors, avalanche photodiodes, laser diodes, fiber optics, laser optics, and photon counting modules.

## Booth S17



NKT Photonics provides new standards for fiber based lasers and light sources. The product portfolio includes photonic crystal fibers (PCF), Bragg grating based Koheras DFB fiber lasers and SuperK supercontinuum white light laser sources including accessories such as filter boxes and delivery fibers to cover the wavelength range from 260 to 4500 nm.

## Booth S18



Fibertech Optica (FTO) is a leader in the manufacture of specialty fiber optic solutions. Offering RAMAN PROBES, micro-lens assemblies, round to line converters, reflectance probes, v-groove arrays, fiber bundles, assemblies, low FRD cables,, and high power laser cables with multimode, singlemode and borosilicate fibers. Fiber options available for applications with wavelengths from the deep UV to the MIR, with NA's from 0.12 to 0.66. FTO also produces fiber coupled LED multi-emitter light sources and vacuum feedthroughs. From prototype through production quantities, FTO supports applications in aerospace, military, astronomy, spectroscopy, research and academics.

Booth S19



Snowy Range Instruments designs and manufactures spectroscopic instrumentation for innovative applications. Our experienced engineering and scientific staff specializes in Raman spectroscopy, and fluorescence spectroscopic instrumentation and applications. Snowy Range Instruments (SnRI) uses a wide range of optical, electrical, mechanical, and software methods to solve difficult problems. Creative, cost-effective solutions are made possible by SnRI's experience with diverse optical technologies, as well as complex applications. Our research grade instrumentation is available in both handheld and bench top systems.

Booth S20



art photonics - founded in Berlin in 1998 – proudly presents:  
New FlexiSpec® Fiber Optic Probes and FlexiSpec® Fiber Probe Couplers - for effective coupling with FTIR-spectrometers enabling process spectroscopy in any spectral range (- 18µm) for industry and lab.  
The brand new FlexiSens® line premieres spectral fiber Moisture Sensor (MoiSens) - the 1st demo of fiber LED-sensor for moisture control in media with our robust fiber probes in diffuse reflection or transmission mode.  
MoiSens enables portable and low cost process-spectroscopy control in pharma, food, building, paper and other industries with remote data analysis from specific IP-address of each sensor.

Booth S21



S.T.Japan is world wide one of the leading providers of spectral libraries. With more than 140.000 ATR-FTIR, Transmission, Raman and NIR spectra S.T.Japan offers more than 120 dedicated spectral libraries meeting a wide range of analytical application needs.  
Additionally S.T. Japan offers innovative and high-quality accessories for FTIR-Spectroscopy and Microanalysis such as sample holders, Diamond knives, and other sample prep tools.

Booth S21



LabCognition provides powerful software solutions and excellent services to manage and evaluate analytical and spectroscopic data and related information. With more than ten years of successful spectroscopy software development, our products cover the fields of chemistry, biochemistry and pharmacology by combining mathematical and scientific approaches with computer science.  
We develop flexible, high quality standard products or custom solutions to increase the efficiency of our customers in everyday work.  
Our products include the panorama spectroscopy software platform; irAnalyze and RAMalyze for spectrum interpretation, and SciGear Scientific Information System for web-based information management and spectral data analysis.

Booth S22



Founded in 2010, Tornado Spectral Systems is developing real-time optical process analyzers and imaging solutions using a portfolio of patents that includes Tornado's foundational and revolutionary High Throughput Virtual Slit (HTVS). The HTVS technology allows the best Raman analysis currently achievable anywhere with innovation and a proprietary nanophotonics platform. TSS's new class of instruments - the HyperFlux PRO Raman series - can acquire chemical signatures of interrogated samples with the speed and accuracy required to perform many quality and safety measurements directly on the production line. To learn more about Tornado, please visit <http://www.tornado-spectral.com>.

## Booth S23



PIKE Technologies, Inc. is located in Madison, Wisconsin. Established in 1989, it is a primary source for spectroscopy accessories and applications worldwide. Products include attenuated total reflectance (ATR), diffuse reflectance, specular reflectance, integrating spheres, polarization, IR microscope, beam condensers, remote sensing, and transmission sampling accessories including gas cells. Many of these products are available with optional heating and automation for increased sampling speed and productivity.

PIKE also manufactures customized optics including mirrors, lenses, optical mounts, and IR microscope objectives. In addition to optical design and prototyping, PIKE offers metrology measurement services, diamond turning, optical thin-film coating, and spherical grinding and polishing.

## Booth S24



Innovative Photonic Solutions (IPS) is the leading manufacturer of high performance wavelength stabilized semiconductor lasers for use in Raman spectroscopy. IPS provides the Raman spectroscopy community with single and multi-mode lasers spanning the entire visible and NIR spectral range. Available packaging configurations range from component level (TO-56 & 14-Pin BF) to complete IEC/UL/CE certified turn-key laser systems. IPS also provides high throughput Raman probes with the excitation laser integrated into the probe, improving efficacy while reducing overall system cost and complexity. Additionally, IPS has extensive experience developing custom systems for a variety of sensing applications.

## Booth S25



Well-known for the high quality of their products, PI is one of the leading players in the global market for precision positioning technology. PI has been developing and manufacturing standard and OEM products with piezo or motor drives for 40 years now. With four German factories and ten subsidiaries and sales offices abroad, the PI Group is represented internationally.

## Booth S26



Infrared Associates, Inc. is a manufacturer of InSb(1 $\mu$ m-5.5 $\mu$ m) and HgCdTe(1 $\mu$ m-25 $\mu$ m) single element detectors and Photoconductive HgCdTe multi element arrays, up to 128 elements! Cooling options include; Thermoelectric, Liquid Nitrogen and Closed Cycle Stirling Coolers! We have recently introduced a series of Room Temperature HgCdTe detectors with response to >6 $\mu$ m! In addition, matched preamplifiers are available as well as accessories including Thermoelectric Temperature Controllers, Power Supplies, Heat Sinks and Pumping Port Adaptors!

## Booth S27



QuantaRed Technologies is a high-tech spin-off company from TU Wien. It develops and distributes instruments for the analysis of liquids based on mid-IR quantum cascade lasers. QuantaRed Technologies has successfully established a new, environmentally friendly method for the determination of total petroleum hydrocarbons (TPH) in water, waste water and soil. The method comprises a liquid-liquid extraction of samples with cyclohexane and subsequent measurement of the extract with a dedicated oil-in-water analyzer (Eracheck) employing quantum cascade laser technology. This method enables trace analytics by infrared technology and has been established as an ASTM standard method (ASTM D7678-11).

Aamer, Khaled	TH501	116	Ashton, Lorna	MO605	27
Abart, Rainer	A104	56	Ashton, Lorna	A008	38
Abdou, Elias	A033	43	Assi, Sulaf	MO803	28
Abeysekara, Samen	B068	89	Assi, Sulaf	C035	133
Ackermann, Roland	C050	136	Assi, Sulaf	A089	54
Agarwal, Parag	C106	146	Assi, Sulaf	B109	98
Agarwal, Shweta	A023	41	Ataka, Kenichi	TU611-inv	75
Agrawal, Megha	TH514	124	Attia, Mohamed	A045	45
Ågren, Matilda	MO802	28	Augustin, Mary A.	C021	130
Agresti, Antonio	TU503	66	Avaldi, Lorenzo	A085	53
Ahlawat, Anju	TH508	120	Avelin, Anders	C037	133
Aichinger, Thomas	A123-pdp	54	Ayora-Cañada, Maria Jose	MO801-inv	28
Aidam, Rolf	TU812	76	Ayora-Cañada, Maria Jose	A058	48
Akiyama, Kotaro	TU501	66	Ayora-Cañada, Maria Jose	A059	48
Albensi, Benedict	MO110	29	Ayora-Cañada, Maria Jose	C014	129
Alcaráz, Mirta R.	C097	145	Babchenko, Oleg	B110	98
Alcaráz, Mirta R.	C099	145	Bache, Michael	TU512	74
Aleksa, Valdemaras	C060	138	Bachmann, Anne	TU809	72
Aleksa, Valdemaras	C072	140	Backus, Ellen	C047	135
Aleksandrova, Daria	A115	58	Bagnaninchi, Pierre	TH101	115
Alikin, Denis	A117	59	Bailey, Matthew	B010	79
Almaviva, Salvatore	B042	84	Baillet-Guffroy, Arlette	MO610	31
Alstrøm, Tommy	TU512	74	Baines, Fiona	TH810	122
Altug, Hatice	TH106	119	Bakeev, Katherine	A062	49
Alula, Melisew	B011	79	Baker, Matthew	TU813	76
Alvarado, Camille	TU613	75	Baker, Matthew	A016	40
Alves, Wagner	TH604	117	Balbekova, Anna	A121-pdp	39
Amenabar, Iban	MO104	25	Balbekova, Anna	MO105	25
Amthauer, Georg	C054	137	Balevičius, Vytautas	C060	138
Andou, Masahiro	A019	40	Balla, Andre	WE101-inv	105
Andre, Erwan	TH511	124	Balling Engelsen, Søren	B113	98
Andre, Erwan	B056	87	Banciu, Horia L.	B093	94
Andre, William	TU613	75	Banno, Motohiro	TH502	116
Andrews, Aaron Maxwell	FR103-inv	153	Bansal, C.	B027	82
Andrews, Aaron Maxwell	TU803	68	Bar-David, Yossi	TU114	73
Andrews, Aaron Maxwell	B003	77	Baranska, Malgorzata	A030	42
Andrey, Chikishev	C028	131	Baranska, Malgorzata	TU104	65
Andrzejak, Marcin	A015	40	Baranska, Malgorzata	A042	45
Antonio, Saverino	C085	143	Baranska, Malgorzata	TH611	125
Argov, Shmuel	MO612	35	Baranska, Malgorzata	A034	43
Ariese, Freek	C051	136	Baranska, Malgorzata	A032	43
Ariese, Freek	MO809	32	Baranska, Malgorzata	WE102	105
Ariizumi, Tohru	A088	53	Barbieri, Donato	A079	52
Arnold, Thomas	C069	139	Baricz, Andreea	B093	94
Arnone, David	MO109	29	Barker, Roger	TH613	125
Artac, Andreas	A104	56	Barone, Angela	WE804	108
Artemenko, Anna	A009	38	Barras, Alexandre	B060	88
Artemenko, Anna	A078	51	Barre, Matt	MO109	29
Artyushenko, Viacheslav	TH809	122	Barre, Matt	TU813	76
Artyushenko, Viacheslav	A041	44	Barszcz, Bolesaw	B080	92
Ascaso, Carmen	B117-pdp	96	Barton, Killian	A118	59
Asenbaum, Augustinus	B097	95	Basar, Gunay	A048	46
Ashton, Katherine	A016	40	Bastu, Ercan	A048	46

Bates, Susan	TH810	122	Boatwright, Mark	WE802	108
Batignani, Giovanni	TH606	121	Bocklitz, Thomas	A021	41
Batista de Carvalho, Ana	TH614	125	Bocklitz, Thomas	MO607	31
Batista de Carvalho, Luís	TH614	125	Bocklitz, Thomas	A046	45
Batista, Victor	TH505	116	Boduszek, Bogdan	C080	142
Bauer, Alexander	C094	144	Boduszek, Bogdan	C081	142
Bauer, Alexander	C095	144	Boehmler, Miriam	MO111	33
Bauer, Michael	A021	41	Bögözi, Timea	TU809	72
Bauer, Michael	A046	45	Bohr, Jakob	MO513	34
Baumruk, Vladimir	B085	93	Boisen, Anja	TU512	74
Baumruk, Vladimir	B086	93	Bolognesi, Paola	A085	53
Baumruk, Vladimir	C009	128	Bonnin, Estelle	TU613	75
Bavili, Nima	A048	46	Bonnist, Eleanor	TH810	122
Bazuin, C. Geraldine	C088	143	Bonoldi, Lucia	A079	52
Bazuin, C. Geraldine	TU507	70	Bornhöfft, Manuel	MO108	29
Beardall, John	MO806-inv	32	Borowski, Piotr	A015	40
Beattie, Aaron D.	B067	89	Borozenko, Kateryna	C088	143
Bec, Julien	MO607	31	Boskovic, Dusan	TU801-inv	68
Bechkoff, Géraldine	B070	90	Botta, Raju	B027	82
Bechtel, Hans	MO103	25	Boubekeur, Bahia	A090	54
Bechtel, Hans	MO106-inv	29	Bouchet, Brigitte	TU613	75
Bechtel, Hans	A013	39	Bour, Petr	B058	87
Beckmann, Toni	C048	135	Bour, Petr	C010	128
Bednářová, Lucie	C009	128	Bour, Petr	WE603	107
Beleites, Claudia	A053	47	Bourotte, Jérémie	TU507	70
Belhaneche-Bensemra, Naima	A090	54	Bourson, Patrice	TH808	122
Belkin, Mikhail	MOPL2	20	Bovi, Daniele	TH602	117
Belkin, Mikhail	MO113	33	Brandán, Silvia	B055	87
Bell, Gavin	TU603	67	Brandl, Christian	TU504	66
Ben Altabef, A.	B115-pdp	95	Brandstetter, Markus	TH803	118
Benko, Aleksandra	TU604	67	Brandstetter, Markus	B002	77
Bent, Julian	C103-pdp	133	Brandstetter, Markus	C015	129
Berer, Thomas	TH803	118	Brandstetter, Markus	C016	129
Bernacki, Bruce	B102	96	Brandstetter, Markus	C097	145
Bernatová, Silva	TU105	65	Branko, Glamuzina	B033	82
Besli, Münir	A087	53	Bratoš Cetinić, Ana	MO810	32
Bhargava, Rohit	WE101-inv	105	Brauer, Carolyn	B102	96
Bianco, Stefano	B024	81	Brodbelt, Andrew	A016	40
Biedermann, P. Ulrich	TU106	69	Brolo, Alexandre	TH112	123
Bigini, Paolo	MO603	27	Bronner, Wolfgang	TU812	76
Bird, Benjamin	TU813	76	Brotin, Thierry	TU109	69
Bird, Benjamin	MO109	29	Brotin, Thierry	C083	142
Bismilla, Yusuf	TH807	122	Brückl, Hubert	TU504	66
Bismuto, Alfredo	TU804	68	Brun, Mickael	TU802	68
Bittner, Roland	A077	51	Buchet, Rene	B070	90
Blackburn, Jonathan	B011	79	Buckow, Roman	C021	130
Blake, Thomas	B102	96	Buczek, Elzbieta	A032	43
Blanch, Ewan	WE603	107	Budde, Janpeter	TH612	125
Blanch, Ewan	C005	127	Buffeteau, Thierry	TU109	69
Blanch, Ewan	A054	47	Buffeteau, Thierry	C083	142
Blaser, Stéphane	TU804	68	Bulgurcuoglu, Sibel	A048	46
Blazejczak, Agnieszka	A032	43	Bunaganic, Bohus	A037	44
Błażewicz, Marta	TU604	67	Buresch, Isabell	C030	132

Burgholzer, Peter.....	TH803.....	118	Chernavskaia, Olga.....	C045.....	135
Bürgi, Thomas.....	WE604.....	107	Chernev, Boril.....	TU504.....	66
Bürgi, Thomas.....	C004.....	127	Chernev, Boril.....	A003.....	37
Burgos, Pierre.....	C042.....	134	Chernyshev, Vladimir.....	TH509.....	120
Butschek, Lorenz.....	TU801-inv.....	68	Chiadò, Alessandro.....	B024.....	81
Buyru, Faruk.....	A048.....	46	Chiadò, Alessandro.....	TH110.....	119
Byrska-Fudali, Magorzata.....	A057.....	47	Chis, Mihaela.....	B092.....	94
Cainap, Calin.....	B092.....	94	Chiş, Vasile.....	B044.....	84
Caldwell, Joshua.....	WE502.....	106	Chiş, Vasile.....	B092.....	94
Camacho, Felipe.....	TH604.....	117	Chiş, Vasile.....	B033.....	82
Camatini, Marina.....	MO511.....	34	Chlopicki, Stefan.....	A030.....	42
Campbell, Colin.....	B009.....	78	Chlopicki, Stefan.....	A032.....	43
Campbell, Colin.....	TH101.....	115	Chlopicki, Stefan.....	A034.....	43
Camus, Victoria.....	B009.....	78	Chlopicki, Stefan.....	A042.....	45
Candeloro, Patrizio.....	MO613.....	35	Chlopicki, Stefan.....	WE102.....	105
Capozzi, Vito.....	A052.....	46	Cho, Minhaeng.....	TH512.....	124
Cappa, Federica.....	A122-pdp.....	48	Choi, Jun-Ho.....	TH512.....	124
Carmichael, Eugene.....	B041.....	84	Chou, Sin-Yi.....	TH103.....	115
Carneiro, Karina.....	MO112.....	33	Christensen, David A.....	B067.....	89
Carney, Paul Scott.....	MO102.....	25	Christensen, David A.....	B068.....	89
Carras, Mathieu.....	TU802.....	68	Chrobok, Łukasz.....	B077.....	91
Carrier, Stacey.....	TU112.....	73	Chun, Hye Jin.....	B096.....	95
Carriere, James.....	MO813.....	36	Chung, Hoeil.....	WE803.....	108
Carron, Keith.....	MO804.....	28	Chung, Hsu-Ming.....	A075.....	51
Carteret, Cedric.....	TH511.....	124	Chuvilin, Andrey.....	MO102.....	25
Carteret, Cedric.....	B056.....	87	Ciaccheri, Leonardo.....	C018.....	130
Casiraghi, Cinzia.....	WE501-inv.....	106	Cialla-May, Dana.....	B075.....	91
Castiglioni, Chiara.....	A092.....	54	Cialla-May, Dana.....	TH102.....	115
Castro, T. J.....	A065.....	49	Cialla-May, Dana.....	B088.....	93
Catalina, David.....	A029.....	42	Cicerone, Marcus.....	TH501.....	116
Cavalcante Freire, Paulo de Traso.....	A112.....	58	Cielecka-Piontek, Judyta.....	B079.....	91
Centintas, Eylem Can.....	C100.....	145	Cielecka-Piontek, Judyta.....	B080.....	92
Centrone, Andrea.....	MO101-inv.....	25	Cielecka-Piontek, Judyta.....	B081.....	92
Ceponkus, Justinas.....	C072.....	140	Cieślak-Boczula, Katarzyna.....	B103.....	96
Čermák, Jan.....	A009.....	38	Cifra, Michal.....	A073.....	50
Cetin, Arif.....	TH106.....	119	Cinque, Gianfelice.....	TH614.....	125
Cha, Myeong Geun.....	A070.....	50	Cîntă-Pânzaru, Simona.....	MO810.....	32
Cha, Myeong Geun.....	MO608.....	31	Cîntă-Pânzaru, Simona.....	B033.....	82
Champagne, Benoît.....	TU606.....	71	Cios, Franciszek.....	TU604.....	67
Chang, Hyejin.....	MO608.....	31	Ciupa, Aneta.....	C057.....	137
Chapron, David.....	TH808.....	122	Ciupa, Aneta.....	A110.....	57
Charwat-Pessler, Johann.....	A024.....	41	Clark, Charlotte.....	C092-pdp.....	141
Chase, Bruce.....	MO514.....	34	Clemens, Graeme.....	A016.....	40
Chase, Bruce.....	A076.....	51	Clemens, Graeme.....	TU813.....	76
Chatterjee, Sangam.....	C048.....	135	Cobos Picot, R. A.....	B115-pdp.....	95
Chavez, Pierre-François.....	B008.....	78	Coles, Benjamin.....	C042.....	134
Chazallon, Bertrand.....	A086.....	53	Coman, Cristina.....	A043.....	45
Chelibanov, Vladimir.....	B048.....	85	Constantin, Florin Lucian.....	B107.....	97
Chelibanov, Vladimir.....	B049.....	86	Constantino, Vera.....	MO604.....	27
Chen, Chi.....	B006.....	78	Contreras, C.....	B115-pdp.....	95
Chen, Hsuen-Li.....	TH103.....	115	Cornaton, Yann.....	B054.....	86
Chen, Li-Wei.....	A080.....	52	Correa-Gomez, Elena.....	A059.....	48
Chen, Yujing.....	C061.....	138	Costa, Sara.....	TU602.....	67

Coste, Ana .....	B073.....	90	Dendisova, Marcela .....	TH105.....	115
Coste, Ana .....	B074.....	91	Deng, Shibin .....	TH111.....	123
Cotter, Colin .....	C072.....	140	Denisova, Anna .....	TU110.....	69
Covert, Paul .....	TU107.....	69	Detz, Hermann .....	FR103-inv.....	153
Cozar, Bogdan I. ....	MO810.....	32	Detz, Hermann .....	TH812.....	126
Craig, Derek .....	A018.....	40	Detz, Hermann .....	TU803.....	68
Csanyi, Gabor .....	A042.....	45	Detz, Hermann .....	B003.....	77
Csilla, Müller .....	B033.....	82	Deval, Vipin .....	B052.....	86
Cuadros-Rodriguez, Luis .....	C014.....	129	Devarenne, Timothy P. ....	B096.....	95
Cuellar, Maryann .....	TH806.....	122	Devaux, Marie-Françoise .....	TU613.....	75
Cui, Li .....	B046.....	85	Dhital, Bharat .....	B037.....	85
Czamara, Krzysztof .....	A042.....	45	Di Bitteto, Arnaud .....	TH511.....	124
Czarnik-Matusewicz, Boguslawa .....	B094.....	94	Di Carlo, Aldo .....	TU503.....	66
Czarnik-Matusewicz, Boguslawa .....	B103.....	96	Di Fabrizio, Enzo .....	MO613.....	35
Dacanin, Ljubica .....	A100.....	56	Di Franco, Simone .....	MO613.....	35
Dadd, Antony .....	TH810.....	122	Di Paola, Eleonora .....	A079.....	52
Dahlquist, Erik .....	C037.....	133	Di Paolo, Lea .....	A079.....	52
Dahms, Tanya .....	A013.....	39	Diaconeasa, Zorita .....	A043.....	45
Dalen van, Gerard .....	A105.....	57	Diaz, S. B. ....	B115-pdp.....	95
Dalen van, Gerard .....	C017.....	129	Dieing, Thomas .....	MO811.....	36
Damaschke, Bernd .....	A114.....	58	Diekmann, Stephan .....	A035.....	43
Davidson, Claudia De Novaes .....	C029.....	132	Dillon, Eoghan .....	MO113.....	33
Davies, Andrew J. ....	C091.....	144	Dillon, Eoghan .....	MO505.....	26
Davies, Charles .....	A016.....	40	Dina, Nicoleta .....	B074.....	91
Davies, Gareth .....	MO809.....	32	Dina, Nicoleta E. ....	B093.....	94
Davies, Julia .....	FR101.....	153	Diomede, Luisa .....	MO603.....	27
Davydov, Anton .....	MO512.....	34	Dixon, Matthew .....	TH611.....	125
Dawson, Paul .....	B039.....	83	Dixon, Matthew W. A. ....	A055.....	47
Dawson, Simon .....	WE804.....	108	Dluhy, Richard .....	TU511.....	74
Dawson, Timothy .....	A016.....	40	Do, Le Duy .....	B070.....	90
de Avila, Jocasta .....	C008.....	128	Dochow, Sebastian .....	MO607.....	31
De Biasio, Martin .....	C074.....	140	Dochow, Sebastian .....	C045.....	135
De Biasio, Martin .....	TH804.....	118	Doctor, Alan .....	TH814.....	126
De Bleye, Charlotte .....	B008.....	78	Doherty, James .....	TH614.....	125
De La Pierre, Marco .....	B056.....	87	Doherty, Matthew .....	B039.....	83
de la Torre-Lopez, Maria Jose .....	MO801-inv.....	28	Domin, Helena .....	B014.....	79
de la Torre, Yolanda .....	A058.....	48	Domin, Helena .....	B017.....	80
de Oliveira, Thales V. A. G. ....	MO104.....	25	Dominguez-Vidal, Ana .....	A059.....	48
de Veij, Marlene .....	TH611.....	125	Dominguez-Vidal, Ana .....	C014.....	129
deBeer, Thomas .....	A091.....	54	Dominguez-Vidal, Ana .....	A058.....	48
Deckert-Gaudig, Tanja .....	TU101-inv.....	65	Dominguez-Vidal, Ana .....	MO801-inv.....	28
Deckert-Gaudig, Tanja .....	B007.....	78	Domonkos, Maria .....	B036.....	83
Deckert, Volker .....	TU111.....	73	Dong, Lei .....	TU814.....	76
Deckert, Volker .....	TH113.....	123	Dong, Zhenchao .....	TUPL1.....	60
Deckert, Volker .....	TU101-inv.....	65	dos Santos, Diego .....	TH112.....	123
Deckert, Volker .....	B007.....	78	Douplik, Alexandre .....	A051.....	46
Degtyareva, Olga .....	B076.....	91	Dovesi, Roberto .....	B056.....	87
Degtyareva, Olga .....	C044.....	135	Drapcho, David .....	B112.....	98
Dekhter, Rimma .....	TU114.....	73	Drees, Markus .....	B064.....	88
Del Campo, Adolfo .....	C053.....	136	Dresselhaus, Mildred .....	B012.....	79
Delbeck, Sven .....	TH612.....	125	Dresselhaus, Mildred .....	TU602.....	67
Demirbilek, Riza .....	C105.....	146	Dresselhaus, Mildred .....	TH111.....	123
Demmler, Stefan .....	C050.....	136	Dresselhaus, Mildred .....	B030.....	82

Driad, Rachid .....	TU812.....	76	Facq, Sebastien .....	A086.....	53
Dropsit, Elise.....	TH808.....	122	Faessler, Thomas F.....	B064.....	88
Duffy, Brendan.....	A118.....	59	Fahel, Jean.....	TH511.....	124
Dugandžić, Vera.....	TH102.....	115	Fahlquist, Henrich.....	WE503.....	106
Dukor, Rina.....	C006.....	128	Faist, Jérôme.....	TU805.....	68
Dumańska-Słowik, Magdalena.....	C101.....	145	Falams, Alexandra.....	B092.....	94
Dumont, Elodie.....	B008.....	78	Fan, Jenyu.....	C096.....	144
Dupont, Sune.....	B113.....	98	Farcas, Anca.....	B061.....	88
Durand, Alain.....	TH808.....	122	Faria, Dalva.....	MO604.....	27
Durand, Sylvie.....	TU613.....	75	Farrant, Stephanie.....	A089.....	54
Duynhoven, John van.....	C017.....	129	Faulds, Karen.....	A018.....	40
Dybal, Jiří.....	MO503.....	26	Faulds, Karen.....	WE603.....	107
Dybal, Jiří.....	A101.....	56	Faulques, Eric.....	TU603.....	67
Eberhardt, Katharina.....	A035.....	43	Fedorowicz, Andrzej.....	WE102.....	105
Ebert, Martin.....	MO807.....	32	Felgitsch, Laura.....	A086.....	53
Eckstein, Nadine.....	B064.....	88	Feng, Lei.....	B019.....	80
Eder, Gabriele.....	TU504.....	66	Fernandes, Rafael.....	C027.....	131
Eder, Gabriele.....	TH804.....	118	Fernandez, Jose Francisco.....	C053.....	136
Ederth, Thomas.....	TU502.....	66	Ferrante, Carino.....	TH606.....	121
Ederth, Thomas.....	B065.....	89	Fiege, Maren.....	B118.....	98
Edlinger, Michael von.....	TU807.....	72	Filho, J. Mendes.....	A119.....	59
Egelkraut-Holtus, Marion.....	B116-pdp.....	95	Filipczak, Paulina.....	B083.....	92
Egelkraut-Holtus, Marion.....	C104-pdp.....	133	Findlay, Catherine.....	FR102-inv.....	153
Ehrenfreund, Eitan.....	MO502.....	26	Findlay, Catherine.....	A013.....	39
Ehrenfreund, Eitan.....	A111.....	58	Finkelstein, Yacov.....	C073.....	140
Eichler, Hans Joachim.....	A041.....	44	Fischer, Marc.....	TU807.....	72
Eitenberger, Elisabeth.....	A084.....	53	Fisher, Kate.....	TH101.....	115
Eitenberger, Elisabeth.....	C100.....	145	Fitzek, Harald.....	A003.....	37
Ek Weis, Johan.....	TU602.....	67	Flego, Cristina.....	A079.....	52
Ekgasit, Sanong.....	B031.....	82	Fleming, Eimear.....	A118.....	59
El-Mashtoly, Samir.....	MO609.....	31	Fokin, Andrey A.....	A072.....	50
El-Mashtoly, Samir.....	A031.....	43	Foltran, Stéphanie.....	C102.....	146
El-Mashtoly, Samir F.....	B071.....	90	Forbrig, Enrico.....	A040.....	44
EL-Zahry, Marwa R.....	WE105.....	105	Forget, Aurelien.....	C006.....	128
Elfvig, Anders.....	MO802.....	28	Foster, Clemens.....	C016.....	129
Elm, Julian.....	A050.....	46	Fotheringham, Edeline.....	MO109.....	29
Elsayed, Badr.....	A045.....	45	Franco Jr., A.....	A065.....	49
Elsenety, Mohamed.....	A045.....	45	Fraser, Michael.....	C092-pdp.....	141
Emmenegger, Lukas.....	TU805.....	68	Freier, Erik.....	A044.....	45
Enengl, Christina.....	A111.....	58	Freier, Erik.....	B071.....	90
Enengl, Christina.....	MO502.....	26	Freire, Paulo de Tarso C.....	A119.....	59
Enengl, Christina.....	B106.....	97	Freitas, Renato.....	C019.....	130
Enengl, Sandra.....	MO502.....	26	Friedbacher, Gernot.....	A084.....	53
Enengl, Sandra.....	B106.....	97	Friedbacher, Gernot.....	C100.....	145
Enengl, Sandra.....	A111.....	58	Fröhling, Kasper.....	TU512.....	74
Engquist, Isak.....	TU502.....	66	Fromm, Felix.....	MO805.....	28
Entacher, Karl.....	A024.....	41	Frosch, Torsten.....	TU809.....	72
Erbe, Andreas.....	TU106.....	69	Frosch, Torsten.....	C025.....	131
Erbe, Andreas.....	C090.....	143	Fuchs, Frank.....	TU812.....	76
Erdas, Dilek.....	A124-pdp.....	59	Fuchs, Frank.....	TU801-inv.....	68
Ertel, Alyssa.....	B102.....	96	Fukuda, Aya.....	C049.....	136
Etezadi, Dordaneh.....	TH106.....	119	Furukawa, Katsuko.....	A113.....	58
Evans, Richard.....	TH810.....	122	Furukawa, Yukio.....	TU501.....	66

Furukawa, Yukio	A097	55	Gironi, Beatrice	B091	94
Çağor, Anna	C057	137	Giubileo, Gianfranco	C038	133
Gaigeot, Marie-Pierre	TH602	117	Giugliarelli, Alessandra	B091	94
Galler, Kerstin	A046	45	Glamuzina, Branko	MO810	32
Galli, Giulia	TU106	69	Glasse, Jarka	WE804	108
Gallo, Crescenzo	A052	46	Glimtoft, Martin	MO802	28
Galvez, Oscar	MO808-inv	32	Glowacki, Eric D.	A111	58
Galyametdinov, Yuri G.	C075	140	Gmachl, Claire	C096	144
Ganster, Lisa	C036	133	Goda, Yukihiko	B082	92
Gao, Danqing	B078	91	Goicoechea, Héctor	C099	145
Garbacik, Eric T.	C017	129	Goicoechea, Héctor	C097	145
Gardner, Benjamin	MO602	27	Golabgir, Aydin	TH801-inv	118
Gardner, Peter	TH614	125	Golabi, Mohsen	B065	89
Garmeister, Roderich	B090	94	Golmar, Federico	MO102	25
Gasser, Christoph	A123-pdp	54	Gonçalves Rubira, Rafael Jesus	B047	85
Gasser, Christoph	B114	98	Gonçalves, Jacqueline	C022	130
Gatemala, Harnchana	B031	82	Gonchar, Mykhailo	B095	94
Gaussmann, Fabian	A010	38	Gong, Liang	A076	51
Gaussmann, Fabian	WE502	106	Gong, Liang	MO514	34
Geier, Eduard	C074	140	González-Miret, Maria Lourdes	C018	130
Geiser, Markus	TU805	68	Goodacre, Roy	MO605	27
Geiser, Peter	C093	144	Goodacre, Roy	A008	38
Gembus, Armin	MO805	28	Gopi, Hosahudya N.	B089	93
Genkawa, Takuma	A088	53	Gordan, Ovidiu	TH506	120
Genner, Andreas	B114	98	Gordillo Arrobas, Belén	C018	130
Geobaldo, Francesco	TH110	119	Gordon, Keith	MO506-inv	30
Geobaldo, Francesco	B024	81	Gordon, Keith	WE805	108
George, Michael	A067	49	Gordon, Keith	A063	49
George, Michael	C092-pdp	141	Gordon, Keith	C092-pdp	141
George, Michael W.	C091	144	Gorshkov, Vadim	A117	59
George, Mike	C040	134	Gorton, Lo	TH109	119
George, Mike	C103-pdp	133	Goryainov, Sergey	WE504	106
Gerwert, Klaus	WEPL2	100	Gough, Kathleen	FR102-inv	153
Gerwert, Klaus	B072	90	Gough, Kathleen	A013	39
Gerwert, Klaus	A025	42	Gough, Kathleen	MO110	29
Gerwert, Klaus	TU612	75	Govyadinov, Alexander	MO102	25
Gerwert, Klaus	TH603	117	Govyadinov, Alexander A.	MO104	25
Gerwert, Klaus	MO609	31	Gowacki, Eric	C046	135
Gerwert, Klaus	A026	42	Grafova, Michaela	B032	82
Gerwert, Klaus	A031	43	Grafova, Michaela	TH105	115
Gerwert, Klaus	A044	45	Graham, Duncan	A018	40
Gerwert, Klaus	B071	90	Graham, Duncan	WE603	107
Ghahghaei Nezamabadi, Mahdi	B029	89	Grahmann, Jan	TU801-inv	68
Ghita, Adrian	A047	46	Gratzl, Reinhard	A098	55
Gierlinger, Notburga	FR104-inv	153	Greetham, Gregory	C042	134
Gierlinger, Notburga	B084	92	Gresch, Tobias	TU804	68
Gil, Otávio	MO604	27	Groenendijk, Petra	A105	57
Gilles, Clement	TU802	68	Größle, Robin	B104	97
Gilliam, Sean	TH806	122	Grothe, Hinrich	A086	53
Giorgis, Fabrizio	B024	81	Gualtieri, Maurizio	MO511	34
Giorgis, Fabrizio	TH110	119	Gudim, Irina	TH507	120
Giovannozzi, Andrea Mario	C085	143	Guidoni, Leonardo	TH602	117
Giovannozzi, Andrea Mario	MO603	27	Guillon, Fabienne	TU613	75

Guilment, Jean	TH808	122	Held, Andreas	A084	53
Guirgis, Gamil	C072	140	Held, Andreas	B007	78
Güldenhaupt, Jörn	TU612	75	Helesicova, Tereza	B021	80
Gupta, Archana	B052	86	Helesicova, Tereza	TH105	115
Gupta, Archana	TH514	124	Hellwig, Petra	TU614	75
Gupta, P.K	TH508	120	Heraud, Philip	WE103	105
Gust, Devens	TH505	116	Heraud, Philip	A055	47
Güven, Hasim	C105	146	Heraud, Philip	MO806-inv	32
Gygi, Francois	TU106	69	Herbst, Johannes	TH811-inv	126
Haas, Julian	C030	132	Heredia, Francisco J	C018	130
Habelitz, Stefan	MO112	33	Hertzberg, Otto	C095	144
Habler, Gerlinde	A104	56	Hertzberg, Otto	C094	144
Hahn, Stephan	A031	43	Herwig, Christoph	TH801-inv	118
Hahn, Stephan	B071	90	Herwig, Christoph	C031	132
Halamkova, Lenka	WE104	105	Hetmanczyk, Joanna	A109	57
Halmagyi, Adela	B073	90	Hetmanczyk, Joanna	C052	136
Halmagyi, Adela	B074	91	Hetmanczyk, Lukasz	A109	57
Hamada, Koji	MO509	30	Hetmanczyk, Lukasz	C052	136
Hamaguchi, Hiro-o	A019	40	Heussen, Patricia	A105	57
Hamra, Patricia	TU114	73	Heussen, Patricia	C017	129
Han, Kiok	A060	48	Heuzé, Karine	TU109	69
Han, Seungho	A107	57	Heuzé, Karine	C083	142
Han, Xue	A067	49	Heyler, Randy	MO813	36
Hands, James	A016	40	Hidi, Izabella Jolan	TH102	115
Hanf, Stefan	TU809	72	Hiederer, Andreas	A098	55
Hangauer, Andreas	TU806-inv	72	Hikima, Yuta	MO509	30
Happe, Thomas	TU102	65	Hikima, Yuta	C068	139
Hara, Risa	A088	53	Hildebrandt, Peter	A040	44
Hardy, Mike	B039	83	Hillenbrand, Rainer	MOPL1	20
Haroniková, Andrea	TU105	65	Hillenbrand, Rainer	MO104	25
Harrer, Andreas	TH812	126	Hillenbrand, Rainer	MO102	25
Harrison, David	TH101	115	Hingerl, Kurt	MO502	26
Hartl, Brad	MO607	31	Hingerl, Kurt	A111	58
Hasegawa, Takeshi	MO510	30	Hintenaus, Peter	TH802	118
Hasegawa, Takeshi	TU509	70	Hirschl, Christina	TH804	118
Hasegawa, Takeshi	C082	142	Hirschl, Christina	C069	139
Hasegawa, Takeshi	C084	142	Hirschl, Christina	C074	140
Hashimoto, Yusuke	C070	139	Hirschmugl, Carol	MO106-inv	29
Hauer, Benedikt	MO108	29	Hirschmugl, Carol	MO110	29
Hauer, Benedikt	A120-pdp	39	Hisatake, Koji	C049	136
Hauer, Juergen	TH610	121	Hitzenberger, Regina	C100	145
Häussermann, Ulrich	WE503	106	Ho, Junming	TH505	116
Havlicek, Marek	MO502	26	Hobro, Alison	MO614	35
Havlicek, Marek	A111	58	Hochreiner, Armin	TH803	118
He, Anqi	A004	37	Hodoroaba, Vasile-Dan	MO603	27
He, Anqi	B078	91	Hoeve, Robert	A105	57
He, Yufan	B037	85	Höfer, Sonja	TU607	71
Heberle, Joachim	TU611-inv	75	Höfer, Sonja	B051	86
Heise, H. Michael	TH612	125	Höfer, Sonja	A094	55
Heise, H. Michael	A049	46	Hoffmann, Helmuth	A077	51
Heise, H. Michael	A050	46	Höfling, Sven	TU807	72
Heise, H. Michael	B090	94	Hofmann, Detlev M.	C048	135
Heise, H. Michael	A025	42	Höhl, Martin	TU103	65

Holland-Moritz, Alexander	B118	98	Itoh, Hiroto	C039	134
Hollricher, Olaf	MO811	36	Itoh, Tamitake	A012	39
Hollywood, Katherine	MO605	27	Itoh, Tamitake	TU601	67
Hollywood, Katherine	A008	38	Ivana, Ujevic	B033	82
Holroyd, Steve	WE805	108	Ivetic, Tamara	A100	56
Holzbauer, Martin	B003	77	Iwamoto, Kei	A096	55
Holzbauer, Martin	TU803	68	Iwamoto, Kei	C070	139
Honorato, Fernanda	C024	131	Iwasawa, Yasuhiro	A097	55
Honorato, Ricardo	A007	38	Iwata, Koichi	TH609	121
Honorato, Ricardo	C024	131	Izak, Tibor	A078	51
Hooijschuur, Jan-Hein	MO809	32	Izak, Tibor	B036	83
Hoppe, Sandrine	TH808	122	Izak, Tibor	B110	98
Horch, Marius	TU102	65	Jacobs, Kevin	B010	79
Hore, Dennis	TU107	69	Jafari, Mohammad Javad	TU502	66
Horvath, Raphael	C092-pdp	141	Jafari, Mohammad Javad	B065	89
Hoshina, Hiromichi	C063	138	Jager, Edwin	B065	89
Hosseinpour, Saman	C047	135	Jahn, Martin	B088	93
Hrubanová, Kamila	TU105	65	Jakobsen, Mogens	TU512	74
Hu, Jiming	B066	89	Jalkanen, Karl	MO513	34
Hu, Qi	A061	48	Jalkanen, Karl	C029	132
Hu, Qichi	MO113	33	James, Sandy	MO807	32
Huang, Dianshuai	A020	41	James, Timothy M.	TU808	72
Huang, Shengxi	B030	82	Jamieson, Lauren	TH101	115
Huang, Shengxi	TH111	123	Jamme, Frédéric	TU613	75
Huang, Shengxi	B012	79	Jantke, Laura-Alice	B064	88
Huang, Stacey	A083	52	Jarisz, Tasha	TU107	69
Huang, Yu-Hsuan	A080	52	Jarvis, Jan	TU812	76
Hubert, Philippe	B008	78	Jaworska, Aleksandra	TH101	115
Huck, Christian	WE801-inv	108	Jearanaikoon, Patcharee	A055	47
Huck, Christians	B045	84	Jegorov, Alexandr	B086	93
Huebner, Uwe	B088	93	Jen, Myungsam	C043	134
Huefner, Anna	TH613	125	Jenkinson, Michael	A016	40
Huefner, Anna	TU513	74	Jensen, Gerard	C029	132
Huff, Gregory	C041	134	Jeong, Dae Hong	A070	50
Hugger, Stefan	TU812	76	Jeong, Dae Hong	B026	81
Hugger, Stefan	TU801-inv	68	Jeong, Dae Hong	MO608	31
Hughes, Caryn	TU813	76	Jeong, Sinyoung	MO608	31
Hugi, Andreas	TU805	68	Jesacher, Alexander	A039	44
Hytönen, Vesa	B040	83	Ježek, Jan	TU105	65
Iacovita, Cristian	B061	88	Ji, Jeong-Eun	A060	48
Ibach, Wolfram	MO811	36	Ji, Qixing	A083	52
Ibrahim, Joyce	B045	84	Ji, Wei	TH104	115
Ichiro, Tanabe	TU601	67	Ji, Wei	B031	82
Idrissi, Abdenacer	WE505	106	Jiang, Jing	TH101	115
Idrissi, Abdenacer	B060	88	Jiang, Ye	A004	37
Igarashi, Yoko	C032	132	Jiang, Ye	B078	91
Ihrig, Dieter	TH612	125	Jimenez-Serrano, Alejandro	A058	48
Ilangovan, Kanaga Vidhya	B089	93	Jin, Mingzhou	MOPL2	20
Ilchenko, Oleksii	A006	38	Jin, Mingzhou	MO113	33
Imbraguglio, Dario	A011	39	Jin, Sila	B025	81
Iramain, Maximiliano	B055	87	Jochum, Tobias	TU809	72
Isakov, Dmitry	A103	56	Johannessen, Christian	WE601-inv	107
Ishikawa, Daitaro	C032	132	Johansson, Niklas	MO802	28

Johns, Robert.....	A013.....	39	Kavetsky, Taras S.....	C075.....	140
Johnson, Tim.....	B102.....	96	Kazakov, Oleksandr.....	WE104.....	105
Jones, Andrew.....	TH810.....	122	Kazarian, Sergei.....	TU506-inv.....	70
Jones, Colin.....	A115.....	58	Ke, Jie.....	A067.....	49
Jonsson, Dan.....	TU609.....	71	Ke, Jie.....	C102.....	146
Jörger, Michael.....	TH607.....	121	Keiderling, Timothy A.....	C010.....	128
Jung, Lena.....	A120-pdp.....	39	Keiner, Robert.....	TU809.....	72
Jung, Lena.....	MO108.....	29	Kelchermans, Mauritz.....	MO505.....	26
Jung, Young Mee.....	B025.....	81	Kelley, Chris.....	TH614.....	125
Jung, Young Mee.....	B094.....	94	Kemper, Mark.....	TH807.....	122
Jung, Young Mee.....	C061.....	138	Kerstan, Andreas.....	MO110.....	29
K Rathore, Ajay.....	C059.....	137	Kesari, Swayam.....	TH510.....	120
Kaczor, Agnieszka.....	TU104.....	65	Kessler, Jiri.....	C010.....	128
Kaczor, Agnieszka.....	A042.....	45	Kessler, Mathias.....	B101.....	96
Kaczor, Agnieszka.....	A032.....	43	Kessler, Mathias.....	B100.....	96
Kadhane, Umesh.....	A085.....	53	Kessler, Rudolf.....	THPL2.....	110
Kadria-Yili, Yara.....	C004.....	127	Khazamov, Timur.....	A103.....	56
Kalbac, Martin.....	TU602.....	67	Khinast, Johannes.....	A091.....	54
Kalbac, Martin.....	A064.....	49	Kholkin, Andrei.....	A117.....	59
Kalbac, Martin.....	A074.....	51	Kholkin, Andrei.....	A103.....	56
Kalbac, Martin.....	B023.....	81	Kholkin, Andrei.....	MO512.....	34
Kalugin, Oleg.....	WE505.....	106	Khoshmanesh, Aazam.....	A055.....	47
Kamada, Ayaka.....	A113.....	58	Kiefer, Johannes.....	WE605.....	107
Kamilli, Katharina A.....	A084.....	53	Kiehntopf, Michael.....	A021.....	41
Kamilli, Katharina A.....	B007.....	78	Kielb, Patrycja.....	TH109.....	119
Kaminskyj, Susan.....	A013.....	39	Kilgus, Jakob.....	B002.....	77
Kamp, Martin.....	TU807.....	72	Kim, Dong-Ho.....	A068.....	50
Kampe, Bernd.....	A033.....	43	Kim, Gil-Sung.....	A066.....	49
Kampe, Bernd.....	B069.....	90	Kim, Gungung.....	MO608.....	31
Kanamori, Toshiyuki.....	C084.....	142	Kim, Gyo-Ho.....	A060.....	48
Kanamori, Toshiyuki.....	MO510.....	30	Kim, Kyung-Hun.....	B026.....	81
Kaneko, Tadaaki.....	TU601.....	67	Kim, Yeseul.....	B094.....	94
Kang, Dai-Il.....	A060.....	48	Kim, Yong-il.....	MO608.....	31
Kang, Homan.....	A070.....	50	Kim, Youngju.....	A107.....	57
Kang, Homan.....	MO608.....	31	Kimura, Kana.....	C056.....	137
Kang, Tingguo.....	B078.....	91	Kinoshita, Yoshikazu.....	A019.....	40
Kang, Xiaoyan.....	A004.....	37	Kiselyov, Eugene.....	A117.....	59
Kano, Hideaki.....	C049.....	136	Kish, Elizabeth.....	TH505.....	116
Kansiz, Mustafa.....	MO110.....	29	Kish, Elizabeth.....	TH602.....	117
Kantner, Wolfgang.....	C015.....	129	Kistler, Magdalena.....	C100.....	145
Kapitan, Josef.....	C010.....	128	Kitahama, Yasutaka.....	A012.....	39
Kapitán, Josef.....	B058.....	87	Kitamura, Sho.....	TH609.....	121
Karlsson, Maths.....	WE503.....	106	Kjoller, Kevin.....	MO505.....	26
Karuppiah, Muruga Poopathi Raja.....	B089.....	93	Kjoller, Kevin.....	MO113.....	33
Kashtiban, Reza.....	TU603.....	67	Klar, Peter J.....	A072.....	50
Kasper-Giebl, Anne.....	C100.....	145	Klar, Peter J.....	C048.....	135
Kaspersen, Peter.....	C093.....	144	Klein, Helmut.....	C016.....	129
Katayama, Norihisa.....	C020.....	130	Klem, Karel.....	B117-pdp.....	96
Katayama, Norihisa.....	A005.....	37	Klug, David.....	FR101.....	153
Kato, Yuichi.....	A069.....	50	Klyamkina, Alla.....	MO508.....	30
Katori, Noriko.....	B082.....	92	Knapp-Mohammady, Michaela.....	MO513.....	34
Katz, Sagie.....	TU102.....	65	Kneafsey, Brendan.....	A118.....	59
Kausteklis, Jonas.....	C060.....	138	Knoll, Christian.....	TU510.....	70

Knoll, Christian.....	C076.....	141	Kristament, Christian.....	C097.....	145
Kobayashi, Yukiko.....	A096.....	55	Kristament, Christian.....	C099.....	145
Kobori, Hikaru.....	C020.....	130	Kristament, Christian.....	TH803.....	118
Kocourkova, Lucie.....	A037.....	44	Krivosudsky, Ondrej.....	A073.....	50
Kocourková, Lucie.....	A036.....	44	Kromka, Alexander.....	B110.....	98
Koeth, Johannes.....	TU807.....	72	Kromka, Alexander.....	A009.....	38
Kögler, Martin.....	B046.....	85	Kromka, Alexander.....	B036.....	83
Koh, Ivan.....	MO604.....	27	Kromka, Alexander.....	A078.....	51
Kojima, Seiji.....	C070.....	139	Krstev, Igor.....	B039.....	83
Kojima, Seiji.....	A096.....	55	Krylov, Alexander.....	TH507.....	120
Kokaislova, Alzbeta.....	B020.....	80	Krylov, Alexander.....	WE504.....	106
Kokaislova, Alzbeta.....	TH105.....	115	Krylov, Alexander.....	MO512.....	34
Kokaislova, Alzbeta.....	B021.....	80	Krylova, Svetlana.....	WE504.....	106
Kokoric, Vjekoslav.....	B111.....	98	Krylova, Svetlana.....	TH507.....	120
Kolada, Oleksandr.....	A006.....	38	Krzuć, Magdalena.....	TU604.....	67
Kondo, Takayuki.....	TH502.....	116	Krzyżánek, Vladislav.....	TU105.....	65
Konegger, Michael.....	C077.....	141	Kuan, Wei-Li.....	TH613.....	125
Kong, Jing.....	B030.....	82	Kubisiak, Piotr.....	A015.....	40
Kong, Jing.....	TH111.....	123	Kuc, Marta.....	B103.....	96
Kong, Jing.....	B012.....	79	Kuca, Kamil.....	B085.....	93
Kong, Kenny.....	A038.....	44	Kuczynski, Szymon.....	A081.....	52
Kong, Kenny.....	MO606-inv.....	31	Küderle, Arne.....	C095.....	144
Konieczny-Molenda, Anna.....	B015.....	89	Küderle, Arne.....	C094.....	144
Kosaka, Kenichi.....	A093.....	55	Kühnemann, Frank.....	TH811-inv.....	126
Kotov, Nikolay.....	A101.....	56	Kukhta, Alexander V.....	C075.....	140
Kötting, Carsten.....	TU612.....	75	Kuligowski, Julia.....	WE105.....	105
Kötting, Carsten.....	B072.....	90	Kuligowski, Julia.....	A027.....	42
Kötting, Carsten.....	TH603.....	117	Kumar B.N., Vinay.....	B069.....	90
Kötting, Carsten.....	MO609.....	31	Kumar, Dharendra.....	C059.....	137
Kötting, Carsten.....	B071.....	90	Kumar, Naresh.....	A011.....	39
Kottke, Tilman.....	TH608.....	121	Kumar, Satish.....	C059.....	137
Koverga, Volodymyr.....	WE505.....	106	Kumaradas, J. Carl.....	A051.....	46
Kowallik, Sarah.....	TU107.....	69	Kunimoto, Ko-Ki.....	B052.....	86
Kowalski, Rafał.....	B077.....	91	Kunkel, Brenda.....	B102.....	96
Kozak, Halyna.....	A009.....	38	Kunsch, Johannes.....	TH814.....	126
Kozak, Halyna.....	B110.....	98	Küpper, Claus.....	A044.....	45
Kozak, Halyna.....	A078.....	51	Kurki, Lauri.....	MO814.....	36
Kozanecki, Marcin.....	MO504.....	26	Kurki, Lauri.....	B038.....	85
Kozanecki, Marcin.....	B083.....	92	Kurouski, Dmitry.....	TU101-inv.....	65
Kozu, Tomomi.....	B005.....	78	Kutsuma, Yasunori.....	TU601.....	67
Kozu, Tomomi.....	B004.....	77	Kutsyk, Andrii.....	A006.....	38
Kozuch, Jacek.....	A040.....	44	Kwon, Jung-Dae.....	A068.....	50
Krafft, Christoph.....	A053.....	47	Kyprianidis, Konstantinos.....	C037.....	133
Kraft, Martin.....	C069.....	139	Laane, Jaan.....	B096.....	95
Kraft, Martin.....	C074.....	140	Ladetto, María.....	B055.....	87
Kraft, Martin.....	TH804.....	118	Lai, Antonia.....	B042.....	84
Krasnenkov, Dmitrii.....	A006.....	38	Lamberti, Andrea.....	TH110.....	119
Kratochvíl, Jaroslav.....	MO503.....	26	Lamberti, Andrea.....	B024.....	81
Krause, Anna.....	B079.....	91	Lambrecht, Armin.....	TH811-inv.....	126
Krauss, Sascha.....	B071.....	90	Landry, Olivier.....	TU804.....	68
Krawczyk, Aleksandra.....	WE102.....	105	Lange, Julia.....	A026.....	42
Kretinin, Andrey.....	WE502.....	106	Langer, Gregor.....	TH803.....	118
Kriegel, Sébastien.....	TU614.....	75	Larkin, Peter.....	MO813.....	36

Larsen, Jan .....	TU512.....	74	Leopold, Nicolae .....	B073.....	90
Lasalvia, Maria .....	A052.....	46	Leopold, Nicolae .....	B092.....	94
Lasch, Peter .....	TH601-inv.....	117	Leopold, Nicolae .....	A043.....	45
Latka, Ines .....	MO607.....	31	Leopold, Nicolae .....	B044.....	84
Latka, Ines .....	C045.....	135	Leopold, Nicolae .....	B093.....	94
Laventure, Audrey.....	TU507.....	70	Leopoldo Constantino, Carlos José.....	B047.....	85
Law, Philippa .....	MO812.....	36	Lerondel, Gilles.....	B045.....	84
Le, Loan .....	C096.....	144	Leş, Anda .....	B093.....	94
Le, Thu .....	B043.....	84	Leslie, Suzanne .....	WE101-inv.....	105
Lea, Robert.....	A016.....	40	Lesniak, Magdalena .....	C064.....	138
Leach, Iain.....	A038.....	44	Lewandowska, Kornelia .....	B080.....	92
Lebel, Olivier .....	TU507.....	70	Lewandowska, Kornelia .....	B081.....	92
Lednev, Igor .....	TU101-inv.....	65	Lewandowska, Kornelia .....	B079.....	91
Lednev, Igor K. ....	WE104.....	105	Lewandowski, Marian H.....	B077.....	91
Ledwith, Deirdre.....	A118.....	59	Lewin, Martin .....	MO108.....	29
Lee, Dong Soo .....	MO608.....	31	Lewin, Martin .....	WE502.....	106
Lee, Han-Hyoung.....	A060.....	48	Lewis, Aaron.....	TU114.....	73
Lee, Ho-Young.....	B026.....	81	Lewis, David.....	TU114.....	73
Lee, Jae Hwan .....	B025.....	81	Lewis, Ian.....	TH806.....	122
Lee, Jiann-Shing.....	A075.....	51	Lewis, Ian.....	C036.....	133
Lee, Minwoo .....	B026.....	81	Li, Chunguang.....	TU814.....	76
Lee, Sang-Kwon .....	A066.....	49	Li, Haibo .....	A020.....	41
Lee, Sebok.....	C043.....	134	Li, Peining.....	WE502.....	106
Lee, Yoon-Sik .....	A070.....	50	Liang, Liangbo.....	B030.....	82
Lee, Yoon-Sik.....	B026.....	81	Liang, Lijia.....	A020.....	41
Lee, Yoon-Sik.....	MO608.....	31	Liao, Catherine.....	MO110.....	29
Lee, Young Jong.....	TH501.....	116	Liberale, Carlo .....	MO613.....	35
Lee, Yuan-Pern.....	A080.....	52	Liegeois, Vincent .....	TU606.....	71
Leiss-Holzinger, Elisabeth.....	TH803.....	118	Lilienfeld-Toal, Hermann von.....	C094.....	144
Leitgeb, Stefan .....	A091.....	54	Limpert, Jens.....	C050.....	136
Leitner, Raimund .....	TH804.....	118	Lin, Chun-Rong .....	A075.....	51
Lembacher, Christian.....	A003.....	37	Lin, Yuan-Chih.....	WE503.....	106
Lemma, Tibebe .....	B040.....	83	Lind, Samuel.....	C092-pdp.....	141
Lenain, Bruno .....	TH806.....	122	Ling, Xi .....	TH111.....	123
Lenarz, Thomas .....	TU103.....	65	Ling, Xi .....	B030.....	82
Lendl, Bernhard .....	C098.....	145	Ling, Xi .....	B012.....	79
Lendl, Bernhard .....	TH805.....	118	Lipina, Olga .....	TH509.....	120
Lendl, Bernhard .....	A123-pdp.....	54	List, Manuela .....	C055.....	137
Lendl, Bernhard .....	C077.....	141	Liu, Jiang.....	TU502.....	66
Lendl, Bernhard .....	MO105.....	25	Liu, Lingxiao.....	B019.....	80
Lendl, Bernhard .....	A121-pdp.....	39	Liu, Yizhen.....	B066.....	89
Lendl, Bernhard .....	A084.....	53	Lizio, Maria Giovanna.....	A054.....	47
Lendl, Bernhard .....	A122-pdp.....	48	Lo, Michael .....	MO505.....	26
Lendl, Bernhard .....	B114.....	98	Lobascio, Cesare .....	C085.....	143
Lendl, Bernhard .....	C099.....	145	Lohninger, Hans.....	B007.....	78
Lendl, Bernhard .....	WE105.....	105	Lohninger, Hans.....	A084.....	53
Lendl, Bernhard .....	C097.....	145	Lohninger, Hans.....	C100.....	145
Lendl, Bernhard .....	TH803.....	118	Lombardi, John R.....	B013.....	79
Lendl, Bernhard .....	B007.....	78	Lombardi, John R.....	C079.....	141
Lendl, Bernhard .....	C100.....	145	López González, Juan Jesús.....	C001.....	127
Lenferink, Aufried.....	TH114.....	123	López González, Juan Jesús.....	C002.....	127
Leonidov, Ivan .....	TH509.....	120	López González, Juan Jesús.....	C003.....	127
Leopold, Loredana Florina.....	A043.....	45	Lopez Ramirez, Maria Rosa .....	TU514.....	74

López-Lorente, Ángela I.....	TU605.....	67	Mandrile, Luisa.....	C085.....	143
López-Tocón, Isabel.....	C086.....	143	Mangold, Markus.....	TU805.....	68
Lorkowski, Stefan.....	A028.....	42	Mänteles, Werner.....	TU811-inv.....	76
Love, Ashley.....	A067.....	49	Mänteles, Werner.....	C095.....	144
Lu, Feng.....	MOPL2.....	20	Mänteles, Werner.....	C094.....	144
Lu, Feng.....	MO113.....	33	Mantsch, Henry.....	TH605.....	117
Lu, H. Peter.....	B037.....	85	Mao, Nannao.....	TH111.....	123
Lu, H. Peter.....	TU113.....	73	Marchet, Pascal.....	C053.....	136
Luber, Sandra.....	WE604.....	107	Marcott, Curtis.....	MO514.....	34
Luber, Sandra.....	C004.....	127	Marcott, Curtis.....	MO505.....	26
Luca, Iannareli.....	MO603.....	27	Marcott, Curtis.....	A076.....	51
Lucaciu, Constantin M.....	B061.....	88	Marcott, Curtis.....	MO113.....	33
Lucas, Herve.....	TH806.....	122	Marcu, Laura.....	MO607.....	31
Luciani, Domenico.....	B042.....	84	Marcus, Katrin.....	A026.....	42
Lucotti, Andrea.....	MO511.....	34	Marek, Andrzej.....	C075.....	140
Lüdeke, Steffen.....	C006.....	128	Marekha, Bogdan.....	WE505.....	106
Ludwig, Roland.....	TH109.....	119	Marisca, Oana.....	B044.....	84
Lukic-Petrovic, Svetlana.....	A100.....	56	Markwart, Robby.....	A046.....	45
Lukic, Aleksandar.....	C045.....	135	Márová, Ivana.....	TU105.....	65
Lux, Oliver.....	A041.....	44	Marques, Maria.....	TH614.....	125
Lyu, Nan.....	B019.....	80	Marquez, Alfredo.....	A022.....	41
Ma, Dinglong.....	MO607.....	31	Márquez, Fernando.....	A056.....	47
Ma, Te.....	C020.....	130	Márquez, Fernando.....	C003.....	127
MacFarland, Donald.....	TU803.....	68	Marrassini, Carla.....	B060.....	88
MacFarland, Donald.....	B003.....	77	Marsh, Christopher.....	C062.....	138
MacFarland, Donald.....	TH812.....	126	Marthandan, Shiva.....	A035.....	43
MacFarland, Donald.....	FR103-inv.....	153	Martin, Michael.....	MO106-inv.....	29
Mackowski, Sebastian.....	A014.....	39	Martin, Michael.....	MO103.....	25
Maczka, Mirosław.....	C057.....	137	Martin, Michael.....	A013.....	39
Maczka, Mirosław.....	A110.....	57	Martin, R. Scott.....	B010.....	79
Maczka, Mirosław.....	A112.....	58	Martra, Gianmario.....	MO603.....	27
Mader, Claudia.....	C030.....	132	Marzec, Katarzyna.....	TH611.....	125
Magg, Martin.....	C004.....	127	Märzinger, Wolfgang.....	TH802.....	118
Maghnouj, Abdelouahid.....	A031.....	43	Maß, Tobias.....	TH107.....	119
Maghnouj, Abdelouahid.....	B071.....	90	Massardier, Valérie.....	A090.....	54
Mahajan, Sumeet.....	TH504.....	116	Mastel, Stefan.....	MO104.....	25
Mahajan, Sumeet.....	TU513.....	74	Mastel, Stefan.....	MO102.....	25
Mahajan, Sumeet.....	TH613.....	125	Matejka, Pavel.....	TH105.....	115
Maier, Konrad.....	B039.....	83	Matejka, Pavel.....	B020.....	80
Maier, Maria E.....	C054.....	137	Matejka, Pavel.....	B032.....	82
Maisons, Gregory.....	TU802.....	68	Matejka, Pavel.....	B021.....	80
Majzner, Katarzyna.....	A030.....	42	Mateuszuk, Lukasz.....	A042.....	45
Maldaner, Adriano.....	C024.....	131	Mateuszuk, Lukasz.....	A034.....	43
Malek, Kamilla.....	WE102.....	105	Matheson, Jane.....	TH810.....	122
Malek, Kamilla.....	A034.....	43	Matousek, Pavel.....	MO602.....	27
Malekfar, Rasoul.....	A116.....	59	Matsui, Hiroshi.....	C070.....	139
Malekfar, Rasoul.....	B028.....	82	Matsui, Hiroshi.....	A096.....	55
Malekfar, Rasoul.....	B029.....	89	Matsumura, Masanori.....	A005.....	37
Malekfar, Rasoul.....	B057.....	87	Matthäus, Christian.....	A028.....	42
Malekfar, Rasoul.....	C058.....	137	Matthäus, Christian.....	A035.....	43
Malon, Petr.....	C009.....	128	Matthäus, Christian.....	C045.....	135
Mandez-Hernandez, Dalvin.....	TH505.....	116	Matthäus, Gabor.....	C050.....	136
Mandrile, Luisa.....	MO603.....	27	Matzl, Julia.....	C100.....	145

Maulini, Richard	TU804	68	Mizaikoff, Boris	B111	98
Maurino, Valter	MO603	27	Mizaikoff, Boris	TU605	67
Mavarani, Laven	A031	43	Mizaikoff, Boris	C030	132
Mavarani, Laven	A044	45	Mizaikoff, Boris	C026	131
Mavarani, Laven	MO609	31	Mizera, Mikoaj	B079	91
May, Caroline	A026	42	Mizera, Mikoaj	B081	92
Mayer, Joachim	MO108	29	Moghe, Prabhas	TH501	116
Mayerhöfer, Thomas	A094	55	Mohammadigol, Reza	B028	82
Mayerhöfer, Thomas G.	TU607	71	Mohammadigol, Reza	B029	89
Mayerhöfer, Thomas G.	B051	86	Mohammadigol, Reza	B057	87
Mayerich, David	WE101-inv	105	Möhler, Ottmar	MO807	32
Mayr, Georg	TH802	118	Mojzes, Peter	B098	95
McBrin, C.J.	MO514	34	Möller, Torgny	B039	83
McBrin, C.J.	A076	51	Monfort, Tual	TH504	116
McCall, David	B041	84	Montague, Gary	WE804	108
McDonnell, Liam	TU603	67	Montejo, Manuel	C001	127
McDowell, Arlene	A063	49	Montejo, Manuel	C002	127
McKinnon, John J.	B067	89	Montejo, Manuel	C003	127
McNaughton, Don	C021	130	Montejo, Manuel	A056	47
McNaughton, Don	WE103	105	Moore, Ana	TH505	116
McNaughton, Don	A055	47	Moore, Thomas	TH505	116
McNaughton, Don	TH611	125	Morais, P. C.	A065	49
McQuillan, A. James	TU108	69	Morávková, Zuzana	A095	55
Mebarek, Saida	B070	90	Mordechai, Shaul	MO612	35
Medema, Jan Paul	MO613	35	Mordechai, Shaul	A017	40
Mehrotra, Ranjana	A023	41	Moreh, Raymond	C073	140
Meinhardt-Wollweber, Merve	TU103	65	Morgner, Uwe	TU103	65
Melin, Frédéric	TU614	75	Mori, Tatsuya	A096	55
Mencaglia, Andrea A.	C018	130	Mori, Tatsuya	C070	139
Mensch, Carl	WE601-inv	107	Morisawa, Yusuke	B105	97
Merten, Andre	TU801-inv	68	Morita, Eugene	C071	140
Merten, Sebastian	A114	58	Morita, Kohei	C084	142
Meunier, Vincent	B030	82	Morita, Kohei	MO510	30
Meyer, Thomas	TU614	75	Morita, Shigeaki	TU508	70
Mezzetti, Alberto	TH602	117	Moritomo, Ikuya	A113	58
Mezzetti, Alberto	B060	88	Morresi, Assunta	B091	94
Michalska, Katarzyna	B081	92	Moselund, Peter M.	B002	77
Michel, Ann-Katrin U.	MO108	29	Moser, Harald	TH805	118
Migdal-Mikuli, Anna	C052	136	Moser, Harald	B114	98
Mignani, Anna G.	C018	130	Moshnyaga, Vasily	A114	58
Milani, Alberto	A092	54	Mosig, Axel	A044	45
Miljevic, Bojan	A100	56	Motahari, Hamid	C058	137
Miloudi, Lynda	MO610	31	Motahari, Hamid	B057	87
Ming, Tian	B012	79	Motobayashi, Kenta	TH108	119
Mink, Janos	WE503	106	Motomura, Asako	C032	132
Mink, Janos	B064	88	Moule, David	B062	88
Mirz, Sebastian	B104	97	Moura, N.S.	A065	49
Misawa, Mayumi	B005	78	Muallem, Merav	B108	97
Misawa, Mayumi	B004	77	Mudronova, Katerina	B098	95
Mishra, Preeti	A085	53	Mueller, Thomas	MO112	33
Misra, Dileep	TU505	66	Müller, Antoine	TU804	68
Misra, Rajkumar	B089	93	Müller, Csilla	MO810	32
Mittal, Shachi	WE101-inv	105	Müller, Danny	C076	141

Müller, Danny	TU510	70	Nishikawa, Yuji	C039	134
Muller, Eric	MO103	25	Nishimura, Ken	C049	136
Muller, Eric	MO106-inv	29	Nishizawa, Seizi	C071	140
Müller, Gerhard	B039	83	Nishizawa, Seizi	A113	58
Müller, Petra	B002	77	Niu, Fang	TU106	69
Mun, ChaeWon	A068	50	Noda, Isao	A076	51
Muntean, Cristina	B073	90	Noda, Isao	C039	134
Muntean, Cristina	B074	91	Noda, Isao	C061	138
Muraki, Naoki	A093	55	Noda, Isao	MO514	34
Muroga, Shun	C068	139	Noda, Isao	A004	37
Musso, Maurizio	A024	41	Noda, Isao	B078	91
Musso, Maurizio	C054	137	Nojima, Yuki	TH609	121
Musso, Maurizio	A102	56	Nolte, Stefan	C050	136
Mutter, Shaun	C005	127	Noothalapati, Hemanth	A019	40
Myers, Tanya	B102	96	Norberg, Ola	MO802	28
Myund, Lubov	TU110	69	Noth, Jens	TU102	65
Nabers, Andreas	TH603	117	Notingher, Ioan	MO606-inv	31
Nabers, Andreas	A026	42	Notingher, Ioan	A038	44
Nafie, Laurence	WE602	107	Novara, Chiara	TH110	119
Nafie, Laurence	C006	128	Novara, Chiara	B024	81
Nagel, Christoph	B090	94	Novokshonova, Lyudmila	MO508	30
Nähle, Lars	TU807	72	Novoselov, Kostya	WE502	106
Nakagomi, F	A065	49	Nowak, Jakub	C075	140
Nam, Ji-Yeon	A060	48	Nowak, Marcus	A001	37
Nasdala, Lutz	A104	56	Nunziante Cesaro, Stella	C038	133
Nasdala, Lutz	A099	56	Nuraeva, Alla	MO512	34
Nasse, Michael	MO106-inv	29	Nuraeva, Alla	A103	56
Natkaniec-Nowak, Lucyna	C101	145	Obruèa, Stanislav	TU105	65
Nattich-Rak, Malgorzata	C080	142	Obst, Martin	A001	37
Nayak, Simantini	TU106	69	Odlare, Monica	C037	133
Nedorezova, Polina	MO508	30	Off, Andreas	TU808	72
Nedwed, Karl	C034	132	Offerhaus, Herman L	C017	129
Negri, Pierre	B010	79	Ofner, Johannes	A084	53
Nerin, Cristina	B022	81	Ofner, Johannes	B007	78
Nessim, Gilbert D.	B108	97	Ofner, Johannes	C100	145
Netchacovitch, Lauranne	B008	78	Ofner, Johannes	TH805	118
Neugebauer, Helmut	B106	97	Ofner, Johannes	C077	141
Neugebauer, Helmut	MO502	26	Ofner, Johannes	A122-pdp	48
Neugebauer, Helmut	A111	58	Ofner, Johannes	B114	98
Neugebauer, Ute	A021	41	Ogrodnik, Karolina	TH813	126
Neugebauer, Ute	A046	45	Ohshima, Masahiro	MO509	30
Neumaier, Lukas	C074	140	Ohshima, Masahiro	C068	139
Neumaier, Lukas	TH804	118	Ohshima, Naoki	A019	40
Niedieker, Daniel	B071	90	Okada, Shigeru	B096	95
Niemiec, Wiktor	TU604	67	Oldemeyer, Sabine	TH608	121
Nikiforov, Anatoliy	TH509	120	Olejniczak, Magdalena	MO504	26
Nikolaeva, Gulnara	MO508	30	Ollesch, Julian	A025	42
Nikolaeva, Gulnara	A115	58	Ollesch, Julian	TH603	117
Nikolai, Brandt	C028	131	Ollesch, Julian	A026	42
Nilges, Tom	B064	88	Olman, Robert	MO106-inv	29
Nilsson, Anders	B100	96	Olmon, Rob	MO103	25
Nilsson, Anders	B101	96	Olsen, Kasper	MO513	34
Nishida, Ken	B005	78	Olszewski, Tomasz K.	C080	142

Olszewski, Tomasz K.....	C081.....	142	Partyka, Janusz.....	C064.....	138
Onishi, Erika.....	C063.....	138	Pashinin, Pavel.....	MO508.....	30
Orozco, Miguel.....	A022.....	41	Pashinin, Pavel.....	A115.....	58
Osawa, Masatoshi.....	TH108.....	119	Pasquini, Celio.....	C027.....	131
Osselton, David.....	MO803.....	28	Pasquini, Celio.....	C023.....	131
Osselton, David.....	A089.....	54	Pasquini, Celio.....	C026.....	131
Osselton, David.....	B109.....	98	Pasquini, Celio.....	A007.....	38
Ostendorf, Ralf.....	TU801-inv.....	68	Pasquini, Celio.....	C022.....	130
Ostendorf, Ralf.....	TU812.....	76	Pastrana-Rios, Belinda.....	MO611-inv.....	35
Österberg, Carin.....	WE503.....	106	Patel, Gaurangkumar.....	A106.....	57
Östmark, Henric.....	MO802.....	28	Patel, Parth.....	TH501.....	116
Ostovar pour, Saeideh.....	WE603.....	107	Patel, Purvi.....	A106.....	57
Ota, Takuma.....	A113.....	58	Paterson, Sarah.....	TH810.....	122
Otero, Juan.....	C086.....	143	Patimisco, Pietro.....	TU810-inv.....	72
Otto, Cees.....	TH114.....	123	Patimisco, Pietro.....	TU814.....	76
Oulevey, Patric.....	WE604.....	107	Patra, Biranchi.....	C029.....	132
Ozaki, Yukihiro.....	C032.....	132	Pavillon, Nicolas.....	MO614.....	35
Ozaki, Yukihiro.....	A014.....	39	Pawliczek, Marcin.....	C015.....	129
Ozaki, Yukihiro.....	B105.....	97	Pawliczek, Marcin.....	C016.....	129
Ozaki, Yukihiro.....	A012.....	39	Pawluczyk, Jaroslaw.....	TH813.....	126
Ozaki, Yukihiro.....	C063.....	138	Pazderková, Markéta.....	C009.....	128
Ozaki, Yukihiro.....	TH104.....	115	Pearson, Charlotte.....	C091.....	144
Ozaki, Yukihiro.....	A088.....	53	Pedrosa-Soares, Antonio.....	C101.....	145
Ozaki, Yukihiro.....	B031.....	82	Pelegov, Dmitry.....	A117.....	59
Ozaki, Yukihiro.....	TU601.....	67	Pellerin, Christian.....	MO501.....	26
Özdemir, Hilal.....	B063.....	88	Pellerin, Christian.....	MO507.....	30
Ozturk, Tugce.....	A048.....	46	Pellerin, Christian.....	C088.....	143
Pacia, Marta.....	A032.....	43	Pellerin, Christian.....	TU507.....	70
Pacia, Marta.....	TU104.....	65	Pellutiè, Letizia.....	MO603.....	27
Paczkowska, Magdalena.....	B080.....	92	Pengel, Stefanie.....	TU106.....	69
Paczkowska, Magdalena.....	B079.....	91	Pennecchi, Francesca.....	C085.....	143
Paiva, Eduardo.....	C023.....	131	Pereira da Silva, Katiane.....	A119.....	59
Palatnik, Alex.....	B108.....	97	Pereira, Claudete.....	C023.....	131
Palucci, Antonio.....	B042.....	84	Pereira, Claudete.....	C022.....	130
Palus, Katarzyna.....	B077.....	91	Pereira, José.....	A007.....	38
Pandya, Aditya.....	A051.....	46	Perez-Guaita, David.....	A055.....	47
Pang, Yoonsoo.....	C043.....	134	Pérez-Guaita, David.....	A027.....	42
Panicker, Yohannan.....	B053.....	86	Perez-Guaita, David.....	TH611.....	125
Pantoja de la Rosa, Jaime.....	C014.....	129	Perna, Giuseppe.....	A052.....	46
Paolantoni, Marco.....	B091.....	94	Pescetelli, Sara.....	TU503.....	66
Paraguassu, W.....	A119.....	59	Petersen, Dennis.....	A044.....	45
Paraguassu, Waldeci.....	A112.....	58	Petersen, Dennis.....	B071.....	90
Parchansky, Vaclav.....	WE603.....	107	Petersen, Dennis.....	MO609.....	31
Parchansky, Václav.....	B058.....	87	Petrenc, Martin.....	B034.....	83
Park, Sung-Gyu.....	A068.....	50	Petrou, Katherina.....	MO806-inv.....	32
Park, Yeonju.....	B025.....	81	Petrov, Vladislav.....	TH509.....	120
Park, Yeonju.....	B094.....	94	Petrovic, Dragoslav.....	A100.....	56
Park, Yeonju.....	C061.....	138	Petutschnigg, Alexander.....	A102.....	56
Parker, Anthony.....	C042.....	134	Petutschnigg, Alexander.....	A024.....	41
Parkinson, Dilworth.....	MO106-inv.....	29	Pham Khac, Duy.....	WE803.....	108
Parkinson, Dilworth.....	WE103.....	105	Picqué, Nathalie.....	TUPL2.....	60
Parlatan, Ugur.....	A048.....	46	Piergies, Natalia.....	B015.....	89
Parras Guijarro, David Jesús.....	A056.....	47	Piergies, Natalia.....	B013.....	79

Piergies, Natalia	C079	141	Prater, Craig	MO505	26
Piergies, Natalia	B014	79	Prats Mateu, Batirtze	B084	92
Piergies, Natalia	C080	142	Preston, Stuart	MO803	28
Piergies, Natalia	B017	80	Previde Massara, Elisabetta	A079	52
Pieta, Ewa	C080	142	Prince, Kevin	A085	53
Pieta, Ewa	C081	142	Procházka, Marek	B085	93
Pieta, Ewa	B017	80	Procházka, Marek	B036	83
Pieta, Ewa	B014	79	Procházka, Marek	B034	83
Pike, Sarah	A054	47	Profant, Václav	C009	128
Pilát, Zdenik	TU105	65	Profant, Václav	B085	93
Pilgun, Yuriy	A006	38	Profant, Václav	B086	93
Pillai, Smitha	TH505	116	Prokhorov, Kirill	MO508	30
Pilling, Mike	TH614	125	Prokhorov, Kirill	A115	58
Pimentel, Fernanda	C023	131	Proniewicz, Edyta	B013	79
Pimentel, Fernanda	A007	38	Proniewicz, Edyta	C079	141
Pimentel, Fernanda	C024	131	Proniewicz, Edyta	B018	80
Pimentel, Fernanda	C022	130	Proniewicz, Edyta	A015	40
Pintus, Valentina	A122-pdp	48	Proniewicz, Edyta	B014	79
Piotrowski, Jozef	TH813	126	Proniewicz, Edyta	B015	89
Pitters, Alexander	TH806	122	Proniewicz, Edyta	B017	80
Pitters, Alexander	C036	133	Proniewicz, Edyta	C081	142
Piza, Pedro	A022	41	Proniewicz, Edyta	A014	39
Plank, Bernhard	A024	41	Proniewicz, Edyta	C080	142
Pleitez, Miguel	C094	144	Proška, Jan	B036	83
Pleitez, Miguel	C095	144	Proška, Jan	B085	93
Poewe, Werner	A039	44	Proška, Jan	B034	83
Polanski, Krzysztof	A081	52	Proška, Jan	B035	83
Polit, Jacek	B095	94	Protti, Stefano	B060	88
Polubotko, Aleksey	B048	85	Pruner, Christian	B097	95
Polubotko, Aleksey	B049	86	Przybya, Marcin	A057	47
Pontecorvo, Emanuele	TH606	121	Ptak, Maciej	A110	57
Popelier, Paul	C005	127	Ptak, Maciej	A119	59
Popp, Jürgen	MO601-inv	27	Ptak, Maciej	C057	137
Popp, Jürgen	C025	131	Pucci, Anne Marie	B045	84
Popp, Jürgen	TU809	72	Pucetaite, Milda	C072	140
Popp, Jürgen	TU607	71	Pudney, Paul	TH810	122
Popp, Jürgen	B051	86	Pudney, Paul	C062	138
Popp, Jürgen	A094	55	Pudney, Paul	C103-pdp	133
Popp, Jürgen	B075	91	Puiatti, M	B115-pdp	95
Popp, Jürgen	A028	42	Puiu, Adriana	C038	133
Popp, Jürgen	A033	43	Pukalski, Jan	TU104	65
Popp, Jürgen	A053	47	Pummer, Bernhard	A086	53
Popp, Jürgen	B069	90	Quaroni, Luca	MO107	29
Popp, Jürgen	TH102	115	Quaroni, Luca	A001	37
Popp, Jürgen	A035	43	Quatela, Alessia	MO610	31
Popp, Jürgen	B088	93	Quintas, Guillermo	A027	42
Popp, Jürgen	A021	41	Quintás, Guillermo	WE105	105
Popp, Jürgen	C045	135	Rabolt, John	MO514	34
Popp, Jürgen	A046	45	Rabolt, John	A076	51
Popp, Jürgen	MO607	31	Radice, Stefano	A092	54
Prahl, Adam	A014	39	Radu, Andreea	B088	93
Pramhaas, Verena	C066	139	Raimundo, Ivo	C026	131
Prater, Craig	MO113	33	Raimundo, Ivo	C027	131

Rajamanickam, Vijayakumar	MO613	35	Rocks, Louise	WE603	107
Rajanikanth, A.	B027	82	Röder, Thomas	TH802	118
Rakhimbekova, Assima	TU110	69	Rodríguez Ortega, Pilar	C002	127
Ramer, Georg	MO105	25	Rodríguez Ortega, Pilar	C003	127
Ramer, Georg	A121-pdp	39	Rodríguez Ortega, Pilar Gema	C001	127
Rameshan, Christoph	C066	139	Rodríguez Vargas, Andrés Ignacio	A099	56
Ramoji, Anuradha	A046	45	Rodríguez-Pulido, Francisco J.	C018	130
Ramoji, Anuradha	A021	41	Rohwedder, Jarbas	C023	131
Ramsay, Jacob	B113	98	Rohwedder, Jarbas	C026	131
Rao, Rekha	TH510	120	Rohwedder, Jarbas	C027	131
Rao, Vishal	B037	85	Roiaz, Matteo	C066	139
Raschke, Markus	MO103	25	Roider, Clemens	A039	44
Raschke, Markus	MO106-inv	29	Román-Pérez, Jéssica	C086	143
Rattunde, Marcel	TU812	76	Romanis, Mariusz	TH813	126
Raus, Vladimír	A101	56	Romano, Elida	B055	87
Raveendran Pillai, Renjith	B053	86	Rooney, Jeremy	A063	49
Rawat, R.	TU505	66	Rösch, Petra	A033	43
Redhammer, Günther J.	A098	55	Rösch, Petra	B069	90
Reece, David	MO812	36	Rösner, Michael	C074	140
Reindl, Christian T.	C048	135	Rospenk, Maria	B103	96
Reininger, Peter	TH812	126	Rossi, Andrea Mario	A011	39
Reininger, Peter	FR103-inv	153	Rossi, Andrea Mario	C085	143
Reint, Andrii	A006	38	Rossi, Andrea Mario	MO603	27
Reischer, Thomas	C015	129	Rössl, Ulrich	A091	54
Reitböck, Cornelia	C046	135	Roth, Andreas	TU811-inv	76
Reja, Rahi M.	B089	93	Roth, Andreas	C095	144
Ren, Zhongyuan	B070	90	Roth, Andreas	C094	144
Requardt, Robert	A046	45	Rowlands, Christopher	MO606-inv	31
Rettenwander, Daniel	C054	137	Rowlette, Jeremy	MO109	29
Reyer, Andreas	A102	56	Rowlette, Jeremy	TU813	76
Reyer, Andreas	A098	55	Roy, Anjan	MO813	36
Rezek, Bohuslav	A009	38	Roy, Anjan	C006	128
Rezek, Bohuslav	B110	98	Roy, Debdulal	A011	39
Rho, Heesuk	A066	49	Roy, Khokan	C051	136
Ricci, Maria	B091	94	Roy, Sandra	TU107	69
Richard-Lacroix, Marie	MO507	30	Rubio-Domene, Ramon	MO801-inv	28
Richard-Lacroix, Marie	C088	143	Rubio-Domene, Ramon	A059	48
Richard-Lacroix, Marie	MO501	26	Rubio-Marcos, Fernando	C053	136
Richter, Robert	A085	53	Rubio, Ignacio	A046	45
Rímal, Václav	B098	95	Rud Keiding, Søren	B113	98
Ringholm, Magnus	TU609	71	Rufoloni, Alessandro	B042	84
Ringholm, Magnus	B054	86	Rugina, Olivia Dumitrita	A043	45
Ringsted, Tine	B113	98	Rupp, Simone	TU808	72
Riordan, Colleen	B010	79	Rupprechter, Günther	C066	139
Rísquez, Carmen	A056	47	Rüther, Anja	C006	128
Ristanic, Daniela	FR103-inv	153	Ruud, Kenneth	TU609	71
Ritsch-Marte, Monika	A039	44	Ruud, Kenneth	B054	86
Rivolo, Paola	TH110	119	Ryabchykov, Oleg	A021	41
Rivolo, Paola	B024	81	Ryabchykov, Oleg	A046	45
Robert, Bruno	TH602	117	Ryan, Kate	MO512	34
Robert, Bruno	TH505	116	Ryzhikova, Elena	WE104	105
Robert, Paul	TU613	75	Sablinskas, Valdas	C072	140
Rocha, Michele	MO604	27	Sacharz, Julia	B077	91

Sackett, Olivia.....	MO806-inv.....	32	Scharber, Markus.....	A111.....	58
Sacré, Pierre-Yves.....	B008.....	78	Scharber, Markus C.....	MO502.....	26
Sadriyeh, Sima.....	A116.....	59	Schartner, Jonas.....	TU612.....	75
Sadriyeh, Sima.....	B057.....	87	Schartner, Jonas.....	TH603.....	117
Saeb-Gilani, Taravat.....	A041.....	44	Schauer, Gerhard.....	C100.....	145
Sagdinc, Seda.....	A124-pdp.....	59	Scheibelhofer, Otto.....	A091.....	54
Sagitova, Elena.....	MO508.....	30	Schenk, Harald.....	TU801-inv.....	68
Sagitova, Elena.....	A115.....	58	Scheuermann, Julian.....	TU807.....	72
Sagmeister, Patrick.....	C031.....	132	Schicker, Johannes.....	C069.....	139
Sahu, Ranjit.....	A017.....	40	Schie, Iwan.....	A053.....	47
Sahu, Ranjit.....	MO612.....	35	Schilling, Christian.....	TU812.....	76
Saiz-Lopez, Alfonso.....	MO808-inv.....	32	Schlesinger, Ramona.....	TU611-inv.....	75
Sakamoto, Tomoaki.....	B082.....	92	Schluecker, Sebastian.....	THPL1.....	110
Salafranca, Jesus.....	B022.....	81	Schmid, Rochus.....	TU106.....	69
Salehi, Mohammad.....	THPL1.....	110	Schmidt, Michael.....	TU512.....	74
Salke, Nilesh.....	TH510.....	120	Schmidt, Mikkel.....	TU512.....	74
Salm, Holly van der.....	C092-pdp.....	141	Schmidt, Ute.....	MO811.....	36
Salman, Ahmad.....	MO612.....	35	Schmitt, Heike.....	TU103.....	65
Salman, Ahmad.....	A017.....	40	Schmitt, Michael.....	C045.....	135
Samek, Ota.....	TU105.....	65	Schmitt, Michael.....	MO607.....	31
Sampaolo, Angelo.....	TU810-inv.....	72	Schmitt, Simon.....	C047.....	135
Samwer, Konrad.....	A114.....	58	Schnaiter, Martin.....	MO807.....	32
Samyn, Pieter.....	A071.....	50	Schneider, Germar.....	C069.....	139
Samyn, Pieter.....	C087.....	143	Schreiner, Elisabeth.....	C100.....	145
Sanchez-Cortes, Santiago.....	B047.....	85	Schreiner, Manfred.....	A122-pdp.....	48
Sánchez-Illana, Ángel.....	WE105.....	105	Schreiner, Peter R.....	A072.....	50
Sánchez-Illana, Ángel.....	A027.....	42	Schrenk, Werner.....	TH812.....	126
Sánchez, Alberto.....	A056.....	47	Schrenk, Werner.....	TU803.....	68
Sanjuan-Herraez, Daniel.....	A027.....	42	Schrenk, Werner.....	B003.....	77
Sanoria, Abhishek.....	C065.....	139	Schrenk, Werner.....	FR103-inv.....	153
Santos, Paulo Sérgio.....	C008.....	128	Schuepfer, Dominique B.....	A072.....	50
Saramak, Jakob.....	MO504.....	26	Schuller-Götzburg, Peter.....	A024.....	41
Sariciftci, Niyazi S.....	B106.....	97	Schulte, Alfons.....	B097.....	95
Sariciftci, Niyazi S.....	MO502.....	26	Schulte, Franziska.....	A041.....	44
Sariciftci, Niyazi S.....	A111.....	58	Schultz, Zachary.....	TU112.....	73
Sariciftci, Niyazi Serdar.....	C046.....	135	Schultz, Zachary.....	B010.....	79
Sarkar, Nirmal.....	TU610.....	71	Schürmann, Klaus.....	B118.....	98
Sasaki, Tetsuo.....	B082.....	92	Schwaighofer, Andreas.....	C099.....	145
Sasaki, Tomoya.....	A097.....	55	Schwaighofer, Andreas.....	C097.....	145
Sassi, Paola.....	B091.....	94	Schwaighofer, Andreas.....	MO105.....	25
Satapathy, Srinibas.....	TH508.....	120	Schwaighofer, Andreas.....	A121-pdp.....	39
Sathe, V.G.....	TU505.....	66	Schwarz, Benedict.....	FR103-inv.....	153
Sathe, Vasant.....	TH508.....	120	Schwarz, Benedikt.....	TH812.....	126
Sathe, Vasant.....	C059.....	137	Schwuchow, Anka.....	C045.....	135
Sato, Harumi.....	C063.....	138	Scopigno, Tullio.....	TH606.....	121
Saulnier, Luc.....	TU613.....	75	Sebbag, Gilbert.....	MO612.....	35
Savela, Jyrki.....	MO814.....	36	Sebbag, Gilbert.....	A017.....	40
Savela, Jyrki.....	B038.....	85	Šeděnková, Ivana.....	A095.....	55
Savranskie, Valerie.....	B076.....	91	Segawa, Hiroki.....	C049.....	136
Sazanovich, Igor.....	C042.....	134	Seifried, Marco.....	TU510.....	70
Scamacchio, Gaetano.....	TU810-inv.....	72	Seitsonen, Ari P.....	B060.....	88
Scamacchio, Gaetano.....	TU814.....	76	Seitz-Moskaliuk, Hendrik.....	TU808.....	72
Schafroth, Nina.....	A087.....	53	Seshadri, Srinivasaiyah.....	B050.....	86

Setnička, Vladimír .....	A037.....	44	Slobodianiuk, Denis .....	A006.....	38
Setnička, Vladimír .....	A036.....	44	Sloufova, Ivana .....	B023.....	81
Seufzer, Siegfried .....	TH804.....	118	Sloufova, Ivana .....	B016.....	80
Shapoval, Oleg .....	A114.....	58	Smith, David .....	TU603.....	67
Sharma, Shekhar .....	B041.....	84	Smith, Geoffrey .....	WE805.....	108
Shashkov, Sergej .....	A002.....	37	Smith, Nicholas .....	MO614.....	35
Shastri, Prasad .....	C006.....	128	Smith, Tim .....	MO812.....	36
Shchur, Yaroslav .....	C073.....	140	Smus, Justyna .....	TH504.....	116
Shen, Aiguo .....	B066.....	89	Smus, Justyna .....	TU513.....	74
Sheregii, Eugeniusz M. ....	B095.....	94	Sobolewski, Dariusz .....	A014.....	39
Shi, Yunjie .....	B046.....	85	Socaciu, Carmen .....	A043.....	45
Shibata, Takanori .....	A097.....	55	Sofronova, Svetlana .....	TH507.....	120
Shibata, Tomohiko .....	A096.....	55	Sokolowska, Katarzyna .....	B015.....	89
Shih, Kun-Yauh .....	A075.....	51	Solonenko, Dmytro .....	TH506.....	120
Shilton, Simon .....	A115.....	58	Solovyeva, Elena .....	TU110.....	69
Shimoaka, Takafumi .....	TU509.....	70	Song, Kigook .....	A107.....	57
Shimoaka, Takafumi .....	MO510.....	30	Song, Wei .....	TH104.....	115
Shimoaka, Takafumi .....	C082.....	142	Song, Yon-Na .....	A060.....	48
Shimoaka, Takafumi .....	C084.....	142	Sonoyama, Masashi .....	C084.....	142
Shinzawa, Hideyuki .....	C013.....	129	Sonoyama, Masashi .....	MO510.....	30
Shioya, Nobutaka .....	C082.....	142	Soohoo, Linda .....	C029.....	132
Shioya, Nobutaka .....	C084.....	142	Soto, Juan .....	C086.....	143
Shioya, Nobutaka .....	MO510.....	30	Sovago, Maria .....	C017.....	129
Shoshi, Astrit .....	TU504.....	66	Sovago, Maria .....	A105.....	57
Shpachenko, Irina .....	C028.....	131	Šovićová, Lucie .....	A036.....	44
Shur, Vladimir .....	A103.....	56	Sowley, Hugh .....	FR101.....	153
Shur, Vladimir .....	MO512.....	34	Sozańska, Agnieszka .....	C075.....	140
Sieger, Markus .....	TU605.....	67	Sozańska, Agnieszka .....	B077.....	91
Sieradzki, Adam .....	C057.....	137	Spagnolo, Angelo .....	TU814.....	76
Sigman, Daniel .....	A083.....	52	Spagnolo, Vincenzo .....	TU810-inv.....	72
Sikora, Antonín .....	MO503.....	26	Spagnolo, Vincenzo .....	TU814.....	76
Silva Santos, Silvio Domingos .....	A112.....	58	Spencer, Joe .....	TU603.....	67
Silva, Carolina .....	A007.....	38	Spezia, Riccardo .....	TH602.....	117
Silva, Igor da .....	C026.....	131	Spizzichino, Valeria .....	B042.....	84
Silva, Neirivaldo .....	C024.....	131	Stables, Ryan .....	A016.....	40
Silva, S. W. da .....	A065.....	49	Stadler, Philipp .....	B106.....	97
Silva, Vitor .....	C022.....	130	Stadler, Philipp .....	A111.....	58
Silvernagel, Michael .....	A083.....	52	Stammer Xia .....	B100.....	96
Simon, Arno .....	TH607.....	121	Stammer, Xia .....	B101.....	96
Simpson, Jonathan .....	A018.....	40	Staniszewska-Slezak, Emilia .....	A034.....	43
Singh, Pushkar .....	TU111.....	73	Staniszewska-Slezak, Emilia .....	WE102.....	105
Sinjab, Faris .....	MO606-inv.....	31	Starchak, Elena .....	MO508.....	30
Sitarz, Maciej .....	C064.....	138	Stassi, Giorgio .....	MO613.....	35
Siurdyban, Elise .....	TU109.....	69	Stavrov, Solomon .....	TH513.....	124
Siurdyban, Elise .....	C083.....	142	Stefanova, Nadia .....	A039.....	44
Sivco, Deborah .....	C096.....	144	Stejskal, Jaroslav .....	A095.....	55
Skakalova, Viera .....	A078.....	51	Stepanov, Andrey L. ....	C075.....	140
Skvaril, Jan .....	C037.....	133	Stiebing, Clara .....	A028.....	42
Slater, Joe .....	TH806.....	122	Stifter, David .....	C046.....	135
Slautin, Boris .....	A117.....	59	Stinco, Carla .....	C018.....	130
Slavov, Svetoslav .....	B062.....	88	Stiufiuc, Rares .....	B061.....	88
Slipets, Roman .....	A006.....	38	Stiufiuc, Rares .....	MO810.....	32
Sloan, Jeremy .....	TU603.....	67	Stodolak-Zych, Ewa .....	TU604.....	67

Štolcová, Lucie .....	B036.....	83	Takagi, Toshiyuki .....	MO510.....	30
Štolcová, Lucie .....	B085.....	93	Takahashi, Takafumi .....	C056.....	137
Štolcová, Lucie .....	B034.....	83	Takalo, Jouni .....	B038.....	85
Štolcová, Lucie .....	B035.....	83	Takamori, Sho .....	A038.....	44
Stone, Nick .....	MO602.....	27	Takaya, Tomohisa .....	TH609.....	121
Stovickova, Lucie .....	A037.....	44	Takayanagi, Masao .....	B099.....	95
Strachan, Clare .....	A063.....	49	Talaczyńska, Alicja .....	B079.....	91
Strachan, David .....	TH806.....	122	Talebian, Ehsan .....	B057.....	87
Strasser, Gottfried .....	FR103-inv.....	153	Talebian, Ehsan .....	A116.....	59
Strasser, Gottfried .....	TH812.....	126	Talebian, Ehsan .....	B028.....	82
Strasser, Gottfried .....	TU803.....	68	Talebian, Ehsan .....	B029.....	89
Strasser, Gottfried .....	B003.....	77	Talebian, Ehsan .....	C058.....	137
Strbac, Goran .....	A100.....	56	Talhavini, Marcio .....	C024.....	131
Stücker, Markus .....	A049.....	46	Tanabe, Ichiro .....	TH104.....	115
Šturcová, Adriana .....	MO503.....	26	Tanaka, Takuo .....	B043.....	84
Šturcová, Adriana .....	A101.....	56	Tanaka, Yoshito .....	A012.....	39
Su, Yin-Fong .....	B102.....	96	Tanaka, Yoshito .....	TU601.....	67
Suda, Jun .....	TU608.....	71	Tanaka, Yoshito .....	B031.....	82
Sudo, Eiichi .....	A069.....	50	Tanaka, Yuki .....	C084.....	142
Sugie, Ryuichi .....	A093.....	55	Tanaka, Yuki .....	MO510.....	30
Sugioka, Mikio .....	C104-pdp.....	133	Tandon, Poonam .....	C011.....	128
Suleiman, Norhidayah .....	C102.....	146	Tandon, Poonam .....	C106.....	146
Sun, Xue-Zhong .....	C091.....	144	Tandon, Poonam .....	B052.....	86
Sun, Xue-Zhong .....	C092-pdp.....	141	Tangl, Stefan .....	A024.....	41
Surat, Ludmila .....	TH509.....	120	Taniguchi, Takashi .....	WE502.....	106
Surducun, Emanoil .....	B074.....	91	Tannapfel, Andrea .....	A044.....	45
Sureshkumar, M. B. .....	A106.....	57	Tarquini, Gabriele .....	C038.....	133
Sutrova, Veronika .....	B016.....	80	Tata, Agnieszka .....	B018.....	80
Sutrova, Veronika .....	B023.....	81	Tata, Agnieszka .....	B015.....	89
Suzuki, Aki .....	A093.....	55	Tatarkovic, Michal .....	A037.....	44
Suzuki, Misao .....	B004.....	77	Tatarković, Michal .....	A036.....	44
Suzuki, Toshiaki .....	A012.....	39	Tatli, Mehmet .....	B096.....	95
Suzuki, Toshiaki .....	TU601.....	67	Tatsumi, Misaki .....	B105.....	97
Suzuki, Yasushi .....	B116-pdp.....	95	Taubner, Thomas .....	TH107.....	119
Suzuki, Yusuke .....	C071.....	140	Taubner, Thomas .....	A010.....	38
Svanqvist, Mattias .....	MO802.....	28	Taubner, Thomas .....	A120-pdp.....	39
Svecova, Marie .....	TH105.....	115	Taubner, Thomas .....	MO108.....	29
Švrček, Vladimír .....	A009.....	38	Taubner, Thomas .....	WE502.....	106
Swider, Joanna .....	B015.....	89	Tecklenburg, Stefanie .....	C090.....	143
Swiech, Dominika .....	A014.....	39	Tecklenburg, Stefanie .....	TU106.....	69
Swiech, Dominika .....	A015.....	40	Telle, Helmut H. ....	TU808.....	72
Swiech, Dominika .....	B017.....	80	Temperini, Marcia .....	TH112.....	123
Swiech, Dominika .....	B018.....	80	Tenhunen, Mari .....	MO814.....	36
Swiech, Dominika .....	C081.....	142	Tenhunen, Mari .....	B038.....	85
Swiech, Dominika .....	B014.....	79	Terazzi, Romain .....	TU804.....	68
Synytsya, Alla .....	A036.....	44	Terpugov, Evgeny .....	B076.....	91
Szabo, Laszlo .....	B044.....	84	Terpugov, Evgeny .....	C044.....	135
Szedlak, Rolf .....	TU803.....	68	Terpugova, Sofia .....	B076.....	91
Szedlak, Rolf .....	B003.....	77	Tetassi Feugomo, Conrard Giresse ..	TU606.....	71
Szybowicz, Mirosław .....	B079.....	91	Tfayli, Ali .....	MO610.....	31
Taha, Hesham .....	TU114.....	73	Thangavel, Karthick .....	C106.....	146
Tahara, Tahei .....	FRPL1.....	148	Thöing, Christian .....	TH608.....	121
Takagi, Toshiyuki .....	C084.....	142	Thomas, Jordan .....	B109.....	98

Tiemessen, David.....	C062.....	138	Ushakova, Tatiana.....	MO508.....	30
Tilley, Leann.....	A055.....	47	Ushida, Takashi.....	A113.....	58
Tilley, Leann.....	TH611.....	125	Vahlsing, Thorsten.....	TH612.....	125
Timmermans, Frank.....	TH114.....	123	Valcárcel, Miguel.....	TU605.....	67
Tirinato, Luca.....	MO613.....	35	Vales, Vaclav.....	A074.....	51
Tischler, Yaakov R.....	B108.....	97	Váňa, Rostislav.....	B035.....	83
Tittel, Frank.....	TU814.....	76	Vandenabeele, Peter.....	A056.....	47
Tittel, Frank.....	TU810-inv.....	72	Vantasin, Sanpon.....	TU601.....	67
Toboła, Tomasz.....	C101.....	145	Vantasin, Sanpon.....	B031.....	82
Todaro, Matilde.....	MO613.....	35	Vapaavuori, Jaana.....	TU507.....	70
Todor, Istvan.....	B044.....	84	Vardaki, Martha.....	MO602.....	27
Tofana, Maria.....	A043.....	45	Varga, Marian.....	A078.....	51
Tomioaka, Ryota.....	TH108.....	119	Varma, Sandeep.....	A038.....	44
Tomšić, Sanja.....	MO810.....	32	Varnholt, Birte.....	WE604.....	107
Tondi, Gianluca.....	A102.....	56	Vasilev, Semen.....	MO512.....	34
Tonkyn, Russell.....	B102.....	96	Vasilev, Semen.....	A103.....	56
Tooze, Robert P.....	C091.....	144	Vasileva, Daria.....	A103.....	56
Toppiari, Jussi.....	B040.....	83	Vega, Sebastián.....	TH501.....	116
Toury, Timothée.....	B045.....	84	Veitmann, Marie.....	TH808.....	122
Towari, Saumya.....	WE101-inv.....	105	Vejpravova, Jana.....	A064.....	49
Towrie, Michael.....	C042.....	134	Vejpravova, Jana.....	TU602.....	67
Trautmann, Steffen.....	TU111.....	73	Vejpravova, Jana.....	A074.....	51
Trbska, Joanna.....	A057.....	47	Vellutini, Luc.....	TU109.....	69
Trchová, Miroslava.....	A095.....	55	Vellutini, Luc.....	C083.....	142
Tripon, Carmen.....	B074.....	91	Velzen, Ewoud van.....	C017.....	129
Tripon, Carmen.....	B073.....	90	Venter, Monica M.....	MO810.....	32
Troccoli, Mariano.....	C096.....	144	Vento, Máximo.....	WE105.....	105
Trybalska, Barbara.....	A057.....	47	Vento, Máximo.....	A027.....	42
Trzcinski, Mariusz.....	C075.....	140	Verhagen, Tim.....	A074.....	51
Tsai, Dung-Sheng.....	B006.....	78	Verkaaik, Mattheus.....	MO809.....	32
Tseng, Shao-Chin.....	TH103.....	115	Vieira, Francisco.....	C022.....	130
Tseng, Yi-Chuan.....	TH103.....	115	Vig, Sarita.....	A085.....	53
Tsuchikawa, Satoru.....	C020.....	130	Viitala, Tapani.....	B046.....	85
Tünnermann, Andreas.....	C050.....	136	Villares, Gustavo.....	TU805.....	68
Tuñón, José Alfonso.....	A056.....	47	Vinteler, Emil.....	B061.....	88
Turnau, Katarzyna.....	TU104.....	65	Viola, Roberto.....	B042.....	84
Turner, Anthony.....	B065.....	89	Viridi, Ajit.....	B059.....	87
Turner, Jack.....	C092-pdp.....	141	Virga, Alessandro.....	B024.....	81
Turrell, Sylvia.....	TU604.....	67	Virga, Alessandro.....	TH110.....	119
Tuttolomondo, María Eugenia.....	B115-pdp.....	95	Vitek, Petr.....	B117-pdp.....	96
Tyutyunnik, Alexander.....	TH509.....	120	Vitiello, Miriam S.....	TU810-inv.....	72
Uchida, Naruya.....	B099.....	95	Vlasova, Tatyana.....	A115.....	58
Uchida, Taro.....	TH108.....	119	Vlckova, Blanka.....	B016.....	80
Uchida, Tomoyuki.....	A093.....	55	Vlckova, Blanka.....	B023.....	81
Uehara, Ryo.....	B005.....	78	Vogt, Patrick.....	TH506.....	120
Uehara, Ryo.....	B004.....	77	Voronov, Vladimir.....	WE504.....	106
Uemura, Suguru.....	A019.....	40	Vovkotrub, Emma.....	TH509.....	120
Uerpmann, Carsten.....	TH806.....	122	Vretenar, Viliam.....	A078.....	51
Ujević, Ivana.....	MO810.....	32	Vtyurin, Alexander.....	WE504.....	106
Ujj, Laszlo.....	TH503.....	116	Vtyurin, Alexander.....	TH507.....	120
Ükermann, Arne.....	B090.....	94	Vuilleumier, Rodolphe.....	TH602.....	117
Umapathy, Siva.....	C051.....	136	Vukosavljevic, Branko.....	B087.....	93
Usenov, Iskander.....	A041.....	44	Wachsmann-Hogiu, Sebastian.....	MO607.....	31

Waclawek, Johannes P.....	C098.....	145	Windbergs, Maike.....	B087.....	93
Wada, Kiyoshi.....	C104-pdp.....	133	Wippermann, Stefan.....	TU106.....	69
Wagner, Joachim.....	TU801-inv.....	68	Witek, Ewa.....	B015.....	89
Wagner, Martin.....	MO112.....	33	Wlodek, Tomasz.....	A081.....	52
Wagner, Reinhard.....	C054.....	137	Wojnarowska, Renata.....	B095.....	94
Wagner, Robert.....	MO807.....	32	Wojtas, Maciej.....	MO512.....	34
Wahl, Verena.....	A091.....	54	Wolf, Sebastian.....	TH811-inv.....	126
Walfisch, Shlomo.....	A017.....	40	Wolferen, Henk van.....	TH114.....	123
Wan Mohamad, Wan Anwar Fahmi.....	C021.....	130	Wong Carter, Katherine.....	TH505.....	116
Wang, Fenglong.....	C047.....	135	Wongravee, Kanet.....	B031.....	82
Wang, Hailong.....	A020.....	41	Wood, Bayden.....	WE103.....	105
Wang, Hao.....	TU112.....	73	Wood, Bayden.....	TH611.....	125
Wang, Jing.....	C078.....	141	Wood, Bayden R.....	A055.....	47
Wang, Pei.....	C026.....	131	Wozniowski, Sebastian.....	B104.....	97
Wang, Wentao.....	B019.....	80	Wriglesworth, Alisdair.....	C040.....	134
Wang, Xiaojun.....	C096.....	144	Wrobel, Tomasz.....	WE101-inv.....	105
Wang, Yandong.....	B019.....	80	Wrona, Magdalena.....	B022.....	81
Wang, Yue.....	TH104.....	115	Wu, Jiang.....	A004.....	37
Ward, Bess.....	A083.....	52	Wu, Jinguang.....	B078.....	91
Warring, Suzanne.....	TU108.....	69	Wu, Kai-Wen.....	A075.....	51
Watanabe, Kazuki.....	A088.....	53	Wu, Yuqing.....	B070.....	90
Watari, Madahiro.....	A088.....	53	Wu, Zitong.....	B066.....	89
Webb, Paul B.....	C091.....	144	Wueppen, Jochen.....	A010.....	38
Webb, Simon J.....	A054.....	47	Wysocki, Gerard.....	TU806-inv.....	72
Weber, Karina.....	B075.....	91	Wysocki, Gerard.....	A083.....	52
Weber, Karina.....	TH102.....	115	Xie, Yunfei.....	A061.....	48
Weber, Karina.....	B088.....	93	Xin, Hangshu.....	B068.....	89
Weddell, Lynette.....	TH810.....	122	Xu, Jing.....	C067.....	139
Weida, Miles.....	MO109.....	29	Xu, Jing.....	C089.....	143
Weidinger, Inez M.....	TH109.....	119	Xu, Shuping.....	C078.....	141
Weigel, Ralf.....	MO807.....	32	Xu, Shuping.....	A020.....	41
Weih, Robert.....	TU807.....	72	Xu, Weiqing.....	C078.....	141
Weinberger, Peter.....	C076.....	141	Xu, Weiqing.....	A020.....	41
Weinberger, Peter.....	TU510.....	70	Xu, Yizhuang.....	B078.....	91
Weisman, R. Bruce.....	C004.....	127	Xu, Yizhuang.....	A004.....	37
Welsh, Calum.....	C103-pdp.....	133	Yamamoto, Jun.....	TU501.....	66
Wenning, Gregor K.....	A039.....	44	Yamamoto, Shigeki.....	WEPL1.....	100
Wentzell, Peter.....	A007.....	38	Yamamoto, Shigeki.....	C063.....	138
Weselucha-Birczynska, Aleksandra.....	TU604.....	67	Yamamoto, Shigeki.....	C010.....	128
Weselucha-Birczynska, Aleksandra.....	A057.....	47	Yamamoto, Tatsuyuki.....	A019.....	40
Weselucha-Birczyńska, Aleksandra.....	B077.....	91	Yan, Di.....	C025.....	131
Westberg, Jonas.....	TU806-inv.....	72	Yan, Di.....	TU809.....	72
Wetzel, David.....	WE802.....	108	Yang, Honghua.....	MO113.....	33
Whelan, Donna.....	WE103.....	105	Yang, In-Sang.....	A060.....	48
Wieda, Mile.....	TU813.....	76	Yang, Ling.....	B067.....	89
Wiegand, Pat.....	TH806.....	122	Yang, Quankui.....	TU812.....	76
Wiercigroch, Ewelina.....	WE102.....	105	Yasuda, Norio.....	A088.....	53
Wierzchos, Jacek.....	B117-pdp.....	96	Yeh, Kevin.....	WE101-inv.....	105
Wietrzyk, Joanna.....	A032.....	43	Yen, Yu-Ting.....	TH103.....	115
Wilhelm, Emmerich.....	B097.....	95	Yliperttula, Marjo.....	B046.....	85
Williams, Hywel.....	A038.....	44	Yoneyama, Hiroaki.....	C049.....	136
Wilk, Andreas.....	B111.....	98	Yosef, Hesham.....	A031.....	43
Willison, Keith.....	FR101.....	153	Yosef, Hesham.....	MO609.....	31

Yoshimura, Masamichi .....	B004.....	77	Zimmerman, Earl A. ....	WE104.....	105
Yoshimura, Masamichi .....	B005.....	78	Zimmermann, Henrik.....	B001.....	77
Yoshimura, Norio.....	B099.....	95	Zobi, Fabio.....	A001.....	37
Yu, Chen-Chieh.....	TH103.....	115	Zubkov, Vladimir.....	TH509.....	120
Yu, Peiqiang .....	B067.....	89	Zverev, Petr.....	TU608.....	71
Yu, Peiqiang .....	B068.....	89			
Yu, Peiqiang.....	C012.....	129			
Yu, Yajun.....	TU814.....	76			
Yu, Zhi Wu.....	C089.....	143			
Yu, Zhi-Wu.....	C067.....	139			
Yui, Hiroharu.....	TH502.....	116			
Yurtseven, Hamit.....	B063.....	88			
Zachhuber, Bernhard.....	MO802.....	28			
Zachmann, Günter.....	TH607.....	121			
Zachmann, Günter.....	B101.....	96			
Zahel, Thomas.....	C031.....	132			
Zahn, Dietrich.....	TH506.....	120			
Zanni, Martin.....	FRPL2.....	148			
Zavgorodnev, Yury.....	MO508.....	30			
Zavoral, Miroslav.....	A037.....	44			
Zebger, Ingo.....	TH109.....	119			
Zebger, Ingo.....	TU102.....	65			
Zederbauer, Tobias.....	TU803.....	68			
Zederbauer, Tobias.....	B003.....	77			
Zederbauer, Tobias.....	TH812.....	126			
Zeerbauer, Tobias.....	FR103-inv.....	153			
Zelenovskiy, Pavel.....	MO512.....	34			
Zelenovskiy, Pavel.....	A103.....	56			
Zelenovskiy, Pavel.....	A117.....	59			
Zemánek, Pavel.....	TU105.....	65			
Zerbi, Giuseppe.....	MO511.....	34			
Zeug, Manuela.....	A099.....	56			
Zhai, Yanjun.....	A004.....	37			
Zhang, Bifeng.....	B046.....	85			
Zhang, Eric.....	A083.....	52			
Zhang, Eric.....	TU806-inv.....	72			
Zhang, Jason.....	WE103.....	105			
Zhang, Jin.....	TH111.....	123			
Zhang, Kaisong.....	B046.....	85			
Zhang, Xuewei.....	B068.....	89			
Zhang, Yu.....	C067.....	139			
Zhang, Yuying.....	THPL1.....	110			
Zhang, Zhenglong.....	TH113.....	123			
Zhao, Bing.....	TH104.....	115			
Zhao, Mengyao.....	A061.....	48			
Zheng, Yan-Zhen.....	C067.....	139			
Zhigunov, Alexander.....	A101.....	56			
Zhou, Xiaodong.....	B066.....	89			
Zhou, Yu.....	C089.....	143			
Ziêba-Palus, Janina.....	B077.....	91			
Ziebell, Arne.....	C077.....	141			
Zielinski, Francois.....	C005.....	127			
Ziemons, Eric.....	B008.....	78			

# Cover more ground, easily

Chances are your research can use the power of Raman to get ahead. It is a key to new discoveries in nanomaterials performance, geological processes, and the treatment of disease. The Thermo Scientific™ DXR™xi Raman imaging microscope is a visually driven system that finds the hidden answers in samples easily, with **all of the performance and none of the learning curve**. You'll be an expert in Raman, covering more ground in your samples and research faster, without missing a detail.

## with smarter Raman imaging

• see the complete picture at [thermoscientific.com/DXRxi](http://thermoscientific.com/DXRxi)



**DXRxi Raman Imaging Microscope**  
High performance in an integrated package



**Thermo Scientific™ OMNIC™xi Raman Imaging Software**  
Simple yet powerful image-centric software

© 2015 Thermo Fisher Scientific Inc. All rights reserved. All trademarks are the property of Thermo Fisher Scientific and its subsidiaries.



NT-MDT is a global leader in the creation of innovation led, cutting-edge devices within the field of instrumentation created for nanotechnology research.

Founded in 1990, NT-MDT has become known internationally for its next-generation instruments in AFM, STM, and Hybrid technologies such as AFM-Raman, TERS, SNOM, Bio and deep vacuum.

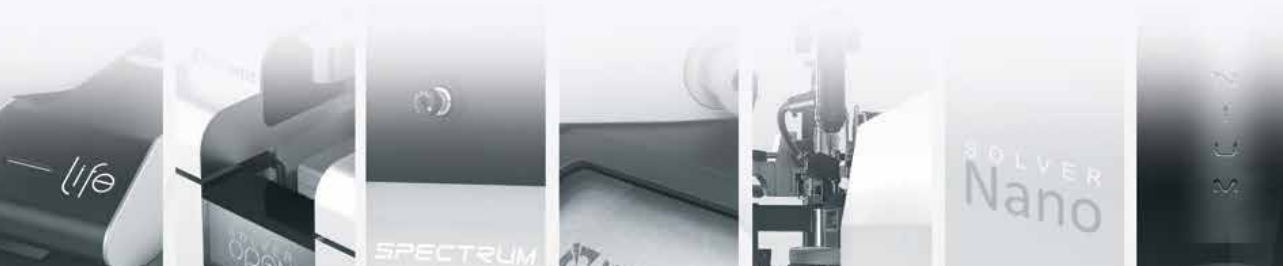
Join us in Vienna, AUSTRIA 12.-17. July 2015



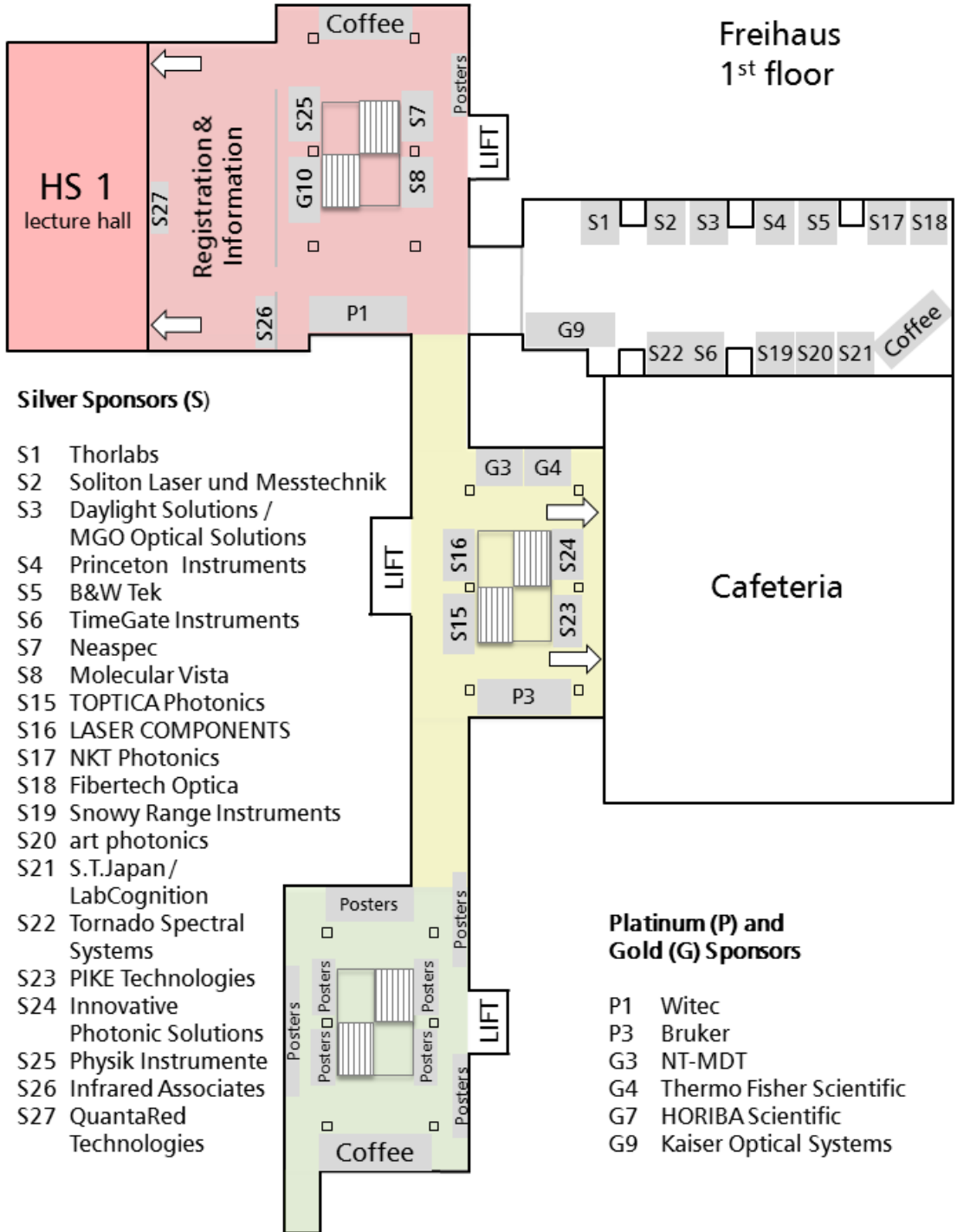
# Booth Number G3

Find Out More  
[www.ntmdt.com](http://www.ntmdt.com)

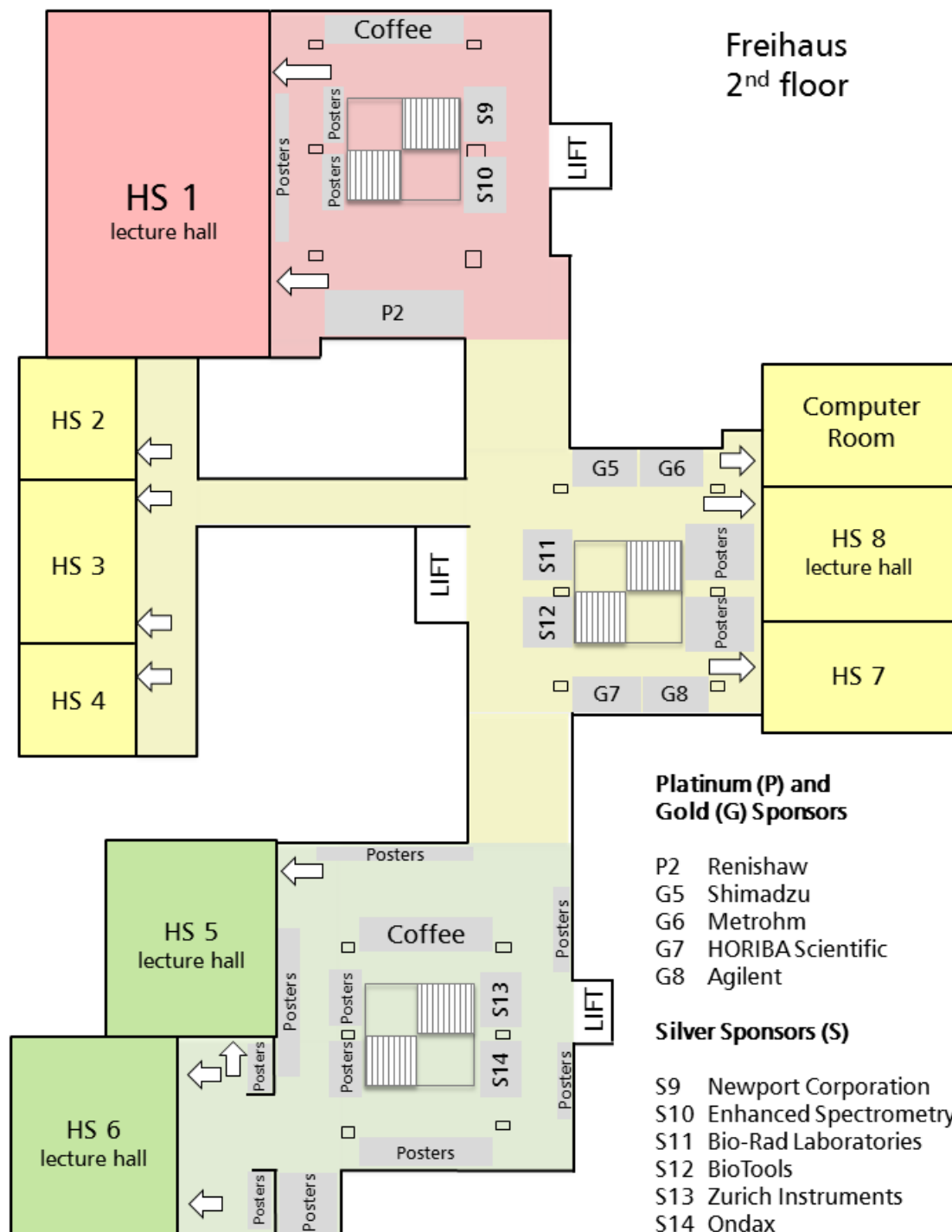
Find Your Local Distributor  
[www.ntmdt.com/distributors](http://www.ntmdt.com/distributors)



## Freihaus 1st floor



## Freihaus 2<sup>nd</sup> floor





- ### Hotels
- 1 AllYouNeed Hotel
  - 2 Hotel Papageno
  - 3 Motel One Wien-Staatsoper
  - 4 Hotel Erzherzog Rainer
  - 5 Hotel Mercure Secession
  - 6 Hotel Beethoven
  - 7 Austria Trend Hotel Europa
  - 8 Hotel Le Meridien

- ### ICAVS 8 Venues
- 1 TU Freihaus: Main Venue, Workshops
  - 2 TU Building BA: Workshops
  - 3 Shimadzu Young Scientists Event
  - 4 Secession bus station
  - 5 Palais Ferstel: Conference Dinner
  - N Naschmarkt

